

**GEOLOGY AND GEOTHERMAL  
RESOURCES OF THE  
CENTRAL OREGON CASCADE RANGE**

1983

STATE OF OREGON  
DEPARTMENT OF GEOLOGY AND MINERAL INDUSTRIES  
DONALD A. HULL, STATE GEOLOGIST



STATE OF OREGON  
DEPARTMENT OF GEOLOGY AND MINERAL INDUSTRIES  
1005 State Office Building, Portland, Oregon 97201

**Special Paper 15**

**GEOLOGY AND GEOTHERMAL  
RESOURCES OF THE  
CENTRAL OREGON CASCADE RANGE**

Edited by  
George R. Priest and Beverly F. Vogt  
Oregon Department of Geology and Mineral Industries

**1983**

Conducted in conformance with ORS 516.030

Funded by U.S. Department of Energy Cooperative Agreement No. DE-FC-07-79ID12044  
to the Oregon Department of Geology and Mineral Industries



**GOVERNING BOARD**

Allen P. Stinchfield, Chairman	North Bend
Donald A. Haagensen	Portland
Sidney R. Johnson	Baker

**STATE GEOLOGIST**  
Donald A. Hull  
**DEPUTY STATE GEOLOGIST**  
John D. Beaulieu



## NOTICE

The Oregon Department of Geology and Mineral Industries (DOGAMI) is publishing this paper because the subject matter is consistent with the mission of the Department. To facilitate timely distribution of data, a draft version of this paper was released as DOGAMI Open-File Report O-82-7. Because additional field and analytical work was done after release of the open-file report, some of the sample numbers used on the maps and tables in the report have been changed in this Special Paper. For that reason, readers wishing to cross reference O-82-7 and Special Paper 15 should refer to field numbers, not sample numbers.

For the reader's convenience, elevations, map distances, unit thicknesses, and well depths are presented in both SI metric and U.S. customary units of measurement. All other units of measurement are in SI metric units.



## CONTENTS

1.	INTRODUCTION AND ACKNOWLEDGMENTS, by George R. Priest .....		1
Figures:	1.1.	Map showing location of drill holes and areas studied in central Cascades of Oregon .....	2
Tables:	1.1.	Heat-flow holes drilled in central Oregon Cascades by DOGAMI .....	1
2.	OVERVIEW OF THE GEOLOGY OF THE CENTRAL OREGON CASCADE RANGE, by George R. Priest, Neil M. Woller, Gerald L. Black, and Stanley H. Evans .....		3
Figures:	2.1.	Map showing physiographic provinces of Oregon .....	4
	2.2.	Diagrammatic cross section of central Cascades of Oregon .....	4
	2.3.	Regional stratigraphic units in Cascades compared to volcanic time categories used in this paper .....	6-7
	2.4.	Map showing major faults, lineaments, hot springs, and Quaternary volcanic centers and heat-flow zones .....	15
	2.5.	Episodes of deformation in northern and central Cascades .....	16
	2.6.	Nepheline-olivine-clinopyroxene-quartz quadrilateral .....	22
	2.7.	$\text{Na}_2\text{O} + \text{K}_2\text{O} - \text{FeO}^* - \text{MgO}$ ternary diagram .....	23
	2.8.	$\text{FeO}^*/\text{MgO}$ versus $\text{SiO}_2$ .....	23
	2.9.	$\text{FeO}^*$ versus $\text{SiO}_2$ .....	24
	2.10.	$\text{Al}_2\text{O}_3$ versus normative plagioclase .....	24
	2.11.	$\text{Na}_2\text{O} + \text{K}_2\text{O}$ versus $\text{SiO}_2$ .....	24
Tables:	2.1.	Parameters of volcanic rocks erupted during various central Oregon Cascade volcanic episodes .....	8
	2.2.	Informal nomenclature used for central Oregon Cascade episodes of volcanism .....	9
3.	PRELIMINARY GEOLOGY OF THE OUTERSON MOUNTAIN-DEVILS CREEK AREA, MARION COUNTY, OREGON, by George R. Priest and Neil M. Woller .....		29
Figures:	3.1.	Map showing location of Outerson Mountain-Devils Creek area .....	29
	3.2.	Map of geology of Outerson Mountain-Devils Creek area .....	30-31
Tables:	3.1.	Stratigraphy of volcanic rock units, Outerson Mountain-Devils Creek area .....	33
	3.2.	Relationship of Outerson Mountain-Devils Creek geologic units to units of previous workers .....	34
	3.3.	Estimated minimum reservoir temperatures and partial analyses from wells and springs in the Breitenbush KGRA .....	38
4.	GEOLOGY OF THE COUGAR RESERVOIR AREA, LANE COUNTY, OREGON, by George R. Priest and Neil M. Woller .....		39
Figures:	4.1.	Map showing location of Cougar Reservoir area .....	40
Tables:	4.1.	Stratigraphy of volcanic rock units, Cougar Reservoir area .....	42
	4.2.	Estimated reservoir temperatures, Terwilliger Hot Springs .....	47
5.	GEOLOGY OF THE LOOKOUT POINT AREA, LANE COUNTY, OREGON, by Neil M. Woller and George R. Priest .....		49
Figures:	5.1.	Map showing location of Lookout Point area .....	50
	5.2.	Map of geology of Lookout Point area .....	52-53
	5.3.	Stratigraphic section of lavas of Black Canyon .....	55
Tables:	5.1.	Stratigraphy of volcanic rock units, Lookout Point area .....	51
6.	GEOLOGY OF THE WALDO LAKE-SWIFT CREEK AREA, LANE AND KLAMATH COUNTIES, OREGON, by Neil M. Woller and Gerald L. Black .....		57
Figures:	6.1.	Map showing location of Waldo Lake-Swift Creek area and areas mapped by various geologists .....	58
	6.2.	Map showing bathymetry of Waldo Lake .....	66
	6.3.	Residual gravity anomaly map of area covered by geologic map on Plate 3 .....	67
Tables:	6.1.	Stratigraphy of volcanic rock units, Waldo Lake-Swift Creek area .....	59
	6.2.	Petrography of Waldo Lake-Swift Creek geologic units .....	60



7.	HEAT FLOW IN THE OREGON CASCADES, by Gerald L. Black, David D. Blackwell, and John L. Steele.....	69
Figures:	7.1. Map showing physiographic provinces of Oregon .....	69
	7.2. Map showing heat flow in Oregon Cascade Range .....	72
	7.3. Geothermal gradient, heat flow, interpreted crustal temperatures, and regional Bouguer gravity in western part of northern Oregon Cascade Range.....	73
	7.4. Models showing relationship of hot springs to the heat-flow transition at Western-High Cascade boundary.....	74
Tables:	7.1. Estimates of the electrical generation potential of the Oregon Cascade Range.....	76
8.	GEOHERMAL EXPLORATION IN THE CENTRAL OREGON CASCADE RANGE, by George R. Priest.	77
Figures:	8.1. Thermal springs in and adjacent to the Oregon Cascade Range .....	78
Tables:	8.1. Analyses of late-stage High Cascade rocks from Mount Hood, Mount Jefferson, and South Sister compared to nearby hypabyssal plutonic rocks.....	86
REFERENCES .....		89
APPENDIX A. NEW K-Ar DATA, OREGON.....		97
Tables:	A.1. New K-Ar data, Oregon .....	97
APPENDIX B. CHEMICAL ANALYSES OF ROCK SAMPLES.....		98
Tables:	B.1. Rock chemistry, Outerson Mountain-Devils Creek area.....	98
	B.2. Rock chemistry, Cougar Reservoir area.....	100
	B.3. Rock chemistry, Lookout Point area.....	103
	B.4. Rock chemistry, Waldo Lake-Swift Creek area.....	105
	B.5. New geochemical data, Outerson Mountain-Devils Creek and Waldo Lake-Swift Creek areas..	109
APPENDIX C. EXPLANATION OF TOWNSHIP-RANGE SYSTEM.....		115
APPENDIX D. TEMPERATURE AND HEAT-FLOW DATA FOR THE OREGON CASCADES .....		116
Tables:	D.1. Temperature and heat-flow data for the Oregon Cascades .....	116
PLATES (in envelope)		
1. Local stratigraphic columns of regional interest in the Oregon Cascades		
2. Geologic map of the Cougar Reservoir area		
3. Geologic map of the Waldo Lake-Swift Creek area		
COVER (repeated on both front and back covers): Segment of SLAR imagery mosaic, central Oregon Cascades. Three Sisters in upper right-hand corner, Waldo Lake below center, and McKenzie River drainage across top. Note contrast between heavily dissected terrain of the Western Cascades (left half) and smooth, more youthful topography of the High Cascades (right half).		



# GEOLOGY AND GEOTHERMAL RESOURCES OF THE CENTRAL OREGON CASCADE RANGE

## CHAPTER 1. INTRODUCTION AND ACKNOWLEDGMENTS

By George R. Priest, Oregon Department of Geology and Mineral Industries

This paper summarizes investigations of the geology and geothermal resources of the central Cascade Range of Oregon conducted by the Oregon Department of Geology and Mineral Industries (DOGAMI) from 1977 through 1982. The project was funded by the State of Oregon and the U.S. Department of Energy (USDOE) (USDOE Contract EG-77-C-06-1040 and Cooperative Agreement DE-FC-07-79ID12044). A draft version of this paper was published in 1982 (DOGAMI Open-File Report O-82-7 [Priest and Vogt, 1982a]). Special Paper 15, however, completely supersedes the open-file report. Users of the information summarized here are encouraged to cite Special Paper 15 instead of Open-File Report O-82-7.

A shallow drilling program and geologic mapping project provided data for heat-flow and geologic analysis. In some areas, detailed geologic maps were produced around individual drill sites, so that heat-flow interpretations could be related to local geology (Figure 1.1). Heat flow was calculated by D.D. Blackwell and J.L. Steele of Southern Methodist University, Dallas, Texas. Interpretation and collection of the heat-flow data were accomplished by G.L. Black (DOGAMI) with the aid of D.D. Blackwell and J.L. Steele (see Chapter 7, this volume). Drilling and geologic mapping were conducted primarily by G.R. Priest and N.M. Woller of DOGAMI (see Chapters 3 and 4, by Priest and Woller, Chapter 5, by Woller and Priest; and Chapter 6, by Woller and Black, this volume). Early phases of the drilling program were supervised by D.A. Hull (DOGAMI) in 1977 and by J.F. Riccio (DOGAMI) in 1979. D.E. Brown (DOGAMI) supervised reconnaissance geologic mapping of the Belknap-Foley and Willamette Pass areas as part of a separate investigation of low-temperature geothermal resources. This paper summarizes the data generated by these workers. Figure 1.1 shows the location of drill holes and map areas, and Table 1.1 lists DOGAMI temperature-gradient holes.

In addition to the above DOGAMI investigations, five separate projects were subcontracted: (1) R.W. Couch of Oregon State University (OSU) supervised production of gravity and aeromagnetic maps of the Cascade Range (DOGAMI maps GMS-8 [Pitts and Couch, 1978], -9 [Couch and others, 1978], -15 [Couch and others, 1981b], -16 [Couch and others, 1981c], -17 [Couch and others, 1981a], and -26 [Couch and others, 1982b] and Open-File Report O-82-9 [Couch and others, 1982a]), exclusive of aeromagnetic coverage of the northern Cascade Range. Gravity field work and calculations were accomplished primarily by G.S. Pitts and M. Gemperle, with assistance from C.A. Veen and D.E. Braman. Aeromagnetic field and laboratory work were completed by M. Gemperle, G.G. Connard, and W.H. McLain. The U.S. Geological Survey (USGS) subcontracted the gravity and aeromagnetic work in the central Cascade Range, while DOGAMI subcontracted gravity surveys of the northern and southern Cascade Range and an aeromagnetic survey of the southern Cascade Range. (2) C.W. Field and S.G. Power of OSU completed a study of Western Cascade mining districts to relate older geothermal systems to modern ones (Power and

others, 1981; Power and Field, 1982). (3) A lineament study of the Cascade Range was accomplished in two parts. The northern Cascade lineaments were described by R. Venkatakrishnan, J.G. Bond, and J.D. Kauffman of Geoscience Research Consultants, Moscow, Idaho (DOGAMI Special Paper 12 [Venkatakrishnan and others, 1980]). The southern Cascade lineaments were studied by C.F. Kienle and C.A. Nelson of Foundation Sciences, Inc., Portland, Oregon, and R.D. Lawrence of OSU (DOGAMI Special Paper 13 [Kienle and others, 1981]). (4) J. Magill and A. Cox of Stanford University conducted a study of paleomagnetism of Western Cascade igneous rocks (DOGAMI Special Paper 10 [Magill and Cox, 1980]). (5) C.M. White, Boise State University, investigated the geology of the Breitenbush Hot Springs quadrangle (DOGAMI Special Paper 9 [White, 1980a]) (Figure 1.1).

Data from the Mount Hood geothermal assessment project (DOGAMI Open-File Report O-79-8 [Hull and Riccio, 1979], Special Paper 8 [White, 1980b], and Special Paper 14

Table 1.1. *Heat-flow holes drilled in the central Oregon Cascades by the Oregon Department of Geology and Mineral Industries in 1979 and 1980*

Twn./Rng./Sec. <sup>1</sup>	Hole name	Drilled depth
8S/8E/31C	Cub Creek <sup>2</sup>	142 m (466 ft)
10S/7E/11Aa	Devils Creek <sup>2</sup>	154 m (505 ft)
11S/7E/10Dc	Minto Creek <sup>2</sup>	122 m (400 ft)
11S/6E/22Db	Buck Mtn. <sup>2</sup>	154 m (505 ft)
11S/10E/5Ac	Castle Rock <sup>2</sup>	154 m (505 ft)
12S/9E/1Bc	Green Ridge	154 m (505 ft)
13S/7E/9Ab	Detroit Road	76 m (249 ft)
13S/9E/5Ab	Fly Creek <sup>2</sup>	119 m (390 ft)
14S/6E/32Dc	Wolf Meadow <sup>2</sup>	154 m (505 ft)
17S/5E/8Ac	Walker Creek <sup>2</sup>	154 m (505 ft)
17S/5E/20Ba	Rider Creek <sup>2</sup>	154 m (505 ft)
17S/6E/25Ad	Mosquito Creek <sup>2</sup>	154 m (505 ft)
18S/5E/11Bd	Rebel Creek <sup>2</sup>	154 m (505 ft)
19S/6E/8Ba	Elk Creek <sup>2</sup>	133 m (436 ft)
19S/5E/27Bc	Brock Creek <sup>2</sup>	154 m (505 ft)
19S/4E/29Cc	Christy Creek <sup>2</sup>	154 m (505 ft)
19S/6E/25Dc	North Fork <sup>2</sup>	154 m (505 ft)
20S/4E/27Dd	Wall Creek <sup>2</sup>	137 m (449 ft)
20S/2E/35Ac	Burnt Bridge Cr. <sup>2</sup>	154 m (505 ft)
21S/5E/16Ac	Black Creek <sup>2</sup>	104 m (340 ft)
23S/5E/8Da	Pinto Creek <sup>2</sup>	154 m (505 ft)
24S/5E/18Ca	Tumblebug Creek <sup>2</sup>	154 m (505 ft)
21S/3E/17Da	Oakridge city well <sup>3</sup>	335 m (1,099 ft) <sup>4</sup>
21S/3E/26Ca	Hills Creek Dam <sup>3</sup>	160 m (525 ft)

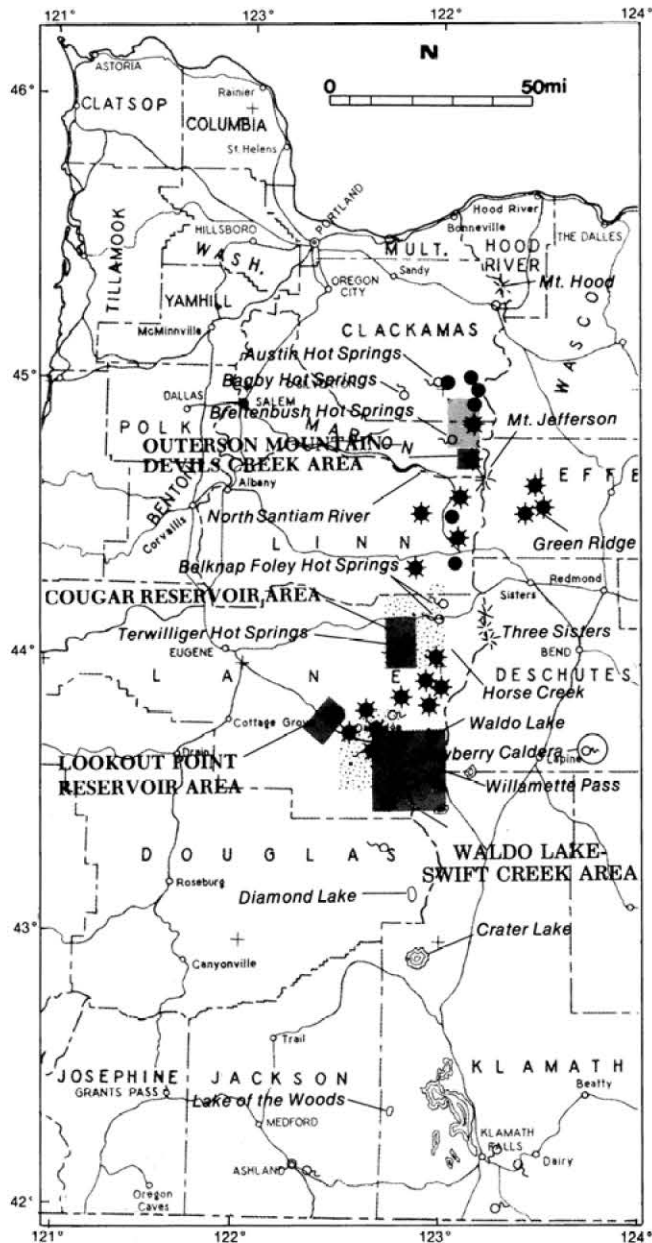
<sup>1</sup> See Appendix C for explanation of township-range location system.

<sup>2</sup> Drilled under contract DE-FC07-79ID12044.







<sup>3</sup> Drilled under contract DE-FC07-79ET27220.

<sup>4</sup> Deepened from 183 m (600 ft) to 335 m (1,099 ft).





#### EXPLANATION

-  Hot springs
-  Gradient hole drilled by DOGAMI
-  Gradient hole drilled by EWEB
-  Detailed geologic mapping by DOGAMI staff
-  Reconnaissance geologic mapping by DOGAMI staff
-  Breitenbush quadrangle, mapped by C. White (1980a)

[Priest and Vogt, 1982b)], are also used in this paper to develop a comprehensive geothermal model. For summaries of Mount Hood data, the reader is referred to DOGAMI Special Paper 14 (Priest and Vogt, 1982b) and a special Mount Hood issue of *Journal of Geophysical Research* (volume 87, number B4). DOGAMI Special Paper 8 by C.M. White (White, 1980b) describes the igneous petrology of Mount Hood.

Temperature and heat-flow data from a drilling project conducted by the Eugene Water and Electric Board, Eugene, Oregon (Figure 1.1) are also summarized here (Chapter 7, Black and others; see also DOGAMI Open-File Report O-80-12 [Youngquist, 1980]). This drilling project was funded primarily by USDOE with smaller contributions by Southland Royalty Company, Fort Worth, Texas; Sunoco Energy Development Company, Dallas, Texas; and the Eugene Water and Electric Board.

Reviews of several drafts of the report, particularly the geological chapters, by George W. Walker, Norman S. MacLeod, and David R. Sherrod of the USGS contributed greatly to the quality of the report. Edward M. Taylor and Gary Smith of Oregon State University, Brian H. Baker of the University of Oregon, Marvin H. Beeson and Paul E. Hammond of Portland State University, and Craig M. White of Boise State University also offered valuable geological reviews. Initial drafts of the geothermal resources and heat-flow chapters of the report were reviewed by Al Waibel and Marshall Gannett of Columbia Geoscience, Hillsboro, Oregon, and by Edward A. Sammel, Melvin H. Beeson, Keith E. Bargar, and Terry E.C. Keith of the USGS.

◁ Figure 1.1 Map showing locations of drill holes and areas studied during the geothermal project in the central Cascades of Oregon.

## CHAPTER 2. OVERVIEW OF THE GEOLOGY OF THE CENTRAL OREGON CASCADE RANGE

*By George R. Priest, Neil M. Woller, Gerald L. Black,  
Oregon Department of Geology and Mineral Industries, and  
Stanley H. Evans, University of Utah Research Institute, Salt Lake City, Utah*

### ABSTRACT

Eruption of voluminous silicic tuffs and lesser volumes of iron-rich basaltic to silicic lavas between about 40 and 18 m.y. B.P. and eruption of intermediate calc-alkaline lavas and subordinate tuffs between about 18 to 9 m.y. B.P. formed most of the volcanic pile in the central Western Cascade Range. The axis of volcanism had shifted to the vicinity of the High Cascade province by about 9 m.y. B.P., when eruption of more mafic, alkaline, and iron-rich lavas began. Slight local folding in the north-central Western Cascade Range also ended by about this time. Widespread north-south- to north-northwest-trending normal faulting accompanied uplift of the Western Cascade block relative to the High Cascade province between about 5 and 4 m.y. B.P. Voluminous basaltic lavas formed a broad platform in the High Cascades in the early Pliocene, and a north-south-trending chain of composite volcanoes developed along the High Cascade axis in the Quaternary as volcanism became slightly more silicic. The youngest composite cones are chiefly andesitic in composition, with local dacitic to rhyodacitic eruptions, although basaltic eruptions have continued to occur on the surrounding platform into the Holocene.

Compositional and textural similarity of some of the 9- to 0-m.y. B.P. basalts in the Basin and Range and the Cascades and the contemporaneity of changes in volcano-tectonic events in the Basin and Range and the Cascades suggest that the geologic histories of the two areas are closely related. A major change in the plate-tectonic regime about 10 to 8 m.y. B.P. may have affected both areas, resulting in increased extensional tectonic influence in the central Cascades. An additional change in the interaction of lithospheric plates at the end of the Miocene is probably necessary to account for the pronounced uplift and north-south faulting which occurred 5 to 4 m.y. B.P. in the Cascades. The central Oregon High Cascade Range is viewed as a subduction-related volcanic arc which has been strongly affected by Basin-and-Range-type extension. Local subsidence of parts of the High Cascade axis is probably caused by magmatic withdrawal and volcanic loading during regional extension.

### INTRODUCTION

This paper summarizes the general geology of the central Oregon Cascade Range, which includes both the Western and High Cascade Ranges, with the goal of achieving a viable geologic model to guide future geothermal exploration (see Chapter 8). One of the most important factors limiting exploration in the Cascade Range of Oregon is the lack of accurate detailed geologic maps. In the following four papers (Chapters 3-6), four new detailed geologic maps (see Figure 1.1 of the

previous chapter) are presented along with numerous new radiometric dates and whole-rock analyses. The new data and maps are utilized in this chapter along with data from other workers (see Schumacher, 1981, and Priest and Vogt, 1982a, Plate 1, for indexes of geologic mapping of the areas covered by this paper) to develop a volcano-tectonic model for the central Oregon Cascade Range. Recommended geothermal exploration areas based on these geologic and geophysical data, especially heat flow (Chapter 7), are discussed in Chapter 8.

Specific topics which will be discussed are the following:

1. The nature of the High Cascade-Western Cascade physiographic boundary (Figure 2.1). Why, for example, is the boundary linear in many places, and why are many parts of the easternmost Western Cascade Range higher than westernmost parts of the High Cascade Range? Does this mean that the High Cascade province is downfaulted in areas other than those already mapped (Figures 2.1 and 2.2)?
2. Compositional changes in Cascade volcanism through time. Why is there so much more olivine-normative diktytaxitic basalt in the sequences less than 8 to 10 m.y. old than in the older sequences, and why are many of the Cascade mafic lavas of Oligocene to early Miocene age so high in both iron and silica relative to younger mafic lavas?
3. Spatial changes in the pattern of volcanism. Why has volcanic activity been focused on the eastern part of the Cascade Range for the last 8 to 10 m.y., and why have diktytaxitic olivine basalts similar to High Cascade basalts also been erupted in the adjacent Basin and Range province during the last 8 to 10 m.y.?
4. Correlation of episodes of tectonic deformation with changes in the composition of volcanic rocks. Why did voluminous eruptions of diktytaxitic basalts occur in the Three Sisters area just after uplift of the Western Cascade block along the McKenzie River-Horse Creek fault (Figure 2.1) 5-4 m.y. B.P.? Did similar diktytaxitic olivine basalt eruptions occurring about 9 to 8 m.y. B.P. east of Cougar Reservoir correspond to a similar faulting and uplift event at the Cougar fault (Figure 2.1; Chapter 4)? If so, did the Groundhog Creek-Waldo Lake fault system (Figure 2.1; Chapter 6) have a volcano-tectonic history analogous to the Cougar-Horse Creek fault system? Do these faults and volcanic events have regional significance?

### PREVIOUS WORK

This study draws on a considerable body of previous geological work by numerous scientists working in the central Cascades. Although there are many new data on the central

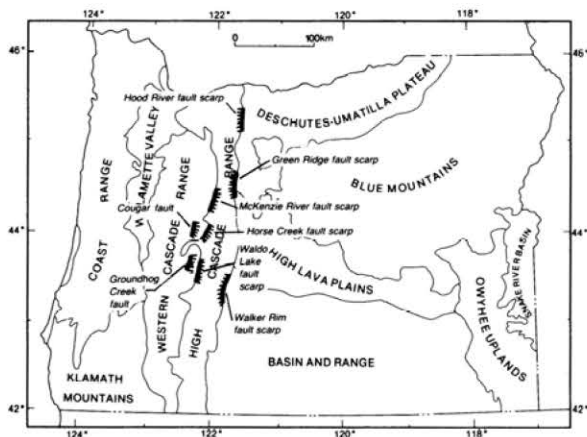


Figure 2.1 Map showing the physiographic provinces of Oregon (after Dicken, 1950). Also shown are several faults and fault scarps at the northern and central High Cascade province boundary. Hachures on faults and fault scarps are on the downthrown side.

Oregon Cascade Range, pioneering work by Williams (1933, 1935, 1942, 1944, 1953, 1957), Thayer (1936, 1939), Callaghan and Buddington (1938), Chaney (1938), and Peck and others (1964) is the foundation for all later studies. Papers by Taylor (1967; 1968; 1973a,b; 1978; 1980; 1981) are important sources on the central High Cascades and Deschutes Basin. Theses by Sutton (1974) on Mount Jefferson and Davie (1980) on Three Fingered Jack include large-scale geologic maps of these important High Cascade cones. Williams' (1935, 1957) and Higgins' (1973) data for Newberry caldera have been recently supplemented by detailed mapping of the volcano by MacLeod (1978a,b), MacLeod and Sherrod (1979), and MacLeod and others (1982).

Geologic map coverage in the Western Cascades is concentrated in the northern part of the range. Anderson's (1978) map of the upper Clackamas River area, White's (1980a,c) work in the Battle Ax and Breitenbush quadrangles, Dyhrman's (1975) work in the Bagby Hot Springs area, Clayton's (1976) map in the Breitenbush Hot Springs area, and Rollins' (1976) and Thayer's (1936, 1939) maps in the North Santiam drainage are the best data at relatively large scales available in

the north-central Western Cascades. Pungrassami (1970) also mapped a small area in the western Detroit Reservoir area. Hammond and others' (1980, 1982) map of the north-central Western Cascades is the best available compilation. The earlier compilations of Wells and Peck (1961) and Peck and others (1964) are more comprehensive but not as detailed as the above maps and lack the age control provided by recent K-Ar studies.

Geologic work in Western Cascade areas south of the North Santiam River has been done mainly by graduate students interested primarily in economic geology, and none of their theses has focused on local volcanic stratigraphy. Recent volcanic stratigraphic theses by Avramenko (1981) and Flaherty (1981) have contributed greatly to knowledge of the structural boundary between the High Cascade and Western Cascade provinces. Both these theses and earlier work by Thayer (1939), Williams (1957), Barnes (1978), Taylor (1978, 1980), Brown and others (1980a), Hammond and others (1980), and White (1980a,c) have helped define the location of the margins of possible central High Cascade axial grabens hypothesized by Allen (1966). Maynard's (1974) work at Lake of the Woods, Naslund's (1977) map of the southernmost High Cascades, and Wells' (1956) map of the Medford quadrangle are among the few large-scale maps of volcanic rocks in the southern Cascades.

There is a great need to update the small-scale compilation maps of Wells and Peck (1961) and Peck and others (1964). New maps in preparation by George W. Walker, Norman S. MacLeod, David R. Sherrod, and James G. Smith of the U.S. Geological Survey (USGS) are providing the needed update (e.g., MacLeod and others, 1982; Smith and others, 1982).

McBirney and others (1974), White and McBirney (1978), and White (1980a,c) have summarized chemical, isotopic, and radiometric-age data on central Cascade rocks. Their syntheses indicate that the central part of the Oregon Cascade Range has been the site of intense episodic volcanism since the Oligocene. They have defined several episodes of chemically distinct magmatism which occurred synchronously along the length of the Oregon Cascades. Many aspects of their model have been confirmed by Hammond (1979), Hammond and others (1980, 1982), Avramenko (1981), Flaherty (1981), and data of this paper. There are, however, differences between our conclusions and interpretations and those of previous workers, primarily because of the larger geographic coverage of new maps, new chemical data, and particularly, new K-Ar dates.

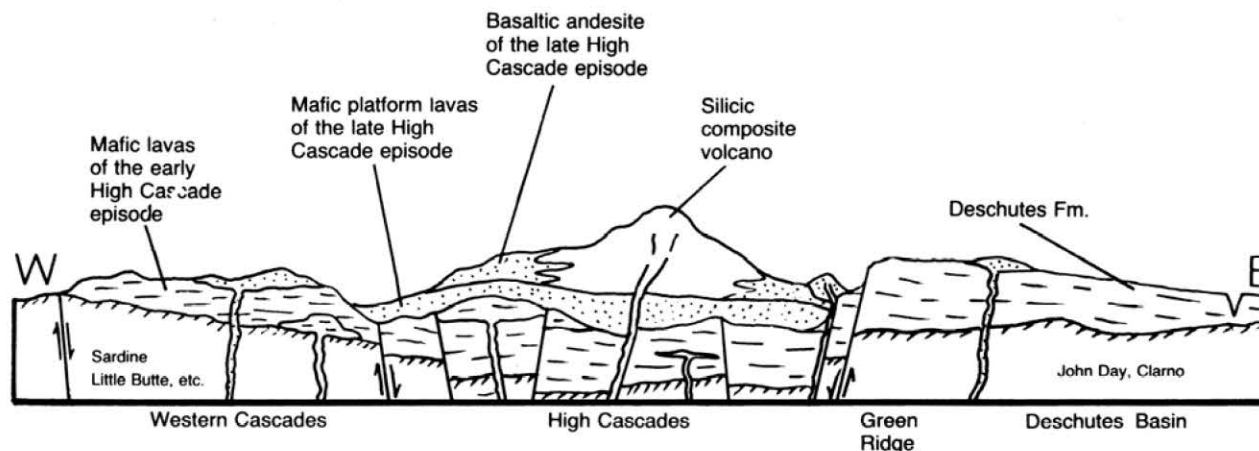


Figure 2.2 Diagrammatic cross section of the central Cascades of Oregon (modified from Taylor, 1980).



## GENERAL GEOLOGY OF THE CASCADES<sup>2.1</sup>

The central Oregon Cascade Range is separable into two physiographic provinces: (1) the Western Cascade Range—a deeply dissected, uplifted block of Miocene and older tuffs and lavas, and (2) the High Cascade Range—a relatively undissected pile of chiefly post-Miocene volcanic rocks (Figure 2.1). Whereas great thicknesses of volcanic rock were accumulating in the area during Oligocene to Miocene time, the Cascade Range was not high enough until the Pliocene to deplete the prevailing westerly winds of their moisture and thereby to create semiarid conditions in eastern Oregon (Chaney, 1938; Williams, 1942). In the early Pliocene (5 to 4 m.y. B.P.), rapid uplift and erosion of the central Western Cascades relative to the area now occupied by the High Cascades created an elevated mountain range in the western part of the province, thereby causing an effective rain shadow (e.g., Chaney, 1938; Williams, 1942, 1953; Taylor, 1980; Flaherty, 1981). Deep valleys were rapidly cut into the elevated western part of the range, and by about 4 to 3 m.y. B.P., most of the relief and the drainage patterns which characterize the present-day Western Cascade physiographic province were well established (e.g., Thayer, 1936, 1939; Williams, 1942, 1953; Flaherty, 1981). Most of the present relief on the High Cascade Range did not exist until the Quaternary, when the majority of the High Cascade composite cones were built on a platform of voluminous mafic Pliocene lavas (e.g., Williams, 1953; Taylor, 1980).

These changes in the physiography of the central Cascades were accompanied by changes in the style of tectonic deformation and the overall composition of the volcanic rocks. During latest Eocene to earliest Miocene time, voluminous silicic ash flows and lesser amounts of black tholeiitic lava and calc-alkaline andesite, dacite, and rhyolite covered all of the area now occupied by the Western Cascades (e.g., Callaghan, 1933; Thayer, 1937, 1939; Peck and others, 1964; White, 1980a,c). At about the same time, similar but more alkaline lavas and tuffs were erupted from the area just east of the High Cascade Range (e.g., see descriptions of the western facies of the John Day Formation by Robinson and Brem, 1981). During the middle Miocene, calc-alkaline andesite, basaltic andesite, and quartz-normative basalt flows were erupted (Thayer, 1936, 1939; Williams, 1953; Peck and others, 1964; Hammond, 1979; Hammond and others, 1980). Toward the end of the Miocene and beginning of the Pliocene, between about 9 to 4 m.y. B.P., eruption of olivine-normative basalt, basaltic andesite, and subordinate andesite and dacite from vents east of many of the earlier Cascade vents began. In the latter part of this episode, basaltic andesite to dacitic volcanism became more common. When the volcanism became increasingly mafic, about 9 m.y. B.P., the local minor folding which characterized the middle Miocene north-central Oregon Cascades was replaced by normal faulting along north to northwest trends, and numerous northwest-trending dikes were injected (e.g., Hammond and others, 1980; Avramenko, 1981; Priest and Woller, Chapters 3 and 4).

Uplift of the Western Cascade Range in early Pliocene time was accompanied by additional north- to northwest-trending normal faulting, especially at the present Western Cascade-High Cascade physiographic boundary. Major north-south faults form the eastern boundary of the uplifted Western Cascade block in the McKenzie River-Horse Creek area (Taylor, 1980; Flaherty, 1981; Avramenko, 1981) and in the Waldo Lake area (Chapter 6).

<sup>2.1</sup> See discussion of nomenclature in section on petrochemistry later in this chapter for a discussion of rock classification used here.

Lineaments in the topography (e.g., Allen, 1966) and regional gravity anomalies (Couch and others, 1982a,b) suggest that similar faults bound the Western Cascade Range in other localities as well. The uplift, faulting, and development of most of the resulting erosional relief on the McKenzie River-Horse Creek escarpment occurred over a very short interval between about 5 and 3.4 m.y. B.P., according to Flaherty's (1981) data. Taylor (1980) concluded that most of the faulting on the east-facing McKenzie River escarpment and west-facing Green Ridge escarpment (Figure 2.1) probably occurred between 5 and 4 m.y. B.P. He suggested that these faults bound a downfaulted block of the High Cascade province.

This major faulting event in the early Pliocene was followed by voluminous eruptions of basalt and basaltic andesite in the High Cascade Range. Highly fluid diktytaxitic basalt flows which dominated the earliest eruptions frequently poured into the Western Cascade drainages, whereas the more silicic lavas were constrained by their higher viscosity to the low shieldlike platform that was developing on the present site of the High Cascade Range (e.g., Taylor, 1980). By Quaternary time, basaltic andesite composite cones were developing as the result of explosive volcanic activity along the central and western parts of the High Cascade province at the same time that effusive eruptions of basalt and basaltic andesite were continuing on the platform (Williams, 1953; Taylor, 1980). Intermediate to silicic composite volcanoes were built in the latter part of the Quaternary at Mount Hood, Mount Jefferson, Mount Bachelor, South Sister, and Mount Mazama, but basaltic eruptions continued in the surrounding platform (e.g., Williams, 1953; Taylor, 1980). The youngest eruptions in the High Cascade Range have been chiefly dacite to rhyodacite (e.g., South Sister, Mount Hood, and Mount Mazama) and basalt to basaltic andesite (the Belknap Crater and Sand Mountain flows).

## VOLCANIC STRATIGRAPHY

### Introduction

A combination of time- and rock-stratigraphic units has traditionally been used for regional stratigraphy in the Cascade Range (e.g., Wells and Peck, 1961; Peck and others, 1964). Because of regional changes in the composition of volcanic rocks along the Cascades through time, certain intervals of geologic time are characterized by distinctive rock-stratigraphic units. Ages of volcanic rock have been judged in the past by both radiometric dates and relative degree of alteration, as well as by the tacit assumption that distinctive compositional types of volcanic rock characterize certain geologic times. Radiometric and compositional data from the present study suggest that the latter assumption is often, though not invariably, justified.

Figure 2.3 summarizes regional and local stratigraphic units defined by various workers in the north-central Cascades and compares them to an informal system of time categories used for this paper (Tables 2.1 and 2.2). The system used here provides a basis for discussion in this paper and is not intended to be used as formal usage or as a replacement for existing rock-stratigraphic nomenclature. It is based on breaks in time which, from mapping in the central Cascades, appear to correspond to broad changes in the overall composition of volcanic sequences. This system avoids some of the confusion generated by previous usage of regional rock-stratigraphic systems which sought to correlate particular type sections over unrealistically large distances along the Cascades. Terms such as "Sardine Formation," whose meaning, in terms of the age of the rocks concerned, is still debated (e.g.,

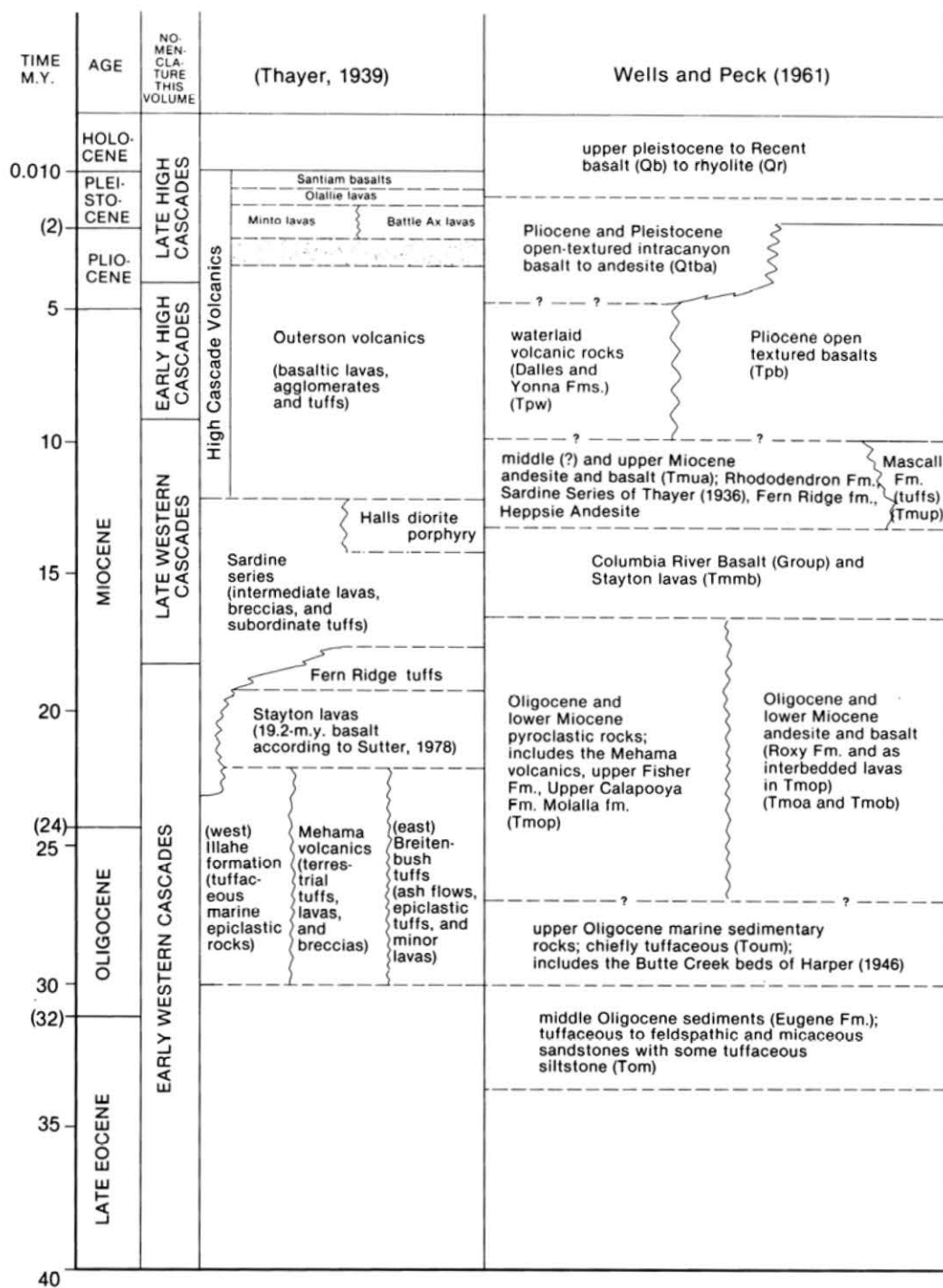


Figure 2.3 (both pages). Regional stratigraphic units used by various workers in the Cascades, compared to time categories of distinctive volcanism utilized in this paper. Time limits of stratigraphic units were estimated. Geologic time boundaries are those of Armentrout (1981).

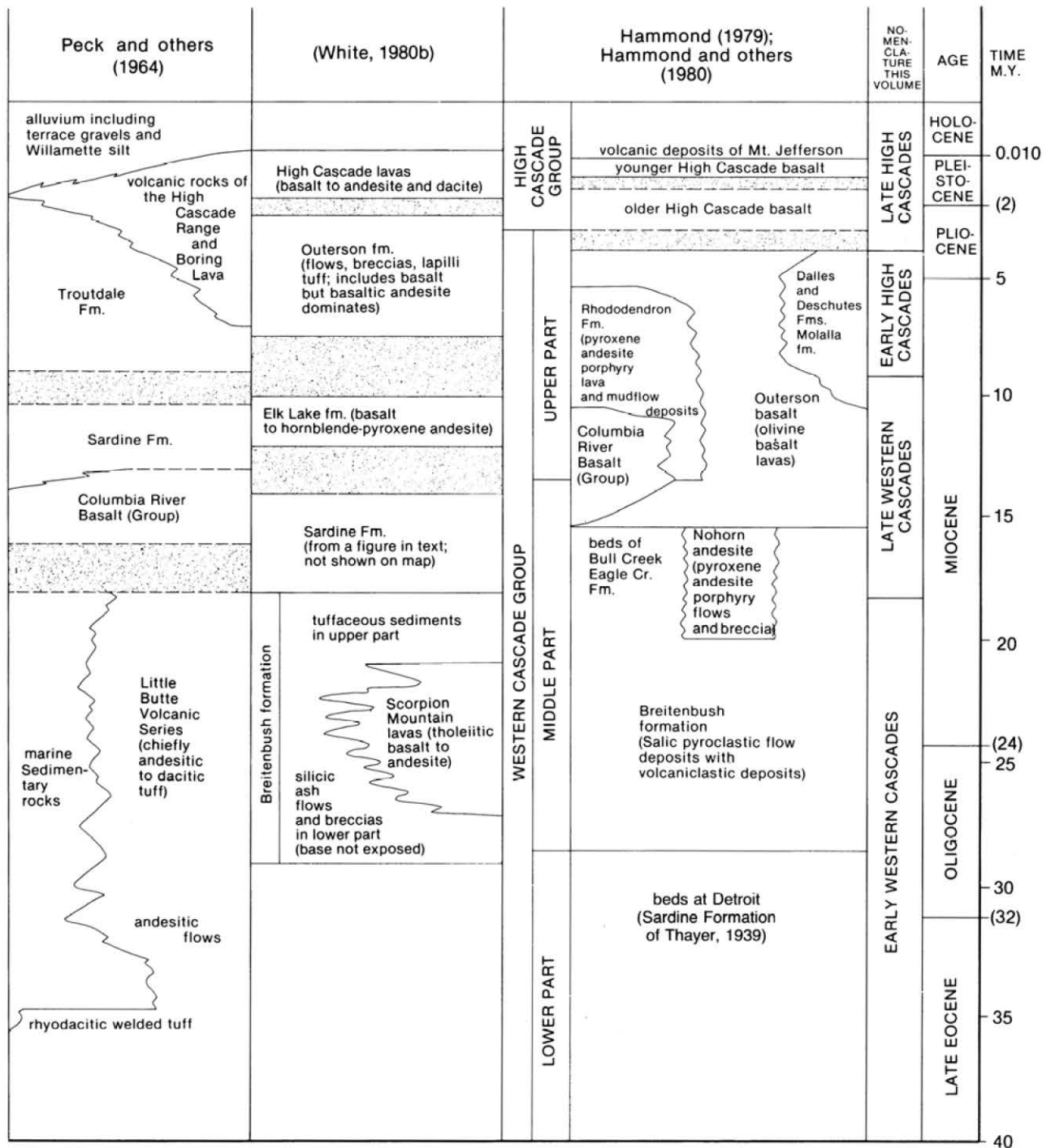




Table 2.1. *Parameters that distinguish volcanic rocks erupted during various central Oregon Cascade volcanic episodes. Andesites, dacites, and tuffs with similar mineralogy and texture occur in all units. Volcanic rocks are not listed if not one of the dominant rock types. Cpx=clinopyroxene; opx=orthopyroxene; px=pyroxene; pl=plagioclase; qtz=quartz; ol=olivine; comp=composition. See nomenclature part of petrochemistry section for rock classification method*

Parameter	Early Western Cascade episode	Late Western Cascade episode	Early High Cascade episode	Late High Cascade episode
Age ( $\pm 1$ m.y.)	(40 to 18 m.y. B.P.)	(18 to 9 m.y. B.P.)	(9 to 4 m.y. B.P.)	(4 to 0 m.y. B.P.)
Characteristic rocks	Dacitic to rhyodacitic laharc, epiclastic, and ash-flow tuff and lava; smaller volumes of Fe-rich, highly qtz-normative, mafic lavas	Two-px andesite + basaltic andesite + dacitic tuff; common autoclastic and epiclastic rocks; basalts are qtz-normative with low Fe	Ol-normative basalt + basaltic andesite; basalts have moderately high Fe and alkalis	Iron-rich ol-normative basalt + basaltic andesite; basalts have moderately high Fe and alkalis.
Distribution (in Western and High Cascades)	Lower valleys of the Western Cascades	Western Cascade ridges and upper valleys	Western Cascade ridge tops; sides of deepest High Cascade valleys	In High Cascade province and present topographic lows outside province.
Degree of alteration	Moderate to heavy in tuffs; light to moderate in tholeiitic lavas	Light to moderate in tuffs and andesites; less in basalts	Light to none	Generally none.
Dominant alteration (excludes local contact metamorphism)	Laumontite-grade zeolite facies to low-grade propylitic alteration	Laumontite-grade zeolite facies; commonly affects pl and glass	Some alteration of opx + ol to saponite; pl is fresh	Deuteric only, unless at volcanic vent.
Main area of eruption	Broad area of Western Cascades	Broad area of Western Cascade Range	In and on margins of High Cascades	Axis of High Cascades.
Dominant texture of lavas	Compact, aphyric, black tholeiitic lavas and glassy flow-banded rhyolite and rhyodacite	Highly phyrlic to megacrystic andesites with nearly aphyric compact mafic lavas	Slightly phyrlic, compact, gray to black, with some moderately diktytaxitic lavas	Slightly phyrlic, highly diktytaxitic gray to black basalt; compact to slightly diktytaxitic basaltic andesite.
Dominant phenocrysts	Rhyodacite and dacite = pl + opx $\pm$ qtz; mafic lavas = rare pl + altered ol or cpx	Dacite = opx + hornblende + pl; andesite = pl + opx + cpx; basaltic andesite = pl + cpx + ol	Basaltic andesite = ol + cpx $\pm$ opx; basalt = ol	Basaltic andesite = ol + cpx; basalt = ol.
Dominant groundmass phases	Rhyodacite = altered glass + pl + qtz; mafic lavas = pilotaxitic to felty pl + cpx + Fe-Ti oxides	Dacite = hyalopilitic with opx + pl + glass; andesite = pilotaxitic to felty pl + opx + cpx; basaltic andesite = felty to pilotaxitic pl + cpx $\pm$ Fe-Ti oxide $\pm$ ol	Basaltic andesite = pilotaxitic to felty pl + cpx + minor Fe-Ti oxide; basalt = felty to diktytaxitic pl with subophitic brownish cpx + Fe-Ti oxide $\pm$ ol	Basaltic andesite = pilotaxitic to felty pl + cpx + minor Fe-Ti oxide; basalt = coarsely diktytaxitic pl with subophitic to ophitic purplish-brown to brownish cpx + Fe-Ti oxide $\pm$ ol.
Chemical character	Calc-alkaline and tholeiitic; both types are qtz-normative	Strongly calc-alkaline	Calc-alkaline to slightly alkaline	Calc-alkaline to slightly alkaline.
Most distinctive characteristic	Abundant tuffaceous volcanoclastic rocks and silicic lavas. Mafic lavas are very Fe rich and highly qtz-normative	Light to moderately altered calc-alkaline lavas of intermediate composition; basalts generally qtz-normative and low in Fe	Distribution; occurrence of some basalts with diktytaxitic texture; basalts generally ol-normative with moderately high Fe and alkalis	Distribution; common highly diktytaxitic basalts; slightly alkaline, Fe-rich comp; basalts generally ol-normative with moderately high Fe and alkalis.

Thayer, 1939; Peck and others, 1964; Hammond and others, 1980; White, 1980a,c), have also been avoided in this paper. The same is also true of the name "Ooterson formation." Data of Priest and Woller (Chapter 3) show that the rocks at Ooterson Mountain are largely older than about 6.3 m.y., whereas earlier data suggested that the Ooterson rocks were between about 4 and 6 m.y. old (e.g., McBirney and others, 1974; White, 1980a,c).

This system also simplifies comparison of widely separated stratigraphic sequences in regional studies. It is particularly useful on compositional diagrams for comparison of units from the major volcanic episodes.

## Introductory summary of the regional time-stratigraphic system

### "Western Cascade" - "High Cascade" division:

The two names "High Cascades" and "Western Cascades" were chosen to conform with previous usage (e.g., Peck and others, 1964; Hammond and others, 1980). Mapping completed for this study and previous work (e.g., Peck and others, 1964; White and McBirney, 1978) indicate that vents in the High Cascade physiographic province and areas immediately adjacent to the province (Figure 2.2) are the sources for most volcanic rocks of latest Miocene and younger age. Relative to the High Cascade Province, more silicic volcanic rocks of

**Table 2.2.** *Informal nomenclature utilized in this paper for compositionally distinctive regional episodes of volcanism in the central Oregon Cascade Range. The system is for purposes of discussion only and should not be considered a revision of rock-stratigraphic nomenclature. See nomenclature part of petrochemistry section for rock-classification method*

Volcanic episode ( $\pm 1$ m.y. B.P.)	Volcanic rocks	Correlative rock-stratigraphic units
Late High Cascade (4 to 0 m.y. B.P.)	Chiefly mafic volcanic rocks; some are slightly alkaline high-alumina basalt; commonly highly diktytaxitic in lower part; more silicic in upper part. Includes the High Cascade composite cones. Includes some andesitic, dacitic, and rhyodacitic to rhyolitic tuff and lava	High Cascade lavas (McBirney and others, 1974; White, 1980a); High Cascades group (Hammond, 1979; Hammond and others, 1980); upper part of volcanic rocks of the High Cascades and Boring Lavas (Peck and others, 1964).
Early High Cascade (9 to 4 m.y. B.P.)	Chiefly mafic lavas and some interbedded tuffs; many lavas are slightly alkaline olivine tholeiites with diktytaxitic texture; includes minor alkali basalt and many compact high-alumina basalts and basaltic andesites. Also includes many andesites and some ash-flow and ash-fall tuff. May be largely absent from the southern Cascades (Smith, 1979)	Uppermost part of Outerson volcanics as mapped by Thayer (1939); uppermost part of Outerson formation as mapped by White (1980a); upper part of Outerson basalt (Hammond and others, 1980); lower part of volcanic rocks of the High Cascades and Boring Lavas (Peck and others, 1964); intermediate series of Avramenko (1981) and Flaherty (1981); probably correlative to Deschutes Formation (Hales, 1975; Taylor, 1981).
Late Western Cascade (18 to 9 m.y. B.P.)	Chiefly intermediate volcanic rocks with common interbedded dacitic tuffs; includes voluminous basaltic andesite and highly phyrlic two-pyroxene andesite with less basalt and dacitic tuff. Basalts of this group are generally compact and quartz normative. This sequence may be very thin or absent in much of the southern Cascades (Smith, 1979)	Possibly the uppermost part of the Sardine series (Thayer, 1936, 1939); Sardine Formation (Peck and others, 1964); Sardine Formation and Elk Lake formation (McBirney and others, 1974; White, 1980a,c); Rhododendron Formation (Hammond, 1979; Hammond and others, 1980, 1982); most of lower part of Outerson volcanics as mapped by Thayer (1939); lower part of Outerson basalt (Hammond and others, 1980).
Early Western Cascade (40 to 18 m.y. B.P.)	Chiefly silicic and tholeiitic volcanic rocks. Interbedded rhyodacitic tuffs and iron-rich quartz-normative tholeiitic basalt, tholeiitic basaltic andesite, and icelandite, with minor rhyodacitic, rhyolitic, and dacitic lavas; local abundant clastic interbeds. This unit contains abundant andesitic lavas in southern Cascades	Breitenbush tuffs (Thayer, 1936, 1939); much of the Sardine series of Thayer (1936, 1939); Little Butte Volcanic Series (Peck and others, 1964); Breitenbush formation and beds of Detroit (Hammond, 1979; Hammond and others, 1980, 1982); Breitenbush formation and Scorpion Mountain flows (White, 1980a,c).

Oligocene to middle Miocene age characterize much of the Western Cascade physiographic province. Numerous vents of these older rocks in the Western Cascade Range and the supposed absence of lithologically similar rocks east of the High Cascade Range suggest that the main Oligocene to middle Miocene volcanic axis was in the Western Cascade physiographic province (e.g., Peck and others, 1964; White and McBirney, 1978). There is, however, no evidence that Oligocene to middle Miocene vents are not abundant beneath the cover of High Cascade lavas; some John Day Formation air-fall tuffs east of the High Cascades are inferred to have come from source areas beneath the Cascade Range (Robinson and Brem, 1981) and could have come from the area now occupied by the High Cascades.

Spatial separation of the High Cascade and Western Cascade volcanic rocks has prompted usage of informal terms such as "volcanic rocks of the High Cascade Range" and "volcanic rocks of the Western Cascade Range" (Peck and others, 1964). Other workers have used terms such as "High Cascades" and "Western Cascades series" or "group" (e.g., Hammond and others, 1980; White, 1980c; Avramenko, 1981; Flaherty, 1981). Mapping and numerous K-Ar dates generated for this report (Appendix A) and other recent studies suggest that both the eastward shift or, more likely, a narrow-

ing of the volcanic axis from the Western Cascades to the High Cascades and the change from andesitic to more mafic volcanism occurred between about 10 and 8 m.y. B.P. over large parts of the central Oregon Cascades. A time boundary of 9 m.y. B.P. is a best fit to the current K-Ar data. The two major episodes, Western Cascade and High Cascade, have been further subdivided into "early" and "late" time periods on the basis of radiometric age data and mappable characteristics of the rocks in each age group (Tables 2.1 and 2.2).

The writers chose to use the terms "early" and "late" High Cascades and Western Cascades rather than "upper" and "lower" in order to avoid any possible confusion with previous or future rock stratigraphic nomenclature. It is hoped that by choosing the terms "early" and "late," it will be clear that volcanic episodes rather than rock-stratigraphic groups of formations are being described.

**Early Western Cascade episode:** Rocks of the early Western Cascade episode are mostly silicic lavas and tuffs, with lesser amounts of mafic flows. Peck and others (1964) mapped these rocks as the Little Butte Volcanic Series, correlating them in part to the Little Butte formation of Wells (1956) in the Medford quadrangle. Included in the upper part of this sequence of early Western Cascade age is a distinctive series of silicic, iron-rich lavas mapped by White (1980a,c) as

the Scorpion Mountain lavas. The Scorpion Mountain magma type is probably compositionally unique enough to serve as a mappable unit throughout the central Cascades. It may be that this petrochemical unit and other similar units in younger and older rocks may serve as regional correlation tools when more data are available.

**Late Western Cascade episode:** The uppermost Eocene to lower Miocene rocks of the early Western Cascade episode are overlain by middle Miocene lavas and subordinate dacite tuffs. Rocks deposited during the middle Miocene episode are here informally termed "volcanic rocks of the late Western Cascade episode." These rocks have been mapped as the Sardine Formation (Peck and others, 1964) and the Sardine Formation and overlying Elk Lake formation (White, 1980a,c). Lavas of the late Western Cascade episode are predominately porphyritic two-pyroxene andesite and fine-grained basalt and basaltic andesite, with typical calc-alkaline chemical composition (i.e., low FeO and high CaO, MgO, and alumina). Based on studies discussed later, the time boundary between the two Western Cascade sequences is between about 19.4 and 17 m.y. B.P. A boundary of 18 m.y. B.P. has been arbitrarily picked to separate the early and late Western Cascade episodes.

**Early and late High Cascade episodes:** Volcanic rocks erupted during the High Cascade episode are generally fresh-appearing basaltic rocks, with subordinate amounts of andesite and still smaller amounts of dacite to rhyodacite tuff and lava, all of which were erupted within the last 9.0 m.y. Diktytaxitic textures and slightly alkaline, iron-rich compositions are common in the basalts but not as common in the more silicic rocks. Examples of these basalts are the lavas of Tipsoo Butte (see Chapter 4) of the early High Cascade episode and lavas of the late High Cascade episode occurring at Cupola Rock and Foley Ridge near McKenzie Bridge (Flaherty, 1981). Although there are some lithologic differences, the units of early and late High Cascade age are distinguished in the field primarily by the degree to which their distribution is controlled by current topography. The rocks of the early High Cascade episode either are in topography strongly reversed from the present-day topography or are obviously displaced into lows created by faulting that occurred about 5 to 4 m.y. B.P. These lavas and tuffs of the early High Cascade episode have been called the Outerson formation (e.g., McBirney and others, 1974; White, 1980a,c). Taylor (1980) gave the informal name "Plio-Cascades" to rocks of early High Cascade age where they are present beneath units of late High Cascade age in the High Cascade physiographic province.

In contrast to flows of the early High Cascade episode, the distribution of flows of the late High Cascade episode is clearly controlled by present topography. The lavas of the late High Cascade episode flowed into canyons cut into the Western Cascade Range (e.g., at Foley Ridge) and banked up against several isolated uplifted fault blocks on the east side of the High Cascade province (e.g., at Green Ridge). The relief in the Western Cascade Range and the age of the earliest intracanyon lavas in the bottom of the valleys indicate that uplift produced more than 1 km (0.6 mi) of erosion in the central Western Cascade Range between 5 and 4 m.y. B.P. (e.g., Flaherty, 1981; Priest and Woller, Chapter 4). These drainages hold numerous basaltic flows of the late High Cascade episode. The late High Cascade episode is informally defined as the period between 4 and 0 m.y. B.P. and can be most easily recognized on the margins of the High Cascade physiographic province where the early Pliocene erosion created a steeply unconformable contact.

Rocks deposited during both the early and late High Cascade episodes have been recognized as a compositionally

related group by earlier workers. The rocks were grouped together as the volcanic rocks of the High Cascades by Thayer (1936, 1939) and Peck and others (1964) after terminology of Callaghan (1933). The two units also correspond to the High Cascade series of Williams (1949), as used by White (1980c). Data of this study suggest that the two units are essentially one compositional type. Because of this close compositional similarity, where the distinction between early and late High Cascade volcanism is not marked by mappable characteristics such as the previously mentioned unconformity, K-Ar dating may be necessary to distinguish between the two units. In such instances, the distinction may not be useful.

In the northern Oregon Cascade Range around Mount Hood, uplift adjacent to downfaulted areas of the High Cascade axis occurred after 3.0 m.y. B.P. (Priest, 1982). Therefore, faulted, high-standing rocks include 3- to 4-m.y.-old units of the late High Cascade episode. Reconnaissance mapping by Smith (1979) in the southern Oregon Cascades suggests that there is no obvious distinction between rocks of the early High Cascade and the late Western Cascade episodes, and they are mapped there as one unit. The nomenclature presented here is thus useful mainly in the central Oregon Cascades, particularly in the Western Cascade province where these writers have mapped, and may not be practical in other parts of the Cascades. We anticipate that this informal nomenclature (Table 2.2) will be replaced by a workable rock-stratigraphic system as detailed map coverage becomes available.

The following sections give more detailed discussions of specific evidence of the four proposed episodes in areas of the central Oregon Cascade Range with relatively good stratigraphic and radiometric-age control. Discussions under each episode proceed from north to south, beginning in the Breitenbush Hot Springs area. This same north-to-south format is used in tables, figures, and plates, where possible.

### **Volcanic rocks of the early Western Cascade episode (40-18 m.y. B.P.)**

**Introduction:** Rocks of the early Western Cascade episode are chiefly ash-flow tuffs, debris flows, lava flows, and epiclastic mudstone and sandstone, with some distinctive siliceous, iron-rich tholeiitic lavas interbedded in the upper part. In the regional mapping of Peck and others (1964), these rocks were generally named the Little Butte Volcanic Series, although the tholeiitic lavas were sometimes mistaken for the Columbia River Basalt Group (e.g., see discussions by White, 1980a,c; Lux, 1981, 1982).

**Breitenbush area:** In the Breitenbush Hot Springs area, the sequence is represented by moderately altered ash-flow tuff and interbedded epiclastic rocks called the Breitenbush tuff or Breitenbush formation (e.g., Thayer, 1935, 1939; Hammond, 1979; Hammond and others, 1980; White, 1980a,c). Similar rocks with some interbedded lavas crop out at Sardine Mountain and were mapped as the Sardine series by Thayer (1936, 1939) and as the beds of Detroit by Hammond and others (1980, 1982).<sup>2.2</sup> The Breitenbush rocks are overlain by a series of black tholeiitic basaltic andesite, icelandite, and iron-rich dacite flows called Scorpion Mountain lavas by White (1980a,c). No radiometric dates which the writers consider reliable are available for the altered pyroclastic rocks, but dates of 27 to 19 m.y. B.P. have been reported by White (1980a,c) for the Scorpion Mountain magma type in various localities in the central Western Cascades.

**Belknap-Foley area:** In the Belknap Hot Springs-Cougar Reservoir area, moderately altered ash-flow tuffs, laharic tuffs, epiclastic rocks, and subordinate rhyodacitic to dacitic

<sup>2.2</sup> See next section (p. 11) for details on Sardine Mountain sequence.



lavas make up the section of early Western Cascade age. These rocks are called the tuffs of Cougar Reservoir by Priest and Woller (Chapter 4) and are intruded by and overlain on a high-relief erosional surface by volcanic rocks of the late Western Cascade volcanic episode. These rocks of the late Western Cascade episode have an oldest K-Ar date of 16.3 m.y. B.P. Immediately west of the Cougar Reservoir area, the older tuffs are intruded by the Nimrod stock, dated by Sutter (1978) at  $16.3 \pm 0.3$  m.y. B.P. (recalculated by Fiebelkorn and others, 1982).

**Lookout Point area:** Rocks of the early Western Cascade episode crop out also in the Lookout Point Reservoir area, where they have been mapped in detail by Woller and Priest (Chapter 5). Ash-flow tuffs, laharic tuffs, epiclastic rocks, and subordinate silicic lavas are overlain by and interbedded with a series of tholeiitic lavas similar to the Scorpion Mountain lavas of White (1980a,c). The tholeiitic lavas (the lavas of Black Canyon) have minimum K-Ar dates of about 22 m.y. B.P. The lavas of Black Canyon are in turn overlain by lavas of the late Western Cascade episode whose oldest K-Ar date is  $15.9 \pm 7.6$  m.y. B.P. A slightly altered basaltic andesite flow in the tuffs underlying the Black Canyon rocks has a minimum age of  $24.7 \pm 2.0$  m.y.

**Hills Creek Dam area:** Rhyolitic lavas occur at the top of the section of early Western Cascade age in the Hills Creek Dam area, immediately south of the Lookout Point area (e.g., Brown and others, 1980b). A minimum age of  $17.3 \pm 0.7$  m.y., which was obtained on a plagioclase separate from a moderately altered rhyolite sample (sample OM-520 of Brown and others, 1980b), probably reflects resetting of the K-Ar age by hydrothermal activity of the late Western Cascade episode. K-Ar ages of  $21.3 \pm 1.0$  m.y. obtained on dacite from Stone Mountain and  $18.7 \pm 0.9$  m.y. obtained on basalt near Groundhog Mountain (see Brown and others, 1980b) in the Hills Creek Dam area are probably better approximations of the ages of the uppermost rocks of the section of early Western Cascade age there.

**Conclusion:** Smith and others (1980, 1982) traced a biotite-bearing ash-flow tuff near the base of the section of early Western Cascade age from the Rogue River to the North Umpqua River. They obtained a K-Ar date of 34.9 m.y. B.P. Lux (1982) considered the base of the Little Butte Volcanic Series to be about 40 m.y. B.P. and listed one date of  $41.5 \pm 0.8$  m.y. B.P. Until other data become available, 40 m.y. is here considered to be the older age limit of the sequence of early Western Cascade age in the central Oregon Cascade Range. The younger age limit is arbitrarily placed at 18 m.y., about 1 m.y. younger than the youngest age obtained for rocks of the Scorpion Mountain magma type and about 1 m.y. older than the oldest dated rocks which probably overlie rocks of the Scorpion Mountain type.

### Volcanic rocks of the late Western Cascade episode (18-9 m.y. B.P.)

**Introduction:** Rocks of the late Western Cascade episode are chiefly calc-alkaline lavas and debris flows of intermediate composition, with subordinate dacitic ash-flow and ash-fall tuff. Basalt and basaltic andesite are locally abundant, but these mafic lavas rarely reach compositions as iron-rich as the overlying High Cascade lavas or underlying tholeiitic lavas of the early Western Cascade episode. Peck and others (1964) mapped these rocks as the Sardine series after terminology of Thayer (1936, 1939).

**Breitenbush area:** Sardine Mountain in the Breitenbush Hot Springs area is the type locality of the Sardine series of Thayer (1936, 1939). Predominance of andesitic lavas over tuffaceous rocks in this sequence was the feature used by

Thayer (1936, 1939) to distinguish these lavas of supposedly late Western Cascade age from underlying rocks of early Western Cascade age (Breitenbush tuff). A disagreement has arisen among workers in the area concerning the relative positions of the Sardine series of Thayer (1939) and the Breitenbush tuff, which are in fault contact on the western limb of the Breitenbush anticline. Disagreement on the direction of displacement on this fault and the absence of detailed mapping at Sardine Mountain have caused confusion about these units. White (1980c) showed the rocks at Sardine Mountain as younger than the Breitenbush tuff, whereas Hammond and others (1980) interpreted the lavas as older than the tuff.

In an attempt to resolve part of the problem, one of us (Priest) traversed the Sardine Mountain sequence and noted that most of the sequence there consists of altered volcanoclastic tuffs identical to sequences of early Western Cascade age in other areas. An altered basaltic andesite plug and flow cap Sardine Mountain, and fine-grained andesite flows cap the adjoining Hall Ridge. A few coarsely glomeroporphyritic two-pyroxene andesite flows of more altered aspect occur immediately below the capping flows in several places. Closely spaced dikes similar to both the fine-grained and glomeroporphyritic lavas account for most of the "lava" outcrops deeper in the Sardine section. The thin capping lavas and the dike swarm resemble rocks of late Western Cascade age in adjacent areas such as Outerson Mountain (see Chapter 3). All thin sections of lavas in the upper part of the section revealed some degree of low-grade alteration. Nevertheless, Sutter (1978) obtained K-Ar dates for the andesites capping Hall Ridge ( $15.9 \pm 0.2$  m.y. B.P. [1.595 percent K, 17.5 percent radiogenic  $\text{Ar}^{40}$ ];  $16.4 \pm 0.2$  m.y. B.P. [1.009 percent K, 17.8 percent radiogenic  $\text{Ar}^{40}$ ]) and for an andesite interbedded in the uppermost part of the sequence on the east side of Sardine Mountain ( $17.2 \pm 0.2$  m.y. B.P. [1.306 percent K, 28.3 percent radiogenic  $\text{Ar}^{40}$ ]) (data recalculated by Fiebelkorn and others, 1982). In view of the probable slight alteration in these samples, the K-Ar dates should probably be considered minimum ages. The top 50 to 100 m (165 to 330 ft) of the sequence at Sardine Mountain is thus probably the basal portion of the section of late Western Cascade age, but the alteration in the area casts some doubt on the reliability of the radiometric ages. The rest of the sequence is composed of rocks of the early Western Cascade episode.

Uppermost lavas of the section of late Western Cascade age in the Breitenbush area have yielded K-Ar dates as young as  $10.6 \pm 1.20$  m.y. B.P. (Rhododendron Formation at Boulder Ridge; sample 13 from Hammond and others, 1980; recalculated by Fiebelkorn and others, 1982), but this sample has low radiogenic  $\text{Ar}^{40}$  (6.5 percent) and K (0.535 percent). The next youngest date in a bedded unit of late Western Cascade age is on Sutter's (1978) and White's (1980a,c) Elk Lake lavas. This andesite sample is  $11.2 \pm 0.8$  m.y. old (1.494 percent K, 16.2 percent radiogenic  $\text{Ar}^{40}$ , recalculated by Fiebelkorn and others, 1982). The stratigraphic position of this sample relative to the rest of the section of late Western Cascade age is, however, not well constrained, as it occurs in an isolated outcrop lying directly on Breitenbush tuff (White, 1980c, sample DMS-40). The top of the section of late Western Cascade age at Outerson Mountain is a sequence of basaltic andesites, andesites, and ash-flow tuffs which forms a highland of late Miocene age (Chapter 3). The highland is overlain by a basaltic andesite flow of the early High Cascade episode dated at  $6.3 \pm 0.2$  m.y. B.P. (Chapter 3). The late Western Cascade episode in the Breitenbush area thus began about 17 m.y. B.P. and ended sometime between 11.2 and 6.3 m.y. B.P.

**Belknap-Foley area:** The Belknap-Foley area (Chapter 4) has a section of late Western Cascade age dominated by highly phyrlic two-pyroxene andesite, with subordinate basal-

tic andesite lava and dacite ash-fall and ash-flow tuff. The oldest radiometric date is 16.3 m.y. B.P. on the glassy plug which forms the abutments of Cougar Dam; the youngest reliable date is  $8.8 \pm 0.3$  m.y. B.P. at the top of the section at Lookout Ridge. The sequence is capped by iron-rich diktytaxitic basalts on the east side of Cougar Reservoir (the lavas of Tipsoo Butte) and at Lookout Ridge. Basal flows of these capping lavas have dates of  $8.34 \pm 0.36$  m.y. B.P. at Lookout Ridge and  $7.80 \pm 0.77$  m.y. B.P. at Cougar Reservoir. Flaherty (1981) noted a small unconformity in the sequence of late Western Cascade age below the uppermost 9.3- to 8.9-m.y. B.P. dacite flows in the Belknap Hot Springs area, although no similar unconformity was noted by Priest and Woller (Chapter 4) to the west at Cougar Reservoir. There is also no evidence of a widespread unconformity between 15 and 11 m.y. B.P. that was noted by McBirney and others (1974) between their Sardine and Elk Lake formations. A large section of lava and tuff at Cougar Reservoir has yielded dates between 15 and 11 m.y. B.P. (Chapter 4).

**Lookout Point area:** A sequence of two-pyroxene andesite lavas occurring in the Lookout Point area have top and bottom flows dated at  $8.3 \pm 5.5$  m.y. B.P. and  $15.9 \pm 7.6$  m.y. B.P., respectively (Chapter 5). At Patterson Mountain, this section of late Western Cascade age is capped by a basaltic flow of the early High Cascade episode dated at  $5.81 \pm 0.30$  m.y. B.P.

**Waldo Lake-Swift Creek area:** In the Waldo Lake-Swift Creek area, the sequence of late Western Cascade age is composed of large volumes of both two-pyroxene andesite and basalt to basaltic andesite (Chapter 6). Although the base of the section is not dated, the oldest reliable date from the sequence is about  $17.0 \pm 0.19$  m.y. B.P., and the youngest dated flow is about  $13.1 \pm 0.6$  m.y. old. These flows are capped by basal basalts of the early High Cascade episode that are K-Ar dated at  $5.56 \pm 0.34$  m.y. B.P. (Chapter 6).

**Conclusion:** Substantial time gaps of 3 to 8 m.y. occur between dated rocks of the early High Cascade and the late Western Cascade episodes in the Breitenbush, Lookout Point, and Swift Creek areas, but no apparent time gap exists in the Belknap Hot Springs area. Whereas local areas have experienced episodic volcanism, it is likely that the central Cascade region as a whole had relatively continuous volcanism during late Western Cascade and early High Cascade time. A large number of volcanic centers of the late Western Cascade episode, however, occur several kilometers west of volcanic centers of the early High Cascade episode (Peck and others, 1964; Priest and Woller, Chapter 4). Both an eastward shift or narrowing of volcanism and a switch to a more mafic composition appear to have occurred about 10 to 8 m.y. B.P. A good compromise with the available dates is 9 m.y. B.P. for the end of the late Western Cascade episode. The beginning of the late Western Cascade episode has been arbitrarily set at 18 m.y. B.P., as previously explained.

## Volcanic rocks of the early High Cascade episode (9-4 m.y. B.P.)

**Introduction:** Volcanic centers of the early High Cascade episode produced voluminous basalts and basaltic andesites. Rocks more silica-rich than basaltic andesite are much less abundant than in the underlying sequence of late Western Cascade age. The eruptions of lavas of the early High Cascade episode occurred from a large area which probably lay mostly within the High Cascade physiographic province. White and McBirney (1978) estimated that volcanic rocks of this episode were erupted from an area about twice as broad as the High Cascade physiographic province. Some vents for these rocks have been recognized a few kilometers west of the

High Cascade province (e.g., Hammond, 1979; Hammond and others, 1980, 1982; White, 1980a,c), and compositionally and temporally similar rocks of the Deschutes Formation were erupted from vents along the central High Cascade Range and its eastern margin (e.g., Hales, 1975; Taylor, 1973b, 1981). In the Western Cascade physiographic province, rocks of the early High Cascade episode are the relatively unaltered mafic to intermediate lavas which cap the highest ridges. These rocks are the extensive ridge-capping units labeled "QTba," "QTp," "Tpb," and "QTV" on various regional compilation maps of the Western Cascade Range (e.g., Wells and Peck, 1961; Peck and others, 1964).

**Breitenbush area:** In the Breitenbush Hot Springs area, the early High Cascade episode is represented chiefly by fresh basalt, basaltic andesite, and subordinate andesite flows which occur along ridge tops in the steep Western Cascade terrain. A few of the basalt flows have a slightly alkaline composition with olivine in the groundmass. Many of the basalts have subophitic to ophitic clinopyroxene in the groundmass (e.g., White, 1980a; Chapter 3). Examples of these alkaline basalts were described by White (1980a, his Figure 8, p. 12) northwest of Breitenbush Hot Springs. The lavas of the early High Cascade episode described by Priest and Woller (Chapter 3) in the Outerson Mountain-Devils Creek area are olivine-normative, somewhat diktytaxitic basalts which give way upward to basaltic andesite. Dacite and andesite intrusions cut the uppermost lavas of the early High Cascade episode in the area (Chapter 3). The oldest flow of the early High Cascade episode so far reliably dated in this area comes from the upper part of the sequence of early High Cascade age where it laps onto a highland of late Miocene age at Outerson Mountain. A single flow of the early High Cascade episode dated at  $6.3 \pm 0.2$  m.y. B.P. caps the sequence of late Western Cascade age at Outerson Mountain (Priest and Woller, Chapter 3). The youngest date from rocks of the early High Cascade episode in this area is 3.7 m.y. B.P. and was obtained from a lava at Breitenbush Mountain listed as Outerson formation by Sutter (1978). The oldest date of a rock that appears to correspond to lavas of the late High Cascade episode is  $4.3 \pm 0.3$  m.y. B.P. (Hammond and others, 1980). Both dates are recalculated by Fiebelkorn and others (1982) using newly established decay constants.

**Belknap-Foley area:** In the Belknap-Foley area (see Priest and Woller, Chapter 4; Flaherty, 1981), volcanic rocks of the early High Cascade episode are iron-rich basalts and basaltic andesites, with subordinate andesite and minor tuff, which occur at the highest elevations on some Western Cascade ridges. Diktytaxitic texture is common in basalts at the base of the section of early High Cascade age at Cougar Reservoir (lavas of Tipsoo Butte, Chapter 4), although the texture is not as coarsely developed as in basal lavas of the late High Cascade episode which occur in the McKenzie River drainage at Foley Ridge and Cupola Rock (see descriptions by Flaherty, 1981). Thin sections of some diktytaxitic samples of the lavas of Tipsoo Butte have subophitic clinopyroxene which is brownish in plain light. The brownish hue and high  $\text{TiO}_2$  in whole-rock analyses suggest that the clinopyroxene is titaniferous. Similar titaniferous clinopyroxene was noted in slightly alkaline lavas of the late High Cascade episode at Cupola Rock (Flaherty, 1981). A basal flow dated at  $7.80 \pm 0.77$  m.y. B.P. at Tipsoo Butte is overlain by a flow dated at  $9.4 \pm 0.4$  m.y. B.P., and a date of  $10.2 \pm 2.0$  m.y. B.P. was obtained at English Mountain on a stratigraphically higher flow (Appendix A). It may be that the mode of eruption or some other factor causes these volatile-rich diktytaxitic basalts to be incompletely degassed of radiogenic argon during cooling. The bulk of K-Ar data obtained by both Flaherty

(1981) and this study suggests that a K-Ar date of  $8.34 \pm 0.36$  m.y. B.P. from a basal diktytaxitic olivine basalt flow at Lookout Ridge is probably the oldest reliable date for rocks of the early High Cascade episode in this area. This olivine basalt (49.8 percent  $\text{SiO}_2$ ) overlies a hornblende two-pyroxene andesite flow (59.7 percent  $\text{SiO}_2$ ) of the late Western Cascade episode dated at  $8.86 \pm 0.34$  m.y. B.P.

The youngest available age of rocks of the early High Cascade episode in the area is 3.98 m.y.<sup>2,3</sup> obtained at Frissel Point by Sutter (1978) (recalculated by Fiebelkorn and others, 1982), but some doubt about the sample location has been voiced by several workers in the area. The youngest reliable date is  $5.5 \pm 0.2$  m.y. B.P. (0.624 percent K, 17.9 percent radiogenic  $\text{Ar}^{40}$ ), obtained on Taylor's (1981) sample of a basaltic andesite ash flow near Trailbridge Reservoir (Armstrong and others, 1975; Fiebelkorn and others, 1982). The youngest available date is 5.19 m.y. B.P. (see footnote 2.3). The oldest K-Ar date in lowermost lavas of the late High Cascade episode at Belknap-Foley is  $3.4 \pm 1.1$  m.y. B.P. (Flaherty, 1981). Taylor (personal communication, 1983) feels that the earliest platform lavas in the Foley Ridge area are about 4.0 m.y. old (see footnote 2.3), based on data of Sutter (1978).

**Deschutes Basin-Green Ridge area:** High-alumina basalt, basaltic andesite, and dacitic to rhyodacitic tuffs of the Deschutes Basin (Taylor, 1973b) are probably, at least in part, units of the early High Cascade episode. Diktytaxitic, iron-rich, slightly alkaline basalts are common in this sequence, although ash-flow and air-fall tuff and epiclastic deposits are also common, especially eastward away from the High Cascade Range (e.g., Taylor, 1973b; Hales, 1975; Taylor, 1980). Rimrock basalts of the Deschutes Basin have yielded several K-Ar ages of about 4.8 m.y. (Taylor, 1973b), although an age of  $10.7 \pm 1.2$  m.y. was recently determined on the same or a similar lava by Bunker and others (1982). The low K (0.281 percent) and low radiogenic  $\text{Ar}^{40}$  (8.1 percent), however, cast doubt on the accuracy of this date of 10.7 m.y. B.P. Basalt flows at the top of the Green Ridge scarp have dates as young as 5.3 m.y. B.P., and a flow near the top of a fault block on the west side of the Green Ridge fault has a K-Ar date of  $4.7 \pm 0.4$  m.y. B.P. (Armstrong and others, 1975). The oldest rocks at Green Ridge are andesites and basaltic lavas from a volcanic center on the north end of the ridge (Hales, 1975). These rocks yielded K-Ar dates of between 9.4 and 8.3 m.y. B.P. (Armstrong and others, 1975; Hales, 1975). Lavas of the late High Cascade episode K-Ar dated at about  $2.2 \pm 0.2$  m.y. B.P. bank up against the Green Ridge fault (Armstrong and others, 1975; Hales, 1975). The oldest part of the Deschutes Formation may be as much as 12 m.y. old (Taylor, 1973b), although Smith (personal communication, 1983) indicated that the base of the part of the formation characterized by tuffs and iron-rich basalt is probably about 6 m.y. old. The part of the Deschutes Formation corresponding compositionally to the volcanic rocks of the early High Cascade episode was therefore probably deposited between about 6 and 4.5 m.y. B.P. All of the above dates were recalculated by Fiebelkorn and others (1982).

<sup>2,3</sup> This age is based on a  $3.98 \pm 0.06$  m.y. age (sample CP-205) obtained by Sutter (1978). Taylor (personal communication, 1982) checked the  $\text{K}_2\text{O}$  content of the rocks at the localities of Sutter's samples numbered CP-205 (listed as at Frissel Point) and CP-208 (listed at Foley Ridge) and found that the CP-205 sample must have come from Foley Ridge and the CP-208 sample (5.19 m.y. B.P.) must have come from Frissel Point. The samples were therefore probably interchanged at some point in processing. Both of the above dates are from recalculations of Fiebelkorn and others (1982) utilizing new constants.

**Lookout Point area:** In the Lookout Point area, one dense basalt near the top of Patterson Mountain yielded a K-Ar age of  $5.8 \pm 0.3$  m.y. A small, locally erupted flow of the late High Cascade episode which was found in a canyon cut into older rocks in the same area at Armet Creek was K-Ar dated at  $0.56 \pm 0.15$  m.y. B.P. The High Cascade section as a whole is very thin and unrepresentative in this area because of the great distance from High Cascade sources.

**Waldo Lake-Swift Creek area:** A sequence of compact basalt flows in the Waldo Lake-Swift Creek area caps basalt, basaltic andesite, and andesite of the late Western Cascade episode. The upper part and bottom of this section of early High Cascade age yielded K-Ar dates of  $4.3 \pm 0.4$  m.y. B.P. and  $5.56 \pm 0.34$  m.y. B.P., respectively (Chapter 6). The oldest flow of the late High Cascade episode is an intracanyon diktytaxitic basalt which yielded a K-Ar date of  $1.98 \pm 0.25$  m.y. B.P. (Chapter 6).

Numerous diktytaxitic basalts capping Western Cascade ridges throughout the area between Lookout Point and Swift Creek have been described by Brown and others (1980b). Basalts with this diktytaxitic texture are thus common in the region, although absent in local areas. Where diktytaxitic texture in basalt is absent, and where underlying rocks of the late Western Cascade episode are nearly unaltered basalts, the contact may be difficult to locate. This was certainly the case at Swift Creek, where there is about a 7.5-m.y. age difference across the contact.

**Conclusion:** The bulk of the K-Ar data supports placing the lower time boundary of the early High Cascade episode at about 9.0 m.y. B.P., based chiefly on the Breitenbush and Belknap Hot Springs data. The upper boundary should be placed at about 4 m.y. B.P., based on the uppermost basalt flows at Breitenbush, Green Ridge, and Swift Creek and the lowermost flow of the late High Cascade episode dated near Belknap Hot Springs. The data presented here suggest the possibility that, in some areas, there may be a time gap between High Cascade and Western Cascade volcanism. It is also possible that, if more dates were available from within the High Cascade province (the probable source for many of the rocks of both the early and late High Cascade episodes), many of the time gaps in High Cascade volcanism might disappear. There is no evidence of a time gap between the two major episodes in the Belknap-Foley area (i.e., at Lookout Ridge).

## Volcanic rocks of the late High Cascade episode (4-0 m.y. B.P.)

**Introduction:** Uplift of the Western Cascade Range relative to much of the central Oregon High Cascades between 5 and 4 m.y. B.P. was followed by eruption of voluminous flows of compact to diktytaxitic basalt and basaltic andesite from contiguous shield volcanoes. This created a low volcanic platform in the High Cascade province (Taylor, 1980). These initial basaltic flows reached deep into the Western Cascade Range by following canyons cut by westward-flowing rivers entrenched into the uplifted Western Cascade block. The distribution of these Pliocene to early Pleistocene intracanyon basalts is clearly related to present topographic lows, distinguishing the lavas of the late High Cascade episode from similar basalt and basaltic andesites of the early High Cascade episode which cap the highest Western Cascade ridges. Basaltic andesite increases in abundance relative to basalt in progressively younger Quaternary flows (Taylor, 1980). Because of their higher viscosity resulting from their higher silica content, these flows tended to be restricted to the High Cascade axis. Basaltic andesite and less abundant andesite, dacite, and rhyodacite form prominent Quaternary composite cones in local areas which, although imposing, are far smaller



in volume than coeval basalt and basaltic andesite on the platform (e.g., Taylor, 1980). Mount Hood, Mount Jefferson, the Three Sisters, Diamond Peak, and Mount Mazama (Crater Lake) are some of the largest composite cones.

**Breitenbush area:** In the Breitenbush Hot Springs area, the late High Cascade episode is represented chiefly by basalt and basaltic andesite flows and cinder cones of very fresh aspect. The distribution of lavas is obviously controlled by existing topography. The volcanic vents often display original volcanic landforms which are preserved with little erosional modification. Hammond and others (1980) listed a  $4.3 \pm 0.3$ -m.y. B.P. date (0.392 percent K, 12.1 percent radiogenic Ar<sup>40</sup>) for a basal High Cascade tephra deposit (date recalculated by Fiebelkorn and others, 1982). Some of the youngest rocks in this area are post-glacial debris flows from Mount Jefferson and volcanic flows around Olallie Butte (Hammond and others, 1980).

**Belknap-Foley area:** In the Belknap Hot Springs area, north-south- to northwest-trending faults dropped the High Cascade province down relative to uplifted areas of the Western Cascades. These faults were first noted by Thayer (1936) and Taylor (1980) and mapped in reconnaissance by Brown and others (1980a). They were later verified by detailed mapping of Flaherty (1981) and Avramenko (1981). A thick sequence of Pliocene basalt, which Jan (1967) and Flaherty (1981) found to be anomalously alkali-rich, banks up against these east-facing fault scarps. The best examples of these alkali-rich basalts occur at Cupola Rock (Flaherty, 1981) and Scott Creek (Jan, 1967). The Scott Creek sequence is particularly interesting, since it contains pillow basalts indicative of lakes (Jan, 1967) which may have been temporarily dammed by lava along the fault scarps (Taylor, 1980). The basal basalts are highly diktytaxitic and, where alkali-rich and nearly holocrystalline, have purplish-brown titaniferous clinopyroxene in the groundmass (Flaherty, 1981). The sequence has more basaltic andesite at higher levels, and the diktytaxitic texture becomes less common in the more siliceous flows. The oldest date so far obtained is about 3.98 m.y. B.P. (see footnote 2.3), and the youngest eruptions are those which occurred from Belknap Crater about 1,500 years ago (Taylor, 1968, 1980).

**Lookout Point area:** The late High Cascade episode is represented in the Lookout Point area by only two flows (see Chapter 5). The High Prairie flow, a diktytaxitic basalt flow dated at  $11.01 \pm 0.15$  m.y. B.P. (Sutter, 1978), flowed from the High Cascades down the North Fork of the Middle Fork of the Willamette River. Woller and Priest (Chapter 5) and others question the date that Sutter obtained on this flow, postulating it is closer to 2 m.y. old. A basaltic andesite flow at Armet Creek was dated at  $0.56 \pm 0.16$  m.y. B.P. and was erupted from a local vent at the head of the creek a few kilometers northeast of Lookout Point Reservoir (Woller and Priest, Chapter 5).

**Waldo Lake-Swift Creek area:** The late High Cascade episode in the Waldo Lake-Swift Creek area is represented chiefly by intracanyon diktytaxitic and compact basalt flows (Woller and Black, Chapter 6). The oldest dated flow, a compact basalt, yielded a K-Ar date of  $1.98 \pm 0.25$  m.y. B.P.; the youngest dated flow had a K-Ar date of  $0.17 \pm 0.48$  m.y. B.P.

**Conclusion:** As explained in the section on volcanic rocks of the early High Cascade episode (9-4 m.y. B.P.), the beginning of the late High Cascade episode is 4.0 m.y. B.P. The most recent High Cascade eruptions in Oregon were at Mount Hood in 1859 and 1865 A.D. (Crandell, 1980).

## STRUCTURAL GEOLOGY

### Introduction

The central Oregon Cascade Range has numerous lineaments and known structures which strike northwest, north-

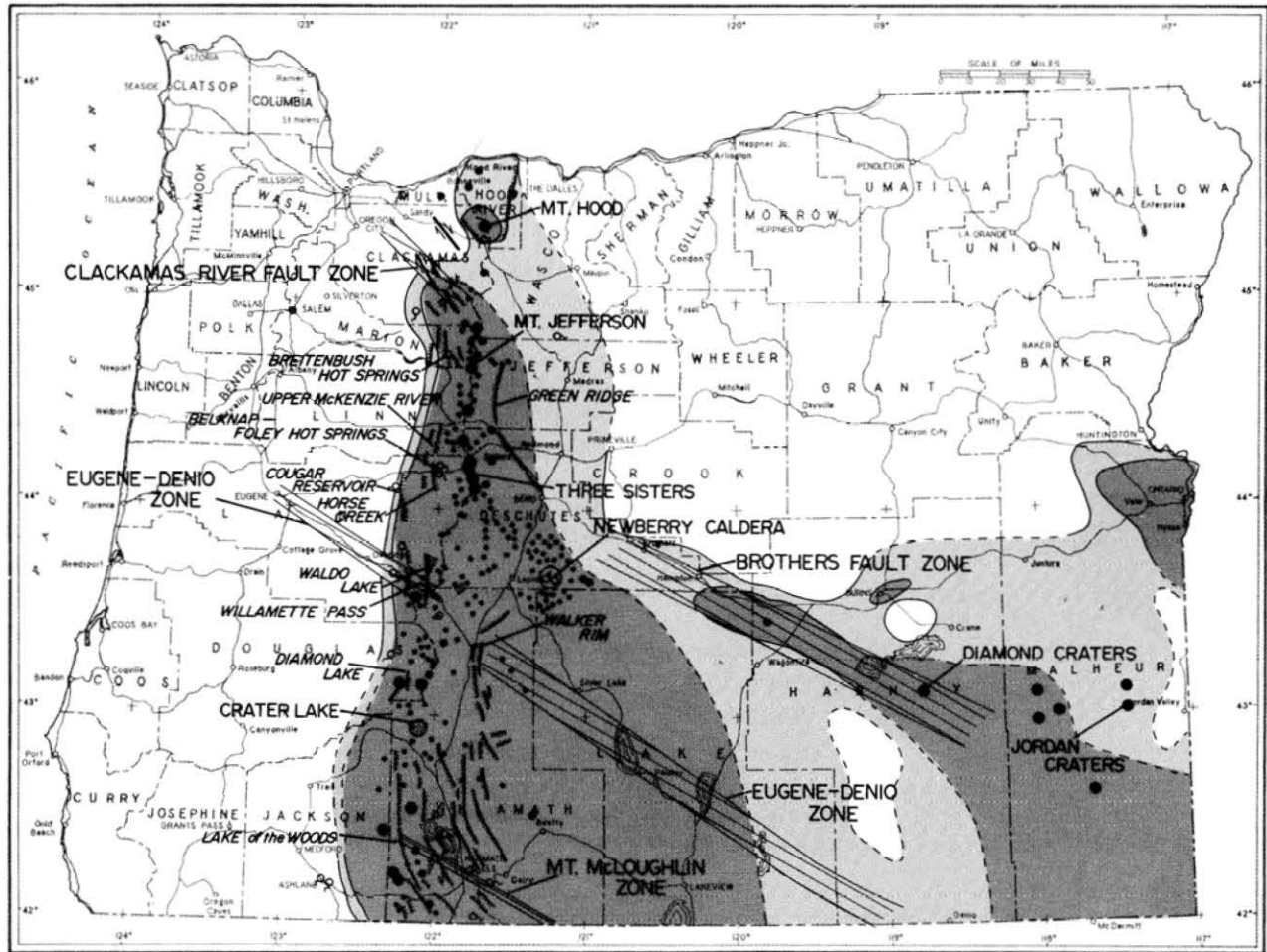
east, and north-northwest to north-south (e.g., Peck and others, 1964; Venkatakrishnan and others, 1980; Kienle and others, 1981). Few of these lineaments and structures have been mapped in detail, so only tentative conclusions can be made on the overall history of deformation in the Cascades. This section will present what is known about the structure from geologic mapping and will suggest some possible interpretations of the limited data base. Various major lineaments of Lawrence (1976) and some mapped faults and Quaternary volcanic centers are shown in Figure 2.4. Figure 2.5 illustrates schematically some periods of faulting and folding in various mapped areas in the northern and central Cascades.

### North-south- and north-northwest-trending faults

North-south faults thus far mapped are concentrated along the eastern half of the Western Cascade physiographic province (Figure 2.4). Williams (1942) inferred from the linearity of the High Cascade-Western Cascade boundary that it was fault controlled. These north-south faults bound blocks in the High Cascade province which are dropped down relative to adjacent areas. The north-south faults occur in the Mount Hood area (Wells and Peck, 1961; Beeson and others, 1982), at Green Ridge (Hales, 1975), in the McKenzie River-Horse Creek area (Taylor, 1973a; Brown and others, 1980a; Avramenko, 1981; Flaherty, 1981), at Cougar Reservoir (Priest and Woller, Chapter 4), and possibly at Walker Rim (Wells and Peck, 1961) and the Mount Bailey-Diamond Lake area (Barnes, 1978).<sup>2.4</sup> Williams (1942) inferred from the high elevation of the Western Cascade Range west of Crater Lake relative to outcrops of High Cascade rocks to the east that there was a major fault scarp on the east boundary of the Western Cascades there, although Peck and others (1964) stated that detailed mapping failed to delineate a fault at this locality. In the area south of Crater Lake, Smith and others (1982) identified a down-to-the-east fault system that extends southward for 50 km (30 mi) from the head of the Middle Fork of the Rogue River. North-south faults have also been mapped in the upper Breitenbush Hot Springs area (Hammond and others, 1980; White, 1980a,c). The Breitenbush faults have a complex pattern of displacement, and it is possible that net subsidence of the High Cascade axis relative to adjacent uplifted areas has occurred there also (Thayer, 1936, 1939; White, 1980c), although Rollins (1976) and Hammond and others (1982) found no evidence of this. Similar unmapped faults may be manifested by lineaments following the western boundary of the High Cascade province from Horse Creek to Crater Lake (e.g., Venkatakrishnan and others, 1980; Kienle and others, 1981). Steep east-dipping gradients on both Bouguer and residual gravity anomaly maps bound the High Cascade province along a north-south zone and have been interpreted to be the result of faults (e.g., Pitts, 1979; Priest and others, 1980; Flaherty, 1981; Couch and others, 1982a,b).

The amount of downward displacement on the High Cascade axis relative to some adjacent areas west and locally east of the axis is probably at least several hundred meters in many places and may exceed 1 km (0.6 mi) in local areas. On the west side of Mount Hood, the middle Miocene Columbia River Basalt Group is displaced downward in the Old Maid Flat area (Beeson and Moran, 1979; Beeson and others, in preparation), and at least another 400 m (1,300 ft) of down-to-the-east displacement probably occurs on a northwest-trending fault at Old Maid Flat (Priest and others, 1982a). At least 600 m (1,970 ft) of down-to-the-west movement has been estimated on the Hood River fault east of Mount Hood (Woller, unpublished mapping, 1981). White (1980c) estimated that

<sup>2.4</sup> Sherrod (personal communication, 1983) found no evidence of this fault in his mapping at Diamond Lake.



#### EXPLANATION


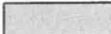







-  = Heat flow over  $100 \text{ mW/m}^2$
-  = Heat flow between  $100 \text{ mW/m}^2$  and  $80 \text{ mW/m}^2$
-  = Major northwest-trending lineaments; names are from Lawrence (1976); Clackamas River fault zone is from Anderson (1978) and Beeson and others (in preparation)
-  = Mapped normal faults, hachured on the downthrown side. Only faults in or closely adjacent to areas of high heat flow in the Cascades are shown; areas west of the high-heat-flow zone tend to have fewer well-defined fault scarps, partly because less mapping has been done in those areas and possibly also because the faulting is older
-  = Lateral fault showing relative displacement
-  = Quaternary volcanic centers. Size of dot is crudely related to the size of the volcanic center relative to other centers. Many more centers exist than are shown, particularly in the High Cascades, but scale does not allow more detail
-  = Calderas (diameter = actual diameter)
-  = Thermal springs in and adjacent to the Cascades
-  = Heat flow isotherm, dashed where inferred

Figure 2.4. Map showing some major faults, lineaments, hot springs, and Quaternary volcanic centers relative to zones of anomalously high heat flow in the Cascade Range and adjacent areas of Oregon. Geologic data are from Wells and Peck (1961), Hales (1975), Peterson and others (1976), Walker (1977), Barnes (1978), Beeson and Moran (1979), Brown and others (1980a), Hammond and others (1980), Avramenko (1981), Flaherty (1981), Priest and others (1982a), Smith and others (1982), Woller and Black (Chapter 6), and Beeson and others (in preparation). Heat-flow data are from Blackwell and others (1978) and Black and others (Chapter 7).

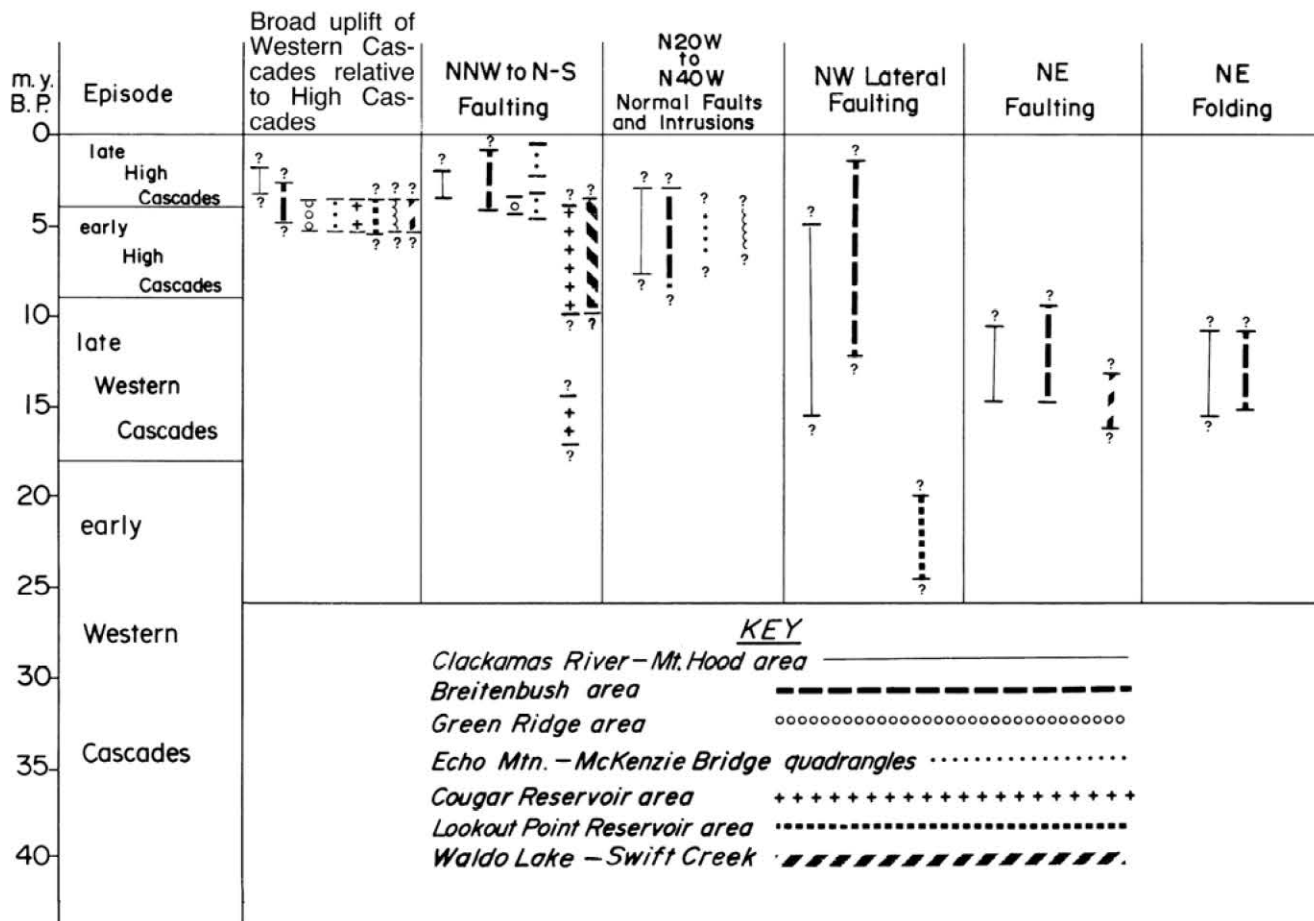


Figure 2.5. Episodes of deformation in some mapped areas of the northern and central Cascades. Data are from Hales (1975), Hammond and others (1980), Taylor (1980), White (1980a,c), Avramenko (1981), Flaherty (1981), Priest and Woller (Chapters 3 and 4), Woller and Priest (Chapter 5), and Woller and Black (Chapter 6).

the Mount Jefferson block has subsided about 750 m (2,460 ft) on north-south-trending faults in the Breitenbush Hot Springs area relative to uplifted adjacent areas. Hammond and others (1982) and Rollins (1976), however, did not see any evidence of these boundary faults. Hales (1975) and Taylor (1980) estimated that the same block is displaced downward on the Green Ridge boundary fault by at least 900 m (2,950 ft). Taylor (1980) emphasized that the Mount Jefferson-Three Sisters block may have subsided much more than 900 m (2,950 ft) and argued that no uplift or tilting is necessary to explain the high-standing Green Ridge fault block. Down-to-the-east faults occur on the west side of the Three Sisters area along the Horse Creek-McKenzie River fault zone, where about 620 m (2,030 ft) of displacement occurs (Flaherty, 1981). Sixteen km (9.6 mi) west of Horse Creek, the older Cougar Reservoir fault zone has at least 152 m (499 ft) of similar displacement (Priest and Woller, Chapter 4).

In the Waldo Lake area, Woller and Black (Chapter 6) present evidence for two major north-south fault zones which may be southerly continuations of the Cougar Reservoir and Horse Creek faults. Gravity anomalies associated with these zones are continuous from Crater Lake to Breitenbush Hot Springs (Couch and others, 1982a,b).

In view of the large number of north-south volcanic vent alignments in the central High Cascade Range, it is possible that additional north-south faults are buried by lavas of the

late High Cascade episode within the High Cascade province. However, these alignments could also be controlled by joints caused by the orientation of the regional stress field (e.g., Nakamura, 1977).

Although vertical stratigraphic offsets on the north-south faults are proof of large dip-slip displacement, some horizontal and near-horizontal slickensides on the north-south-trending faults show that some lateral movement has also occurred. Beeson and Moran (1979) and Beeson and others (in preparation) found subhorizontal slickensides with 90° rakes on north-trending faults in the Mount Hood area. Priest and Woller (Chapter 4) noted horizontal slickensides on north-trending shears within the dacite of Cougar Dam.

#### Age of north-south- and north-northwest-trending faults

Most of the movement on major north-south-trending faults in the central Cascades occurred during late Miocene and early Pliocene time, although older and younger displacements have been documented in various places. Hammond and others (1980) concluded that most of the north-trending faulting in the Breitenbush area occurred during the last 5 m.y. Most of the offset on faults bounding the central High Cascade province occurred in the early Pliocene between 4 and 5 m.y. ago (e.g., Taylor, 1980; Flaherty, 1981). Faults which bound the western side of the central High Cascade block in



the upper McKenzie River area had last movements between 1.0 and 0.7 m.y. B.P., although large movements probably also occurred during the early Pliocene (Avramenko, 1981). North-south- to northwest-aligned Holocene basaltic vent strings associated with the Belknap Crater-Nash Crater-Sand Mountain eruptions west of the Three Sisters suggest that the north-south-trending faults may still be active enough to channel magma to the surface. As previously mentioned, however, there is no documented example of faults cutting these Holocene deposits, and the vent alignments could be joint systems.

The oldest documented north-south fault in the central Cascades could be the Cougar fault (Figure 2.1). Unlike the younger Horse Creek fault, the Cougar fault has no well-defined topographic scarp. The fault may control a  $16.3 \pm 1.8$ -m.y. B.P. glassy dacite intrusion which is strongly elongated north-south and which is adjacent to the fault (Priest and Woller, Chapter 4). Within the intrusion, dikes filled with both magmatic material and explosion breccias follow northwest- to north-northwest-trending shears and fissures. The fault, however, definitely offsets lavas dated at  $13.2 \pm 0.7$  m.y. B.P. by at least 152 m (499 ft). The proven movement on the Cougar fault is thus younger than 13.2 m.y. Stratigraphic relationships between lavas of the early High Cascade episode and the Cougar fault suggest that the fault may have had major movement immediately prior to eruption of the lavas which occurred between 8.3 and 7.8 m.y. B.P. (Priest and Woller, Chapter 4). It is not known whether additional offset occurred during the 5- to 4-m.y. B.P. faulting episode which occurred at Horse Creek to the east, but the absence of a large topographic scarp analogous to that of the Horse Creek scarp casts doubt on large 5- to 4-m.y. B.P. displacements at Cougar Reservoir (see Chapter 4; Plate 2). The Cougar fault is capped by unbroken Pleistocene sedimentary strata (Chapter 4).

The Waldo Lake fault scarp may be of similar or younger age than the Horse Creek fault; the stratigraphic control at Waldo Lake is not adequate to further specify its age (Chapter 6). The Groundhog Creek fault, unlike the Waldo Lake fault to the west, has no well-defined scarp and, by analogy to the arguments for the Horse Creek and Cougar faults (Chapter 4), may be older than the Waldo Lake fault (Chapter 6). The Groundhog Creek fault definitely cuts rocks of the late Western Cascade episode with probable ages in the 13- to 15-m.y. range, and lavas of the early High Cascade episode do not appear to crop out west of it (Chapter 6). These relationships in addition to the similarities of the gravity signatures of the Groundhog Creek and Cougar Reservoir faults strongly suggest that they are the same age.

The north-south faults with the largest displacements in the central Cascades thus appear to fall into two age groups:

1. Those with most movement immediately preceding basaltic eruptions of the early High Cascade episode.
2. Those immediately preceding eruptions of the late High Cascade episode.

Small displacements appear to have also occurred throughout the last 5 m.y.

### Northwest-trending faults with possible lateral movement

A N. 40° W.-trending right-lateral fault zone at the Clackamas River (Anderson, 1978) and three major N. 60° W.-trending lineaments (Lawrence, 1976) intercept the High Cascade axis (Figure 2.4). The Clackamas River fault zone was interpreted by Beeson and Moran (1979) and Beeson and others (in preparation) to be an extension of the Brothers fault zone (Figure 2.4), which is a zone of right-lateral shear bounding the Basin and Range province (Lawrence, 1976). Davis

(1981), however, argued that there is evidence of left-lateral shear on the Brothers fault zone. It is also apparent that all of the mapped faults in the Brothers fault zone are largely, if not completely, dip-slip (e.g., Walker, 1977). The Green Ridge-Tumalo fault (e.g., Peterson and others, 1976) has been interpreted as the deflection of the northwest-trending Brothers fault zone into the north-south High Cascade trend (Lawrence, 1976). Northwest-trending faults with right-lateral oblique-slip displacement in the Breitenbush area (White, 1980a,c; Hammond and others, 1980) may be part of the overall Clackamas River-Brothers fault system postulated by Beeson and Moran (1979) and Beeson and others (in preparation).

The Eugene-Denio zone of Lawrence (1976) is a northwest-trending lineament which occurs in pre-High Cascade rocks on both sides of the High Cascade axis in the Willamette Pass area (Figure 2.4). Parts of this lineament in the Western Cascade Range were mapped by Woller and Black (Chapter 6) adjacent to the High Cascades, by Brown and others (1980b) in the Oakridge-McCredie Hot Springs area, and by Woller and Priest (Chapter 5) in the Lookout Point Reservoir area (see Figures 1.1 and 2.4 for locations). Northwest-trending shear zones in the lineament were found only at Lookout Point. In the Lookout Point area, numerous northwest- to west-northwest-trending shear zones with subhorizontal slickensides were found in tuffaceous rocks of the early Western Cascade episode. However, no lateral displacement of 22-m.y.-old lavas overlying the tuffs at Lookout Point could be documented (Chapter 5).

On the east side of the High Cascades, the Eugene-Denio zone appears as a series of northwest-trending faults which cut across the Walker Rim (e.g., Wells and Peck, 1961; Kienle and others, 1981). Kienle and others (1981) inferred from photogeologic analysis that some of these faults have right-lateral strike-slip displacement; however, MacLeod (unpublished mapping, 1982) found no evidence of lateral displacements. All mapped faults in the Eugene-Denio lineament in the Basin and Range appear to have chiefly or entirely dip-slip displacement (e.g., Walker, 1977).

Although some authors (e.g., Lawrence, 1976) have inferred that there is some lateral offset of the High Cascade axis across the Eugene-Denio zone, Woller and Black (Chapter 6) found no evidence to support this hypothesis. Basalts mapped by Wells and Peck (1961) and Peck and others (1964) as High Cascade units south of the Eugene-Denio lineament in the Swift Creek area are actually the lower part of the volcanic rocks of the late Western Cascade episode. This changes the inferred eastern boundary of the uplifted Western Cascade block to the area on the east side of Diamond Peak and largely eliminates any possible lateral offset of this boundary across the Eugene-Denio zone (Chapter 6).

The Mount McLoughlin zone of Lawrence (1976) is a poorly defined lineament which terminates at the High Cascade Range near a north-south-trending fault mapped by Maynard (1974) and Smith and others (1982). No lateral faults have been described in this zone.

### Age of northwest-trending faults with possible lateral movement

Beeson and Moran (1979) showed that some documented movement on the Clackamas River right-lateral wrench-fault zone is younger than the Sardine Formation of Peck and others (1964), although Beeson and others (in preparation) indicated that a fault scarp parallel to the Clackamas River may have also acted as a barrier to the Grande Ronde Basalt, flood basalt which at that time was flowing into the area from fissure eruptions that were occurring in eastern Oregon,



southeastern Washington, and western Idaho (Swanson and others, 1979). Lux's (1982) radiometric dates on Grande Ronde Basalt found in western Oregon indicated that it was erupted over a short time span about  $15.3 \pm 0.4$  m.y. B.P. The Clackamas River wrench fault was thus probably active prior to 15.3 m.y. B.P. Hammond and others (1980) inferred from mapping in the Clackamas River-Breitenbush Hot Springs area that northwest-trending oblique-slip faults began movement about 12 m.y. B.P. and remained active during later episodes of more northerly trending faulting. White (1980a) inferred that some of these northwest-trending oblique-slip faults in the Breitenbush Hot Springs area have displaced Pleistocene units. There appears to be evidence of a long history of northwest-trending lateral to oblique-slip faulting in the northern Oregon Cascades from before 15.3 m.y. B.P. to Pleistocene times.

Mapping by Woller and Priest (Chapter 5) in the Lookout Point area and Woller and Black (Chapter 6) in the Waldo Lake-Swift Creek area has revealed no northwest-trending lateral faults younger than about 22 m.y. in the Western Cascade segment of the Eugene-Denio lineament. Although a few small lateral shears were found in the 22-m.y.-old lavas of Black Canyon in the Lookout Point area, there was no obvious lateral offset of a paleocanyon filled with these lavas, even though the paleocanyon crosses the Willamette River portion of the Eugene-Denio lineament at right angles (see Chapter 5). Northwest- to west-northwest-trending lateral shear zones are, however, abundant in tuffs underlying the lavas of Black Canyon (Chapter 5). As mentioned previously, the tuffs have a minimum age of  $24.7 \pm 2.0$  m.y. and may be somewhat older.

On the east side of the Cascades, northwest-trending faults within the Eugene-Denio lineament cut lavas mapped as Quaternary-Tertiary volcanic rocks by Wells and Peck (1961). These rocks are probably of early High Cascade age (MacLeod, unpublished mapping, 1982), but none of these faults have any documented lateral displacement (e.g., Walker, 1977).

It appears that there is evidence of a long history of lateral movement on northwest-trending faults in the Clackamas River-Breitenbush area, perhaps starting before 15.3 m.y. B.P. and continuing into Pleistocene time. Similar movements in the area of the Eugene-Denio lineament had largely ceased prior to 22 m.y. B.P. A few minor oblique-slip faults in 22-m.y.-old rocks in the Lookout Point area, however, indicate that some small lateral movements occurred in the post-22-m.y. B.P. period.

Hammond and others (1980) speculated that lateral faulting during the last 5 m.y. in the northern Oregon Cascades may have occurred in a stress environment different from that during previous periods of lateral deformation. This hypothesis arose because Pliocene and younger north-south normal faulting has accompanied northwest-trending lateral faulting in the Rhododendron Ridge-Clackamas River area (Hammond and others, 1980).

#### **N. 20°-40° W. normal faults and intrusives**

Numerous dikes and normal faults with trends between N. 20° W. and N. 40° W. occur in the Western Cascade Range. Peck and others (1964) noted that northwest-trending faults are the dominant structures in the Cascades and cited several examples of them, including youthful normal faults which cut rocks of the late High Cascade episode south of Crater Lake. Callaghan and Buddington (1938) also noted that mineralized veins and intrusive rocks of the Western Cascade episode tend to preferentially follow northwest-trending structures. Only a small percentage of these faults and dikes have been documented in the central Western Cascade Range because of the

paucity of detailed mapping.

N. 20°-40° W.-trending faults with both normal and lateral offsets are common in the Clackamas River-Mount Hood area (Beeson and Moran, 1979; Beeson and others, in preparation). The faults were interpreted by Beeson and others (in preparation) as the result of an overall system of right-lateral wrenching along a N. 45° W. trend.

Reconnaissance maps of the Breitenbush area (White, 1980a,c; Hammond and others, 1980, 1982) show numerous N. 20°-40° W. normal faults which appear to be terminated by north-south faults (Hammond and others, 1982). Priest and Woller (Chapter 3) found two small N. 30°  $\pm$  10° W.-trending normal faults which displace uppermost tuffs of the late Western Cascade episode. These small faults are parallel to nearby basaltic andesite dikes of the early High Cascade episode (see Chapter 3).

Avramenko (1981) noted swarms of dikes of early High Cascade age and a few parallel normal faults with an average trend of N. 30° W. in the Echo Mountain quadrangle in the upper McKenzie River area. There appear to be only a few minor faults with this trend in the Cougar Reservoir and Waldo Lake-Swift Creek areas.

#### **Age of N. 20°-40° W. normal faults and intrusives**

No definite age estimates for the N. 20°-40° W. faulting in the Clackamas River-Mount Hood area are known, but the faults do cut the Columbia River Basalt Group and overlying units of the late Western Cascade episode (Beeson and Moran, 1979; Beeson and others, in preparation). Hammond and others (1982) noted on their reconnaissance map that some of these faults have had recurrent movement into late High Cascade time in the Breitenbush area. The two small faults mapped in detail in the same area by Priest and Woller (Chapter 3) appear to have experienced offset in the interval prior to 6.3 m.y. B.P. but after the end of late Western Cascade volcanism. The faults and dikes in the Echo Mountain quadrangle are apparently roughly coincident with the early High Cascade episode (see Avramenko, 1981). Peck and others (1964) and Naslund (1977) noted that the northwest-trending faults in the southern Cascades cut units of late High Cascade age. Naslund (1977) showed examples of these faults cutting lavas erupted within the last normal polarity epoch (i.e., within the last 770,000 years).

The northwest-trending faults seem to have chiefly begun movement sometime prior to the north-south-trending faults, probably during the beginning of early High Cascade time. Observations of Callaghan and Buddington (1938), however, suggest that older intrusive rocks of the Western Cascade episode also followed northwest-trending structures. Movement on these faults has apparently been recurrent into late High Cascade time.

#### **Northeast-trending faults**

Although there are many northeast-trending photogeologic and geophysical lineaments in the Cascades (e.g., Venkatakrishnan and others, 1980; Kienle and others, 1981; various geophysical studies by Couch, Gemperle, Pitts, McLain, and Veen), there are fewer northeast-trending faults verified by geologic mapping than faults with other trends. Some northeast-trending reverse faults occur in northeast-trending folds in the Mount Hood area (Beeson and Moran, 1979; Vogt, 1979, 1981; Beeson and others, in preparation). Northeast-trending faults also occur in the Breitenbush Hot Springs area, where both lateral and normal movements have occurred (e.g., Hammond and others, 1980, 1982; White 1980a,c). Moderate- to large(?) displacement northeast-

trending normal faults occur in the Willamette Pass area (Woller and Black, Chapter 6). Barnes (1978) inferred that a northeast-trending dip-slip fault mapped by Wells (1956) in the Medford quadrangle continues into the Diamond Lake area.

### Age of northeast-trending faults

Many northeast-trending faults are middle to late Miocene in age, and younger faults with this trend also occur. Provided generalizations about the age of folds in the Mount Hood area apply to the intimately associated northeast-trending faults, movement on the faults probably began about 15.3 m.y. B.P. during the time of extrusion of the Grande Ronde Basalt of the Columbia River Basalt Group (Vogt, 1979, 1981; Beeson and others, 1980, in preparation). The youngest movement on these faults, however, is not well constrained (Beeson and Moran, 1979; Beeson and others, in preparation). Northeast-trending faults in the Breitenbush Hot Springs area are associated with a fold of middle to late Miocene age, and some of these faults cut the 11.8- to 9.8-m.y. B.P. Elk Lake formation (White, 1980a). A northeast-trending fault in the Swift Creek area cuts lavas dated at 5.5 m.y. B.P. (Woller and Black, Chapter 6). Barnes (1978) showed that northeast-trending faults near Diamond Lake cut lavas of Mount Bailey of late High Cascade age. He related these faults to the response of northeast-trending Klamath Mountain structures to High Cascade extension.

### Folds

Folds occur in Western Cascade rocks chiefly in the northern part of the Oregon Cascade Range. Northeast-trending folds with local thrust-faulted limbs occur in the Mount Hood-Columbia Gorge area (Hodge, 1938; Beeson and Moran, 1979; Vogt, 1979, 1981; Beeson and others, in preparation). Along the North Santiam River, north-northeast to northeast-trending folds were described and named by Thayer (1936), from west to east, the Mehama anticline, Sardine syncline, and Breitenbush anticline. Wells and Peck (1961) and Peck and others (1964) mapped these and related folds throughout much of the northern Oregon Western Cascades, but Hammond and others (1980, 1982) showed these folds as small disjointed structures extending only a few kilometers in any one area. Most of these folds have limbs dipping less than 20°, although limbs of the Breitenbush anticline locally dip as much as 60° (e.g., Peck and others, 1964; White, 1980a,c). No evidence for the Breitenbush anticline has been found to the south in the Cougar Reservoir area (Priest and Woller, Chapter 4), although Wells and Peck (1961) and Peck and others (1964) showed the axis of the anticline extending west of Cougar Reservoir.

Flaherty (1981) measured easterly dips of 7°-10° in the lavas of Cupola Rock of late High Cascade age near Belknap Hot Springs. He interpreted this as evidence of subsidence along the High Cascade axis. Most cross sections drawn on regional geologic maps also infer a broad synclinal structure under the High Cascades (e.g., Wells and Peck, 1961; Peck and others, 1964).

The small eastward dip on the contact between rocks of the late Western Cascade-early Western Cascade episodes in the Willamette Pass area has been interpreted as evidence of some downwarping in the general area of the High Cascades (e.g., cross sections of Wells and Peck, 1961; Peck and others, 1964). There is, however, no evidence of local compressional folding in the Willamette Pass area (Chapter 6), although Wells and Peck (1961) showed the axis of the Breitenbush anticline several kilometers west of the area.

Although folding in the North Santiam drainage and areas

north of the Clackamas River is well documented, the gentle dips which Wells and Peck (1961) and Peck and others (1964) interpreted as folds in areas to the south could be explained by local tilting of, or compression between, fault blocks and, in some cases, by primary depositional dips. There is, in fact, no reason that the folds in the North Santiam area could not have been caused by interactions between local fault blocks. The folds are of very limited extent and are everywhere unique to individual fault blocks (e.g., Hammond and others, 1980, 1982). Walker (personal communication, 1982), in preliminary mapping of the McKenzie River drainage, also found no evidence of Western Cascade folds resulting from regional compression. The gentle downwarping of the High Cascades noted in the Belknap-Foley area (Flaherty, 1981) may have resulted from isostatic forces rather than from an episode of compressive deformation.

### Age of folds

The local folds in the northern Oregon Western Cascade Range are probably middle Miocene in age, although the age control is poor. As previously mentioned in the section on northeast-trending faults, folding in the Mount Hood area had probably begun by about 15.3 m.y. B.P., but the age of the youngest folding is not well constrained (e.g., see Beeson and Moran, 1979; Beeson and others, in preparation). Similar folding in the Breitenbush area occurred between 15 and 11 m.y. B.P. (White, 1980a,c). Folding hypothesized by Flaherty (1981) in the Belknap Hot Springs area ended between 8.9 and 7 m.y. B.P. There is thus some evidence that, in the Breitenbush-Belknap area, stress conditions which favored local folding ended by about 11 to 7 m.y. B.P.

The gentle eastward tilting of rocks along the eastern margin of the Western Cascade Range may have occurred in the Pleistocene. In the Belknap Hot Springs area, Flaherty (1981) interpreted some gentle easterly dips in 3.4- to 2.9-m.y. B.P. Foley Ridge lavas as evidence of tectonic tilting.

### Structural interpretations and speculations

According to Venkatakrishnan and others (1980) and Kienle and others (1981), the general pattern of northwest, northeast, and north-south lineaments and mapped structures in the Cascades can be explained by a stress field with a horizontal north-south to north-northwest maximum compressive stress axis, a horizontal east-west minimum stress axis, and a vertical intermediate stress axis. The northwest-trending lateral faulting along the Clackamas River and similar shears in the Lookout Point Reservoir area could also have been caused by this stress regime. Likewise, north-south to north-northwest normal faults could be accommodated because they are parallel to the maximum stress axis and perpendicular to the minimum compressive stress axis. These extensional faults could, however, just as easily be explained by east-west extension with the maximum compressive stress axis vertically oriented.

It is difficult to account for the north-northeast-trending folds in the Breitenbush area by simple north-south to north-northwest compression; presumably some local compression in a west-northwest to east-southeast direction would be necessary to cause the folds. It is also difficult to obtain the northeast-trending folds and associated thrust faults north of the Clackamas River from simple north-south compression unless local stresses associated with the right-lateral wrench faults have somehow produced the folds (Beeson and Anderson, personal communication, 1982).

One problem with the assumption that the regional stress regime has remained more or less constant during the Neogene (and perhaps earlier) is the change in both volcanism and

style of deformation which occurred between late Western Cascade time and High Cascade time. About 10 to 8 m.y. B.P. mafic lavas began to dominate eruptions, and the focus of volcanism became limited chiefly to the eastern part of the Cascade Range. Northeast to north-northeast folding in the Breitenbush Hot Springs-North Santiam River area had terminated by about this same time (White, 1980a,c).

North-south, down-to-the-east faulting along the Cougar Reservoir zone was apparently underway by about 9 m.y. B.P. when the mafic lavas of the early High Cascade episode were erupted, because they apparently banked up against the east-facing Cougar scarp (Chapter 4). If the Groundhog Creek fault in the Willamette Pass area (Chapter 6) is an analogue of the Cougar fault, then contemporaneous down-to-the-east north-south faulting probably also occurred south of the Cougar Reservoir area. North of Cougar Reservoir, northwest-trending mafic dike swarms of the early High Cascade episode and small normal faults which formed in the Echo Mountain area (Avramenko, 1981) are evidence of extensional stress there as well. Dikes of the early High Cascade episode also invaded northwest-trending fractures and small normal faults in the Outerson Mountain area (Chapter 3). This period of normal faulting and mafic volcanism is evidence of a more extensional tectonic environment in early High Cascade time relative to the late Western Cascade time.

About 4 to 5 m.y. ago, widespread uplift of the central Western Cascade Range relative to the High Cascade province was contemporaneous with extensive north-south to northwest-trending faulting at the High Cascade-Western Cascade boundary (e.g., Williams, 1942, 1953; Taylor, 1980, 1981; Flaherty, 1981). A period of very rapid downcutting of the Western Cascade Range then occurred, producing most of the present kilometer or so of relief in about 1.6 to 3 m.y. (e.g., Flaherty, 1981). North-south faulting continued in the central Oregon Cascade Range, but not on the same scale as in this 5- to 4-m.y. B.P. interval. Perhaps equally important events are the abrupt restriction of High Cascade volcanism to the present area of the High Cascade physiographic province and the eruption of extensive flows of highly fluid diktytaxitic basalt. This period of strong down-to-the-east deformation and diktytaxitic basalt eruption is strongly reminiscent of the eruption of diktytaxitic basalt of the early High Cascade episode and preceding down-to-the-east, north-south faulting documented at Cougar Reservoir (Chapter 4). In a manner analogous to the beginning of the early High Cascade episode, the late High Cascade episode began probably with another abrupt increase in extensional forces.

The abrupt changes in volcanism and deformation summarized above are best accounted for by equally abrupt changes in the stress regime perhaps resulting from changes in the interaction of major lithospheric plates. Changes in the direction of spreading on the Juan de Fuca Ridge between 7 and 4 m.y. B.P. and possible partial coupling of the Juan de Fuca Plate with the North American Plate in this interval (Atwater, 1970) may have caused these changes in deformation and volcanism. It may also be significant that Atwater's (1970) models require a change of 20° in direction of plate motion at about 10 m.y. B.P. Intense uplift and thrusting of sediments on the outer Oregon continental margin about 10 m.y. ago are evidence that the rate of subduction off the Oregon coast increased at this time (Drake, 1982). Continued deformation of sediments on the outer Oregon continental shelf indicates that subduction has continued into the Holocene (Drake, 1982). The present pattern of crustal heat flow also supports continued subduction (Blackwell and others, 1973, 1978, 1982).

In some way, the changes in plate interaction about 10 to 8 m.y. B.P. appear to have caused an episode of mafic magmatism and somewhat greater extensional stresses to affect the central Oregon Cascade Range. Fault-plane solutions for modern earthquakes indicate east-west extension (Couch and Lowell, 1971), implying that extensional stress may still be predominant.

None of the previously discussed plate interactions directly account for the uplift of the Western Cascade block about 5 to 4 m.y. B.P. or the major episode of diktytaxitic basaltic volcanism which formed the lower platform of the modern High Cascade Range. Taylor (1980) postulated that this period of faulting and volcanism corresponded to a time of crustal relaxation, when subduction changed or ceased. In view of the above-mentioned evidence of modern subduction, a model suggesting modification of subduction seems more likely than one hypothesizing cessation. About 5 to 4 m.y. B.P., a modification of the plate boundary between the Farallon Plate and the North American Plate caused the opening of the Gulf of California (Atwater, 1970), but it is not known if this event could have affected the Cascade stress regime.

Another factor which may have influenced the style of deformation in the Cascades is the relative strength of various parts of the crust. The high heat flow characteristic of the High Cascade province should cause the High Cascade crust to be more plastic and less rigid than the cooler Western Cascade crust. Concentration of faulting in areas of weak crust, especially where thermally weakened crust is adjacent to cooler crust, might explain (1) the poorly defined aspect of structures and lineaments in the cooler Western Cascade crust relative to areas to the east, and (2) the localization of the eastern boundary faults of the Western Cascade block. High rainfall and many tuffaceous sequences in the Western Cascade Range do not favor fault scarp preservation, but one would expect to see scarps if dip-slip displacements of 600 m (1,970 ft) or more had occurred in the last few million years. Well-defined fault scarps and associated lineaments are, however, rare in the Western Cascade Range relative to the High Cascade and Basin and Range provinces (e.g., Kienle and others, 1981). Concentration of well-defined fault scarps on the margins of the highest part of the High Cascade heat-flow anomaly of Blackwell and others (1978) and Black and others (Chapter 7) might be explained by this hypothesis (Figure 2.4). Elevated temperatures in the upper crust in the upper Klamath Lake area, postulated from Curie-point isotherm studies of McLain (1981), may cause Basin and Range faults associated with the Klamath graben to swing toward parallelism with the High Cascade axis (Figure 2.4). The Tumalo and Walker Rim faults both appear to swing toward the very hot crust which must underlie Newberry volcano (Figure 2.4). Likewise, concentration of lateral faults in the Clackamas River area may reflect interaction between somewhat cooler crust to the north and hotter crust to the south of the Clackamas River (Figure 2.4). The margins of a local heat-flow anomaly (Figure 2.4) associated with Mount Hood are also associated with a late Pliocene(?) fault at Old Maid Flat (Priest and others, 1982a) and with the Hood River fault. The youthful age of the Hood River fault (less than 3 m.y.) compared to the large 5- to 4-m.y. B.P. faults in the central Cascades might correlate with the age of this local heat-flow anomaly which, in turn, probably correlates with the age of volcanism at the Mount Hood volcano.

Williams and others (1982) pointed out that apparent net subsidence of the fault-bounded Mount Hood block was probably caused by magmatic withdrawal and crustal loading.



Allen (1966) considered the entire northern and central Oregon High Cascade Range to be in a volcano-tectonic depression. Correlation of heat flow and faulting could thus be a function of the amount of magmatic withdrawal and volcanic loading. It is likely that both regional extension and volcano-tectonic processes worked together to localize the faults.

The above hypotheses imply that the western Oregon lithosphere south of the Clackamas River fault zone and west of the faults concentrated at the westernmost edge of the High Cascade heat-flow anomaly may have acted as a relatively cool, stable block or microplate. Crustal spreading in the Basin and Range province to the east has, according to paleomagnetic models of Magill and Cox (1980), rotated western Oregon about 25° in a clockwise manner during the last 25 m.y. The axis of rotation in their model is in southern Washington. If the boundaries of this relatively undeformed microplate were governed by relative heat flow, then rotation of the Western Cascade lithosphere across a north-south zone of magma generation, possibly a north-south subduction zone, could explain the migration of both active volcanism and tectonic deformation from the Western Cascade Range toward the present High Cascade Range during the Neogene.

This eastward migration of the volcanic arc might also explain the location of the major zone of north-south faulting at the Cougar Reservoir fault west of the younger McKenzie River-Horse Creek fault (Chapter 4). The period of extensional deformation which caused the Cougar fault may have occurred when the boundary between the rigid Western Cascade crust and plastic High Cascade crust was west of the analogous, but several million years younger, Horse Creek-McKenzie River boundary. This may explain why many of the volcanic centers of the early High Cascade episode, such as in the Belknap-Foley area (Brown and others, 1980a; Flaherty, 1981), Echo Mountain quadrangle (Avramenko, 1981), and the Outerson Mountain area (Chapter 3), were located a few kilometers west of the current margin of the High Cascades.

The discontinuous nature of both the faulting and the volcanic episodes in the Cascade Range is, however, incompatible with a constant rate of rotation and Basin and Range spreading throughout the last 25 m.y. It is more likely that an acceleration of Basin and Range spreading occurred between about 10 and 8 m.y. B.P., coincident with the beginning of High Cascade mafic volcanism and the switch to the easterly position of the volcanic axis. It was also at about this time that (1) the current Basin and Range topography became well defined (Stewart, 1978), (2) the direction of Basin and Range spreading may have changed (Zoback and Thompson, 1978), (3) the eruption of dike-taxitic to compact high-alumina olivine tholeiites in the Basin and Range of Oregon began (Hart, 1982; Hart and Mertzman, 1983; McKee and others, 1983), and (4) rhyolitic volcanism began to migrate westward from easternmost Oregon along the northern margin of the Basin and Range (MacLeod and others, 1975). Compositional similarities of high-alumina basalts erupted from the High Cascade province in the last 9 m.y. to basalts of this age in the Basin and Range (see the following sections) further suggest that Basin and Range type of extensional tectonism may have strongly modified Cascade volcanism during the last 8 to 10 m.y. Increases in the rate of Basin and Range spreading may have produced the increases noted by Drake (1982) in the rate of subduction of the Juan de Fuca Plate about 10 m.y. B.P. The extension could be the product either of regional deformation of the North American Plate by interactions at the San Andreas transform boundary (Atwater, 1970) or of a combination of those interactions and back-arc spreading processes (e.g., Scholz and others, 1971).

## PETROCHEMISTRY

### Introduction

Numerous rocks have been chemically analyzed from each of the four map areas studied in detail for this report (see Appendix B). These analyses are by no means a comprehensive representation of the Western and High Cascade sequences, but the compositional fields of these samples and selected analyses from the literature are probably typical of the range of compositions in other areas.

Compositional fields from the literature are shown on various diagrams for comparison. Analyses of some samples of alkali-rich High Cascade mafic lavas were taken from the literature and plotted on compositional diagrams to illustrate this petrologically important group of rocks. It is beyond the scope of this report, however, to show all the available literature data.

### Analytical methods

All rocks except those from the Devils Creek area; Swift Creek samples P-604, TMO, P-509, P-626, and P-PHL; Cougar Reservoir samples Ri-22, Ri-46, Ri-60, and LB; and Look-out Point sample BB-PPAT were chemically analyzed by standard atomic absorption methods at the University of Oregon (Christine McBirney, analyst). The samples noted above were analyzed by standard induced argon coupled plasma techniques at the University of Utah Research Institute, Salt Lake City, Utah (Ruth Kroneman, analyst). All samples are listed in Appendix B with locations.

### Recalculation of data

Where specific oxide percents are listed in the text or on the chemical diagrams, the value is from an analysis which has been recalculated to a 100-percent total without volatiles and with all iron as Fe<sup>2+</sup>. This applies to values presented in this chapter and all following chapters. This recalculation removes some variations caused solely by weathering and low-grade metamorphism.

Normative mineral compositions have been calculated using an oxide analysis which has been recalculated to a 100-percent total without volatiles and with Fe<sub>2</sub>O<sub>3</sub>/FeO in a weight ratio of 0.31 (molecular ratio of Fe<sup>3+</sup>/Fe<sup>2+</sup> of 0.28). CIPW norms are listed in Appendix B, but the compositional diagrams utilize cation norms (e.g., see recommendations of Irvine and Baragar, 1971, p. 526).

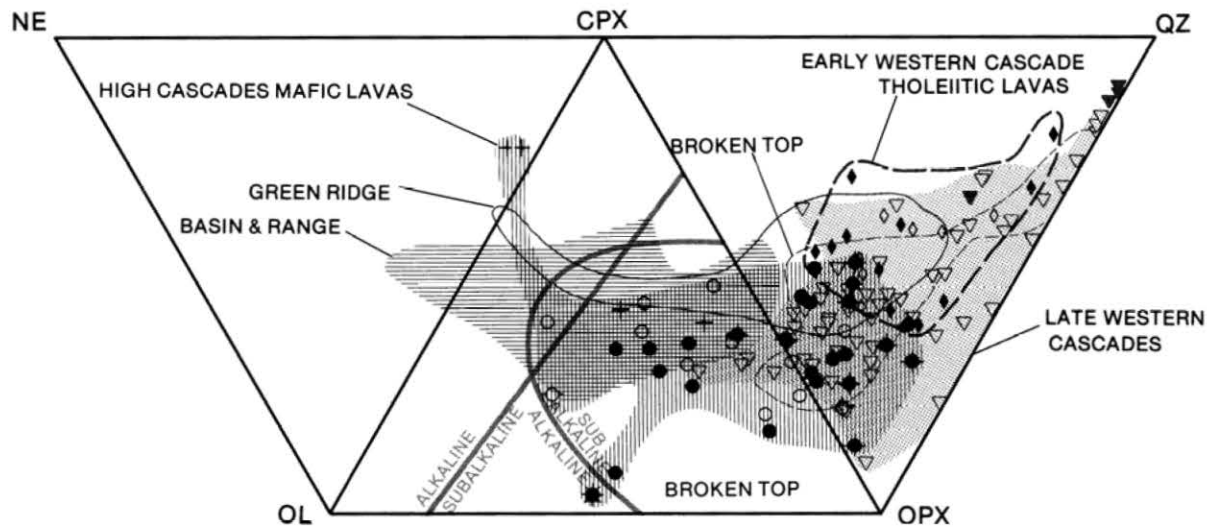
### Nomenclature

Volcanic rocks are named in this and following chapters primarily by means of a simple system based on SiO<sub>2</sub> (silica) of recalculated analyses (see previous section). The following rock names apply to rocks with silica contents in the designated ranges:

1. Silica <53 percent = basalt.
2. Silica ≥53 and ≤57 percent = basaltic andesite.
3. Silica >57 and <63 percent = andesite.
4. Silica ≥63 and <70 percent = dacite.
5. Silica ≥70 percent = rhyodacite.

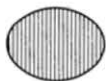
Rocks with silica contents of more than 70 percent and K<sub>2</sub>O contents greater than 4 percent are termed "rhyolite" rather than rhyodacite. Basalts which are not nepheline normative are nevertheless classified as "alkaline" if they plot in the smaller alkaline field on Chayes' (1965, 1966) normative clinopyroxene-olivine-orthopyroxene ternary diagram and "subalkaline" if they plot in the smaller subalkaline field (see Figure 2.6). Samples which plot in the borderline area on Chayes' (1965, 1966) diagram are termed "slightly alkaline." Nepheline-normative basalt is termed "alkali basalt." Rocks



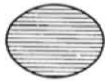


### LEGEND FOR COMPOSITIONAL DIAGRAMS

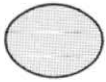
- Late High Cascade sample of this study
- Early High Cascade sample of this study
- ⊕ Plio-Cascade sample of Maynard (1974)
- + Cascades Formation sample of Jan (1967) along Scott Creek
- ◆ Mafic lavas of Devils Canyon of Barnes (1978)
- ★ Alkali-rich sample of Outerson Formation from White (1980 a)
- ▽ Late Western Cascades sample of this study
- ♦ Scorpion Mountain lavas sample of White (1980 a, c)
- ◇ Lavas sampled in this study which are correlative to the Scorpion Mountain lavas. All samples but two are from the lavas of Black Canyon at Lookout Point Reservoir. The other two samples are from the lavas of Hardesty Mountain (Lookout Point Reservoir) and the tuffs of Cougar Reservoir
- ▼ Non-tholeiitic early Western Cascades sample of this study. Samples suffer from slight hydrothermal alteration in most cases



Field of composition for early and late High Cascade mafic lavas (less than 58% silica)



Field of composition for 9 to 0 m.y. B.P. Basin and Range lavas of Hart (1982)



Full field of composition for late Western Cascade samples of this study



Field of composition for Broken Top volcano; includes only samples from the flanks of the volcano. Data taken from Taylor (1978)



Field of composition for early High Cascade mafic lavas of Green Ridge ( $\text{SiO}_2$  less than 58%). Data is from Hales (1975)



Field of composition of the diamond-shaped symbols above. Shows the range of composition of early Western Cascade tholeiitic lavas

Figure 2.6. Nepheline-olivine-clinopyroxene-quartz-quadrilateral. NE=nepheline; OL=olivine; CPX=clinopyroxene; OPX=orthopyroxene; QZ=quartz. The subalkaline-alkaline boundaries are those of Chayes (1965, 1966).

which are iron-rich enough to plot in the tholeiitic field of Irvine and Baragar's (1971) AFM diagram (Figure 2.7) are termed "tholeiitic" if they are not alkaline as defined in Figure 2.6. The term "icelandite" is used for andesites which plot in the tholeiitic field of Figure 2.7. The term "high-alumina basalt" is used for basalts with  $\text{Al}_2\text{O}_3$  over about 17 percent (e.g., see recommendations of Carmichael and others, 1974, p. 33).

### Methods of comparison

In this study, compositional variation diagrams utilizing simple oxides and normative mineral values (Figures 2.6-2.11) are used to compare and contrast groups of rocks from the Western Cascade, High Cascade, and Basin and Range provinces. The Cascade values are from this study and the literature, while the Basin and Range values are from samples of eastern Oregon basalts of Hart (1982) K-Ar dated between about 9 and 0 m.y. B.P. Neither the number of samples nor the size of compositional fields bears any relation to the volume of the rock units.

Because many processes of differentiation lead to silicic magmas of similar eutectic or thermal minimum compositions, it is often more profitable to compare the compositions of mafic volcanic rocks, which tend to reflect fundamental differences in parent magmas. Differentiation causes the compositional fields of silicic rocks from the different groups to completely overlap one another. To reduce the resulting clutter on the diagrams, lavas with more than 58 percent  $\text{SiO}_2$  from High Cascade, Green Ridge, and Basin and Range units were excluded so that compositions of the dominantly intermediate to silicic Western Cascade samples could be shown. The complete compositional spread of samples from the flanks of Broken Top volcano in the High Cascades was also shown to illustrate an entire High Cascade magma series (data taken from Taylor, 1978).

Useful compositional parameters for mafic rocks are the degrees of alumina, iron, and alkali enrichment of differentiation series. These parameters are sensitive indicators of petrogenesis (e.g., see discussions by Yoder and Tilley, 1962; O'Hara, 1965; Green and Ringwood, 1968; Ringwood, 1975; Yoder, 1976). The iron enrichment relative to magnesium

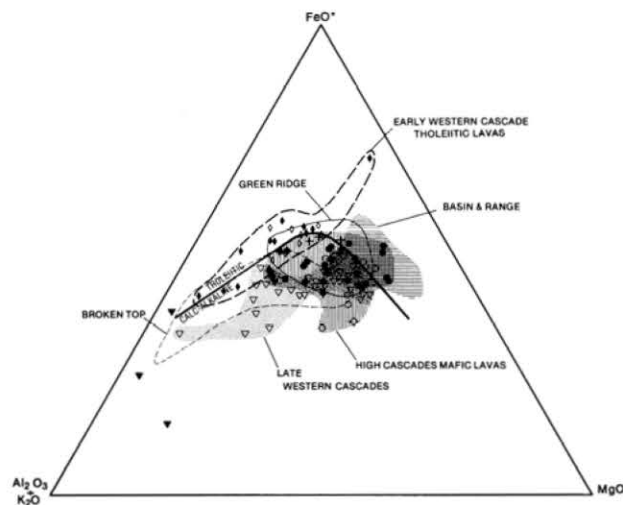


Figure 2.7.  $(\text{Na}_2\text{O}+\text{K}_2\text{O})\text{-FeO}^*\text{-MgO}$  ternary diagram. The tholeiitic-calc-alkaline boundary is taken from Irvine and Baragar (1971).  $\text{FeO}^*$ =all iron recalculated to  $\text{Fe}^{+2}$ ; other symbols as in Figure 2.6.

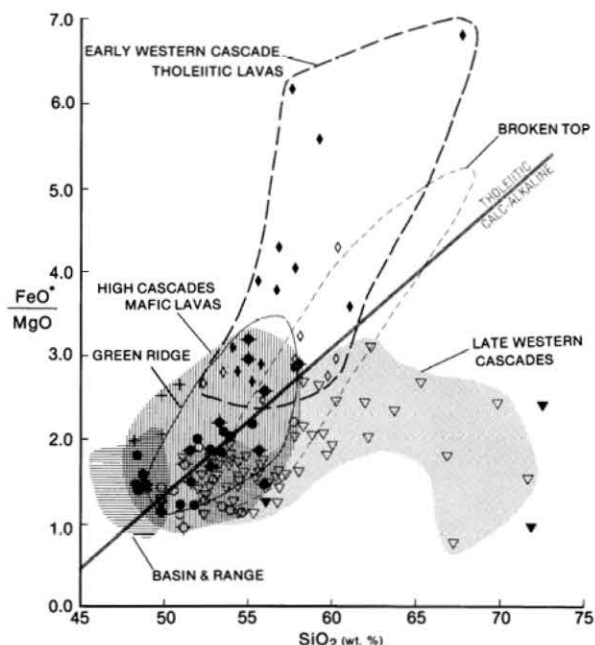


Figure 2.8.  $\text{FeO}^*/\text{MgO}$  versus  $\text{SiO}_2$  with Miyashiro's (1974) boundary between the calc-alkaline and tholeiitic compositional fields.  $\text{FeO}^*$ =all iron recalculated to  $\text{Fe}^{+2}$ . See Figure 2.6 for explanation of other symbols.

content can be shown on an AFM diagram and on a plot of  $\text{SiO}_2$  versus  $\text{FeO}^*/\text{MgO}$  ( $\text{FeO}^*$  = all iron recalculated to  $\text{Fe}^{+2}$ ) (Figures 2.7 and 2.8, respectively). Total iron enrichment is best shown on an  $\text{FeO}^*$  versus  $\text{SiO}_2$  diagram (Figure 2.9). Alumina content is shown on the  $\text{Al}_2\text{O}_3$  versus normative plagioclase diagram of Irvine and Baragar (1971) (Figure 2.10). The alkalinity is best shown by the amount of total alkalis versus the silica content (Figure 2.11) or as the amount of silica saturation in the previously mentioned diagram of Figure 2.6.

The samples presented here are compared to fields of composition of samples from other parts of the world by means of lines separating major types of differentiation series. Kuno (1966) described a suite of tholeiitic lavas from the outer margins of the Japanese volcanic arc which differ in composition from more alkaline and aluminous lavas in the main central part of the arc, which he called the "high-alumina basalt series." Both of these suites differ strongly from alkaline back-arc lavas, which he termed the "alkali basalt series." Macdonald and Katsura (1964) described similar alkali and tholeiitic basalt differentiation series in the Hawaiian Island chain but did not recognize the high-alumina basalt type noted by Kuno in the subduction-related island-arc terrane. Miyashiro (1974) plotted numerous island-arc differentiation series and arbitrarily split them on the  $\text{FeO}^*/\text{MgO}$  versus  $\text{SiO}_2$  diagram into iron-rich tholeiitic and iron-poor calc-alkaline series (Figure 2.8). Irvine and Baragar (1971) similarly divided basaltic suites into iron-rich, alumina-poor tholeiitic fields and iron-poor, alumina-rich calc-alkaline fields on the AFM and alumina versus normative plagioclase plots (Figures 2.7 and 2.10). Irvine and Baragar's fields took into account tholeiitic compositions from the ocean basin and continental flood basalts, both of which tend to be very iron-rich and alumina-poor compared to subduction-related island-arc suites.

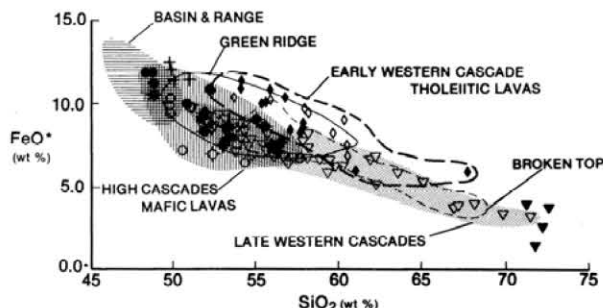


Figure 2.9.  $\text{FeO}^*$  versus  $\text{SiO}_2$ .  $\text{FeO}^*$  = all iron recalculated to  $\text{Fe}^{+2}$ ; symbols as in Figure 2.6.

All of the above systems were designed to deal with mafic rock series and produce definitions of calc-alkaline appreciably different from the original definition by Peacock (1931). Peacock designated a differentiation series "calc-alkaline" if it had samples with  $\text{alkalies}/\text{CaO} = 1.0$  at  $\text{SiO}_2$  contents between 56 and 61. It is now recognized that subduction-related, mature island arcs and continental margin arcs typically have iron-poor differentiation series with Peacock indices in this range.

The other methods of defining calc-alkaline are distinctly easier to apply than Peacock's method, since they do not necessarily require that a complete spectrum of comagmatic differentiates be available. The other methods are also more applicable to mafic magmas, which are of principal interest here.

## Comparisons

Whereas there is considerable compositional overlap between all of the Cascade units, there are some overall compositional differences, particularly between the mafic end members. In the extremes of their compositional range, the High Cascade basalts tend to be somewhat less silicic and richer in alkalies than the Western Cascade basalts. Lavas from the tholeiitic series of the early Western Cascade episode (the Scorpion Mountain magma type) which have been plotted on the diagrams are from mapped areas in the upper part of the sequence and have  $\text{SiO}_2$  contents no lower than 52.4 percent (e.g., field no. BB-30, Appendix B, Table B.3). Although not plotted on the compositional diagrams, data of Lux (1981) showed that the tholeiitic series of the early West-

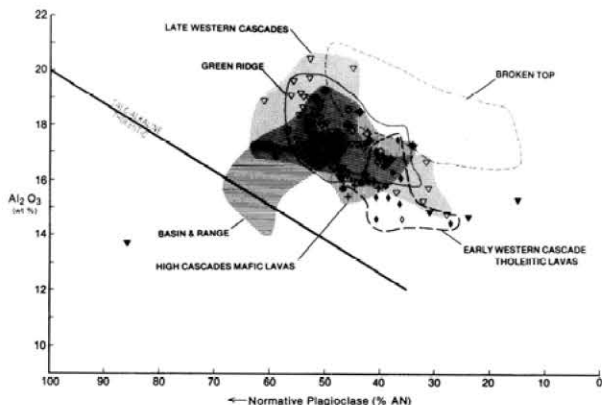


Figure 2.10.  $\text{Al}_2\text{O}_3$  versus normative plagioclase (AN = anorthite). The calc-alkaline-tholeiitic field boundary is from Irvine and Baragar (1971); other symbols as in Figure 2.6.

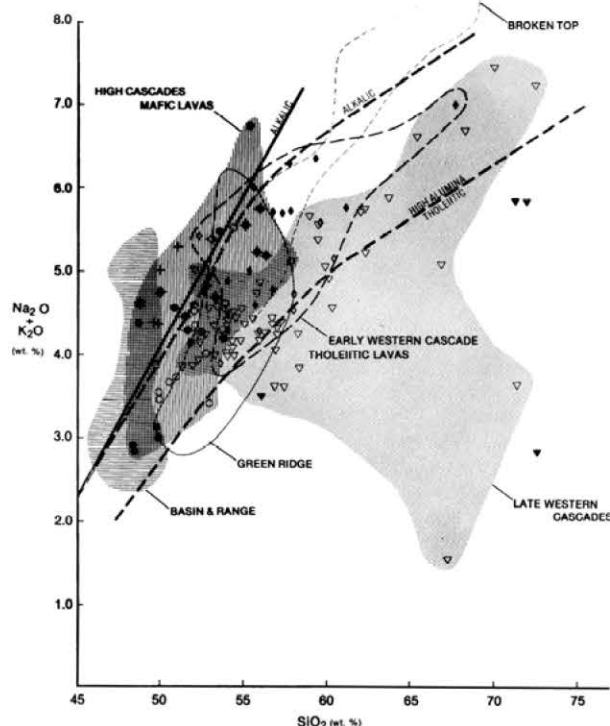


Figure 2.11.  $\text{Na}_2\text{O} + \text{K}_2\text{O}$  versus  $\text{SiO}_2$  with the alkali basalt and tholeiitic basalt fields of Macdonald and Katsura (1964) for the Hawaiian rocks. Also shown are the boundaries of alkali basalt, high-alumina basalt, and tholeiitic basalt fields of volcanic rocks of the Japanese arc (Kuno, 1966). Other symbols as in Figure 2.6.

ern Cascade episode has  $\text{SiO}_2$  as low as about 49.8 and 52.0 percent (recalculated volatile-free). All of these tholeiitic-series samples are, however, quartz normative (e.g., Figure 2.6; Lux, 1981), whereas some basalts of the late Western Cascade episode and a large number of the High Cascade basalts are undersaturated with respect to quartz. Aside from the Basin and Range compositional field, only the High Cascade samples plot into the alkaline compositional space on Figure 2.6 (see also Figure 2.11).

The sequence of late Western Cascade age is iron-poor relative to both the tholeiitic lavas of the early Western Cascade episode and the High Cascade lavas (Figures 2.7, 2.8, and 2.9). Rocks of the late Western Cascade episode are strongly calc-alkaline on all of the diagrams which show calc-alkaline fields. Calc-alkaline lavas and tuffs are also common in the sequence of early Western Cascade age (e.g., see Lux, 1981), although few of these rocks were collected in this study. All of the compositional fields of rocks of the High Cascade episode completely overlap those of rocks of the late Western Cascade episode. Iron-poor calc-alkaline rocks are thus very common in all of the Cascade units, and a general calc-alkaline composition is characteristic of Cascade rocks erupted throughout the last 40 m.y. Differences in the range of compositions within each group of rocks, however, are consistent and may be related to important differences in petrogenesis.

The fields of composition for the mafic lavas of the south-



eastern Oregon Basin and Range do not overlap the Western Cascade compositional fields at all, yet the High Cascade fields overlap both the Western Cascade and Basin and Range fields. If the Basin and Range field included samples from an area such as the Yamsay Mountain complex (Hering, 1981), which is part of the Basin and Range near the Cascades, there would be a great deal of overlap with Western Cascade compositions, because the Basin and Range volcanic centers near the Cascades, while having many compositional dissimilarities, also have a significant amount of calc-alkaline rock of intermediate composition. Because the petrologic interpretation and tectonic setting of the volcanoes near the Cascades are probably complex, chemical data from these volcanoes were excluded to facilitate comparison of Cascade rocks to rocks unquestionably generated within an area of Basin and Range tectonism free of any effects of late Tertiary Cascade processes. With this in mind, it is apparent from the compositional plots that the most mafic lavas of both the early and late High Cascade episodes have many attributes of contemporaneous Basin and Range basalts including (1) moderate iron enrichment, and (2) moderate alkali enrichment with some nepheline-normative basalt.

In terms of Kuno's (1966) fields of composition for island-arc rocks, both the Basin and Range and the most mafic and most alkaline of the High Cascade basalts are similar to Kuno's back-arc alkali basalt series (e.g., Figure 2.11). Alkali basalts, while very rare, occur in both sequences of early and late High Cascade age. Nepheline-normative basalts were collected by Jan (1967) from units of the late High Cascade episode in the Scott Creek drainage north of Belknap Hot Springs, and a slightly nepheline-normative sample of basalt of the early High Cascade episode from Green Ridge was analyzed by Hales (1975). Most nepheline-normative samples from the Basin and Range were erupted contemporaneously with rocks of the late High Cascade episode in the late Pliocene to Holocene (e.g., Hart, 1982; Hart and Mertzman, 1983).

The textures of many of the 9- to 0-m.y. B.P. Basin and Range basalts also resemble those of the High Cascade basalts. Both groups have abundant diktytaxitic lavas with colored subophitic to ophitic clinopyroxene. The most mafic end members of both groups also frequently have olivine in the groundmass and show no reaction relationship of olivine with pyroxene. Examples of High Cascade lavas of this type include the late High Cascade age Cupola Rock lavas of Flaherty (1981), early High Cascade age basalts collected by White (1980a,c) in the Breitenbush area, and some samples of the early High Cascade age lavas of Tipsoo Butte at Cougar Reservoir (Priest and Woller, Chapter 4).

The Western Cascade tholeiites generally show no alkaline tendencies and plot in fields characteristic of primitive to mature island-arc series (i.e., the tholeiitic and high-alumina fields, respectively, shown in Figure 2.11). The tholeiitic series of early Western Cascade age is similar in composition to the island-arc tholeiitic series characteristic of the outer margin of the Japanese arc on Kuno's (1966) diagram (Figure 2.11). The mafic lavas of the late Western Cascade episode plot instead in the high-alumina basalt series, typical of the main part of the mature andesitic arc in the Japanese islands (Figure 2.11).

Most of the Cascade basalts plotted here have alumina contents greater than 17 percent and can be called high-alumina basalt (see nomenclature section and Figure 2.10). A large number of the Basin and Range basalts of Hart (1982) are also high-alumina by this definition, although many have alumina contents less than 17 percent (Figure 2.10). Hart's (1982) average  $Al_2O_3$  for his "high-alumina olivine tholeiite" was 17.02 percent (his Table 3.11, p. 158), indicating that the

average sample is a borderline high-alumina basalt by the nomenclature of Carmichael and others (1974). Hart (1982) used Yoder and Tilley's (1962) definition of olivine tholeiite (i.e., a basalt which is neither quartz nor nepheline normative but which has significant olivine and hypersthene in the norm). By this definition, most High Cascade basalts are olivine tholeiites and the basalts of the early and late Western Cascade episodes are chiefly tholeiite to quartz tholeiite. This is a result of the high silica saturation characteristic of rocks of the Western Cascade episode (e.g., see Figure 2.6). Using both the classification of this paper and Yoder and Tilley's (1962) classification, the Basin and Range basalts are best described as alkaline olivine tholeiite to high-alumina alkaline olivine tholeiite; the Western Cascade basalts are subalkaline high-alumina olivine tholeiite to high-alumina quartz tholeiite.

One feature not shown on the diagrams is the bimodal nature of the southeastern Oregon Basin and Range sequence. In addition to the basalts, Basin and Range volcanic assemblages typically contain a large volume of highly silicic lavas and tuffs which are also very alkali-rich, primarily because of high  $Na_2O$ . This has given rise to such names as "soda rhyolite" to describe these silicic rocks. This bimodal basalt-rhyolite assemblage is typical of other parts of the Basin and Range province as well (e.g., Christiansen and Lipman, 1972). Whereas volcanic rocks of intermediate composition occur in the Basin and Range sequence, particularly in the westernmost part of the province, both the High Cascade and Western Cascade sequences contain a much larger volume of intermediate lavas and tuffs of andesitic to dacitic composition. This assemblage of mafic and intermediate rocks is typical of subduction-related volcanism on island arcs and continental margins throughout the world (e.g., Dickinson, 1968).

Another feature not illustrated by the compositional diagrams is the upward increase in more silica-rich volcanic rocks of both the early High Cascade and late High Cascade episodes. The sequence of early High Cascade age in the Outerson Mountain area has the most mafic rocks concentrated at the base of the section, with more basaltic andesite upward and high-silica dacite plugs at the top (Chapter 3). Likewise, the base of the section of early High Cascade age at Cougar Reservoir is diktytaxitic basalt (Chapter 4), but andesitic rocks are common in the upper part of the sequence farther east (Flaherty, 1981). The upward increase in frequency of andesite, basaltic andesite, and dacite relative to basalt in the High Cascade platform (sequence of late High Cascade age) has been recognized by many workers in many parts of the central Oregon High Cascade Range (e.g., Williams, 1942; Walker and others, 1966; Taylor, 1980).

To summarize, the Cascade sequence is fundamentally calc-alkaline in character but has changed in composition through time. Rocks of the early Western Cascade episode are chiefly iron-rich quartz normative basalt to dacite and iron-poor calc-alkaline andesite to rhyodacite, with a large proportion of iron-poor dacite to rhyodacite tuff. The sequence of late Western Cascade age is free of the iron-rich, tholeiitic differentiates but has a large volume of calc-alkaline basalt to andesite and a smaller volume of dacitic tuff. In both early and late High Cascade times, a larger proportion of basalt was erupted than in earlier times, and the range of basalt compositions reached compositions more alkaline and silica-poor than earlier basalts. The High Cascade basalts tend to have  $FeO^*$  contents and  $FeO^*/MgO$  ratios that are somewhat higher than those of the basalts of the late Western Cascade episode but lower than tholeiites of the early Western Cascade episode. The most alkaline and least silicic of the High Cascade basalts resemble high-alumina olivine tholeiites erupted contemporaneously in the Basin and Range province of south-

eastern Oregon. The volume of rocks more silicic than basalt increases upward in both sequences of early and late High Cascade age.

The Cascade volcanic rocks resemble volcanic rocks erupted from subduction-related island-arc terranes. The iron-rich lavas of the early Western Cascade episode resemble island-arc tholeiites from the early stages of island-arc development and tholeiites erupted on the outer margin of island arcs. The lavas of the late Western Cascade episode resemble the rocks of Kuno's (1966) high-alumina basalt series which characterize the mature stage of island-arc development in the central part of an island arc. The High Cascade rocks have characteristics of both the high-alumina basalt series and Kuno's (1966) alkali basalt series characteristic of back-arc areas.

Finally, the reader should not expect to be able, on the basis of a few whole-rock analyses, to definitively place a Cascade rock sequence within one of the volcanic episodes described above. There is a very large volume of compositionally identical calc-alkaline basalt to rhyodacite in every episode. Only by detailed mapping and comprehensive sampling and mineralogic analyses can the episodes be distinguished. Even after all of this work, radiometric dates on the rocks are often necessary to establish which episode of volcanism is present.

## SPECULATIONS ON THE TECTONIC SETTING OF VOLCANIC EPISODES FROM COMPOSITIONAL EVIDENCE

### Introduction

It is beyond the scope of this paper to quantitatively evaluate possible petrologic models which might generate the volcanic rocks of the Cascades. In order to adequately treat petrogenesis in a quantitative manner, it is necessary to have much more data, especially trace-element and isotopic data, on individual volcanic centers. This would allow detailed modeling of comagmatic rock series. Approximate pressures, temperatures, and the fugacities of  $H_2O$  and  $O_2$  of magmas at the site of last equilibration in the crust or mantle can be estimated using microprobe data (e.g., see Carmichael and others, 1974). Unfortunately, neither microprobe nor adequate trace-element data are available from this study to quantitatively test partial melting or differentiation models. Even with additional data, it is likely that the study would yield a large number of petrologic models which could be related to a variety of tectonic processes.

It is nevertheless important that some petrologic speculation be developed, if for no other reason than to generate enough lively debate to encourage good quantitative studies of central Cascade volcanism. A few observations and assumptions, which in themselves are speculative, are made in this study in order to provide a basis for discussion:

1. The composition of volcanic rocks is chiefly a function of the following variables:
  - (a) The mineralogy and chemical composition of source rocks.
  - (b) Conditions of partial melting ( $T$ ,  $P$ ,  $f_{O_2}$ ,  $f_{H_2O}$ , percent melting).
  - (c) Path and rate of rise of magmas to the surface. These factors are important controls on the degree and conditions of equilibration of the magma with various wall-rock compositions and the amount of differentiation by crystal settling, vapor-phase transport, and other processes.
2. Since high rates of magma generation are commonly associated with active tectonic processes such as subduction and extensional faulting, it is likely that tec-

tonic and petrogenetic processes are intimately related. For example, Bacon (1983a) demonstrated a direct relationship between crustal stress and magma type at the Coso volcanic field.

3. Although far from perfect, there nevertheless is a correlation between specific compositional types of volcanic rock and specific tectonic environments (e.g., calc-alkaline andesites at convergent plate boundaries and tholeiitic basalts at divergent boundaries).
4. Observations 2 and 3 imply that tectonic processes very often have a characteristic effect on one or more of the variables of observation 1. This, in turn, implies that the composition of volcanic rocks may be used as a clue to the tectonic environment which prevailed when they were erupted.
5. It is apparent that composition of volcanic rocks does not represent proof of tectonic environment, because any of the variables of observation 1 can probably be duplicated in a number of tectonic environments under special circumstances. For example, a mantle source might be altered by subduction processes in such a way that calc-alkaline melts could be derived. The same source could then be tapped by some unrelated process in a different tectonic environment. The following models must be considered only unproven hypotheses.

### Early Western Cascade episode

The tholeiitic series of early Western Cascade age (the Scorpion Mountain magma type) consistently plots in the compositional fields of island-arc tholeiite (Figure 2.11), although White (1980c) pointed out that trace-element abundances of the Scorpion Mountain rocks are more similar to tholeiitic series from orogenic continental margins. The few available analyses of silicic rocks of the early Western Cascade episode are similar to calc-alkaline silicic fields on all of the chemical diagrams considered here. Island arcs in the initial stages of development typically erupt voluminous, relatively iron-rich basalts (Jakes and White, 1972). Island arcs overlying continental crust are characterized by the eruption of voluminous silicic rocks chiefly in the form of ash flows and falls (e.g., Jakes and White, 1969; Carmichael and others, 1974). The volcanic series of early Western Cascade age may represent the early stages of development of a subduction-related volcanic arc in an area underlain by significant continental crust. The series has tholeiitic lavas similar to primitive island arcs and voluminous silicic tuffs typical of island-arc terranes underlain by continental crust.

### Late Western Cascade episode

Rocks of the late Western Cascade episode have compositions typical of mature andesitic volcanic arcs. Andesitic volcanism of this kind is very commonly associated with areas of active subduction which have had well-developed subduction regimes for some time (e.g., Jakes and White, 1969). The late Western Cascade volcanism may be the result of partial melting which occurred in a maturing subduction regime initiated during early Western Cascade time.

### High Cascade episode

The High Cascade and Basin and Range volcanic series have chemical affinities to both the back-arc alkali basalt series and the high-alumina volcanic series on Kuno's (1966) diagrams. The Basin and Range basalts are part of a bimodal basalt-rhyolite assemblage which is typical of the extensional Basin and Range tectonic regime throughout the western United States (e.g., Christiansen and Lipman, 1972). The High Cascade sequence, however, has a significant volume of intermediate volcanic rocks and has been characterized by

eruption from a linear, north-south-trending volcanic axis with numerous composite cones. The overall composition and distribution of the High Cascade sequence, as well as previously mentioned heat-flow and plate-tectonic arguments (see structural geology section), suggest that subduction is presently occurring.

The definite compositional and textural affinities of contemporaneous High Cascade and Basin and Range basalts, however, argue for a petrogenesis for High Cascade magmas which is also partially related to processes which generated Basin and Range magmas. It is highly unlikely that eruption of alkaline high-alumina basalts in both the High Cascades and a large area of the Basin and Range beginning between 10 and 8 m.y. B.P. could be sheer coincidence.

The linkage of some High Cascade volcanic processes to processes operative in the Basin and Range province is central to understanding the nature of High Cascade volcanism. Similarities in composition and probably in petrogenesis between mafic lavas of the late High Cascade episode and mafic lavas of the eastern Oregon Basin and Range were first noted by Taylor (1980) and more completely discussed in a later study by Flaherty (1981). Priest and others (1981) pointed out the chemical and textural affinity of basalts of the early High Cascade episode to the eastern Oregon basalts. All of these workers concluded that basaltic magmatism in the Cascades may have been affected by partial melting processes linked to Basin and Range-like extensional tectonism.

Petrologic arguments of Flaherty (1981) suggested that extensional faulting may be necessary to explain the eruption of basalts of the early High Cascade episode. He showed that compositions of mafic end members of lavas of early High Cascade age in the Belknap Hot Springs area probably last equilibrated at about 10 kb (30-km [18-mi] depth). He called on crustal extension during early High Cascade time to bring these magmas rapidly to the surface without extensive re-equilibration and differentiation at shallower levels. Similar arguments for rapid ascent to the surface were advanced by him for basalts of late High Cascade age.

The above evidence points to increased extensional stresses in the Oregon Cascade Range during the last 8 to 10 m.y. These conclusions are in harmony with arguments in the structural geology portion of this report.

## Conclusions

The compositional data favor a tectonic history for the Cascades which includes three major stages:

1. A subduction zone formed and developed between about 40 and 18 m.y. B.P. This early Western Cascade episode was characterized by eruption of magmas similar to those evolved from primitive island arcs or from shallow subduction on the outer margins of mature island arcs.
2. Maturation of the subduction zone continued between about 18 and 9 m.y. B.P. This late Western Cascade period was characterized by eruption of calc-alkaline andesite and high-alumina basalt typical of mature island arcs over well-developed active subduction zones.
3. Modification of the pattern of structural deformation between 10 and 8 m.y. B.P. probably caused eruption of magmas more mafic and alkaline than previous magmas. The most mafic basaltic lavas of this High Cascade episode of magmatism resemble back-arc lavas of island arcs and even more closely resemble contemporaneous basalts of the Oregon Basin and Range province. The structural modification probably involved increased extensional deformation related to Basin and Range spreading. Continued eruption of

magmas similar to magmas of the late Western Cascade episode and presence of a north-south-trending line of composite calc-alkaline volcanoes argue for continued operation of an active subduction zone beneath the High Cascade province.

## SUMMARY AND CONCLUSIONS

The central Oregon Cascades has been the site of eruption of subduction-related volcanic rocks for the last 40 m.y. Calc-alkaline lavas and tuffs typical of subduction-related terranes have erupted throughout this time, but changes in the tectonic regime and evolution of the volcanic arc have caused some modification of both the composition and location of the Cascade volcanoes. Four episodes of volcanism can be recognized:

1. The early Western Cascade episode (40-18 m.y. B.P.): Eruption of silicic tuffs and lavas, lesser amounts of intermediate calc-alkaline lava, and a distinctive series of quartz-normative, highly iron-rich mafic lavas occurred over a broad area of the Western Cascade Range. These iron-rich rocks resemble island-arc tholeiites and are characteristic of the outer margins of subduction-related volcanic arcs in an early stage of development. Similar but more alkaline lavas and tuffs were erupted just east of the present High Cascade Range (i.e., western facies of the John Day Formation). The John Day Formation rocks may be the products of back-arc volcanic processes.
2. The late Western Cascade episode (18-9 m.y. B.P.): Calc-alkaline andesite, high-alumina quartz-normative to subalkaline basalt, and dacitic lavas and tuffs typical of mature, subduction-related island arcs were erupted during this episode. Again, the volcanism was spread over a large part of the Western Cascade Range and may have occurred within the present High Cascade Range as well.
3. The early High Cascade episode (9-4 m.y. B.P.): Voluminous flows of olivine-normative subalkaline to alkaline high-alumina basalt, often with diktytaxitic texture and moderately high  $\text{FeO}^*/\text{MgO}$ , characterized the initial eruptions of the early High Cascade episode. More basaltic andesite, andesite, and dacite than basalt were erupted toward the end of the episode. The volcanism was centered east of most of the vents of the late Western Cascade episode in and closely adjacent to the current High Cascade province. Westward-flowing lavas and ash flows probably banked up against east-facing north-south fault scarps in some areas, as at Cougar Reservoir, but numerous basalts and ash flows flowed without obstruction into the Deschutes Basin to the east.
4. The late High Cascade episode (4-0 m.y. B.P.): At about 5 to 4 m.y. B.P., broad uplift of the Western Cascade block and formation of major east-facing fault scarps preceded a major episode of basaltic volcanism from the High Cascade province. These basalts of the late High Cascade episode were even more highly diktytaxitic, and, in local areas, more mafic than the analogous initial pulse of basalt of the early High Cascade episode. The overall composition of basalts of both the early and late High Cascade episodes is, however, essentially the same. As in the sequence of early High Cascade age, the frequency of basaltic andesite and more siliceous rocks increases upward in the sequence of late High Cascade age, although diktytaxitic basalts are common throughout the volcanic pile. Basalts are



more abundant in sequences of both early and late High Cascade age than in those of Western Cascade age.

The eruption of diktytaxitic, olivine-normative alkaline to subalkaline high-alumina basalts during High Cascade time (9-0 m.y. B.P.) also occurred throughout a large part of the Basin and Range province of Oregon (Hart, 1982; Hart and Mertzman, 1983; McKee and others, 1983). Except in areas close to the Cascades, this Basin and Range volcanism produced a low volume of probably subduction-related intermediate calc-alkaline volcanic rocks which characterize the upper parts of volcanic piles of both early and late High Cascade age. The compositional and textural similarity of contemporaneous basalts in the Basin and Range and High Cascade provinces, along with the extensional faulting typical of both provinces during the last 8 to 10 m.y., leads to the speculation that Basin and Range type of tectonism may have modified subduction-related central Oregon volcanism. Other events in the Basin and Range which also began about 10 to 8 m.y. B.P. include (1) the beginning of westward migration of silicic volcanism across the High Lava Plains and Basin and Range provinces from a starting point east of the Harney Basin (MacLeod and others, 1975), (2) definition of the present physiography of the Basin and Range province (Stewart, 1978), and (3) possible change in the direction of Basin and Range spreading (Zoback and Thompson, 1978).

The contemporaneity of the above events with a major modification of Cascade volcanism and with major changes in the plate-tectonic regime of western North America suggests that the volcano-tectonic histories of the High Cascades and Basin and Range are closely linked. A model was proposed whereby a microplate of cool, relatively stable Western Cascade lithosphere migrated westward in response to Basin and Range spreading during the Neogene. The eastern boundary of this microplate at any given time was the zone of high heat flow and partial melting at the Cascade arc.

An acceleration of Basin and Range spreading and concomitant increase in the rate of subduction of the Juan de Fuca Plate about 10 to 8 m.y. B.P. (see Drake, 1982, for rate of subduction) caused localization of extensional deformation and mafic magmatism in the vicinity of the High Cascade province. A possible second episode of accelerated extension about 5 to 4 m.y. B.P. caused additional extensional faulting and mafic volcanism at the eastern margin of the Western Cascade microplate. The eastern margin of the 5-4 m.y. B.P. microplate was about 16 km (10 mi) east of its position in the 10-8 m.y. B.P. episode in the Cougar Reservoir-Belknap Hot Spring area. The 10-8 and 5-4 m.y. B.P. microplate boundaries in that area are marked by major down-to-the-east, north-south normal faults. The younger fault set still has well-defined topographic scarps. The boundary farther north is less well defined and appears to break up into a series of right-lateral wrench faults where the High Cascade heat flow decreases across the Clackamas River area. Continuation of the High Cascade zone of high, albeit reduced, heat flow northward into Washington suggests that some extensional deformation may be localized at the boundaries of hot High

Cascade crust to the north as well. Magmatic withdrawal and loading of the crust in local areas of highly active volcanism have caused additional downfaulting of the High Cascade axis; the Mount Hood subsidence block (Williams and others, 1982) is an example.

One final question might be worth further investigation. Could the transition from volcanism of the early Western Cascade episode to that of the late Western Cascade episode have been caused by Basin and Range spreading? It is well established that Basin and Range spreading in a large part of Western North America began about 17 m.y. B.P. (Stewart, 1978). The oldest rocks typical of the late Western Cascade episode so far dated are also approximately 17 m.y. old.

Other lines of evidence which support linkage between the initiation of late Western Cascade volcanism and Basin and Range spreading include the following:

1. The proposed northern boundary of the Western Cascade microplate at the Clackamas right-lateral wrench fault was probably already active when the Grande Ronde Basalt flowed into the area about 15.3 m.y. B.P. (Beeson and Moran, 1979; Beeson and others, in preparation; see Lux 1981, 1982, for the age of the Grande Ronde Basalt).
2. The lower part of the sequence of late Western Cascade age is characterized by basalts (albeit basalts less mafic than High Cascade basalts) in the Outerson Mountain and Waldo Lake-Swift Creek areas. Could these episodes of mafic volcanism be analogous to basaltic eruptions which initiated the early and late High Cascade episodes? Some of the basalts at the base of the Waldo Lake-Swift Creek sequences of late Western Cascade age are slightly diktytaxitic, similar to some basal High Cascade basalts (Chapter 6).
3. Many of the volcanic centers of the late Western Cascade episode appear to be concentrated somewhat east of vents of the early Western Cascade episode (e.g., see observations of Peck and others [1964] about their Little Butte versus Sardine vents and of Power and others [1981] about the distribution of intrusive rocks of late Western Cascade age).
4. There was a widespread mid-Miocene episode of basaltic volcanism throughout the southeast Oregon Basin and Range, which was the time of eruption of the Columbia River Basalt Group from fissure systems east of the Cascade Range (e.g., see Walker's [1977] map which indicates that most of these eastern Oregon basalts have ages between 13 and 16 m.y.).

It may be that the less mafic compositions of the basaltic sequence of late Western Cascade age relative to the High Cascade basaltic sequence are a function of slower Basin and Range spreading and less extension in the Cascades during late Western Cascade time. A slower rate of Basin and Range spreading between about 17 and 10 m.y. B.P. relative to the 10- to 0-m.y. B.P. period is supported by the low relief of the paleotopography of the Basin and Range during the 17- to 10-m.y. B.P. period (e.g., see Stewart's [1978] review).

## CHAPTER 3. PRELIMINARY GEOLOGY OF THE OUTERSON MOUNTAIN-DEVILS CREEK AREA, MARION COUNTY, OREGON

By George R. Priest and Neil M. Woller,  
Oregon Department of Geology and Mineral Industries

### ABSTRACT

The Outerson Mountain-Devils Creek area was the site of mafic and subordinate andesitic to dacitic volcanism from about the middle Miocene (before 11.5 m.y. B.P.) to about 4.8 m.y. B.P. Rock sequences of both the late Western Cascade and the early High Cascade episodes occur in the area. Both sequences begin with basal mafic flows which give way to more silicic volcanic rocks upward. The late Western Cascade episode culminated with eruption of andesitic and dacitic ash flows (the tuffs of Outerson Mountain), and the early High Cascade episode culminated with emplacement of dacite and andesite plugs and dikes.

Normal faulting on a N. 30° W. trend preceded volcanism of the early High Cascade episode (the Miocene-Pliocene lavas), and many of the basaltic flows in the sequence of early High Cascade age are olivine-normative, unlike the quartz-normative basalts of the late Western Cascade episode (lavas of Outerson Mountain). Uplift of the area some time after 4.8 m.y. B.P. was accompanied by a resurgence of highly mafic volcanism from the Mount Jefferson area to the east outside of the study area. Basaltic flows of the late High Cascade episode, followed the canyon of the ancestral North Santiam River as it cut into the uplifted Western Cascade block. The late High Cascade volcanic episode, while beginning with basalt flows more mafic than basalts of the early High Cascade episode, culminated with andesitic and minor dacitic to rhyolitic eruptions in the High Cascade Range to the east. The late High Cascade episode, like the early High Cascade episode, was accompanied by extensional faulting.

### INTRODUCTION

The Outerson Mountain-Devils Creek area lies in the Western Cascade physiographic province about 7 km (4.2 mi) southeast of Breitenbush Hot Springs (Figure 3.1). Local relief in the Devils Creek valley is about 620 m (2,034 ft). The South Fork of the Breitenbush River lies about 1.9 km (1.1 mi) north of Devils Creek. The area is characterized by steep, mature topography and poor bedrock exposure. A preliminary geologic map covering an area of about 15.5 km<sup>2</sup> (6 mi<sup>2</sup>) was produced in order to evaluate the drilling results from a temperature-gradient hole drilled near Devils Creek in 1979 (Figure 3.2).

Specific goals of the project were to (1) locate faults which might influence the circulation of hydrothermal waters, and (2) decipher a mass of conflicting geologic data which have been generated by numerous previous workers who have mapped in the area. K-Ar data (Appendix A) generated by Stanley H. Evans of the University of Utah Research Institute were particularly helpful with respect to the latter goal.

Because of time limitations, it was not possible to complete all of the needed detailed geologic mapping, and the small amount of mapping completed for this study should be considered to be very preliminary in nature. In order to resolve the most critical problems in the area, a detailed geologic map covering the area from Sardine Mountain to Mount Jefferson is needed.

### PREVIOUS WORK

The geology of the study area has been mapped either wholly or in part by six different workers. The area was first studied by Thayer (1936, 1939) during his mapping of the North Santiam River drainage. Thayer (1939) mapped all of the rocks of the area as the Outerson volcanics, which he termed the oldest formation of the High Cascade series. He

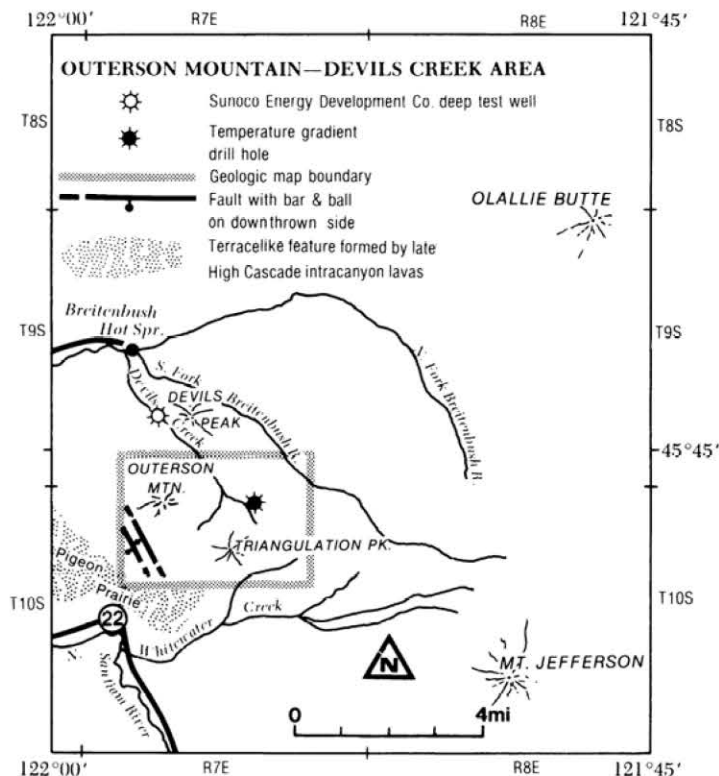
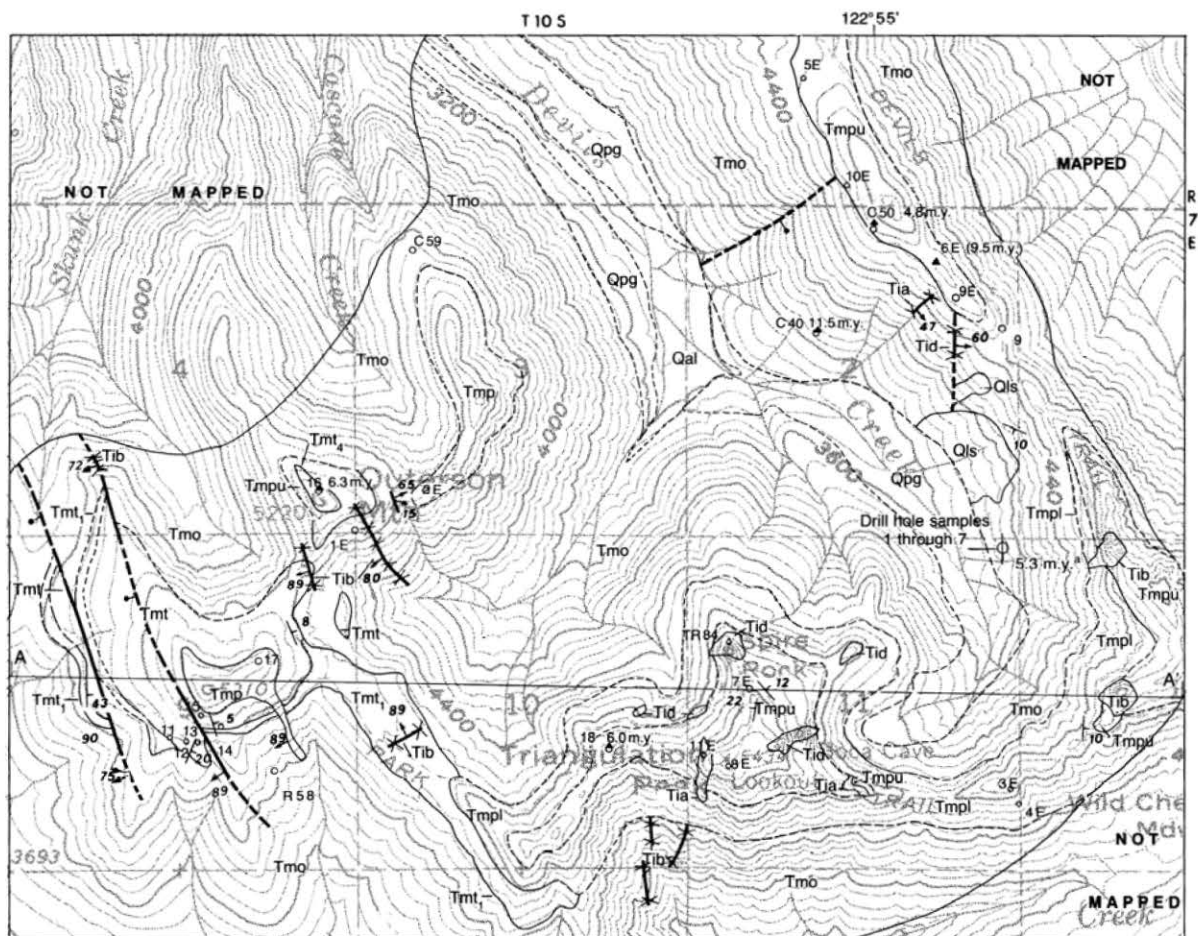
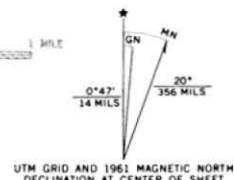
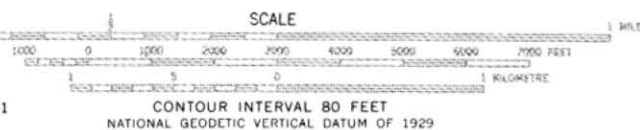


Figure 3.1. Map showing location of the Outerson Mountain-Devils Creek map area and other localities mentioned in the text.



Base map by U.S. Geological Survey — enlarged version of Mount Jefferson-Devils Creek 15' quadrangle (original scale 1:62,500). Control by USGS and USC&GS  
Topography by photogrammetric methods from aerial photographs taken 1949 and 1958. Field checked 1961  
Polyconic projection. 1927 North American datum



Geology by G.R. Priest and N.M. Woller  
Field work dates: 1979, 1981, 1982

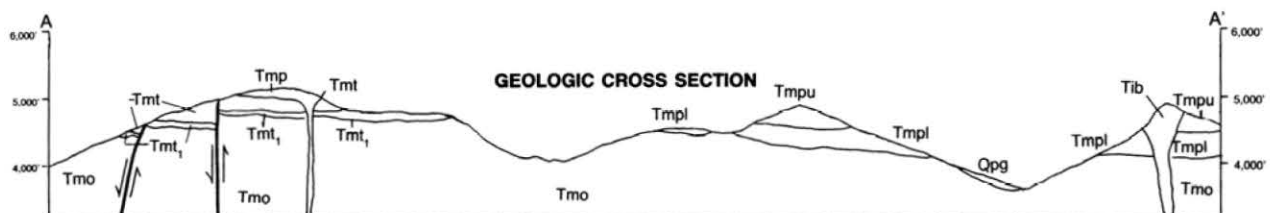


Figure 3.2. Map of the geology of the Outerson Mountain-Devils Creek area (both pages). Map is a modification of the maps of Clayton (1976) and Rollins (1976). See Tables 3.1 and 3.2 for detailed descriptions and correlations.



## EXPLANATION

### SURFICIAL DEPOSITS

Qal	<b>Recent alluvium (Quaternary):</b> <i>Unconsolidated sands and gravels of Holocene age</i>
Qpg	<b>Pleistocene glacial deposits (Pleistocene):</b> <i>Till and outwash sediments</i>
Qls	<b>Landslide debris (Quaternary)</b>

### BEDROCK GEOLOGIC UNITS

#### Volcanic rocks of the early High Cascade episode

Tmp	Tmpu	<b>Miocene-Pliocene lavas, undifferentiated (upper Miocene-lower Pliocene):</b> <i>Locally vented, fine-grained basaltic andesite lavas. Where possible, unit has been divided into (1) upper Miocene-Pliocene lavas (Tmpu), which are chiefly glomeroporphyritic olivine-plagioclase-clinopyroxene basaltic andesite lavas for which highest quality K-Ar data indicate ages between 4.8 and 6.3 m.y., and (2) lower Miocene-Pliocene lavas (Tmpl), which are chiefly fine-grained basalts and low-silica basaltic andesites with olivine as the only phenocrystic phase and which are probably latest Miocene in age</i>
	Tmpl	

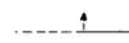



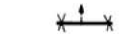
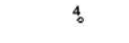
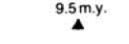
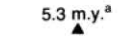


#### Volcanic rocks of the late Western Cascade episode

Tmt	Tmt <sub>4</sub>	<b>Tuffs of Outerson Mountain (upper Miocene):</b> <i>Five nonwelded ash-flow sheets with minor interbedded volcanoclastic sediments. Unit is underlain by unit Tmo and overlain by flow dated at 6.3 m.y. B.P. at Outerson Mountain. Two of the ash flows are thick and extensive enough to be mapped separately in this area: (1) unit Tmt<sub>4</sub>, a thick, nonwelded gray andesite ash-flow sheet composed of two or more individual ash flows, and (2) unit Tmt<sub>1</sub>, a cream-colored, nonwelded dacite ash-flow tuff</i>
	Tmt <sub>1</sub>	
Tmo	<b>Lavas of Outerson Mountain (middle-upper Miocene):</b> <i>Chiefly basaltic andesite with some quartz normative basalt and two-pyroxene andesite; bedded and massive hyaloclastic, partially palagonitized units are interbedded in the upper part. A sill K-Ar dated at 11.5 m.y. B.P. occurs in lower part; unit is below flow of unit Tmp dated at 6.3 m.y. B.P.</i>	

### SUBVOLCANIC INTRUSIVES

Tid	<b>Dacitic plugs and dikes (upper Miocene-lower Pliocene):</b> <i>Glassy, glomeroporphyritic orthopyroxene dacite; some plugs and dikes cut unit Tmpu; dike not found in this study reportedly yielded date of 5.75 m.y. B.P. (Sutter, 1978; White, 1980c; Fiebelkorn and others, 1982)</i>
Tia	<b>Andesitic plugs and dikes (upper Miocene-lower Pliocene):</b> <i>Two-pyroxene andesite; one plug cuts unit Tmpu at Triangulation Peak</i>
Tib	<b>Basaltic andesite plugs and dikes (middle Miocene-lower Pliocene):</b> <i>Dark, fine-grained basaltic andesite; locally glomeroporphyritic with olivine, plagioclase, and clinopyroxene phenocrysts; cuts unit Tmpu on east edge of map; sill reported at lower elevations by White (1980c) yielded a K-Ar date of 11.5 m.y. B.P. (Sutter, 1978; Fiebelkorn and others, 1982)</i>

### GEOLOGIC SYMBOLS

	<b>Bedrock contact:</b> Dashed where inferred beneath thin colluvial deposits or in areas not traversed. Arrow = dip
	<b>Normal fault:</b> Bar and ball on downthrown side; arrow indicates dip. Dashes where inferred beneath thin colluvial deposits or in areas not traversed
	<b>Strike and dip of fault zone:</b> Arrow = dip; diamond arrow = rake of slickensides
	<b>Strike and dip of bedded units</b>
	<b>Dike:</b> Arrow indicates dip
	<b>Chemically analyzed sample:</b> Number = sample number of this study, Appendix B, Table B.1; or, with an E suffix, from Appendix B, Table B.5. C prefix = sample number of White's (1980c) Appendix 2; TR prefix = sample number of Rollins' (1976) Appendix F
9.5 m.y. 	<b>K-Ar date with radiogenic argon greater than 10 percent.</b> Dates from White's (1980c) samples were generated by Sutter (1978) and recalculated by Fiebelkorn and others (1982)
5.3 m.y. <sup>a</sup> 	<b>K-Ar date, but sample has been affected by low-grade alteration</b>
(9.5 m.y.) 	<b>K-Ar date with radiogenic argon 10 percent or less</b>
	<b>Geothermal temperature-gradient hole:</b> 152 m deep, 16.58°C @ 152 m; terrain-corrected gradient = 72.6°C/km; heat flow = 101 mW/m <sup>2</sup> ; seven samples chemically analyzed (see Appendix B, Table B.1, where field numbers indicate depth in feet below surface). K-Ar date was from a slightly altered sample at 134-m depth

described the rocks as a varied assemblage of mafic lavas, flow breccias, and tuffs.

On their geologic map of western Oregon, Wells and Peck (1961) mapped the study area as Pliocene-Pleistocene basalt and andesite, with a mafic intrusion on the south flank of Outerson Mountain. The regional geologic map of Peck and others (1964) showed the area as Quaternary-Tertiary basalt and andesite, with a volcanic plug in the same locality as the mafic intrusion on Wells and Peck's (1961) map. The intrusive rocks shown on both maps, however, according to this study, are gray ash-flow tuff intruded by a very small dike.

Clayton (1976) mapped most of the area as part of his master's thesis. His map included a much larger area than the area in Figure 3.2 and encompassed Breitenbush Hot Springs. He recognized seven rock units in the area but had neither radiometric age data nor chemical analyses of rock units. Two of his units, the Lake Leone sediments and the Outerson tuff, do not occur in the mapped area but are present outside of it. Differences between the nomenclature adopted here and Clayton's (1976) names are a result of differences in placement of rock-unit boundaries. This is discussed in detail in the following sections. The western part of the map shown in Figure 3.2 is a small revision of part of Clayton's (1976) map.

The northern edge of Rollins' (1976) master's thesis map overlaps the study area. Rollins divided the rocks cropping out in this overlap zone into three units and showed the detailed distribution of dikes and plugs in the area. For this study, the distribution of many of the dikes and plugs in the Triangulation Peak area has been taken directly from his map, and the contacts of many of his units match the contacts mapped in this study. Rollins (1976) conducted extensive chemical and petrographic analyses of rock units but had no radiometric data. There are also some minor differences between the separation of rock units between this study and Rollins' study, but the southern part of the map in Figure 3.2 should be considered a slightly revised version of the northern part of his excellent map.

Hammond and others (1980) published a compilation map which combined all of the units recognized by Rollins (1976) and Clayton (1976) into two major units: the Outerson basalt and overlying older High Cascade basalt. Their map also showed some of the local intrusive rocks and included some inferred faults not recognized by previous workers. The inferred faults were not found in this study, but the general age relationships inferred by Hammond and others (1980) are similar to those found here. Hammond and others (1980) had access to new K-Ar data from their own study and work of Sutter (1978) and White (1980a,c).

The 1:62,500-scale map of Hammond and others (1982) showed the geology for a large area from the Clackamas River to the North Santiam River. Contacts on this map within the study area corresponded closely with those of Clayton (1976), although there were a few additional faults and some differences in the contacts and the names assigned to the units. The absolute ages of units are similar to ages inferred by Hammond and others (1980).

White (1980c) mapped the area as part of his doctoral dissertation. His map covers a much larger area, and the Outerson Mountain-Devils Creek area was not the focus of his research. Consequently, he made no attempt to do detailed volcanic stratigraphy in the Outerson Mountain area, although he did add several new chemical analyses and summarized all of the available radiometric dates. He combined the units of the Outerson Mountain area into two major units: the Elk Lake-Sardine formations (undifferentiated) and Pliocene-Pleistocene lavas (undifferentiated). White (1980c) showed also the distribution of some of the local intrusive rocks. The

units and faults of Hammond and others (1980) and White (1980c) do not closely correspond to one another in the study area.

In his map of the Breitenbush quadrangle, which includes the north side of the study area, White (1980a) used somewhat different terminology than in his dissertation (1980c). Also, some faults on his 1980a map extend farther south than on his 1980c map. Because the Breitenbush quadrangle extends well east of White's (1980c) dissertation map, his (1980a) Breitenbush map was able to show structures and rock units of the High Cascade province. A significant finding of White's 1980a study was an inferred north-south-trending fault which separates a thick section of young High Cascade rocks to the east from older rocks to the west. The fault projects just east of the present study area and may be the western boundary of a major graben along the High Cascade axis. Hammond and others (1980, 1982) did not show this fault, although Thayer (1936) did show a fault in this approximate location. Further detailed mapping should be done to resolve this problem.

To summarize, the map completed for this study is a revision of the maps of Clayton (1976) and Rollins (1976). The map also covers a small area east of both of their maps.

## VOLCANIC STRATIGRAPHY

### Introduction

General lithologic summaries and thicknesses of bedrock units occurring in this area are listed in Table 3.1, and chemical analyses are given in Appendix B. Rock names are assigned according to the classification of Chapter 2. The relationship of geologic map units to units of previous workers is shown in Table 3.2. The following text descriptions stress the characteristics of map units which served to distinguish them from one another. Evidence will be given for relative and absolute ages assigned to each formation.

The rock units are grouped for convenience into the regional volcanic episodes discussed in Chapter 2. Only rocks of the late Western Cascade and early High Cascade episodes occur in the immediate study area, but closely adjacent lavas of the late High Cascade episode are also discussed in order to give a complete geologic history.

### Volcanic rocks of the late Western Cascade episode

**The lavas of Outerson Mountain (unit Tmo):** Basal flows of the lavas of Outerson Mountain are chiefly quartz-normative basalts which give way to basaltic andesite and some glomeroporphyritic two-pyroxene andesites in the upper part. The basaltic lavas differ from the overlying basaltic rocks of the early High Cascade episode by having several generations of stubby random to pilotaxitic groundmass plagioclase and by having much less olivine relative to orthopyroxene in the groundmass. Olivine tends also to be mostly altered to greenish or yellowish saponite, whereas the younger rocks generally have either iddingsitized or fresh olivine. Diktytaxitic lavas, which occur locally in overlying units, are absent from the Outerson Mountain lavas.

The Outerson Mountain lavas also have many more pyroclastic units than basaltic units of the early High Cascade episode. Hyaloclastic debris flows and bedded, possibly surge, deposits are common in the upper part of the sequence. The overlying tuffs of Outerson Mountain represent the culmination of a general trend toward higher silica contents and more frequent pyroclastic eruptions upward in the sequence of late Western Cascade age.

The lavas of Outerson Mountain are probably middle Miocene in age. They are capped at Outerson Mountain by a

Table 3.1. *Stratigraphy of volcanic rock units in the Outerson Mountain-Devils Creek area, central Cascade Range, Oregon.*  
*Opx = orthopyroxene, cpx = clinopyroxene, px = pyroxene, pl = plagioclase, ol = olivine, hb = hornblende*

Regional volcanic episode	Informal formation and map symbol	Informal member and map symbol	K-Ar dates (m.y. B.P.)	Maximum exposed thickness	Typical SiO <sub>2</sub> <sup>1</sup> (wt. %)	Chief phenocrysts	Average total percent phenocrysts	Lithologic description
Early High Cascade	Miocene-Pliocene lavas, undifferentiated (Tmp)	Upper Miocene-Pliocene lavas (Tm <sub>pu</sub> )	6.3 ± 0.2 (6.0 ± 0.2) <sup>2</sup> (9.5 ± 1.3) <sup>2</sup> 4.8 ± 0.2 <sup>3</sup>	242 m (794 ft)	53	Pl, cpx, ol	10	Dark-gray glomeroporphyritic basaltic andesite lavas with 1- to 2-mm subhedral phenocrysts in a pilotaxitic to felty groundmass.
		Lower Miocene-Pliocene lavas (Tmpl)	—	98 m (320 ft)	52	Ol	3	Dark-gray fine-grained basalt and basaltic andesite flows with 0.1- to 0.5-mm ol phenocrysts in an insert to subophitic groundmass of pl+ol+cpx; flows with pilotaxitic textures and/or pl+cpx ± opx phenocrysts occur locally.
	Subvolcanic intrusives	Dacitic intrusives (Tid)	5.75 ± 0.10 <sup>3</sup>	—	69	Pl, opx	7	Medium-gray glassy glomeroporphyritic plugs and dikes; unaltered; 1- to 2-mm subhedral phenocrysts.
		Andesitic intrusives (Tia)	—	—	59	Pl, cpx, opx	1-15	Dark-gray fine-grained to highly porphyritic andesites with very fine-grained, felty groundmasses; unaltered; 0.5- to 2-mm subhedral to euhedral phenocrysts.
Late Western Cascade to early High Cascade	Subvolcanic intrusives	Basaltic andesite intrusives (Tib)	11.5 ± 0.2 <sup>3</sup>	—	54	Pl, cpx, ol	5-10	Dark-gray, somewhat glomeroporphyritic plugs and highly phyrlic to fine-grained dikes and sills; ol altered to saponite in some samples; 1- to 3-mm subhedral phenocrysts.
Late Western Cascade	Tuffs of Outerson Mountain (Tmt)	Ash flow #5	—	18 m (60 ft)	69.8 (pumice)	Pl(2%), opx(1%) (pumice)	3	Cream-colored nonwelded high-silica dacite ash-flow tuff; 25% pumice lapilli, 65% ash, 10% dark-reddish-gray lithic fragments; slightly flattened pumice; 0.3-mm subhedral phenocrysts.
		Ash flow #4 (Tmt <sub>4</sub> )	—	85 m (280 ft)	58.1 (pumice)	Pl, cpx, opx, ol (pumice)	2	Medium-gray nonwelded low-silica andesite ash-flow tuff; at least two partings in the unit; 15% yellowish pumice, 55% ash, 30% gray scoriaceous pumice and andesitic lithic fragments; minor obsidian chips.
		Ash flow #3	—	9 m (30 ft)	65.2 (pumice)	Pl + opx (pumice)	<1	Yellowish-gray nonwelded dacite ash-flow tuff; 36% pumice lapilli, 55% ash, 6% andesitic lithic fragments, 2% obsidian fragments, 1% cinders; nearly aphyric.
		Ash flow #2	—	9 m (30 ft)	61.9 (pumice)	Pl(2%), cpx (1%), opx (<1%) (pumice)	3	Light-yellowish-gray nonwelded andesite ash-flow tuff; 50% pumice lapilli, 30% ash, 20% andesitic and palagonitic cinder fragments; 0.1- to 1-mm subhedral phenocrysts.
		Ash flow #1 (Tmt <sub>1</sub> )	—	49 m (160 ft)	67.0 (pumice)	Pl, opx, hb (pumice)	2	Cream-colored nonwelded dacite ash-flow tuff; 20% pumice lapilli, 60% ash, 20% andesitic lithic fragments; moderate deformation of pumice; 0.1- to 1-mm subhedral phenocrysts.
	Lavas of Outerson Mountain (Tmo)	—	(5.3 ± 0.6) <sup>4</sup>	372 + m (1,220 + ft) (bottom not exposed)	54	Pl, ol, cpx, opx	10	Dark-gray ol basaltic andesite flows and hyaloclastic deposits with numerous medium-gray two-px andesite flows interbedded in the upper part. Subhedral phenocrysts are 1- to 2-mm and are set in groundmass that is intergranular in the basaltic andesites and hyalopilitic in the andesites and hyaloclastites. Basalts are interbedded locally; ol and opx commonly partially or completely altered to smectite.
		—	—	—	—	—	—	—

<sup>1</sup> Recalculated to a 100-percent total, volatile-free.

<sup>2</sup> 10-percent or less radiogenic argon. Parenthesis indicates questionable date.

<sup>3</sup> Data from Sutter (1978), recalculated by Fiebelkorn and others (1982).

<sup>4</sup> Altered drill hole sample. Parenthesis indicates questionable date.



Table 3.2. Relationship of geologic units of the Outerson Mountain-Devils Creek area to units of previous workers. See Table 2.1 for descriptions of units

Regional volcanic episode	Unit and map symbol	Relationship
Early High Cascade	Miocene-Pliocene lavas, undifferentiated (Tmp)	Mapped as Triangulation Peak volcanics by Clayton (1976), Plio-Pleistocene lavas by White (1980c), older basalt and basaltic andesite by Hammond and others (1982), unit QTv by Hammond and others (1980), unit QTba by Wells and Peck (1961), unit QTv by Peck and others (1964), and Outerson volcanics by Thayer (1939).
Late Western Cascade to early High Cascade	Subvolcanic intrusives (Tid, Tia, Tib)	Mapped as Plio-Pleistocene dikes of Clayton (1976) and White (1980c), unit QTm of Wells and Peck (1961), and unit QTa of Peck and others (1964).
Late Western Cascade	Tuffs of Outerson Mountain (Tmt)	Mapped as the upper part of Clayton's (1976) Cheat Creek sediments and Rollins' (1976) Cheat Creek beds; mapped as part of White's (1980c) Plio-Pleistocene lavas, QTba of Wells and Peck (1961), unit QTv of Peck and others (1964), Outerson basalt of Hammond and others (1980), Rhododendron Formation of Hammond and others (1982), and the Outerson volcanics of Thayer (1939).
	Lavas of Outerson Mountain (Tmo)	Mapped as Outerson lava and breccia and lower part of the Cheat Creek sediments by Clayton (1976); mapped as the Nan Creek volcanics and lower part of the Cheat Creek beds by Rollins (1976); probably equivalent to Rollins' (1976) Grizzly Creek lavas below about 1,098-m (3,600-ft) elevation; mapped as unit QTba by Wells and Peck (1961), unit QTv by Peck and others (1964), Outerson basalt by Hammond and others (1980), basalt of Outerson Mountain and Rhododendron Formation by Hammond and others (1982), and Outerson volcanics of Thayer (1939).

flow dated at 6.3 m.y. B.P., and, according to White (1980c), a sill dated by Sutter (1978) at 11.5 m.y. B.P. (Fiebelkorn and others, 1982) occurs in the lower part of the sequence at Devils Creek.

**Tuffs of Outerson Mountain (unit Tmt):** Five small, nonwelded andesitic to dacitic ash-flow tuffs and some interbedded volcanoclastic deposits crop out on the unnamed ridge on the southwest side of Outerson Mountain. These ash flows, here informally named the tuffs of Outerson Mountain, occur in the area between Triangulation Peak and Skunk Creek where they fill an irregular erosional surface cut in the underlying lavas of Outerson Mountain (Figure 3.2). No flow directions were obtained in this study, but Clayton (1976) noted in exposures of the fourth ash-flow from the bottom that "alignment and blockage of some scoriaceous fragments indicate that flow direction was to the southeast." His observation is in agreement with the distribution of the tuffs, which indicates that they filled a northwest-trending paleocanyon.

The position of the paleocanyon appears to have been controlled by the distribution of easily eroded hyaloclastic and cindery deposits in the underlying lavas of Outerson Mountain. Therefore, the tuffs of Outerson Mountain directly overlie hyaloclastites of the lavas of Outerson Mountain in numerous localities, and, for this reason, previous workers combined the tuffs and hyaloclastites into one unit (e.g., the Cheat Creek sediments and Cheat Creek beds of Clayton [1976] and Rollins [1976], respectively). The tuffs, however, lie in steep intracanyon relationship with the older hyaloclastites and interbedded lavas of Outerson Mountain on the south slope of Outerson Mountain (Figure 3.2). The writers hypothesize that the ash flows are compositionally distinct from the underlying, dominantly mafic hyaloclastite and lava sequence and may have been deposited after a significant period of erosion. For these reasons, the tuffs are mapped separately in this study. To avoid confusion, this revision of previous

nomenclature required use of unit names different from those of previous workers.

One consequence of mapping the tuffs separately is that the detailed mapping of the Cheat Creek beds by Rollins (1976) in the Triangulation Peak area could not be directly used here. Rollins (1976) found the first ash flow of the tuffs in the uppermost part of his Cheat Creek sequence near Triangulation Peak, but the writers could not follow the first ash flow past the question-marked point on Figure 3.2 (southwest of Triangulation Peak). It is possible that the tuffs reappear along the contact between the Miocene-Pliocene lavas, undifferentiated, and the lavas of Outerson Mountain on the south side of Triangulation Peak. That contact was not examined.

Of the five ash flows, only the first and fourth are thick and areally extensive enough to be mapped separately. Lithologic characteristics which distinguish the ash flows from one another are as follows:

1. The first (lowermost) ash flow is the most altered of the five and has many more crystals in the ash-size fraction than the fifth ash flow, which is the one most similar to it. The first ash flow, unlike the other ash flows, has minor amounts of hornblende phenocrysts.
2. The second ash flow has the least ash and most pumice of any of the ash flows.
3. The third ash flow is characterized by ubiquitous obsidian fragments which are more abundant than in any of the other ash flows. It is also the least phyrlic of all of the ash flows.
4. The mafic composition of the fourth ash-flow unit (nearly basaltic andesite) and its darker color are distinctive. Crudely bedded surge(?) deposits in the lower part of the unit may be difficult to distinguish from the lavas of Outerson Mountain, where the ash-flow sheet lies on hyaloclastites of the lavas of Outerson Mountain.

tain. This problem led Clayton (1976) to include some of those hyaloclastites with the fourth ash flow. Close inspection of hyaloclastites of the lavas of Outerson Mountain will, however, disclose a complete absence of the yellowish pumice which comprises about 15 percent of the fourth ash flow.

5. The fifth ash flow is the most silicic of all of the ash flows, being nearly a rhyodacite by the classification of Chapter 2. It most closely resembles the first ash flow but has a much smaller crystal component in the ash fraction.

Some peculiar textural characteristics of the fourth tuff unit lead to the conclusion that it may have interacted with meteoric water during eruption. Where it lies in the bottom of a steep paleocanyon cut through the underlying ash flows, the fourth ash-flow unit has at its base several meters of irregularly bedded material resembling hyaloclastites of the underlying lavas of Outerson Mountain (hence the comment in number 4 above). These rocks may have been deposited by phreatic surge blasts prior to deposition of the main ash-flow sheet.

In some outcrops of the fourth tuff unit, the lower part of the main ash-flow sheet has a vague planar bedding and is much finer grained and better sorted than the rest of the ash-flow sheet. This facies of the ash-flow sheet may represent base surge blasts ahead of the advancing ignimbrite.

There are no radiometric dates on the tuffs of Outerson Mountain, but the tuffs clearly flowed into canyons cut into the lavas of Outerson Mountain. At Outerson Mountain, a flow of the upper Miocene-Pliocene lavas which caps the fourth tuff unit yielded a high-quality K-Ar date of 6.3 m.y. B.P. The lower Miocene-Pliocene lavas appear to overlie the first ash flow in the Triangulation Peak area.

### Volcanic rocks of the early High Cascade episode

**General observations:** As a whole, the volcanic rocks of the early High Cascade episode, like the underlying rocks of the late Western Cascade episode, appear to become somewhat more silicic upward, although some basalts occur throughout the section. The basal flows in the sequence are basalts which are more mafic than any of the basalts thus far analyzed from the underlying lavas of Outerson Mountain (e.g., all of the rocks of the lavas of Outerson Mountain are quartz normative unlike those of the Miocene-Pliocene lavas; see Appendix 2). The upper part of the sequence is mostly basaltic andesite, with minor basalt and andesite. Numerous glassy orthopyroxene andesite and dacite plugs which intrude the entire section of early High Cascade age in the Triangulation Peak area demonstrate the silicic nature of some of the final early High Cascade eruptions.

The distribution of the upper and lower parts of the sequence of early High Cascade age indicates that it buried a paleotopography with maximum local relief of about 240 m (800 ft). Outerson Mountain and the adjacent ridge to the southwest were the highest points in this map area when the eruptions of lavas of the early High Cascade episode began. The tuffs of Outerson Mountain and the hyaloclastic units in the upper part of the lavas of Outerson Mountain have been protected from erosion by the capping Miocene-Pliocene lavas of the early High Cascade episode.

K-Ar dates of  $6.0 \pm 0.9$  m.y. B.P. (0.49 percent K, 9 percent radiogenic  $Ar^{40}$ ),  $6.3 \pm 0.2$  m.y. B.P. (1.61 percent K, 63 percent radiogenic  $Ar^{40}$ ), and  $9.5 \pm 1.3$  m.y. B.P. (0.66 percent K, 10 percent radiogenic  $Ar^{40}$ ) have been obtained on the upper Miocene-Pliocene lavas in this study. The location from which the sample with the age of 9.5 m.y. was taken was originally thought to have been in the uppermost lavas of

Outerson Mountain (Priest and Woller, 1982), but this location was later found to have been plotted incorrectly. It is plotted correctly in Figure 3.2 as sample no. 6E. Sutter (1978) listed a date of  $4.8 \pm 0.2$  m.y. B.P. (0.747 percent K, 17.6 percent radiogenic  $Ar^{40}$ ) on a sample of the upper Miocene-Pliocene lavas at Devils Peak close to the sample which yielded a 9.5-m.y. B.P. date. The 6.3- and 4.8-m.y. B.P. dates are probably the most reliable, because both samples have higher radiogenic  $Ar^{40}$  and K than the other samples dated. No K-Ar data are available for the lower Miocene-Pliocene lavas.

The Miocene-Pliocene lavas are older than the nearby Pigeon Prairie and Minto Mountain lavas. The Minto Mountain and Pigeon Prairie lavas are intracanyon flows of the late High Cascade episode within the North Santiam River valley to the south. There are no K-Ar dates on the Minto Mountain or Pigeon Prairie lavas. If these intracanyon flows of the late High Cascade episode are similar in age to analogous flows at Foley Ridge to the south, then they could be 2 to 4 m.y. in age (e.g., Flaherty, 1981; Chapter 2).

**Miocene-Pliocene lavas, undifferentiated (unit Tmp):** The early High Cascade episode is represented in this area by locally vented, fine-grained basaltic andesite lavas. Where possible, the unit has been divided into the two subunits listed below:

**Lower Miocene-Pliocene lavas (unit Tmpl)—**The lower Miocene-Pliocene lavas, which lie at the base of the sequence of early High Cascade age, are the most mafic rocks in the map area. About 122 m (400 ft) of these lavas fill a northwest-trending paleocanyon cut in the lavas of Outerson Mountain.

The lower Miocene-Pliocene lavas are chiefly basalts characterized by abundant groundmass and phenocrystic olivine. Slender, unimodal plagioclase with intersertal to subophitic olivine and clinopyroxene characterize the groundmass. This is in contrast to the lavas of Outerson Mountain, which have various sizes of stubby groundmass plagioclase and intergranular textures. The lower Miocene-Pliocene lavas also have very few plagioclase phenocrysts, unlike the underlying lavas of Outerson Mountain and overlying upper Miocene-Pliocene lavas, both of which tend to have abundant, commonly glomeroporphyritic plagioclase phenocrysts. The only type of phenocryst in most lower Miocene-Pliocene lavas is olivine.

**Upper Miocene-Pliocene lavas (unit Tmpu)—**The upper Miocene-Pliocene lavas are chiefly basaltic andesite, with minor basalt and andesite, and generally have medium to coarse plagioclase phenocrysts in glomeroporphyritic intergrowth with olivine and clinopyroxene. Similar glomeroporphyritic lavas are common in the lower part of the lavas of Outerson Mountain near Outerson Mountain, but the greater alteration, coarser groundmass textures, and association with numerous andesite flows in the Outerson sequence are distinctive. The finer grain size, more mafic composition, and sporadic diktytaxitic texture of the lower Miocene-Pliocene lavas distinguish them from the upper Miocene-Pliocene lavas. Some fine-grained lavas are also interbedded in the upper Miocene-Pliocene lavas, but they are generally somewhat less mafic in composition than the lower Miocene-Pliocene lavas, with the exception of an olivine basalt flow at the top of Triangulation Peak.

**Intrusive rocks:** Numerous basaltic to dacitic dikes and small volcanic plugs occur throughout the area. The plugs account for many of the prominent peaks such as Spire Rock and Triangulation Peak. Plugs in the Triangulation Peak area are chiefly andesite, as at Triangulation Peak itself (58.8 percent  $SiO_2$ ), or dacite, as at Spire Rock (68.8 percent  $SiO_2$ , according to Rollins, 1976). The two plugs north of Wild Cheat Meadow are olivine-clinopyroxene-plagioclase-phyr

basaltic andesite with glomeroporphyritic textures similar to those of the upper Miocene-Pliocene lavas. As previously mentioned, these two plugs are probable vents for some of the upper Miocene-Pliocene lavas.

Most of the dikes trend north to northwest, and, like the sequence of early High Cascade age, most are basaltic andesites. Many of the dikes are definitely related to the early High Cascade volcanic episode. A large northwest-trending dike southwest of Outerson Mountain is the feeder for a flow of the early High Cascade episode which caps the tuffs of Outerson Mountain (Figure 3.2). A similar large basaltic andesite dike cuts the lavas of Outerson Mountain at Outerson Mountain and has slightly diktytaxitic texture—a texture characteristic of many of the units of the early High Cascade episode.

Dacite and andesite dikes and plugs are intimately associated with vent complexes of the upper Miocene-Pliocene lavas in the Triangulation Peak area, and a dacite dike reported by White (1980c) in the Outerson Mountain area had a K-Ar age of  $5.75 \pm 0.1$  m.y. (Sutter, 1978; Fiebelkorn and others, 1982). These silicic rocks are probably the youngest units in the map area.

Some of the subvolcanic intrusives were probably emplaced during the late Western Cascade episode. A basaltic andesite sill reported by White (1980c) near the base of Devils Peak yielded a K-Ar date of  $11.5 \pm 0.2$  m.y. B.P. (Sutter, 1978; Fiebelkorn and others, 1982).

### Volcanic rocks of the late High Cascade episode

No lavas of late High Cascade age (4 to 0 m.y.) occur in the map area, but a sample of basalt from the uppermost Pigeon Prairie lavas near the southern boundary of the map area was chemically analyzed (field no. PP in Appendix B, Table B.1). This flow is a slightly diktytaxitic basalt (49.4 percent  $\text{SiO}_2$ , volatile-free) with about 2 percent subhedral to anhedral olivine (0.6 mm long) and about 1 percent subhedral plagioclase phenocrysts (0.4 to 1.5 mm long) set in a pilotaxitic groundmass of plagioclase with intergranular clinopyroxene and Fe-Ti oxide. This sample and samples of Rollins (1976) are higher in normative olivine than any of the basalts from older units. Flows of the Pigeon Prairie lavas are present as intracanyon flows that followed canyons cut into all bedrock units of the study area as well as into a sequence of older lavas, the Minto Mountain lavas, of the late High Cascade episode (e.g., Rollins, 1976). The distribution and morphology of both the Pigeon Prairie and Minto Mountain lavas suggest that they originated from sources in the High Cascade province and flowed into ancestral North Santiam River valleys cut into the uplifted Western Cascade block (e.g., Rollins, 1976). No radiometric data are available for these rocks, but they are younger than the lavas dated at 4.8 m.y. B.P. at Devils Peak (see Sutter, 1978; White, 1980c). Intracanyon flows in this same geologic setting in other parts of the Cascades are generally less than about 4.0 m.y. in age (Priest and others, Chapter 2).

The Minto Mountain and Pigeon Prairie basaltic eruptions were followed by eruption of increasing quantities of basaltic andesite, andesite, and minor dacite from the Mount Jefferson area (e.g., Walker and others, 1966; Sutton, 1974). Walker and others (1966) described some rocks of late High Cascade age east of the study area which have silica in the 69 to 75 percent range, based on the refractive index of fused beads. About 2 km (1 mi) east of the study area, Walker and others (1966) mapped an outcrop of silicic volcanic rock (their unit QTr), which could, however, be part of either the early or late High Cascade episode and could be either dacite or rhyolite. The age and composition of these silicic volcanic rocks should be carefully investigated in order to evaluate the potential of

the area for geothermal resources.

## STRUCTURAL GEOLOGY

### Folds and regional tilting

The area lies on the eastern limb of the north-northeast-trending Breitenbush anticline of Thayer (1939). Where not adjacent to faults, dips in a few thinly bedded epiclastic units in the tuffs of Outerson Mountain vary between  $5^\circ$  and  $8^\circ$  to the east-northeast. The distribution of the first ash flow in the tuffs southwest of Triangulation Peak indicates that the tuffs there are subhorizontal (Figure 3.2). Working in a wider area, Rollins (1976) measured dips of about  $10^\circ$  to the southeast within rocks older than his Minto lavas. The Minto lavas are intracanyon lavas of the early part of the late High Cascade episode. Clayton (1976) measured  $5^\circ$  to  $15^\circ$  dips in the sediments within the lavas of Outerson Mountain and inferred an angular unconformity between these lavas of Outerson Mountain and the overlying tuffs of Outerson Mountain (his Cheat Creek sediments); Rollins (1976) came to similar conclusions. Clayton, however, also found evidence of tilting of a few degrees in lavas of late High Cascade age. It is difficult to differentiate such small dips from depositional dips in lavas, so Clayton's (1976) observations on the lavas of late High Cascade age are probably questionable. No evidence of tilting could be demonstrated in the upper Miocene-Pliocene lavas. Slight regional eastward tilting, perhaps related to folding on the Breitenbush anticline, probably ended prior to extrusion of lavas of the early High Cascade episode at Outerson Mountain and Triangulation Peak (i.e., before about 6.3 m.y. B.P.).

### Faults in the study area

Two small, northwest-trending faults are exposed on the south slope of the ridge southwest of Outerson Mountain. Both Rollins (1976) and Clayton (1976) recognized the easternmost fault of this fault set. Strikes and dips on these faults are not well constrained because of irregularities of the fault planes, but both appear to trend about  $N. 30^\circ W. \pm 10^\circ$  and dip between  $72^\circ$  and  $89^\circ$  to the west. Slickensides on the westernmost fault have a rake of  $90^\circ$  within the fault plane. The tuffs of Outerson Mountain are offset about 30 m (100 ft) down to the west at each fault. Tilting and minor shearing which affect the tuffs of Outerson Mountain adjacent to these faults do not appear to affect the overlying upper Miocene-Pliocene lavas. A feeder dike of the upper Miocene-Pliocene lavas trends  $N. 30^\circ W.$  and may follow a small shear or fracture zone associated with the other  $N. 30^\circ W.$  faults. The faulting took place after deposition of the tuffs of Outerson Mountain but before 6.3 m.y. B.P., the oldest high-quality date on the upper Miocene-Pliocene lavas.

Other small northwest- and northeast-trending faults occur in numerous localities, but many are too small to map. Most of these faults have only 1 to 2 m ( $3\frac{1}{2}$  to 7 ft) of movement at most. They are shown on the map (Figure 3.2) with symbols for the strike and dip of the fault zone where possible, but in many areas they were left off to avoid clutter at the map scale.

Hammond and others (1980) showed a northwest-trending and a northeast-trending fault between Outerson Mountain and Triangulation Peak. The oldest ash flow of the tuffs of Outerson Mountain forms a topographic low between the two peaks, but the ash flow is nowhere offset by faults in this low. They also recognized one of the northwest-trending faults noted in Figure 3.2.

Hammond and others (1982) showed five north- to northwest-trending faults in the study area. Only one of these faults closely matches the faults shown on Figure 3.2.



### Faults in adjacent areas—the “Cascade fault”

Thayer (1936) hypothesized that a 610-m (2,000-ft) high, east-facing fault scarp extended N. 10° E. from the eastern side of Mount Bruno (south of the study area), going beneath Outerson Mountain, to Collawash Mountain (north of the study area) prior to burial by “Pliocene” lavas. Following the contact of these “Pliocene” lavas with older rocks, he estimated an eastward slope on the topographic scarp of “500 ft per mile in Mount Bruno” and “1,500 ft per mile in Collawash Mountain.” Thayer (1939), however, found no evidence of this fault in his later mapping, although he was not certain it was not there.

White (1980a) showed some down-to-the-east, north-south faults east and southeast of Collawash Mountain which offset his Outerson formation down to the east. One of these faults cuts High Cascade lavas younger than 2 m.y., according to White’s (1980a) map. Whereas Thayer (1936, 1939) hypothesized a single fault scarp dipping toward the east, White (1980a) showed a complex series of step faults at Collawash Mountain. There is no evidence of this fault scarp at Outerson Mountain, where Thayer (1936) believed it was buried by these Outerson volcanics (part of his “Pliocene” lavas).

Rollins (1976) showed his Nan Creek and underlying Grizzly Creek lavas (both units combined as the lavas of Outerson Mountain in Figure 3.2) wedging out against a western highland of Breitenbush tuff at Bruno Mountain. Rollins (1976), however, interpreted this highland of Breitenbush tuff as an erosional unconformity rather than a fault scarp. He also concluded from his detailed mapping that the north-south course of the North Santiam River east of Bruno Mountain is not fault controlled.

Hammond and others (1980, 1982) showed no large down-to-the-east faults along the trend of Thayer’s (1936, 1939) “Cascade fault.” Hammond and others (1982), instead, showed most contacts between major sequences dipping toward the east in the southern part of their map area (near Mount Bruno). The contacts are cut by northwest-trending faults in the northern and central part of the area (Collawash Mountain and the Clackamas River), but no large down-to-the-east fault is shown. They concluded that there is no evidence that a large down-to-the-east fault separates the High Cascade Range and Western Cascade Range in their area. Hammond and others (1980), however, concluded that north-south normal faulting accompanied High Cascade volcanism during the last 5 m.y.

The Collawash Mountain area clearly needs some detailed mapping to determine whether it is, in fact, one outcrop of the scarp of a fault system analogous to the one hypothesized by Thayer (1936, 1939). Recognition of this structure in the Breitenbush area will depend on the ability to discriminate between older and younger mafic lavas—a task which is very difficult, if not impossible, without tight control from radiometric age determinations.

If there is a “Cascade fault” in the Breitenbush area analogous to the one in the Horse Creek-upper McKenzie River area (e.g., Avramenko, 1981; Flaherty, 1981), then it will have undergone offset chiefly during the interval between 5 and 4 m.y. B.P. and will probably be found east of high-standing outcrops of rocks older than this. Areas east of the study area of Figure 3.2 would be logical localities for this structure, if it is present. The work of Rollins (1976) and Hammond and others (1982), however, suggests that a search for this fault may be in vain.

### Conclusions

The study area has been dominated by mafic volcanism from before 11.5 m.y. B.P. to at least 4.8 m.y. B.P., although

subordinate amounts of andesite and dacite were erupted toward the end of both the late Western Cascade and early High Cascade episodes.

The late Western Cascade episode began with effusive eruptions of quartz-normative basalt, but basaltic andesite and lesser amounts of andesite dominated later eruptions. Near the close of the late Western Cascade episode, phreatic eruptions occurred when mafic magmas encountered surface water and ground water. Numerous andesite and basaltic andesite flows and autobreccias were erupted between the explosive eruptions. Sometime before 6.3 m.y. B.P., eruptions of dacitic to andesitic ash flows (the tuffs of Outerson Mountain) occurred from a nearby vent, possibly to the northwest or west. These ash flows represent the culmination of the tendency toward eruption of more highly evolved, silicic magmas in the latter part of the late Western Cascade episode.

Following the formation of small N. 30° W.-trending normal faults, eruption of olivine-normative basalt to basaltic andesite lavas occurred. These lavas of the early High Cascade episode are more mafic than lavas of the earlier late Western Cascade episode and include some slightly diktytaxitic flows. The basalts give way upward to basaltic andesites which were erupted between 6.3 and about 4.8 m.y. B.P. Sometime in the latter part of this early High Cascade episode, andesitic to dacitic lavas were erupted from the Triangulation Peak area. Numerous dacitic plugs and dikes in that area are the sub-volcanic equivalents of this closing phase of the early High Cascade episode.

Following a period of uplift and erosion, basaltic lavas from the High Cascade Range to the east flowed down a deep canyon south of the study area. Many of the basalts of the late High Cascade episode are more mafic than earlier basalts and are often diktytaxitic. Basaltic andesite, andesite, and minor dacite to rhyolite eruptions followed the basaltic activity in the High Cascade Range. This late High Cascade episode of activity probably occurred within the last 4 m.y. and, according to Hammond and others (1980), coincided with north-south normal faulting in surrounding areas.

### GEOTHERMAL RESOURCES

The study area is located adjacent to the southern margin of the Breitenbush Hot Springs Known Geothermal Resource Area (KGRA). The KGRA boundary runs east-west through Devils Peak. The KGRA is predominantly on U.S. Forest Service land, although areas around the hot springs are privately owned. Several springs have temperatures up to 92° C and discharge at about 3,400 liters (898 gallons) per minute (Brook and others, 1979). From chemical geothermometry, Brook and others (1979) estimated reservoir temperatures of 99° to 149° C, with a mean temperature of  $125 \pm 10^\circ$  C. They also listed a sulfate-water isotopic temperature estimate of 195° C (see discussion in Chapter 8).

Table 3.3 lists some analyses of well and spring samples collected for this study. The various minimum reservoir temperatures are similar to those calculated by Brook and others (1979), although the range goes to somewhat higher temperatures (e.g., 171° C for the silica geothermometer). The high silica values obtained here may, in part, be due to two factors. First, both samples which yielded high SiO<sub>2</sub> were from unfiltered samples acidified with ten drops of dilute hydrochloric acid. It is possible that some suspended silica-bearing material was partially dissolved by the acid, thereby enhancing the SiO<sub>2</sub>, although some other samples treated in this fashion did not yield high SiO<sub>2</sub> (Table 3.3). Also, silica appeared to be actively precipitating from the sample of boiling well water taken in 1980, and silica gel was removed from the filter paper. This filtered 1980 sample yielded a relatively

Table 3.3. *Estimated minimum reservoir temperatures and partial analyses from new samples of wells and springs in the Breitenbush Known Geothermal Resource Area (KGRA). Calculations were made according to methods of Fournier and Rowe (1966), Fournier and Truesdell (1973), Fournier (1979), and Mariner and others (1980)*

	Wellhead	Spring	Wellhead	Wellhead	Wellhead	Spring
Collection date	1980	12/79	2/23/78	2/10/78	2/10/78	?
Temperature	97.8	98.0	110.0	?	?	81.0
Filtered	Yes	No	No	No	No	?
SiO <sub>2</sub> (ppm)	116	175	44.2	96	173	128.6
Li (ppm)	1.5	1.78	0.03	1.41	1.9	0.0
Na (ppm)	600	651.0	85.5	675	690	707.4
K (ppm)	27	15.5	8.9	20	34	31.5
Ca (ppm)	81	103.0	21.7	77	90	96.6
Mg (ppm)	< 0.5	1.51	0.8	< 0.5	0.8	1.8
*Si (conductive)	145	171	96	135	170	152
*Si (adiabatic)	140	161	98	131	160	145
*Si (chalcedony)	120	149	66	108	148	127
*Si (amorphous)	25	48	19	15	47	30
*Si (cristobalite)	95	121	46	84	120	101
*Na-K	125	92	178	102	130	124
*Na-K-Ca 4/3β	125	98	92	116	134	129
*Na-K-Ca 1/3β	150	121	170	133	155	150
*Mg-corrected Na-K-Ca	—	100	64	—	105	137

\* Minimum reservoir temperature in °C.

low SiO<sub>2</sub> content of 116 ppm compared to the 175- and 173-ppm values obtained on the unfiltered samples. It may be that the unfiltered samples are more representative in that silica gel was not removed by filtering. The second factor which might have caused one of the two high SiO<sub>2</sub> values is the fact that one of the samples was taken from an artesian well rather than a surface spring. If there is less time for re-equilibration in a rapidly flowing well than in a spring, then the well sample may be more representative of the water at depth. Additional sampling needs to be done using various filtering and acidification procedures to determine the actual SiO<sub>2</sub> content of the water.

There are no hot springs in the immediate area of Figure 3.2, but there is evidence of a relatively high geothermal gradient. A 152-m (499-ft) well which was drilled specifically for temperature-gradient measurement had a bottom-hole temperature of 16.3° C and a relatively high gradient of 83.5° C/km. When this gradient is corrected for terrain and microclimate effects, it reduces to 72.6° C/km, with a calculated heat flow of 2.43 HFU (Black and others, Chapter 7; number T10S/R7E/11Aa, Appendix D). In the nearby Sisi Butte and Twin Meadows holes, which are about the same distance west of the High Cascade Range as the Devils Creek hole, gradients of about this same magnitude persist to depths of 460 and 600 m (1,509 and 1,968 ft), respectively (see numbers T8S/R8E/6Dd and T12S/R7E/9Da, Appendix D). It is thus likely that the Devils Creek gradient also persists to greater depths and represents conductive background heat flow. A heat flow of 2.43 HFU places the Devils Creek area within the main part of the High Cascade heat-flow anomaly of Blackwell and others (1978, 1982; also see Figure 7.2).

In the fall of 1981, Sunoco Energy Development drilled a deep test well about 1.2 km (0.72 mi) north of the map area of Figure 2.2 (SE¼ sec. 28, T. 9 S., R. 7 E.). The well was targeted to about 2,744 m (9,000 ft); the final drilled depth and results of testing are confidential. If the terrain-corrected gradient at Devils Creek persisted to 2,744 m (9,000 ft), a temperature of about 200° C would be expected (Priest and others, 1982b).

At present there are no firm data on possible thermal aquifers at depth in the area. The presence of many small faults and fractures, especially in the area southwest of Outer-son Mountain, may create some fracture permeability. There are insufficient publicly available drilling data to evaluate the permeability of stratigraphic units in possibly high-temperature rocks at depths of 3 km (1.8 mi). Tuffaceous epiclastic and pyroclastic rocks should occur at those depths (e.g., see Thayer, 1936; Hammond and others, 1982), but no measurements of their permeability are available. For a general discussion on geothermal exploration in Western Cascade terranes, the reader is referred to relevant portions of Chapter 8.

## CHAPTER 4. GEOLOGY OF THE COUGAR RESERVOIR AREA, LANE COUNTY, OREGON

*By George R. Priest and Neil M. Woller,  
Oregon Department of Geology and Mineral Industries*

### ABSTRACT

Volcanic rocks of the early and late Western Cascade episodes crop out at Cougar Reservoir west of the major north-south Cougar fault. Volcanic rocks of the late Western and early High Cascade episodes crop out on the east block of the Cougar fault. A drill hole on the east block revealed that at least 152 m (499 ft) of down-to-the-east movement has occurred on the fault and that the dip on the fault plane is greater than 74° to the east. The fault cuts units of late Western Cascade age (lavas of Walker Creek) that have been K-Ar dated at 13.2 m.y. B.P. Pleistocene outwash gravels that overlie the fault zone are not offset. Stratigraphic arguments suggest that 366 m (1,200 ft) to possibly more than 1,033 m (3,388 ft) of down-to-the-east movement on the fault may have occurred. Stresses similar to those producing the fault may have caused the north-south elongation of a dacite intrusion dated at 16.2 m.y. B.P., but there is only permissive evidence for this. Lavas of the early High Cascade episode which began to flow into the area between about 8.3 and 7.8 m.y. B.P. were probably prevented from flowing west by the scarp of the Cougar fault. Although most of the displacement probably occurred immediately prior to those eruptions, it is possible that displacements may have also occurred on the Cougar fault about 4 to 5 m.y. ago, when north-south faults formed east of the area. However, absence of an obvious topographic scarp today suggests that 5- to 4-m.y. B.P. displacements, if they occurred, were small.

Slight southward tilting of the area may have occurred during late Western Cascade time between about 13 and 9 m.y. B.P. Between early and late Western Cascade time, which was a period of nondeposition and erosion, a topography with at least 366 m (1,200 ft) of relief developed. A period of rapid erosion and uplift produced about 1 km (0.6 mi) of relief in the area between 5 and 4 m.y. B.P.

The gravity signature of the Cougar fault continues north and south of the study area for many kilometers and coincides with an analogous fault at McCredie Hot Springs to the south (see Chapter 6). The Cougar fault may thus be a regional structure older than and west of analogous north-south faults at the Western Cascade-High Cascade boundary at Horse Creek and Waldo Lake (see Chapter 6).

### INTRODUCTION

Cougar Reservoir is located on the South Fork of the McKenzie River between the towns of Blue River and McKenzie Bridge (Figure 4.1). The area is about 80 km (50 mi) east of Eugene on State Highway 126.

The area is in steep, mature topography of the Western Cascade physiographic province. The northern boundary of the area is the McKenzie River, which runs almost east-west.

The central part of the area is dominated by the north-south-trending V-shaped valley of the South Fork of the McKenzie River. Cougar Dam forms a 9.2 km (5.7 mi)-long lake on the South Fork. Local relief is about 1,037 m (3,400 ft).

Geologic mapping was undertaken at a scale of 1:24,000 to define structures and rock units which control the local hydrothermal systems (see Plate 2). The area is only a few kilometers west of the Belknap-Foley Known Geothermal Resource Area (KGRA). There is one local thermal spring, Terwilliger Hot Springs, where water at about 44° C issues from fractured andesitic lavas on the west side of Cougar Reservoir at Rider Creek. Other workers, including Bowen and others (1978) and Brown and others (1980a), mentioned another thermal spring, the "Cougar Reservoir hot spring," located under what is now Cougar Reservoir. The earliest reference to this spring comes from Waring (1965), who mentioned a warm spring 12.9 km (7.7 mi) southwest of McKenzie Bridge. No spring, however, was noted by geologists of the U.S. Army Corps of Engineers at the site of "Cougar Reservoir hot spring" when constructing Cougar Dam. The mislocation of Terwilliger Hot Springs and the deletion of the correct name for the hot spring in Waring's (1965) compilation have probably created this confusion. Only one hot spring, Terwilliger Hot Springs, is known to be in the area.

### PREVIOUS WORK

Many workers have mapped near the Cougar Reservoir area, but until this study, the only available maps of the area were reconnaissance maps by Wells and Peck (1961) and Peck and others (1964). The authors of this present paper contributed the Cougar Reservoir portion of the larger reconnaissance map of Brown and others (1980a), but the present 1:24,000-scale map (Plate 2) represents a considerable refinement of the 1:62,500-scale map of Brown and others (1980a).

Wells and Peck (1961) mapped the entire area as middle and upper Miocene andesite roughly equivalent to the Sardine series of Thayer (1936, 1939). Peck and others (1964) mapped the entire area as Sardine Formation, except for a small area of the older tuffaceous rocks at Cougar Dam. Peck and others (1964) mapped the tuffaceous rocks as Little Butte Volcanic Series. Neither Wells and Peck (1961) nor Peck and others (1964) showed faults in the area. The correspondence of map units of this study to the rock units of earlier workers is discussed in detail on Plate 2.

### PRINCIPAL CHANGES FROM PREVIOUS MAPPING

Relative to these earlier maps, the present map shows a much larger area of the older tuffaceous sequence, here informally called the tuffs of Cougar Reservoir. It also shows exten-



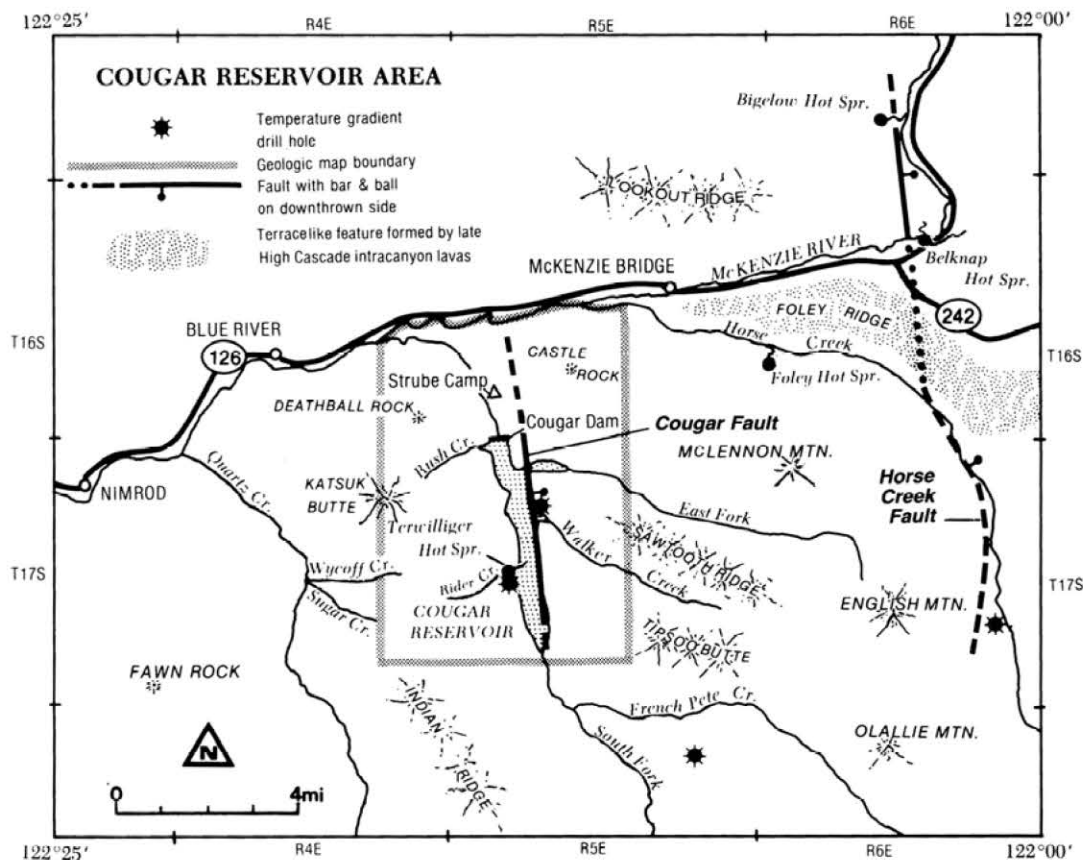


Figure 4.1. Map showing location of the Cougar Reservoir map area and other localities mentioned in the text. The Horse Creek fault is from Brown and others (1980a) and Flaherty (1981).

sive areas of basalts of the early High Cascade episode, the lavas of Tipsoo Butte, which cap the ridges east of Cougar Reservoir. The present map shows a large north-south-trending fault along the East Fork of the McKenzie River and other smaller subsidiary faults not shown on earlier maps. Earlier maps show a general easterly dip to the Western Cascade sequence, but only a very slight ( $7^\circ$ ) southerly dip was recognized in the present study. The easterly dip of the sequence in the earlier maps (Wells and Peck, 1961; Peck and others, 1964) was used as evidence of a regional anticline in the area (the Breitenbush anticline). The dominance of rocks younger than the Little Butte Volcanic Series on the limbs of the structure and the dominance of the Little Butte Volcanic Series on the axis were used as evidence for existence of an anticline. Our work suggests that younger rocks dominate east of the presumed anticlinal axis principally because of down-to-the-east step faulting along a north-south trend.

## GEOLOGIC HISTORY

During early Western Cascade time (40 to 18 m.y. B.P.), the area was the site of intense silicic volcanism, principally in the form of large, tuffaceous, pumice-poor, lithic-fragment-rich lahars (tuffs of Cougar Reservoir). Although some ash-flow tuffs, rhyodacite, and moderately iron-rich andesite lavas occur in the sequence, laharic tuffs and interbedded epiclastic sandstones and mudstones dominate the volcanic pile. Between about 22 m.y. B.P. (?) and about 14 m.y. B.P., a steep

topography with at least 366 m (1,200 ft) of relief developed. Andesitic lavas (andesites of Walker Creek), dacitic ash-flow tuffs and lapilli and ash-fall tuffs (tuffs of Rush Creek and tuffs of Tipsoo Butte), basaltic flows (basaltic lavas of the East Fork), and numerous andesitic to dacitic plugs (dacite intrusive of Cougar Dam and other andesitic intrusions) invaded the area during late Western Cascade time about 16.2 to 8.9 m.y. B.P. These rocks buried the earlier topography to a depth of at least 470 m (1,542 ft). The sequence of late Western Cascade age was then capped by iron-rich diktytaxitic basalts (lavas of Tipsoo Butte) during early High Cascade time (about 8.3 to 5 m.y. B.P.). These flows of the early High Cascade episode filled a topography east of Cougar Reservoir that had very little relief and flowed in from sources to the east.

Between about 5 m.y. and 4 m.y. B.P., the area was deeply dissected by the current drainage system, and numerous mudflows subsequently poured off the steep slopes. Later, in the Pleistocene, glacial outwash deposits covered the floor of the valley of the East Fork. Steep slopes in the area are very unstable and form large landslides where underlain by tuffs of the late Western Cascade episode. These landslides and glacial outwash deposits are being incised by present-day streams.

The major structure in the area is the north-south-trending Cougar fault zone, which offsets rocks dated at 13.2 m.y. B.P. by at least 152 m (499 ft) and probably by more than 366 m (1,200 ft). The relative motion on the fault is down to the east. North-south elongation of the 16.2-m.y. B.P. dacite intrusion of Cougar Dam adjacent to the Cougar fault suggests

that regional stresses similar to those which caused the Cougar fault may have been active during initial volcanism of the late Western Cascade episode. Breccia dikes and magmatic dikes along small northwest-trending faults and fissures within the Cougar Dam intrusive suggest that some faulting was closely associated with the intrusion. Slight tilting of the Western Cascade sequence about 7° or less to the south probably occurred during late Western Cascade time.

## STRATIGRAPHY

### Introduction

Volcanic rocks of the early and late Western Cascade episodes and early High Cascade episode dominate the area (see Chapter 2 for definitions of these units). Ages have been assigned by K-Ar dating of the tops and bottoms of major sequences where possible. Stanley H. Evans of the University of Utah Research Institute determined a total of 11 K-Ar dates from rocks collected within the map area and other parts of the McKenzie Bridge quadrangle (Appendix A). All stratigraphic units used in this paper are informal and have been divided according to mappable characteristics of the rocks. The chemical classification system used to give rock names is summarized in the nomenclature section in Chapter 2. The chemical petrology and regional significance of the chemical compositions of the rocks are discussed in Chapter 2 and are not repeated here.

Detailed lithologic descriptions of volcanic bedrock units are given in Table 4.1, and correlation of all map units with units of previous workers is summarized in the geologic map legend (Plate 2). Only features useful for stratigraphic correlation and petrologic interpretation are discussed in the text.

### Volcanic rocks of the early Western Cascade episode

**Tuffs of Cougar Reservoir (unit Totc):** Thick tuffaceous laharic and mudflow deposits, nonwelded ash-flow tuffs, epiclastic mudstone and sandstone, and minor interbedded rhyodacite to moderately iron-rich andesite flows crop out in the lowest elevations of the South Fork of the McKenzie River. These rocks are here informally called the tuffs of Cougar Reservoir. The lowest part of the sequence, which is exposed downstream from Cougar Dam, consists of abundant tuffaceous mudstone. Diamond core samples from holes drilled in the area by the U.S. Army Corps of Engineers indicate that additional lithic-fragment-rich laharic tuffs underlie the epiclastic mudstone. Most of the unit is dominated by a series of crystal-poor, pumice-poor, tuffaceous lahars with numerous mudstone and sandstone interbeds.

Laharic flows in the uppermost part of the sequence above Cougar Dam at Rush Creek are locally crystal rich and contain numerous plagioclase and hypersthene crystals. A dark, hackly, aphyric, iron-rich andesite flow (sample 20, Appendix B, Table B.2) crops out at the head of Rush Creek near the top of the sequence, and a series of rhyodacite flows occurs near the base east of Strubes Forest Camp.

All of the rocks show some alteration to fine-grained birefringent phyllosilicates. Most of these phyllosilicates are probably smectite clays which totally replace glass in most rocks and affect plagioclase and orthopyroxene in many places. In some samples, chlorite and calcite were also noted replacing mafic phases and plagioclase, respectively. Alteration of plagioclase is unknown in the overlying rock units.

Microscopic examination of the ash-flow tuffs reveals the broken nature of matrix pyroxene and plagioclase crystals and the paucity of crystals in pumice. The fine-grained vitric ash component was partially winnowed out of the matrix during

transport. Pumice lapilli are not common in the ash flows and are rare in the tuffaceous mudflows and lahars. Coarse ash is common in the ash-flow tuffs. The mudflows contrast with the ash-flow tuffs by having a lithic-fragment content equal to, or in some cases exceeding, the vitric component.

The mudflows commonly contain carbonized wood fragments, as well as abundant lithic lapilli. Lithic fragments seldom exceed 1 m (3 ft) in size in the mudflows in this area, and most are less than 10 cm (4 in). The pyroclastic and epiclastic rocks generally form rounded slopes with frequent cliffs and some "hoodoos." The overall color of the tuffs is greenish gray, with abundant dark-gray to reddish-purple aphyric lithic fragments. The units are well lithified and, unlike younger tuffs, show no tendency to form major landslides.

The tuffs of Cougar Reservoir are too altered to provide material for accurate radiometric dates, but some constraints can be placed on the age of the sequence. The intrusion at Cougar Dam which cuts the tuffs has a K-Ar date of 16.2 m.y. B.P. Sutter (1978) listed a K-Ar date on the Nimrod stock of  $15.86 \pm 0.18$  m.y. B.P. (which recalculates to  $16.3 \pm 0.2$  m.y. B.P. according to Fiebelkorn and others, 1982). This quartz monzonite stock appears to intrude tuffs similar to the tuffs of Cougar Reservoir. Lavas chemically similar to the iron-rich andesite lava found near the top of the sequence occur at the top of a similar tuffaceous sequence near Lookout Point Reservoir where they have a K-Ar date of about 22 m.y. B.P. (see Chapter 5). Similar lavas in other parts of the Western Cascade Range have K-Ar dates of between 27 and 19 m.y. B.P. (White, 190a,c).

### Volcanic rocks of the late Western Cascade episode

**Introduction:** Volcanic rocks of the late Western Cascade episode are a series of basaltic to dacitic lavas and tuffs which fill a steep topography cut into the underlying tuffs of Cougar Reservoir. The sequence thins against an east-west-trending highland formed of tuffs of Cougar Reservoir in the northwestern part of the map area. The adjacent paleovalley was at least 366 m (1,200 ft) deep, based on the rise of the lower contact of rocks of the late Western Cascade episode from the Rider Creek area to the Katsuk Butte area (Figure 4.1; Plate 2). About 470 m (1,542 ft) of rocks of the late Western Cascade episode overlie this highland at Katsuk Butte. The highland terminates abruptly at the Cougar fault. About 792 m (2,598 ft) of the sequence of late Western Cascade age is exposed on the east side of the Cougar fault, but no older rocks are exposed. The minimum offset across the fault which could displace this highland below the lowest exposure of rocks of the late Western Cascade episode on the east block of the fault is 562 m (1,843 ft). Because the lowest exposed unit on the east block of the fault (the basaltic lavas of the East Fork) is absent from the upthrown west block, it is logical to assume that these lavas may have been present on the west block but have been removed by erosion. If they were present just above the highest point on the west block (Katsuk Butte) prior to erosion, they would have been vertically displaced 1,033 m (3,388 ft) from the lowest exposure on the east block. It is possible that the displacement exceeds this amount, if the East Fork basalt were once present on the west block at an elevation higher than Katsuk Butte.

An alternative hypothesis to the above arguments is that the paleohighland in the northwest part of the area was an isolated high flanked on both the east and south by valleys when the sequence of late Western Cascade age was deposited. This would require a thicker sequence east of the fault and cause units low in the eastern section of late Western Cascade

Table 4.1. *Stratigraphy of volcanic rock units in the Cougar Reservoir area, central Cascade Range, Oregon.**Pl=plagioclase, ol=olivine, px=pyroxene, cpx=clinopyroxene, opx=orthopyroxene, qtz=quartz, hb=hornblende*

Regional volcanic episode	Unit and map symbol	K-Ar dates (m.y. B.P.)	Maximum exposed thickness	Typical SiO <sub>2</sub> <sup>1</sup> (wt. %)	Lithologic description
Early High Cascade	Lavas of Tipsoo Butte (Tml)	Near top 9.41 ± 0.42 <sup>2</sup>  Bottom at Tipsoo Butte, 7.80 ± 0.77  Bottom at Lookout Ridge, 8.34 ± 0.36	457 m (1,500 ft)	48-53	Light- to dark-gray fine-grained fresh ol- to qtz-normative basalts; diktytaxitic with brownish subophitic to intersertal cpx; ½-2% 0.6-1.0 mm anhedral ol phenocrysts ± pl and cpx phenocrysts; one qtz-normative sample with felty opx-pl-cpx groundmass.
	Tuffs of Tipsoo Butte (Tmtt)	—	122 m (400 ft)	—	Cream-colored bedded tuffs with some hb-bearing and cpx-opx-pl-phyric ash-flow tuffs.
Late Western Cascade	Andesites of Castle Rock (Tmcr)	9.31 ± 0.44	183 m (600 ft)	60	Fine-grained gray andesite lavas with 1.2-mm subhedral pl(2%) + opx(1%) phenocrysts, with microphenocrysts of pl + cpx + opx + altered ol(?) in a pilotaxitic groundmass; xenocrystic qtz with reaction coronas in some samples.
	Andesitic intrusives (Tmvi)	—	—	—	Highly porphyritic, pl-rich two-px andesites similar to unit Tmw.
	Andesites of Walker Creek (Tmw)	Top at Katsuk Butte, 11.4 ± 0.5  Top at Lookout Ridge, 8.80 ± 0.34  Middle at Walker Creek, 13.2 ± 0.7  Bottom east of Katsuk Butte, (12.4 ± 2.5) <sup>3</sup>	837 m (2,745 ft)	57-62	Dominantly with phyric pl-rich two-px andesites with dark-gray to reddish-gray color. Many megacrystic units with phenocrysts of 1 cm or larger size. Some slightly diktytaxitic flows at top near Tipsoo Butte; numerous epiclastic interbeds.
	Basaltic lavas of the East Fork (Tme)	Lower part, (8.1 ± 2.3) <sup>3</sup>	91 m (300 ft)	52-54	Dark-gray fine-grained qtz-normative basalt and basaltic andesite; less than 10% 1-mm subhedral phenocrysts of altered ol ± pl ± cpx ± opx in a felty to pilotaxitic groundmass.
	Tuffs of Rush Creek (Tmrt)	Upper part, 13.8 ± 0.8	274 m (900 ft)	67-71	Cream to gray dacite to rhyodacite non-welded ash flows and epiclastic tuff; minor welded tuff; opx + pl ± hb phenocrysts in pumice; glass altered to very fine-grained clays in nonwelded units.
	Dacite intrusive of Cougar Dam (Tmvic)	16.2 ± 1.8	—	63.6	Black glassy two-px low-silica dacite; glomeroporphyritic with subhedral 1-mm opx(3%), cpx(4%), and pl(18%); 1% altered 2.2-mm ol(?) phenocrysts; hyalopilitic groundmass.
	Tuffs of Cougar Reservoir (Totc)	—	470 m (1,542 ft)	61-72	Lithic-fragment-rich, pumice-poor laharic tuffs and minor ash flows; abundant epiclastic tuffaceous mudstone and sandstone; minor iron-rich andesite and rhyodacite lavas; pl + opx partially affected by smectite alteration; glass totally altered to smectite; rocks are dull greenish gray.

<sup>1</sup> Recalculated to a 100-percent total, volatile-free.<sup>2</sup> Sample may have excess radiogenic argon.<sup>3</sup> Sample has 10 percent or less radiogenic argon; date probably affected by low-grade alteration.



age to pinch out to the west. This highland could have been partially formed by movements on the Cougar fault prior to or during deposition of most of the sequence of late Western Cascade age. Arguments below suggest that the 16.2-m.y. B.P. dacite intrusive of Cougar Dam was roughly contemporaneous with some movement on the Cougar fault. This supports the latter hypothesis.

Additional deep drilling on the east block of the Cougar fault will be necessary to discriminate among these hypotheses. Only then will the amount of offset on the fault be known with any certainty.

**Dacite intrusive of Cougar Dam (unit Tm<sub>vic</sub>):** A dark, glassy, porphyritic two-pyroxene dacite forms the east and west abutments of Cougar Dam. The dacite is a cliff-forming unit which causes a narrows on the South Fork of the McKenzie River at Cougar Dam. The unit appears to have a conformable upper contact with the tuffs of Cougar Reservoir on the west abutment but obviously intrudes and alters the tuffs in the upper contact on the east abutment. Numerous dike-like protrusions are injected along the west contact in exposures just north of the dam along U.S. Forest Service Road 19. The lower contact on the west abutment also appears to be conformable with underlying, nearly horizontal tuffaceous mudstones of the tuffs of Cougar Reservoir. No lower contact is exposed on the east abutment, where the dacite appears to be a long, dike-like mass extending about 2.74 km (1.7 mi) in a north-south- to north-northwest direction. However, abutment exploration by geologists of the U.S. Army Corps of Engineers revealed pods of pyroclastic rock within and below the intrusive at the east abutment (U.S. Army Corps of Engineers, 1964). Northwest-trending shears cut through the east abutment in several places and in some cases are filled with nearly aphyric dikes. Breccia dikes filled with comminuted wall-rock and quartz-diorite fragments also fill west-northwest-trending fissures in the east abutment. One large north-trending shear at the top of the east abutment has prominent horizontal slickensides.

Lateral contacts between the intrusion and tuffs of Cougar Reservoir on the east abutment are complex. Most contacts are very sharp and steeply dipping, but others show signs of complex interactions between the intrusion and the walls. In one locality near the top of the intrusion, rounded block-size pieces of the dacite are completely surrounded by structureless, fine-grained tuff adjacent to an obscure, steeply dipping contact. Thermal metamorphic effects on wall rocks include slight bleaching and very low-grade epithermal alteration with some iron-oxide staining, possibly from minute quantities of weathered sulfides. The intrusion is slightly discolored to a darker, more stony appearance at the contact. The general appearance of the east abutment contact is indicative of interactions between moist tuffaceous wall rocks and a highly viscous, very shallow intrusion.

A plagioclase separate from the dacite yielded a K-Ar date of  $16.2 \pm 1.8$  m.y. B.P. (0.237 percent K, 13 percent radiogenic Ar<sup>40</sup>). This corresponds to the early part of the late Western Cascade episode.

**Tuffs of Rush Creek (unit Tm<sub>rt</sub>):** Light-colored ash-fall, ash-flow, and epiclastic tuffs interfinger with two-pyroxene andesite flows in the lower part of the sequence of late Western Cascade age at Rush Creek. Most of the ash-flow tuffs are nonwelded, but welded tuffs crop out in three localities. In the Sugar Creek drainage west of the map boundary, a densely welded, glomeroporphyritic two-pyroxene dacite ash-flow tuff crops out at about 915-m (3,000-ft) elevation (Blue River quadrangle). This tuff can be traced into the map area near the headwaters of Rider Creek. Similar partially welded to nonwelded ash-flow tuffs without the

glomeroporphyritic texture are found at about the 1,006-m (3,300-ft) elevation in road cuts on the east flank of Harvey Mountain. A densely welded two-pyroxene dacite ash-flow tuff occurs in one outcrop at about the 732-m (2,400-ft) elevation (McKenzie bridge quadrangle) at the base of the section below the above-mentioned Harvey Mountain ash-flow tuffs. Although it is possible that one of the Harvey Mountain ash-flow tuffs is the distal facies of the Sugar Creek welded tuff, no certain correlation was established for any of the ash-flow tuff units over significant distances. This may be a function of the high relief which probably characterized the area. All of these welded to partially welded tuffs pinch out to the north at Rush Creek against an old highland formed by the tuffs of Cougar Reservoir. The lower contact of the tuffs of Rush Creek is exposed at the head of Rush Creek, where the peak of this old highland is covered by the tuffs. The uppermost tuffs of Cougar Reservoir at this location are a series of gray mudflows. Pieces of the white- to cream-colored Rush Creek tuff are intermixed in the gray mudflow material at the contact. This mixture is probably a mudflow formed from rocks of the underlying sequence during Rush Creek time.

Most of the tuffs of Rush Creek are composed of light-colored hypersthene-bearing dacite pumice lapilli and ash. Welded and partially welded ash-flow tuffs are dark gray to black with eutaxitic texture. Very low-grade alteration commonly has caused glass in the nonwelded and epiclastic units to alter to clay minerals. Welded ash-flow tuffs have hydrated but otherwise unaltered glass. Broken plagioclase and subordinate orthopyroxene and clinopyroxene make up most of the crystal fraction which forms up to 10 percent of the tuffs, although minor hornblende is present in some of the rocks. The tuffs generally form low-angle slopes and serve as slip planes for major landslides throughout the western half of the map.

A nonwelded ash-flow tuff at the head of Rush Creek (976-m [3,200-ft] elevation) near the top of the tuffs of Rush Creek yielded a K-Ar date of  $13.8 \pm 0.8$  m.y. B.P. (0.349 percent K, 26 percent radiogenic Ar<sup>40</sup>) on a plagioclase separate. At the 1,447-m (4,745-ft) elevation, a sample stratigraphically above the tuffs of Rush Creek yielded a K-Ar date of  $11.4 \pm 0.5$  m.y. B.P. (0.208 percent K, 35 percent radiogenic Ar<sup>40</sup>) from a plagioclase separate. A slightly altered flow of two-pyroxene andesite stratigraphically below most of the tuffs of Rush Creek yielded a K-Ar date of  $12.4 \pm 2.5$  m.y. B.P. (0.44 percent K, 7 percent radiogenic Ar<sup>40</sup>). The alteration and low radiogenic argon of the andesite flow cast doubt on the accuracy of that date.

**Basaltic lavas of the East Fork (unit Tm<sub>e</sub>):** Fine-grained basalt to basaltic andesite lavas crop out on both sides of the East Fork of the McKenzie River. These flows dip gently toward the south and are about 91 m (300 ft) thick. They do not crop out anywhere else in the map area. They are in fault contact with the lavas of Walker Creek to the east and are cut off by the Cougar fault on the west. They are overlain by the lavas of Walker Creek to the north and south.

One sample collected at about the 537-m (1,760-ft) elevation on the south side of the East Fork yielded a K-Ar date of  $8.1 \pm 2.3$  m.y. B.P. (0.52 percent K, 5 percent radiogenic Ar<sup>40</sup>). This date is far too young, since a lava higher in the sequence of Walker Creek has a date of  $13.2 \pm 0.7$  m.y. B.P. The lavas are chemically and mineralogically similar to the rest of the section of late Western Cascade age, and so they are probably no older than about 16.2 m.y. They are older than about 13.2 m.y.

**Andesites of Walker Creek (unit Tm<sub>w</sub>):** Highly phryc two-pyroxene andesite lavas and minor debris flows crop out in a 610-m (2,000-ft) section at Walker Creek, where they are capped by the lavas of Tipsoo Butte. Lavas chemically and

mineralogically similar to the lavas at Walker Creek crop out intermittently over a vertical distance of 837 m (2,745 ft) on the west side of Cougar Reservoir, where they interfinger with the tuffs of Rush Creek in the lower part of the section of late Western Cascade age. The writers were not able to demonstrate that individual flow units cropping out on the west side of Cougar Reservoir correlate with specific flows on the east side. An apparent single flow unit on the west side of the reservoir was traced from an elevation of 1,220 m (4,000 ft) near Ridge Creek to an elevation of 488 m (1,600 ft) at Rider Creek. This would indicate that flows of the sequence may have flowed from the west toward the east into a valley similar in relief and position to the current valley of the East Fork. If lavas on the east side of the East Fork flowed from local source areas to the east into this same topographic low, then there is no reason for individual flow units to correlate across the East Fork. It is still puzzling that very distinctive units like the tuffs of Rush Creek and the basaltic lavas of the East Fork are not found across the South Fork. The Cougar fault zone, which will be discussed in a later section, may have sufficient displacement to juxtapose very different parts of the section of late Western Cascade age, making outcrop correlation across the fault impossible. If this is the case, then much of the section cropping out on the west side of the fault may lie at depth on the east side.

The most common rock type in the unit is a two-pyroxene andesite with 2- to 5-mm-long phenocrysts of plagioclase and subordinate orthopyroxene and clinopyroxene set in a partially devitrified hyalopilitic groundmass. Minor olivine, hornblende, Fe-Ti oxides, and apatite are also commonly present. Phenocrysts and glomerocrysts are up to 1.5 cm in their longest dimension, and such glomerocrystic rocks are quite common. Nearly aphyric lavas with minor pyroxene phenocrysts are also common locally. In the upper part of the sequence, on the east side of the fault, flows tend to be slightly diktytaxitic. The lavas form spectacular curving colonnades where the flows are thick in steep intracanyon sections.

A sample from the middle part of the Walker Creek section (720-m [2,360-ft] elevation) yielded a whole-rock K-Ar date of  $13.2 \pm 0.7$  m.y. B.P. (1.32 percent K, 28 percent radiogenic  $Ar^{40}$ ). Basal Tipsoo Butte lavas above this flow at about the 1,171-m (3,840-ft) elevation have a K-Ar date of  $7.9 \pm 0.8$  m.y. B.P. On the west side of the reservoir, the tuffs of Rush Creek, which are K-Ar dated at  $13.8 \pm 0.8$  m.y. B.P., interfinger with the lower part of the west-side two-pyroxene andesite section. The top flow of the west-side section at Katsuk Butte (elevation of 1,415 m [4,640 ft]) has a K-Ar date on plagioclase of  $11.4 \pm 0.5$  m.y. B.P. (0.28 percent K, 35 percent radiogenic  $Ar^{40}$ ).

At Lookout Ridge across the McKenzie River from the northern margin of the map area, the top flow of the section of late Western Cascade age is a hornblende-bearing two-pyroxene dacite with a whole-rock K-Ar date of  $8.80 \pm 0.34$  m.y. B.P. (1.12 percent K, 61 percent radiogenic  $Ar^{40}$ ). This unit is considered to be the top of the section of late Western Cascade age and may be about the same age as the undated top flow at Walker Creek. At Lookout Ridge, the basal basalt of early High Cascade age has a K-Ar date of  $8.34 \pm 0.36$  m.y. B.P. There is thus no evidence in either the Walker Creek or Lookout Ridge areas of a significant time break between the andesitic volcanism of the late Western Cascade episode and the basaltic volcanism of the early High Cascade episode.

**Andesites of Castle Rock (unit TmcR):** Light-gray, nearly aphyric two-pyroxene andesite lavas (60 percent  $SiO_2$ ) cap Castle Rock in the northeastern part of the area. It is possible that these lavas are at their vent area and that they merge into a plug dome at Castle Rock. Field relationships are

ambiguous, but wide variations in dip and strike of flow foliation and the limited distribution of the lavas (only at Castle Rock) suggest that this may be a plug dome.

At least two rock types are present, but it is unclear whether they are separate cooling units. Both have similar textures, but one has minor xenocrystic quartz and idding-sitized olivine phenocrysts, whereas the other has both clinopyroxene and orthopyroxene pseudomorphs after minor olivine(?) phenocrysts, but no quartz. The quartz, where present, has reaction coronas of clinopyroxene and minor idding-sitized olivine. Aside from xenocrystic quartz, the lavas are similar.

A K-Ar age of  $9.31 \pm 0.44$  m.y. (0.755 percent K, 34 percent radiogenic  $Ar^{40}$ ) was determined from a whole-rock sample containing xenocrystic quartz. This unit was probably erupted at the end of the late Western Cascade episode.

**Tuffs of Tipsoo Butte (unit Tmtt):** At Tipsoo Butte, three easterly trending paleocanyons incised in the underlying lavas of Walker Creek are filled with from 98 to 122 m (320 to 400 ft) of nonwelded dacitic ash-flow tuff and possibly ash-fall tuff. These tuffs are probably part of the sequence of late Western Cascade age, although their presence at the top of the Walker Creek section and the relief on their lower contact suggest that they could have been deposited in early High Cascade time (i.e., after 9.0 m.y. B.P.). Subtle bedding within the sequence, inclusion of some wood fragments, and the large number of lithic fragments relative to pumice are permissive evidence that some of these tuffs may be surge deposits. Layers that are more rich in pumice are free of wood fragments, lack the subtle bedding, and appear to be ash flows. Unfortunately, these observations apply only to the units in the lower part of the sequence; the upper part was inaccessible because it was exposed only on cliffs.

Unlike pumice in nonwelded tuffs at Rush Creek, pumice in thin sections from two samples of the tuffs of Tipsoo Butte is unaltered; one of these samples, however, contains carbonized wood fragments, and the ash and lithic fragments in it are extensively altered to chlorite and smectite. Pumice in the other sample has a minor amount of hornblende phenocrysts, whereas the sample with altered lithic fragments has a minor amount of orthopyroxene phenocrysts. Two-pyroxene andesites and hornblende two-pyroxene andesites are the chief lithologies of the lithic fragments. Broken clinopyroxene, orthopyroxene, plagioclase, and hornblende crystals are at least ten times as abundant in the matrix as they are in the pumice. Winnowing during ash-flow or base-surge transport apparently reduced the volume of the vitric component relative to the crystal component in the matrix.

No K-Ar data are available for the tuffs of Tipsoo Butte, but they lie at least 366 m (1,200 ft) above a Walker Creek flow K-Ar dated at 13.2 m.y. B.P. and are capped by basal lavas of Tipsoo Butte K-Ar dated at 7.8 m.y. B.P. The tuffs could have been erupted in either the late Western Cascade or early High Cascade episode.

## Volcanic rocks of the early High Cascade episode

**Lavas of Tipsoo Butte (Tml):** About 457 m (1,500 ft) of dark-gray diktytaxitic basalts and basaltic andesites cap McLennen Mountain, Sawtooth Ridge, and Tipsoo Butte in the eastern half of the area. The lower contact is at nearly the same elevation from ridge to ridge, except for a slight rise in elevation toward the east. The westward slope of the lower contact suggests that the lavas flowed from vents at higher elevations east of the map area.

The absence of the lavas of Tipsoo Butte in the western half of the area can be explained by three hypotheses. Either (1) thinning or (2) a topographic barrier prevented the lavas

from reaching the western part of the area, or (3) they were eroded from the western ridge tops. The lavas do not seem to thin significantly from west to east, so thinning is not likely. Elevations of ridges in the western part of the area are between 1,220 and 1,525 m (4,000 and 5,000 ft), whereas the lower contact on the lavas of Tipsoo Butte, which slopes toward the west, is at about 1,098 to 1,220 m (3,600 to 4,000 ft). The lavas should thus crop out below 1,098 m (3,600 ft) on the west side of the map unless they were stopped by a topographic barrier or uplifted after deposition and eroded off. Because relative down-to-the-east movement has been demonstrated along the Cougar fault zone, the resulting fault scarp or uplifted western half of the area may have created a possible barrier to the lavas of Tipsoo Butte. Swanson and James (1975) noted pillowed units in lavas correlative to the lavas of Tipsoo Butte north of the map area, suggesting a lake-filled lowland at the western terminus of the flow units there. If the Cougar fault extends to the north, it may have produced a scarp against which the lavas ponded. Lava-dammed lakes may have formed, and lava flows entering the lakes could have produced pillowed basalts. No pillow basalts, however, were noted in the map area. The reason for termination of the basalts in the Cougar Reservoir area is not known, but it is probable that it was caused by uplift of the western part of the area (or downdrop of the eastern part) by an amount equal at least to the exposed thickness of the basalts, or about 457 m (1,500 ft). This relief could have been produced by the Cougar fault anytime from shortly before to shortly after early High Cascade time. Pleistocene outwash gravels are not faulted along the trace of the Cougar fault in the East Fork area. The minimum offset necessary to simply erode the basalts from the western part of the area, assuming that they were deposited before uplift, would be the difference in elevation between their lower contact and the elevation of the highest ridges in the western part of the area, or about 427 m (1,400 ft). This last estimate assumes that the topography in the western area had relatively low relief, similar to the relief along the lower contact of the lavas of Tipsoo Butte in the eastern part of the area.

Absence of a current topographic scarp on the west block of the fault and the previously mentioned evidence of ponding of the lavas of Tipsoo Butte suggest that the offset probably occurred shortly before and possibly during eruption of the lavas of Tipsoo Butte. If this is the case, then the total offset may have been as much as, or somewhat more than, the exposed thickness of the lavas of Tipsoo Butte, or greater than 457 m (1,500 ft).

The lavas of Tipsoo Butte are chemically and mineralogically distinct from earlier basaltic rocks. They reach lower silica contents (48.3 percent) and higher iron contents (11.9 percent total iron oxide recalculated volatile-free to FeO) than any of the older basaltic rocks. High  $P_2O_5$  contents of 0.32 to 0.87 percent also characterize the Tipsoo Butte basalts (e.g., compare to the underlying basalts of the East Fork with 0.11 to 0.18 percent  $P_2O_5$ ). The lavas are also diktytaxitic and commonly contain, in the most mafic samples, brownish ophitic to subophitic clinopyroxene in the groundmass. The groundmass clinopyroxene is a darker color in a sample with 2.44 percent  $TiO_2$  than in a sample with 1.48 percent  $TiO_2$ , so the color is probably a function of titanium content in the clinopyroxene. Olivine is present in all samples and shows no reaction with the former liquid. The absence of a reaction relationship between olivine and liquid, the high  $TiO_2$  and  $P_2O_5$  contents, and the presence of probable titaniferous clinopyroxene are attributes of basalts with alkaline affinities. Basalts with these same characteristics occur also in the section of late High Cascade age described at Cupola Rock north-east of the area (Flaherty, 1981). The chemical affinity of

basalts of both the late and early High Cascade episodes to one another and to alkaline basalts is described more completely in Chapter 2.

The lavas of Tipsoo Butte are generally light gray to dark gray and weather to a tan color. They characteristically have widely scattered, large (1- to 3-cm) spherical vesicles in addition to a diktytaxitic texture. They tend to form precipitous cliffs and are generally of fresher appearance than all but the uppermost flows of the underlying sequence of late Western Cascade age.

A K-Ar age at the base of the section at Tipsoo Butte is  $7.80 \pm 0.77$  m.y. (0.48 percent K, 14 percent radiogenic  $Ar^{40}$ ). A K-Ar date of  $8.34 \pm 0.36$  m.y. B.P. (0.365 percent K, 39 percent radiogenic  $Ar^{40}$ ) was obtained at the base of the section at Lookout Ridge. A K-Ar date of  $9.41 \pm 0.42$  m.y. B.P. (1.39 percent K, 36 percent radiogenic  $Ar^{40}$ ) was determined for a flow near the top of Tipsoo Butte. As explained previously (Chapter 2), it is possible that the 9.41-m.y. B.P. date is caused by incomplete degassing of radiogenic argon at the time of eruption. Alternatively, since the 9.41-m.y. B.P. date is characterized by more radiogenic argon than the 7.80-m.y. B.P. date, it may be the more accurate age, making the lower part of the sequence somewhat older than 9.41 m.y.

### **Pliocene-Pleistocene mudflow deposits (unit QTpm)**

Partially lithified mudflow deposits occur on the east side of Cougar Reservoir between Walker Creek and the East Fork. One outcrop of these deposits also occurs in a roadcut on the west side of the reservoir 1.6 km (1 mi) north of Terwilliger Hot Springs. The mudflows appear to have flowed from local areas into a river valley essentially identical to the present one. All clasts examined were of rock types common to the sequence of late Western Cascade age.

The deposits are friable but more consolidated than overlying Pleistocene gravels. They lack the sorting and rounding of pebble- to cobble-size clasts characteristic of the Pleistocene deposits. They generally contain abundant subrounded to subangular pebble- to cobble-size clasts of highly phyrlic two-pyroxene andesite set in poorly sorted, argillaceous, partially lithified sand. Overall color is dark gray to dark brownish gray, and the deposits form low slopes.

No radiometric dates are available, but the mudflow deposits may be pre-Pleistocene, since at the East Fork they are overlain by Pleistocene gravels which are much less indurated. Because their distribution is clearly controlled by the current topography, they must be younger than the age of the South Fork river valley. Flaherty's (1981) work at McKenzie Bridge suggests that the McKenzie River drainage system had attained its present relief by at least 2.0 m.y. B.P. and may have been in existence as early as about 4 m.y. B.P. (oldest local K-Ar date on intracanyon lavas of the late High Cascade episode; see structural geology section).

### **Glacial and fluvial deposits (unit Qgfl)**

Glacial deposits are found in the vicinity of Katsuk Butte. Till, small moraines, and glacial outwash are composed of lithologies of the late Western Cascade episode. No mafic lavas of Tipsoo Butte lithology were observed within the deposits, probably because the glacial deposits have provenances west of possible outcrops of the section of early High Cascade age.

### **Glacial outwash deposits (unit Qpg)**

Moderately well-sorted gravels, sands, and gravelly sands occur at the mouth of the East Fork where they fill a shallow



paleocanyon incised into the Cougar fault zone. They are not cut by the fault. The deposits also occur extensively in terraces at the junction of the South Fork with the main McKenzie River. They are probably outwash gravels from melting of Pleistocene valley glaciers.

### **Unconsolidated Recent colluvium (Qc), alluvium (Qal), and landslide deposits (Qls)**

Colluvium, as shown on the geologic map, includes all talus and thin unconsolidated residual soils which mantle bed rock. Alluvium is unconsolidated sand and gravel in overbank deposits and beds of the current streams. Landslide deposits include slump blocks and totally disaggregated landslide debris. All of these deposits are probably Holocene in age, although some of the landslides may well have begun to occur during the Pleistocene.

## **STRUCTURAL GEOLOGY**

### **Introduction**

The main structure in the area is the Cougar fault (Figure 4.1; Plate 2), which cuts through the middle of the map area along a N. 5° W. trend. This very steeply dipping fault offsets the east half of the area downward relative to the west half.

Generally, the tuffs of Cougar Reservoir appear to dip a few degrees to the south or southwest, although local dips to the east, west, and northeast were also measured. Fine-grained sediments near the Cougar Dam powerhouse are horizontally bedded. The sequence of late Western Cascade age also probably dips very gently toward the south. The regional tectonic significance of the Cougar fault and other deformation in the area is discussed in Chapter 2 and is not repeated here.

### **Cougar fault**

The Cougar fault appears to be nearly vertical with chiefly dip-slip movement. Although one north-south fault in the dacite intrusion at Cougar Dam has horizontal slickensides, all documented stratigraphic offset is dip-slip. A drill hole located about 46 m (151 ft) east of where the Cougar fault zone crops out at the mouth of Walker Creek encountered 152 m (499 ft) of the lavas of Walker Creek, whereas the tuffs of Cougar Reservoir crop out on the west side of the fault. This hole demonstrates that (1) there is at least 152 m (499 ft) of apparent dip-slip offset on the fault, and (2) the minimum easterly dip is 73°. Previously discussed stratigraphic arguments presented in the section on volcanic rocks of the early High Cascade episode suggest that the offset on the fault since about 13.2 m.y. B.P. is probably at least 427 m (1,401 ft). In the previous introductory section on late Western Cascade volcanism, various hypotheses led to estimates of displacement on the Cougar fault from 562 m (1,843 ft) to more than 1,033 m (3,388 ft), although the minimum offset which can be constrained by units of the late Western Cascade episode is the 152-m (499-ft) offset estimated from the Walker Creek hole.

The age of movements on the Cougar fault is constrained by the following observations:

1. The 16.2-m.y. B.P. Cougar Dam intrusion is immediately adjacent to the Cougar fault and is elongate parallel to the trace of the fault.
2. Breccia dikes and lava-filled dikes, probably generally related to magmatic activity during the Cougar Dam intrusive event, follow small northwest-trending faults adjacent to the Cougar fault.
3. The fault definitely cuts lavas of Walker Creek dated at 13.2 m.y. B.P.
4. If the Cougar fault or related faults extend northward into the area mapped by Swanson and James (1975),

then the scarp may have been responsible for creation of lakes which caused basaltic lavas of the early High Cascade episode to be pillowed in that area. These lavas began to flow into the area about 8.34 m.y. B.P., according to a date from Lookout Ridge.

5. A fault zone essentially parallel to the Cougar fault has been mapped to the east in the upper McKenzie River and Horse Creek (Figure 4.1). This fault zone formed between 5 and 4 m.y. B.P. (Taylor, 1980; Flaherty, 1981; Taylor, personal communication, 1983).
6. The Cougar fault does not cut Pleistocene gravels overlying it at the mouth of the East Fork.
7. Unlike the McKenzie River-Horse Creek fault, the Cougar fault has no well-developed topographic scarp.

The above observations are consistent with movement on the Cougar fault shortly before 16.2 m.y. B.P. and after 13.2 m.y. B.P. If the Cougar fault or related faults caused ponding of lavas of the early High Cascade episode mapped by Swanson and James (1975), then it may have been active about 8.34 m.y. B.P. If the fault experienced additional displacement when the Horse Creek fault formed, then it may have moved between 5 and 4 m.y. B.P. Movement on the fault apparently ceased before deposition of Pleistocene outwash gravels in the area, but the exact age of the gravels is not known.

The Cougar fault also appears to have affected the pattern of gravity and aeromagnetic anomalies in the area. The west block of the fault has a complete Bouguer gravity value of about -102 mgal, whereas the east block has a value of about -110 mgal (Pitts and Couch, 1978; Pitts, 1979). The decrease in Bouguer gravity values occurs approximately along the Cougar fault. Using a reduction density of 2.43 g/cm<sup>3</sup>, Pitts (1979) produced a residual gravity anomaly map which shows a decrease in gravity values of 6 mgal from the west block to the east block (also see Couch and others, 1982a,b). This decrease in residual gravity occurs over an east-west distance of only 3.9 km (2.3 mi), producing a very steep north-south-trending gradient. The Cougar fault follows the east side of this steep gradient. The residual and Bouguer gravity gradients continue toward the north across Lookout Ridge into the area mapped by Swanson and James (1975), suggesting that the Cougar fault also continues toward the north, which lends credence to observation number 4 above on the age of movement on the fault. The same gradients continue toward the south, where they coincide with another down-to-the-east, north-south fault in the McCredie Hot Springs area (Woller and Black, Chapter 6).

The aeromagnetic map of Couch and others (1978) also shows a steep change in the pattern of magnetism at the Cougar fault. The west block of the fault has a magnetic high of +250 gammas centered on Harvey Mountain, while the east block of the fault from Walker Creek to Castle Rock is characterized by a broad magnetic low of between -50 and -150 gammas. The transition between these two areas occurs at a steep north-south-trending gradient which terminates at the Cougar fault. A magnetic low along the McKenzie River to the north and an east-west-trending magnetic high at Tipsoo Butte changes the north-south pattern of contours. The north-south pattern, however, appears to reestablish itself north of Lookout Ridge in the area mapped by Swanson and James (1975).

### **Local tilting and folding**

There is no evidence of a major fold in the area. Wells and Peck (1961) plotted the axis of the Breitenbush anticline a few kilometers west of the map area, but the general easterly dip of 10° to 20° inferred from their map could not be demonstrated in the map area. Dips measured in the section of early and late

Western Cascade age have many orientations over very small areas, because of initial slopes during deposition and local deformation related to small faults and probable mass movements.

Dips in fine-grained epiclastic units along the west shore of Cougar Reservoir, however, consistently show tilting of about 7° or less toward the south to southwest. Although there is considerable relief on the contact between rocks of the late Western Cascade and early Western Cascade episodes, there is little difference in dips across the contact, and the sequence of late Western Cascade age appears also to slope gently toward the south to southwest. South of the map area, rocks of the late Western Cascade episode totally dominate surface outcrops, whereas to the north, the sequence of early Western Cascade age crops out at higher elevations. As previously explained, this is partly due to a local topographic high which existed in the northern part of the map area when the lavas of late Western Cascade age began to erupt, but some southerly tilting of the Western Cascade sequence is probably necessary to explain dominance of the sequence of late Western Cascade age over the region beyond the map area to the south.

There is no indication of any measurable southerly tilting of the sequence of early High Cascade age. This suggests that a slight angular discordance may exist between the sequences of early High Cascade and late Western Cascade age. If the tilting occurred gradually throughout late Western Cascade time, units of the latest Western Cascade age may be conformable. The close similarity between the age of an uppermost lava of the late Western Cascade episode at Lookout Ridge (8.80 m.y. B.P.) to an overlying lava of the early High Cascade episode (8.34 m.y. B.P.) suggests that the latter hypothesis is probably correct. In any case, the total amount of tilting is quite small and not easily measured in this type of volcanic terrane.

The 1-km (0.6-mi)-deep entrenchment of the McKenzie River drainage system into the rocks west of the Horse Creek fault zone probably occurred between 5 and 4 m.y. B.P. Essentially all of the current relief in the McKenzie River area was developed before the Foley Ridge flows entered the McKenzie River canyon. Taylor (1980; personal communication, 1983), utilizing Sutter's (1978) radiometric data, concluded that the oldest Foley Ridge date is about 3.98 m.y. B.P. (see footnote 2.3, Chapter 2). The presence of 6- to 5-m.y. B.P. flows of the early High Cascade episode on ridgetops as much as 1,238 m (4,060 ft) above the intracanyon Foley Ridge flows indicates that the McKenzie River cut down over a kilometer into the area over a period of about 1 m.y. (also see Flaherty, 1981). MacLeod (personal communication, 1982) believes substantial uplift of the Western Cascades rather than only passive subsidence of the High Cascades is necessary to explain this rapid erosion. It may be that both uplift of the Western Cascades and subsidence of the High Cascade axis occurred simultaneously. The similarity of the elevations of both the base of the Foley Ridge flows and the current McKenzie River indicates that the streams may have been at approximately base level for the past 4 m.y. (MacLeod, personal communication, 1982), except for periodic influxes of glacial outwash sediments during the Pleistocene.

## GEOHERMAL RESOURCES

Terwilliger Hot Springs, the only hot springs in the map area, has flow rates of 114 to 200 liters (30 to 53 gallons) per minute and measured temperatures between 38° and 44° C (Table 4.2). Calculated reservoir temperatures from chemical geothermometers range between about 48° and 104° C (Table 4.2). The silica geothermometer, based on the assumption of

equilibrium with opal, gives negative reservoir temperatures and so obviously does not apply to the Terwilliger Hot Springs waters. The good agreement among the silica geothermometers, which assume equilibrium with quartz, and the Na:K:Ca ( $1/3\beta$ ) geothermometer suggests that these chemical systems are most applicable to the Terwilliger Hot Springs waters. The range of reservoir temperatures using the latter systems is 95° to 104° C.

Table 4.2. *Estimated reservoir temperatures of Terwilliger Hot Springs from chemical geothermometers of Fournier (1979), Fournier and Rowe (1966), Fournier and Truesdell (1973), and Mariner and others (1980). Data are from Brown and others (1980a)*

	Lower spring	Upper spring	Upper spring
Date sampled	3/76	1973	3/76
Surface temperature (°C)	38	44	42
Flow rate (liters/min.)	114	200	200
Na:K (°C)	87	74	86
Na:K:Ca, $1/3\beta$ (°C)	104	95	103
Na:K:Ca, $4/3\beta$ (°C)	52	48	51
SiO <sub>2</sub> , conductive (°C)	99	102	99
SiO <sub>2</sub> , adiabatic (°C)	100	103	100
SiO <sub>2</sub> , chalcedony (°C)	68	72	69
SiO <sub>2</sub> , opal (°C)	-17	-14	-16

A temperature-gradient hole about half a kilometer (a third of a mile) east of the hot springs intercepted a heavily celadonitized tuffaceous unit at 125 m (410 ft). Upon penetrating the lower contact of the unit at 140 m (459 ft), about 378 liters (100 gallons) per minute of 23°-C water began to blow from the hole during airhammer drilling. Water continued to blow from the hole as the drill penetrated a holocrystalline, plagioclase-pyroxene-bearing lava flow to a depth of 153.5 m (503.5 ft). The average stabilized temperature gradient within the well was 134.7° C/km. The gradient was roughly linear throughout the aquifer; temperatures varied from 23.2° C at 140 m (549 ft) to 24.7° C at 153.5 m (503.5 ft), giving a gradient within the aquifer of 112° C/km. The average gradient, corrected for local terrain effects, is 102° C/km (Black and others, Chapter 7).

A hole drilled northeast of the above well, at the mouth of Walker Creek and adjacent to the Cougar fault, had an average gradient of 54.1° C/km in the lower 50 m (164 ft) of the 155-m (508-ft) hole (sampled to 152 m [499 ft]). The terrain-corrected gradient was 52.0° C/km, resulting in a heat-flow value of 83 mW/m<sup>2</sup> (Black and others, Chapter 7). The terrain-corrected value is similar to terrain-corrected gradients measured in other holes near Cougar Dam which range from about 48.0° C/km to 53° C/km. The heat flow from the Walker Creek hole is thus probably characteristic of the background heat flow in the map area.

This background heat-flow value of 83 mW/m<sup>2</sup> roughly matches the regional heat flow predicted by Blackwell and others (1978). This heat flow is characteristic of the transition zone between the low heat flow (approximately 40 mW/m<sup>2</sup>) of the Willamette Valley-Coast Range provinces and the high heat flow (greater than 100 mW/m<sup>2</sup>) of the High Cascades (see Blackwell and others, 1978, 1982). The Belknap-Foley Hot Springs area east of the map area (Figure 4.1) has heat flow characteristic of the High Cascades. Three conclusions may be drawn from the above observations:

1. The hole near Terwilliger Hot Springs has a gradient which is raised by convective upflow of thermal water related to the hot springs.
2. The Walker Creek hole, even though it is next to the largest fault in the area, shows no evidence of temperature disturbance by upwelling thermal waters.
3. Heat flow probably increases from west to east across the map area toward the main part of the High Cascade heat-flow anomaly.

Terwilliger Hot Springs is located on strike with a small N. 35° W. shear zone which dips 79° to the southwest. No shear zone was found at the actual hot springs, but the thermal water issues from a complex series of joints and fractures. A similar observation applies to Foley Hot Springs to the east, where hot water issues from northwest-trending fractures and small shears. Both Foley and Terwilliger Hot Springs are on upthrown blocks adjacent to major north-south- to northwest-trending fault zones (Figure 4.1), but neither of the springs issues directly from the main fault. It may be that jointed rocks and splinter faults adjacent to the main fault zones offer more permeability than the fault zones themselves. Alternatively, water may rise from depth in certain places along the main faults until it encounters impermeable rock units which force the water into lateral zones of permeability. The water might then reach the surface along local splinter faults or joints. There are insufficient data in the map area to distinguish between these two possibilities, but significant smectite-calcite-zeolite alteration within the Cougar fault zone suggests that some hydrothermal circulation occurred there in the past.

If local terrain-corrected conductive gradients hold up to a depth of 3 km (1.8 mi) (the maximum practical drilling depth), a temperature of about 165° C could be encountered. Fluids at this temperature are adequate for Rankine-cycle electrical generators but not for direct-flash generators. Unless drilling can intercept upwelling thermal fluids, it is not likely that the area can be economically exploited for generation of electricity, inasmuch as drilling to 3 km (1.8 mi) and use of expensive Rankine-cycle generators may well prove to be uneconomic. Drilling of additional temperature-gradient holes along the Cougar fault zone might reveal disturbances of the background heat flow indicative of significant transport of heat from depth by upward-moving thermal water.

The higher heat flow associated with the Horse Creek fault zone to the east of the map area (Figure 4.1; see Black and others, Chapter 7) makes that area a more attractive exploration target than the Cougar Reservoir area. Curie-point isotherm calculations of Connard (1980) confirm that the depth of the Curie-point isotherm is probably shallow (i.e., 8 to 14 km [4.8 to 8.4 mi] below sea level) under the High Cascades in the main part of the heat-flow anomaly outlined by Blackwell and others (1978). Connard's model suggests that the Curie-point isotherm may be significantly deeper under the Cougar Reservoir area, although his data were not at all definitive on this point. Geothermal exploration models relating to the Horse Creek area and other areas in the main part of the High Cascade heat-flow anomaly of Blackwell and others (1978) are discussed in Chapter 8.

## CONCLUSIONS AND SPECULATIONS

The Cougar Reservoir area is cut by a north-south fault which displaces rocks of the late Western Cascade episode at least as young as 13.2 m.y. The relative motion on the fault is down to the east by at least 152 m (499 ft) and possibly by more than 1,033 m (3,388 ft). The fault may have begun to displace rocks of the area as early as 16.2 m.y. B.P. Geologic and geophysical interpretations suggest that a fault scarp may have existed in the area when distinctive, iron-rich diktytaxitic basaltic lavas of the early High Cascade episode began to flow from the east about 8.3 to 7.8 m.y. B.P. The fault does not cut Pleistocene outwash gravels and does not have an obvious topographic scarp like the 5- to 4-m.y. B.P. Horse Creek fault. It is reasonable to assume that most movement on the fault occurred prior to 4 m.y. B.P., otherwise a large topographic scarp would probably be present.

The Cougar fault and the parallel, but younger, Horse Creek fault are probably two small parts of regional north-south zones of down-to-the-east faulting. This conclusion is supported by the continuation of gravity signatures characteristic of both faults for many kilometers to the north and south (Couch and others, 1982a,b). Where this hypothesis was tested by mapping in the Waldo Lake-Swift Creek area, two major north-south faults which appear to be nearly exact analogues of the Horse Creek and Cougar faults were found (see Chapter 6). Regional tectonic implications of these two major zones of faulting are discussed in Chapter 2.

The area as a whole has not been significantly folded, but slight tilting toward the south probably occurred during late Western Cascade time (i.e., between 13 and 9 m.y. B.P.). Although deep erosion produced about 366 m (1,200 ft) or more of relief between the time of deposition of the tuffs of Cougar Reservoir and the time of eruption of lavas and tuffs of the late Western Cascade episode, no certain evidence of an angular unconformity was found between these two sequences. Most of the current drainage system probably developed between 5 and 4 m.y. B.P. during formation of faults in the Horse Creek area. Uplift of the Western Cascades and possible subsidence of the High Cascades occurred between 5 and 4 m.y. B.P. Deep dissection (1 km [0.6 mi]) of the area occurred during this interval.

After the Western Cascades were uplifted in the early Pliocene, lavas of the late High Cascade episode banked up against the bounding fault scarp of the Western Cascade block and, where the McKenzie River cut across it, flowed into the uplifted block (Taylor, 1980; Flaherty, 1981). These basal lavas of the late High Cascade episode closely resemble the distinctive iron-rich diktytaxitic basalts at Tipsoo Butte which mark the base of the early High Cascade volcanic episode. The Tipsoo Butte basalts may also bank up against a major north-south fault at Cougar Reservoir.

It appears, from the above evidence, that there is a close, perhaps completely analogous, relationship between the Horse Creek area and the Cougar Reservoir area. The Cougar fault of late Miocene age may be an analogue of the Horse Creek fault of early Pliocene age. Likewise, the eruptions of diktytaxitic basalts probably occurred after formation of topographic fault scarps at both Cougar Reservoir and Horse Creek.



## CHAPTER 5. GEOLOGY OF THE LOOKOUT POINT AREA, LANE COUNTY, OREGON

By Neil M. Woller and George R. Priest,  
*Oregon Department of Geology and Mineral Industries*

### ABSTRACT

A sequence of tholeiitic lavas, here called the lavas of Black Canyon, was identified within the predominantly calc-alkaline middle and upper Tertiary terrane of the Western Cascade province. These lavas are dated at 22 m.y. B.P., which is in good accordance with the dates of other identified tholeiitic sequences in the Western Cascades.

The lavas of Black Canyon flowed through a paleocanyon that was perpendicular to the Eugene-Denio lineament. It has been suggested by other researchers that this lineament is a zone of right-lateral strike-slip displacement. The authors could show no substantial lateral offset on the paleocanyon filled with tholeiitic lavas.

Most mapped faults and shears in the Lookout Point area strike to the northwest, and the Eugene-Denio lineament in this area appears to be controlled by these northwest-trending structures. There is no evidence that these structures cut rocks younger than 18 m.y.

### INTRODUCTION

The Lookout Point area is located 7 km (4.2 mi) northwest of Oakridge and 58 km (35 mi) southeast of Eugene in Lane County, Oregon (see Figure 5.1). It is a rugged, heavily forested mountain area located within the Western Cascade physiographic province. The northwest-flowing Middle Fork of the Willamette River provides the principal drainage and flows into Lookout Point Reservoir in the northwest part of the map area. Access is by State Highway 58 and the extensive logging-road network of the Willamette National Forest.

### VOLCANIC STRATIGRAPHY

#### Introduction

The informal nomenclature used by Priest and others (Chapter 2) to discuss and compare petrologic and chemical similarities of temporally equivalent stratigraphic units throughout the central Oregon Cascade Range is also used in this chapter. Figure 2.3 shows distinctive lithologic and field characteristics that typify, on a regional basis, each of the four age groups. Correlative rock stratigraphic units of Cascade researchers corresponding to each division are shown on Plate 1.

All four age groups of Priest and others (Chapter 2) are represented in the Lookout Point area. The authors attempted to identify the age breaks between each stratigraphic unit with K-Ar dates supplied by Stanley H. Evans and F.H. Brown of the University of Utah Research Institute, and these data are summarized in Table 5.1.

Lookout Point geochemical data and related discussions are incorporated into the petrologic discussions and diagrams of Priest and others (Chapter 2) and are not duplicated here in detail. The geologic map of this area is presented in Figure 5.2.

### Volcanic rocks of the early Western Cascade episode

**Introduction:** Volcanic rocks of the early Western Cascade episode in the Lookout Point area are represented by the Oligocene to lower Miocene tuffs and lavas, undifferentiated. Distinctive lithologies within this unit are the lavas of Lookout Point, the lavas of Hardesty Mountain, and the lavas of Black Canyon. These rock units comprise most of the total exposed section in the map area. The bottom of the section of early Western Cascade age is not exposed in the map area.

**Oligocene and lower Miocene tuffs and lavas, undifferentiated (unit Totl):** The oldest rocks in the area are Oligocene to lower Miocene tuffs and lavas, previously mapped as the Little Butte Volcanic Series (Peck and others, 1964; Kays, 1970). They are probably roughly equivalent to the tuffs of Cougar Reservoir (Priest and Woller, Chapter 4) and the Oligocene-Miocene lavas, undifferentiated, of Woller and Black (Chapter 6).

Tuffs predominate in the unit. In the exposures at river level, the tuffs are green, lithic-fragment rich, pumice poor, and generally massive. They contain abundant silicic aphyric clasts of many pastel colors. The matrix is generally green or yellow ash, altered to celadonite, chlorite, or smectite. The texture of these units suggests an origin that is in large part laharic. Large clasts up to half a meter (1½ ft) in diameter are locally found in the flows. Pumice is rarely present. Charred wood occurs in some outcrops. In nearby exposures at Hills Creek Dam, similar deposits contain fragments of volcanic flow rock many meters in diameter. The rare interbeds, which can be seen in excellent roadcut exposures along State Highway 58, are typically thin, fine-grained epiclastic units sandwiched between identical overlying and underlying laharic(?) lithic-fragment-rich tuff. In the heat-flow hole drilled at the mouth of Burnt Bridge Creek, 150 m (492 ft) of uninterrupted green, lithic-fragment-rich tuff was penetrated without reaching the bottom of the unit.

Above the lithic-fragment-rich tuffs, ash-flow and air-fall tuffs predominate. They are altered and phenocryst poor, with yellow, red, purple, or green color commonly resulting from alteration. Common types of alteration include devitrification and the alteration of pumice and ash to smectite and/or chlorite. Many ash-flow tuffs are nonwelded, but in others, slight collapse of pumice lapilli indicate that incipient welding may be present. All are probably dacitic or rhyodacitic in composition, but no chemical analyses were obtained. Interbedded lavas range in composition from rhyodacite to basaltic andesite, but silicic lavas predominate. Most are aphyric or slightly plagioclase phyric and have smectite alteration. The total thickness of the ash- and lava-flow sequence exceeds 600 m (1,968 ft). The dips of the sequence, although highly variable from exposure to exposure, appear to be to the north and northeast.

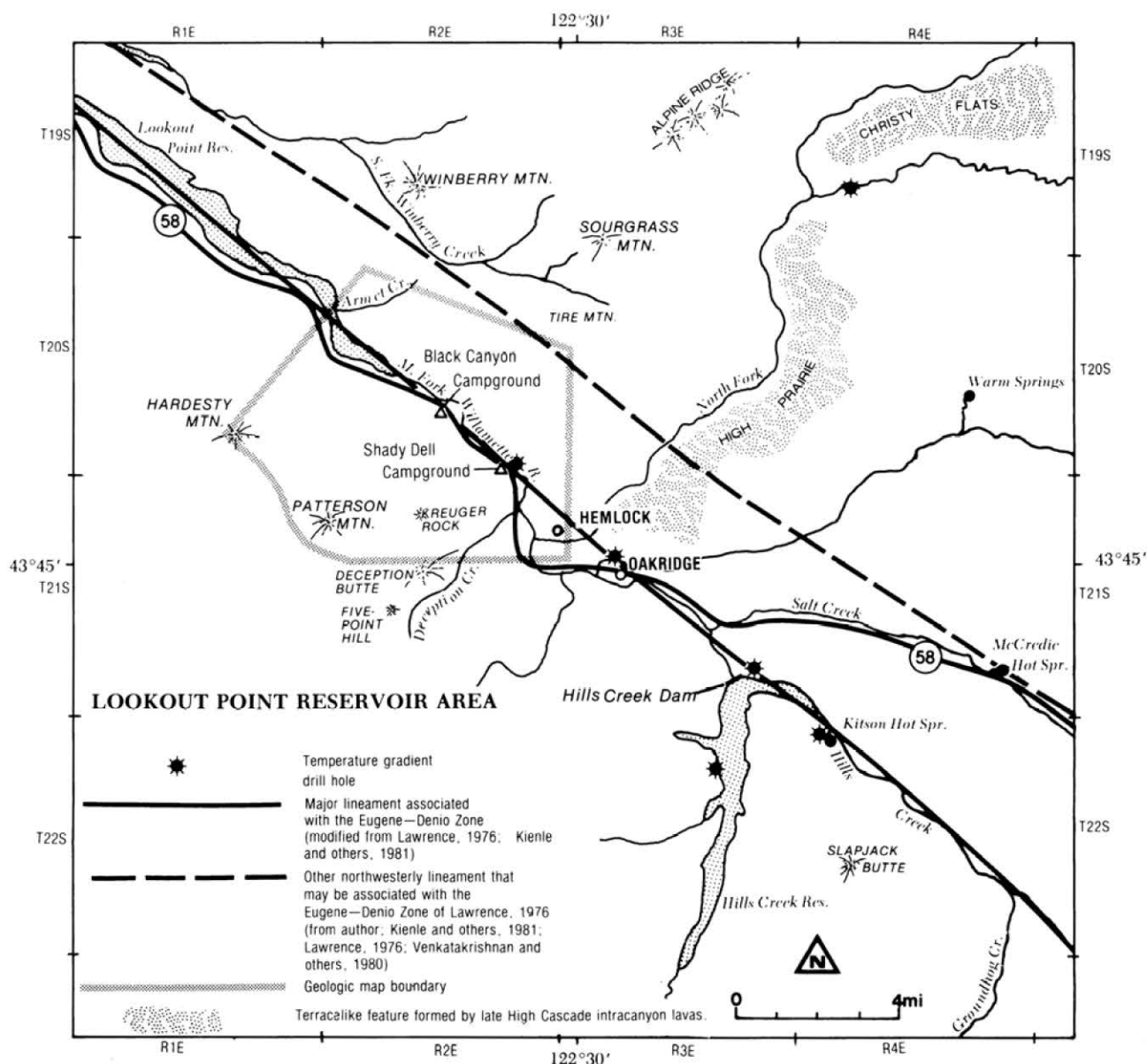


Figure 5.1. Map showing the location of the Lookout Point map area, the Eugene-Denio lineament, and other localities mentioned in the text.

A basaltic andesite from fairly high in the section was dated at  $24.7 \pm 2.0$  m.y. B.P. (0.81 percent K, 17 percent radiogenic  $Ar^{40}$ ). However, the presence of smectitic alteration may have caused some loss of radiogenic argon, which would cause the date to be too young.

The rocks of the early Western Cascade episode tend to form gentle slopes which are characterized by frequent slumps and slides. Exposures other than in roadcuts and railway cuts are rare, making it difficult to trace individual flows for any distance. Three distinctive units within the section of early Western Cascade age are extensive enough to be mapped separately, however. These are the lavas of Lookout Point, the lavas of Hardesty Mountain, and the lavas of Black Canyon.

**Lavas of Lookout Point (unit Tolp):** The lavas of Lookout Point are exposed mainly at river level on both sides

of the Willamette River. The flows, which are more resistant to erosion than are the enveloping tuffs, tend to form knobs. Lookout Point, a prominent, plug-shaped outcrop on the northeast side of the Willamette River, may be a source for these lavas.

Rocks from these flows have sparse plagioclase phenocrysts and rare pyroxene phenocrysts. They are black when fresh and pink or gray when altered. Individual flows cannot be distinguished from one another in the field.

**Lavas of Hardesty Mountain (unit Toh):** Over 450 m (1,476 ft) of plagioclase-phyric andesitic lavas form a resistant cap on Hardesty Mountain. These rocks are altered and typically brown, pink, or gray. Clinopyroxene is more abundant than orthopyroxene; other ferromagnesian phases are unrecognizable because of alteration to smectite.

Table 5.1. *Stratigraphy of volcanic rock units in the Lookout Point area, central Cascade Range, Oregon*

Regional volcanic episode <sup>1</sup>	Name and map symbol	K-Ar dates (m.y. B.P.)	Maximum exposed thickness	SiO <sub>2</sub> content <sup>3</sup> (wt. %)	Lithologic description
Late High Cascade	Pliocene-Pleistocene basaltic lavas (QTb)	0.56 ± 0.16	49 m (160 ft)	54.5	Olivine-bearing basalt; diktytaxitic to compact; dark-gray; fresh. Flowed into canyons cut into all older units in Quaternary drainages.
Early High Cascade	Upper Miocene lavas (Tmu)	5.81 ± 0.30	73 m (240 ft)	50.9	Olivine-bearing basalt; compact; fresh; gray; caps Patterson Mountain.
Late Western Cascade	Miocene andesitic lavas (Tma/Tmi)	Upper part, 8.3 ± 5.5 <sup>2</sup> ; lower part, 15.9 ± 7.6 <sup>2</sup>	610+ m (2,000+ ft)	58.3-68.1	Two-pyroxene andesite with subordinate two-pyroxene dacite, olivine-bearing basaltic andesite, and epiclastic interbeds; dark-gray to black; generally altered.
Early Western Cascade	Oligocene and lower Miocene tuffs (Totl)	24.7 ± 2.0 <sup>2</sup>	762+ m (2,500+ ft)	56.1-71.2	Silicic ash-flow tuffs, sediments, laharic(?) lithic-fragment-rich tuffs and lavas, generally dacitic to rhyodacitic; altered, with celadonite, chlorite, and/or smectite.
	Lavas of Black Canyon (Tml/Tmli)	Top, 22.0 ± 1.0; bottom, 21.9 ± 2.9 <sup>2</sup>	366+ m (1,200+ ft)	52.4-58.1	Tholeiitic basaltic andesite, basalt, and andesite; aphyric to plagioclase-phyric; dark-gray to black; fresh to altered. Interbedded with ash-flow tuffs and epiclastic deposits. Flowed into canyons cut into older units.
	Lavas of Hardesty Mountain (Toh)	—	488 m (1,600 ft)	60.4	Pyroxene andesite and dacite; plagioclase-phyric; extensive alteration of mafic phenocrysts, brown, pink, gray. Clinopyroxene generally present in larger percentages than orthopyroxene; caps Hardesty Mountain.
	Lavas of Lookout Point (Tolp)	—	213 m (700 ft) at Lookout Point	71.9	Rhyodacitic lavas; dark-gray; sparsely plagioclase phyric; also contains rare megascopic clinopyroxene. Generally altered.

<sup>1</sup> See Priest and others (Chapter 2) for explanation and regional rock-stratigraphic correlation.<sup>2</sup> K-Ar date may be affected by alteration.<sup>3</sup> Recalculated to a 100-percent total, volatile-free.

**Lavas of Black Canyon (unit Tml/Tmli):** The lavas of Black Canyon are a sequence of intracanyon tholeiitic basaltic to iron-rich andesitic lavas that flowed to the northeast from vents at Kreuger Rock and Deception Butte (immediately south of the map area). Other vents may exist, but they were not located during this study. These flows are stratigraphically and geochemically equivalent to the Scorpion Mountain lavas of White (1980a,c). The chemistry of six flows is shown in Appendix B, Table B.3, samples 45-50.

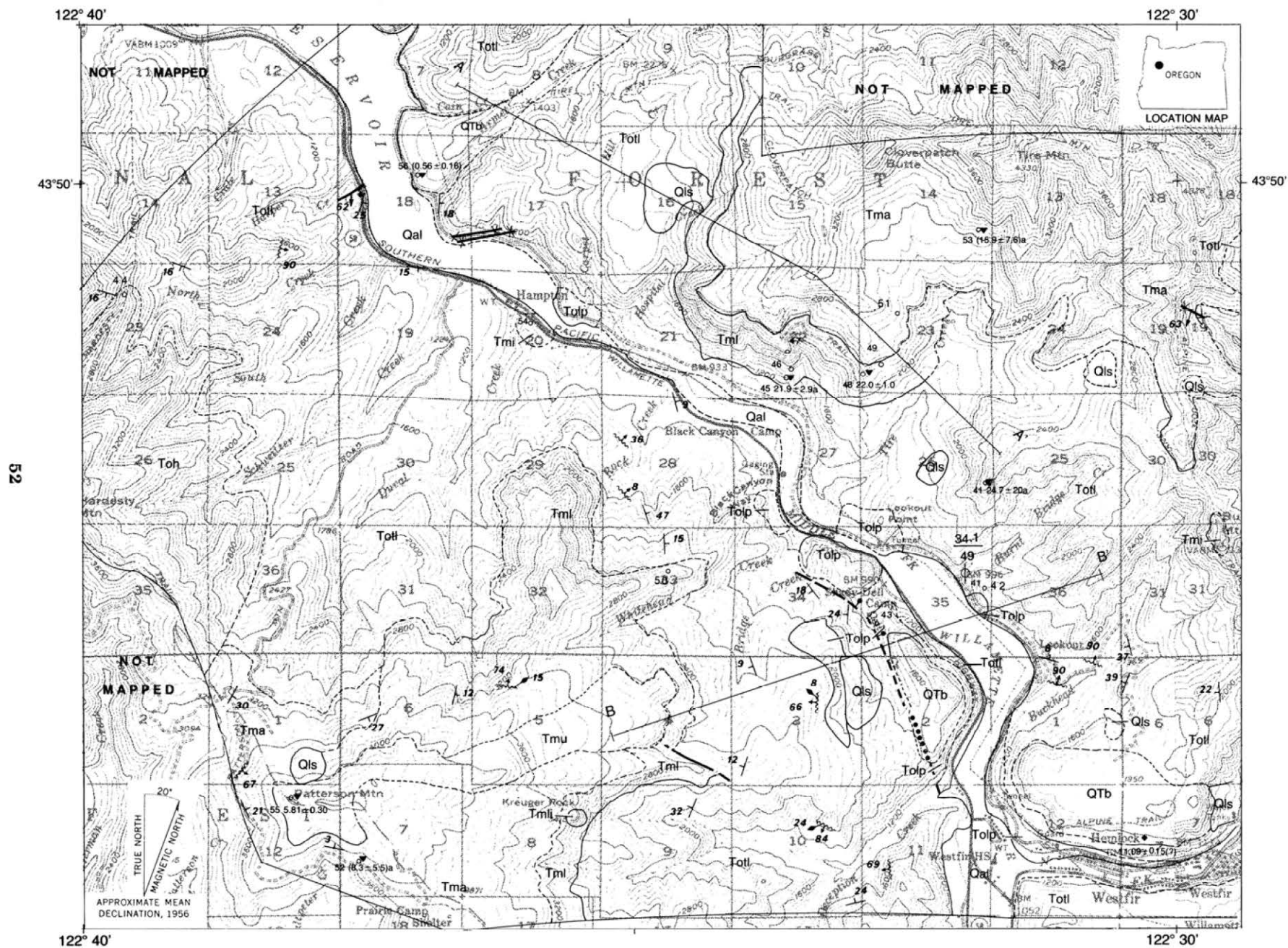
The lavas are compact, dark gray to black, and generally aphyric. In thin section, most are pilotaxitic with rare plagioclase and very rare augite and olivine microphenocrysts. Ash-flow tuffs and fine-grained sediments very similar in appearance to those of the Oligocene and lower Miocene tuffs and lavas which constitute the paleocanyon walls are interbedded with the Black Canyon lavas on the north side of Patterson Mountain.

On the Deception Creek side of the paleocanyon, the Black Canyon sequence can be followed for miles along a cliff exposure. Dips along the cliff face are low and to the north, but

on the north side of Patterson Mountain, dips of 12° to 17° are more common, and at one location a 30° dip to the southeast was measured. On the northeast side of the Willamette River, the dips are gentle (e.g., 2° to the north).

K-Ar dates obtained on the lowest flow and a flow moderately high in the sequence at Black Canyon were, respectively, 21.9 ± 2.0 m.y. B.P. (0.52 percent K, 11 percent radiogenic Ar<sup>40</sup>) and 22.0 ± 1.0 m.y. B.P. (0.54 percent K, 35 percent radiogenic Ar<sup>40</sup>). Extensive low-grade smectitic alteration of the lower flow may have affected accuracy of the K-Ar date. The upper dated flow was much fresher, and its K-Ar age is probably more reliable. Similar tholeiitic lavas in the same stratigraphic position in other Western Cascade locations have yielded similar dates (White, 1980a; Lux, 1981; see discussion and conclusions section of this chapter). In addition, the composition (high normative quartz and iron, low MgO) and field relations (continuous stack of lavas with few interbeds) suggest that the lavas of Black Canyon may be a genetically related magma series from a single volcanic source and thus may not span much time. Therefore, the authors feel 22

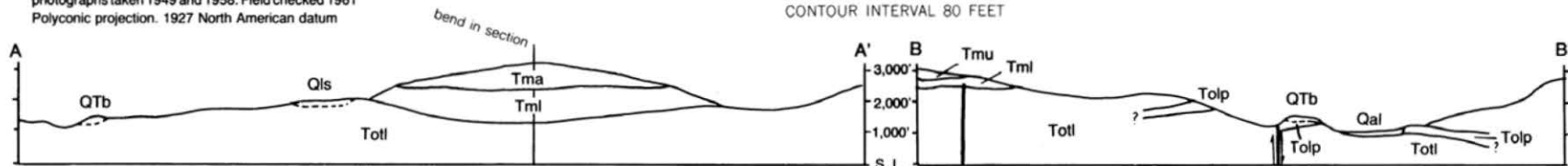




Base map by U.S. Geological Survey —  
Hardesty Mountain and Sardine Butte 15' quadrangles  
Control by USGS and USC&GS  
Topography by photogrammetric methods from aerial  
photographs taken 1949 and 1958. Field checked 1961  
Polyconic projection. 1927 North American datum



Geology by N.M. Woller and G.R. Priest  
Field work dates: 1980, 1981



### EXPLANATION SURFICIAL DEPOSITS

- Qal** Recent alluvium (Quaternary): Recent unconsolidated sediments located in present river and creek channels
- Qls** Landslide deposits (Quaternary): Unconsolidated landslide deposits, including slumps and slide blocks

### BEDROCK GEOLOGIC UNITS

#### Volcanic rocks of the late High Cascade episode

- QTb** Pliocene-Pleistocene basaltic lavas (Pliocene-Pleistocene): Olivine basalts and basaltic andesites, diktytaxitic to compact, gray, fresh. Found as intracanyon flows in canyons cut into all other rock units in drainages related to Quaternary topography. Equivalent to the basalts of High Prairie of Brown and others (1980b) and the upper part of the volcanic rocks of the High Cascades . . . [undivided] of Peck and others (1964). Armet Creek flow dated at  $0.56 \pm 0.16$  m.y. B.P.

#### Volcanic rocks of the early High Cascade episode

- Tmu** Upper Miocene lavas (upper Miocene): Olivine basalt, fresh, gray, compact. Caps Patterson Mountain. Equivalent to Pliocene volcanic rocks of Brown and others (1980b) and the lower part of the volcanic rocks of the High Cascades . . . [undivided] of Peck and others (1964). Dated at  $5.81 \pm 0.3$  m.y. B.P.

#### Volcanic rocks of the late Western Cascade episode

- Tma** **Tmi** Miocene andesitic lavas (Miocene): Two-pyroxene plagioclase-rich andesites with interbeds of epiclastic volcanic rocks and minor flows of olivine basalt and dacite. Equivalent to Sardine Formation of Peck and others (1964) and Miocene volcanic rocks of Brown and others (1980b). Unit **Tmi**: intrusive equivalent of unit **Tma**. One flow low in section dated at  $15.9 \pm 7.6$  m.y. B.P.; another flow high in the section dated at  $8.3 \pm 5.5$  m.y. B.P.

#### Volcanic rocks of the early Western Cascade episode

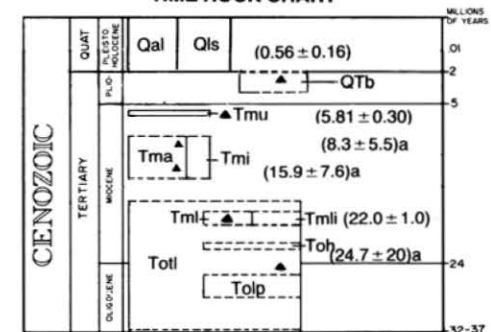
- Totl** Oligocene and lower Miocene tuffs and lavas, undifferentiated (Oligocene and lower Miocene): Lower part: lithic-fragment-rich tuff, possibly partly laharic in origin. Upper part: ash-flow tuff, air-fall tuff, silicic lavas, and sedimentary interbeds. Generally altered, stained, and deformed. Equivalent to Little Butte Volcanic Series of Peck and others (1964) and Breitenbush formation of White (1980a) and Hammond and others (1982). A lava high in section was dated at  $24.7 \pm 2.0$  m.y. B.P. Three distinctive units within this sequence were mapped separately and are described below:

- Tml** **Tmli** Lavas of Black Canyon (lower Miocene): Basalt to andesite, aphyric to slightly plagioclase phyrlic, black, gray, or brown. Follows canyon cut into unit **Totl**. Contains interbeds of sediments and ash flows of unit **Totl**. Equivalent to Scorpion Mountain lavas of White (1980a,c). Unit **Tmli**: plug of these lavas. Sequence extruded in short period of time about 22 m.y. B.P.

- Toh** Lavas of Hardesty Mountain (upper Oligocene-lower Miocene): Intermediate lavas, generally plagioclase phyrlic. Caps Hardesty Mountain

- Tolp** Lavas of Lookout Point (upper Oligocene): Rhyodacitic lavas; black, gray, or pink; glassy field appearance with sparse plagioclase and rare pyroxene phenocrysts. Resistant compared to surrounding tuffs; forms knobby hills along the river

### TIME ROCK CHART



### GEOLOGIC SYMBOLS

- Contacts: Solid where visible; dashed where inferred below cover or from aerial photo interpretation
- Fault: Solid where visible; dashed where approximately located; dotted where concealed by alluvium, landslide, or colluvium. Dip on fault plane indicated where known; bar and ball on downthrown side
- \* \* \* Dike: Mafic to intermediate dike, dip indicated
- Shear: With dip of plane and orientation of striations within plane
- Shear: With dip of plane and slickensides
- Strike and dip: Of thinly bedded epiclastic units or volcanic flow tops
- Geochemical sample location**
- K-Ar date:** Age in millions of years (this study). Parentheses around date indicate that sample had less than 10 percent radiogenic argon. "a" indicates date may be affected by low-grade rock alteration
- K-Ar date:** Age in millions of years (Sutter, 1978)
- Drill hole location:** Terrain-corrected gradient in °C/km and heat-flow values in mW/m<sup>2</sup>

Figure 5.2 (both pages). Map of the geology of the Lookout Point area.

m.y. B.P. represents a reasonable date for this sequence of flows.

The Black Canyon lavas can be seen best along the Willamette River across from the Black Canyon Campground (Figure 5.1), where the section is 350 m (1,148 ft) thick. The measured section at this location is described in Figure 5.3. Although the lower contact with the underlying Oligocene and lower Miocene tuffs and lavas, undifferentiated, is obscured by colluvium, it is marked by a sharp change in slope. The upper contact with the Miocene andesitic lavas appears conformable at Black Canyon but is unconformable at Patterson Mountain.

### Volcanic rocks of the late Western Cascade episode

**Introduction:** The volcanic rocks of the late Western Cascade episode are represented in the Lookout Point area by Miocene andesitic lavas. These rocks are stratigraphically equivalent to the Sardine Formation of Peck and others (1964) and the Miocene volcanic rocks of Brown and others (1980b).

**Miocene andesitic lavas (unit Tma/Tmi):** Miocene andesitic lavas are characterized mainly by andesitic lava flows, with subordinate dacitic and basaltic andesite flows and interbedded epiclastic volcanic rocks and rare olivine basalt flows. The andesites are typically dark gray to brown and plagioclase rich. Both orthopyroxene and clinopyroxene are commonly found in flows of intermediate composition.

Very few of these flows are unaltered. Smectite is the most common alteration mineral, usually replacing mafic phenocrysts and groundmass minerals.

A dacite flow from low in the section was dated at  $15.9 \pm 7.6$  m.y. B.P. (0.241 percent K, 3 percent radiogenic  $\text{Ar}^{40}$ ), and an andesitic flow from high in the section on Patterson Mountain was dated at  $8.3 \pm 5.5$  m.y. B.P. (0.100 percent K, 8 percent radiogenic  $\text{Ar}^{40}$ ). Both rocks have experienced low-grade alteration, characterized by the presence of smectite in plagioclase phenocrysts. The alteration may have caused the loss of radiogenic argon, which would make the rocks older than the ages reported here. Despite the high statistical error and low potassium and radiogenic argon of both samples, the older date is consistent with the age of the lower part of the sequence of late Western Cascade age, and the Patterson Mountain date approximately corresponds to the latest volcanism of the late Western Cascade episode as dated in other areas (Priest and others, Chapter 2).

### Volcanic rocks of the early High Cascade episode

**Upper Miocene lavas (unit Tmu):** Lavas of the early High Cascade episode which are present at Patterson Mountain are called upper Miocene lavas. They are olivine basalts which are light gray, compact, and unaltered. Two flows were recognized, the lower one of which is very poorly exposed. The unit is equivalent to the lavas of Tipsoo Butte (Priest and Woller, Chapter 4), Miocene-Pliocene basaltic lavas (Woller and Black, Chapter 6), and Pliocene volcanic rocks (Brown and others, 1980a,b). A K-Ar date of  $5.81 \pm 0.3$  m.y. B.P. (0.91 percent K, 30 percent radiogenic  $\text{Ar}^{40}$ ) was obtained on the upper flow.

### Volcanic rocks of the late High Cascade episode

**Pliocene-Pleistocene basaltic lavas (unit QTb):** Lavas of the late High Cascade episode are present at two locations within the Lookout Point area. The terminus of the intracanyon basalt flows at High Prairie (previously mapped by Callaghan and Buddington, 1938; Peck and others, 1964; Brown and others, 1980b) is located northwest of the town of Hemlock. These diktytaxitic olivine basalts, which originated in the Christy Creek area to the east (MacLeod and Sherrod,

personal communications, 1982) form the topographic features of Christy Flats and High Prairie (Figure 5.1).

The High Prairie flows were dated by McBirney and others (1974) at  $11.09 \pm 0.15$  m.y. B.P., but that date is probably too old, because it is much greater than ages of lavas at the tops of the local ridges (e.g., upper Miocene lavas). The flows followed Quaternary canyons and are identical in mineralogy, chemistry, and field aspect to other nearby lavas of the late High Cascade episode which possess dates of 2 to 3 m.y. B.P. (e.g., see Flaherty, 1981; Priest and others, Chapter 2).

The other Pleistocene flow in the Lookout Point area forms a fan-shaped lobe which protrudes into the Willamette River channel at the mouth of Armet Creek. The source is located 3 km (1.8 mi) up Armet Creek from its junction with the Willamette River. The flow is a nearly aphyric basaltic andesite which bears olivine and augite microphenocrysts. The Armet Creek flow is normally polarized (Sherrod, personal communication, 1982) and has a K-Ar age of  $0.56 \pm 0.16$  m.y. (1.18 percent K, 5 percent radiogenic  $\text{Ar}^{40}$ ).

## STRUCTURE

### Structural configuration of rocks of the early Western Cascade episode

Landsliding and dense vegetation obscure the rocks of the early Western Cascade episode to such an extent that it is difficult to see the structural configuration of the sequence as a whole. Within specific localities, formational attitudes can be measured, but the location and nature of the transitions between specific localities are not evident.

The Black Canyon lavas dip to the north and northeast, which is in accordance with the attitude of the sequence of early Western Cascade age visible in the Deception Creek area. The overall dip of the same sequence in the southern part of the Lookout Point map area is apparently  $10^\circ$  to  $20^\circ$  to the north. North of the Willamette River, the northerly dips appear to be somewhat shallower ( $2^\circ$  to  $10^\circ$ ), although westerly dips of  $22^\circ$  to  $39^\circ$  were measured near Buckhead Mountain.

### Shear orientations in rocks of the early Western Cascade episode

Many low-angle shears occur within rocks of the early Western Cascade episode in the Lookout Point area, and many of these shears possess low-angle rakes indicative of strike-slip motion. Most of the low-angle shears with low rake angles are northwest striking. Bedding-plane movement was noted in two exposures.

### Shady Dell fault

A northwest-trending lineament above Shady Dell Campground on the southwest side of the Willamette River may be a fault which vertically offsets the Lookout Point lavas by as much as 122 m (400 ft). The trace of the lineament, which trends N.  $15^\circ$  W., implies a steep, nearly vertical dip. Sediments crop out in a switchback roadcut directly across a ravine from the Lookout Point rhyodacite. Above the sediments, an altered, decomposed outcrop of what may be the same rhyodacite is exposed. The apparent relative displacement is down to the northeast. The possible fault zone in the ravine is obscured by landslides, colluvium, and vegetation. We were not able to show that the fault zone cuts younger units.

### Deformation of the Black Canyon lavas

The Black Canyon lavas are not sheared, deformed, or altered to the same extent as the underlying rocks. The minimum interval between extrusion of the Black Canyon lavas



## Stratigraphic section of the lavas of Black Canyon



\*Volatile free, total iron as  $\text{Fe}^{+2}$  Complete raw chemistry is listed in appendix.

Figure 5.3. Stratigraphic section of the lavas of Black Canyon.

and older units is 3 m.y. A minimum age of 24.7 m.y. was obtained on a slightly altered sample of underlying rocks of the early Western Cascade episode, while the Black Canyon lavas have been dated at about 22 m.y. B.P. The contrast in degree of shearing between the Black Canyon lavas and older units and the development of a 250-m (820-ft)-deep paleocanyon into which the lavas of Black Canyon flowed suggest that significant deformation and possible uplift occurred in the time interval between the eruption of the older units and the Black Canyon lavas. The change from calc-alkaline to tholeiitic volcanism also suggests a change in tectonic environment.

Deception Butte and Kreuger Rock, vents for the Black Canyon lavas, are aligned on a trend of N. 15° W., roughly parallel to the Shady Dell fault. Other vents south of Deception Butte may also exist, in view of the presence of Black Canyon intracanyon sequence south of the map area.

As mentioned previously, the Black Canyon lavas dip to the northeast. The bottom contact on the southwest side of the Willamette River is located at an elevation of approximately 488 m (1,600 ft), while on the northeast side it is at an elevation of 366 m (1,200 ft). The drop of the paleovalley across the river is 122 m (400 ft) in a lateral distance of 2.5 km (1.5 mi), which is not anomalous considering the estimated dip of about 3° to 5° on the sequence in this vicinity. The apparent displacement of the lavas of Lookout Point on the Shady Dell fault is 122 m (400 ft). This fault, if it exists, is probably older than the Black Canyon lavas, as it does not obviously displace the Black Canyon lavas and does not appear in the roadcuts of State Highway 58 and the cliffs of the Black Canyon lavas.

Faults are rare in the Black Canyon lavas. Two faults, probably related, can be seen in secs. 4 and 5, T. 21 S., R. 2 E. The fault in sec. 5 possesses an attitude of N. 80° W. 74° N. Oblique slickensides on the fault plane possess a rake of 15° E. The direction of movement and amount of displacement are not known. While there may be some lateral offset on the fault, the course of the main channel of the paleocanyon does not appear to have been appreciably affected. In view of the width of the paleocanyon and relative positions of the intracanyon lavas on either side of the river, it is safe to say that there has been no substantial lateral movement in the map area since extrusion of the Black Canyon lavas 22 m.y. ago. No other offsets on the Black Canyon sequence have been found in the map area.

## DISCUSSION AND CONCLUSIONS

### Tholeiitic lavas of the early Western Cascade episode

The tholeiitic lavas of Black Canyon are an ideal marker sequence within rocks of the early Western Cascade episode because of their distinctive chemistry, widespread occurrence, and the relatively small range of their K-Ar ages. Stratigraphically and chemically equivalent lavas are described by White (1980a,c) in the Breitenbush and Detroit areas, where they are called the Scorpion Mountain lavas. White (1980a) also noted tholeiitic lavas of the same age in the North and Middle Santiam, Calapooia, and North Collawash drainages and in the Western Cascade foothills near Eugene. They thus appear to have regional distribution in the Western Cascade Range.

The tholeiitic Black Canyon lavas were dated in the Lookout Point area at 22 m.y. B.P. Lux (1981) dated equivalent tholeiitic lavas within the Little Butte Volcanic Series at Foster and Sweet Home at 25.3 m.y. B.P. and at Bear Creek (midway between Cottage Grove and Eugene) at 23.4 m.y. B.P. White (1980a) obtained dates of between 27 and 19 m.y. B.P. on his Scorpion Mountain lavas. Therefore, there appears to be agreement among researchers on a late

Oligocene-early Miocene age for the episode of tholeiitic volcanism represented by the lavas of Black Canyon.

### Eugene-Denio fault zone

The Eugene-Denio fault zone of Lawrence (1976) is commonly shown following the valley of the Middle Fork of the Willamette River northwest of Oakridge and the Hills Creek drainage southeast of Oakridge (Lawrence, 1976; Kienle and others, 1981) (see Figure 5.1). North of the above-mentioned drainages, another expression of the lineament is formed by the Salt Creek-Winberry Creek drainages. This second lineament is not shown on the map or discussed here.

Lawrence (1976) suggested that the Eugene-Denio zone forms part of the northern boundary of the Basin and Range province and that right-lateral strike-slip movement along the lineament accommodated relative motion between the Basin and Range province and more stable areas to the north. Lawrence noted that, in the Basin and Range province, the lineament seems to form the boundary between an area of younger faulting to the north and an area of predominantly older faulting to the south. He cited a 10- to 20-km (6- to 12-mi) right-lateral offset of the High Cascade axis across the lineament as evidence for dextral movement on the lineament. Woller and Black (Chapter 6), however, find neither offsets on the western margin of the High Cascades nor major north-west-trending structures.

The lavas of Black Canyon flowed through a paleocanyon on a course which crossed the Eugene-Denio lineament at approximately right angles (Figure 5.2). No substantial displacement on the 22-m.y. B.P. Black Canyon sequence was identified.

There is, however, abundant shearing and alteration in older rock units that may indicate an earlier episode of structural deformation. Nearly horizontal slickensides on north-west-trending shears in these rocks suggest that lateral faulting paralleling the Eugene-Denio lineament may have occurred prior to the eruption of the 22-m.y. B.P. lavas of Black Canyon. The lineament is apparently controlled by faulting, although it has not yet been clearly established that the Eugene-Denio lineament is a unique zone of weakness and deformation. It is possible, instead, that it is just one well-defined lineament within a broad zone of northwest faulting. Further detailed mapping in adjacent areas will be necessary to determine the importance and uniqueness of the Eugene-Denio zone of Lawrence (1976).

### Recent volcanism in the Lookout Point area

The Lookout Point area has been volcanically active from the late Oligocene to the Neogene. Volcanic rocks of both the early and late Western Cascade and the early and late High Cascade episodes are present.

The Pleistocene basaltic andesite flow at Armet Creek is of the same geochemical petrologic type as the High Cascade lavas to the east. The Armet Creek center and other centers of late High Cascade age in the Western Cascades (e.g., Battle Ax and Harter Mountains [White, 1980c; Taylor, 1981]) are evidence that partial melting processes like those occurring beneath the High Cascade province are taking place beneath the Western Cascade province as well, albeit at a much reduced volume. The sharply reduced volume of magmatism of the late High Cascade episode in the Western Cascade Range is reflected in the sharp decline in heat flow. Heat flow of 48 mW/m<sup>2</sup> was measured at Burnt Bridge Creek near the Armet Creek vent, whereas heat flow in the High Cascades to the east is greater than 100 mW/m<sup>2</sup> (Black and others, Chapter 7). If the partial melting is linked to tectonic forces, then tectonic forces affecting the High Cascades (e.g., east-west extension discussed by Priest and others, Chapter 2) must be having much less effect on the Western Cascade Range.

## CHAPTER 6. GEOLOGY OF THE WALDO LAKE-SWIFT CREEK AREA, LANE AND KLAMATH COUNTIES, OREGON

*By Neil M. Woller and Gerald L. Black,  
Oregon Department of Geology and Mineral Industries*

### ABSTRACT

The Waldo Lake-Swift Creek area contains rocks representative of each of the four major age divisions which have been recognized in the central Oregon Cascades. Rocks of the early Western Cascade episode consist of tuffs and flows which range in composition from basaltic andesite through rhyolite. The oldest volcanic rocks of the late Western Cascade episode are olivine basalts to basaltic andesites which occur in the Koch Mountain and Tumblebug Creek area. The basalts are overlain by a thick sequence of two-pyroxene andesitic flows which grade into olivine clinopyroxene basaltic andesites near the top of the section. Rocks of the early High Cascade episode consist of olivine basalt and basaltic andesite which cap ridges in the western portion of the map area. Olivine basalts of the late High Cascade episode cover the High Cascade platform in the eastern portion of the map area and flow into the canyons of the deeply dissected Western Cascade province.

Two major north-south-trending, down-to-the-east faults have been inferred in the Waldo Lake-Swift Creek area. One fault occurs along the west side of Waldo Lake and extends southward, possibly as far as the Lakeview-Redtop Mountain area. The second fault occurs farther west at Groundhog Creek. The geologic evidence, while not completely compelling, is highly suggestive of faulting at both locations. Associated residual gravity anomalies provide further support for interpreting faults. The structures appear to be analogous to similar structures identified farther north in the Horse Creek-McKenzie River and Cougar Reservoir areas.

No lateral offset of the High Cascade Range axis across the Eugene-Denio lineament was identified in the study area. No major zones of northwest-trending faulting were found.

Uplift and deep dissection of the Western Cascades relative to the High Cascades probably occurred between 4.32 m.y. B.P. and 1.98 m.y. B.P.

### INTRODUCTION

This paper is a refinement and expansion of previous work by Woller (1982). Detailed mapping of the upper Salt Creek area and refinements of previous geologic mapping in the Pinto Creek area by Woller and detailed mapping of the Black Creek canyon by Black (see Figure 6.1) are here presented as a new geologic interpretation of this portion of the Cascade heat-flow transition zone (see Black and others, Chapter 7, and Blackwell and others, 1978).

### LOCATION AND PHYSIOGRAPHY

The Waldo Lake-Swift Creek area is located 75 km (45 mi) southeast of Eugene, Oregon. The map area covers the entire Waldo Lake 15-minute quadrangle and adjoining portions of

the Summit Lake, Toketee Falls, and Oakridge quadrangles. The area is administered predominantly by the Willamette and Deschutes National Forests.

Major drainages are the South Fork of the Willamette River, Hills Creek, Salt Creek, and Black Creek. All of these westward-flowing streams are deeply incised into the middle and upper Tertiary terrane of the Western Cascade physiographic province.

The most prominent topographic features in the map area are Diamond Peak (elev. 2,667 m [8,744 ft]), Mount Yoran (elev. 2,165 m [7,100 ft]), and Fuji Mountain (elev. 2,179 m [7,144 ft]), all of which are Quaternary composite volcanoes which have been deeply eroded by glaciation. Waldo Lake (27.2 km<sup>2</sup> [10.5 mi<sup>2</sup>]), the second largest lake in Oregon, is located in the northeast quarter of the map area.

The topography in the western portion of the map area has been formed primarily by the processes of stream erosion and glaciation. The topography in the eastern portion of the map area consists of constructional volcanic landforms which have been modified primarily by glaciation. The division between the High and Western Cascade physiographic provinces approximately bisects the study area along a north-south line through Diamond Peak.

Primary access to the area is by State Highway 58 from Eugene. Logging roads of the Willamette National Forest provide additional access to much of the area. The Diamond Peak Wilderness Area is a roadless natural area, and no effort other than aerial photo interpretation was made by the authors to map within it. Geologic mapping by Sherrod and others (in press), however, adequately covers the wilderness area, and their work is incorporated into the map (see Figure 6.1).

### VOLCANIC STRATIGRAPHY

#### Introduction

This report uses the informal stratigraphic nomenclature discussed by Priest and others (Chapter 2, see Figure 2.2). General geochemical and petrologic discussions are incorporated into Chapter 2 and will not be repeated here. Chemical data are presented in Appendix B. Summaries of lithologic, chemical, and petrographic characteristics of each described map unit in the Waldo Lake-Swift Creek area are presented in Tables 6.1 and 6.2. All K-Ar data in this section were generated by Stanley H. Evans of the University of Utah Research Institute.

#### Volcanic rocks of the early Western Cascade episode

**Introduction:** Oligocene-Miocene lavas, undifferentiated, and Oligocene-Miocene rhyodacitic lavas are included in the volcanic rocks of the early Western Cascade episode. They are equivalent to the Little Butte Volcanic Series of Peck and





Table 6.1. *Stratigraphy of volcanic rock units in the Waldo Lake-Swift Creek area, central Cascade Range, Oregon*

Regional volcanic episode <sup>1</sup>	Name and map symbol	K-Ar dates (m.y. B.P.)	Maximum exposed thickness	SiO <sub>2</sub> content <sup>2</sup> (wt. %)	Lithologic description
Late High Cascade	Mazama pumice-fall deposit	Holocene	Variable 3 m (10 ft)	67.1	Unconsolidated, well-winnowed pumice-fall; yellow; with voids between pumice clasts. Appears bedded where undisturbed. Mantles topography.
	Pleistocene basaltic lavas (QTb/QTv)	Oldest, 1.98 ± 0.25; youngest, 0.17 ± 0.48	854 m (2,800 ft)	49.6-57.7	Olivine-bearing basalts and basaltic andesites; black to gray; fresh, undeformed; compact to diktytaxitic. Found in bottoms of glaciated valleys and related to Recent drainages, also as products of Quaternary volcanic activity in constructional area of eastern part of map area.
Early High Cascade	Miocene-Pliocene basaltic lavas (Tpb/TPv)	5.53 ± 0.41; 5.56 ± 0.34; 4.32 ± 0.40	366 m (1,200 ft)	48.6-52.9	Olivine-bearing basalts and basaltic lavas; compact; gray; fresh. Caps highest ridges of the Western Cascade province.
Late Western Cascade	Andesitic lavas of Moss Mountain (Tma/Tmv)	17.3 ± 0.8(?)	732 m (2,400 ft)	53.8-62.4	Pyroxene-bearing andesites, dacites, and basaltic andesites. Highest members are olivine augite-bearing. Black to gray; very plagioclase phyrlic.
	Tuffs of Black Creek (Tmtb)	—	105 m (345 ft)	—	Dacitic(?) pumiceous ash-flow tuffs, ash, and pumice falls; buff to pink; fresh to weathered; with thin, local andesite flow interbeds.
	Basaltic lavas of Tumblebug Creek (Tmb/Tmbv)	Upper part, 13.1 ± 0.6; lower part, 17.0 ± 0.9	915 m (3,000 ft)	51.9-55.8	Olivine-bearing basalts and basaltic andesites; fresh in appearance; compact to diktytaxitic; black to gray.
	Basaltic lavas of Koch Mountain (Tmk)	—	—	52.5-55.0	Olivine basalts and basaltic andesites; fresh to weathered in appearance; compact to diktytaxitic; fine-grained; gray.
Early Western Cascade	Oligocene-Miocene lavas (Toml/Tomv)	—	366 m (1,200 ft)	51.9-57.7	Rhyolite to basalt; commonly aphyric or with alteration of mafic phenocrysts to nontronite, saponite, magnetite, or other products; commonly altered, stained, sheared, amygdaloidal.
	Oligocene-Miocene rhyodacites (Tomr)	—	305 m (1,000 ft)	73.2-74.1	Rhyodacite and rhyolite; aphyric; holohyaline, cryptocrystalline, banded.

<sup>1</sup> See Priest and others (Chapter 2) for explanation and regional rock stratigraphic correlations.

<sup>2</sup> Recalculated to a 100-percent total, volatile-free.

Table 6.2. Generalized petrography of Waldo Lake-Swift Creek geologic units. Pl=plagioclase; hb=hornblende; qtz=quartz; cpx=clinopyroxene; opx=orthopyroxene; ol=olivine; mg=magnetite

Name and map symbol	Common rock types	Common phenocryst assemblages	Common groundmass textures	Common alteration of rocks within map unit
Upper Tertiary-Quaternary lavas, undifferentiated (QTu/QTuv)	Basalt Basaltic andesite	Ol, ol+pl Ol, ol+pl	Intergranular Intergranular	Ol→iddingsite.
Pleistocene basaltic lavas (QTb/QTv)	Basalt Basaltic andesite	Ol, ol+pl Ol, ol+pl	Intergranular Intergranular	Ol→iddingsite.
Miocene-Pliocene basaltic lavas (Tpb/Tpv)	Basalt Basaltic andesite	Ol, ol+pl Ol, ol+pl	Intergranular Intergranular	Ol→iddingsite.
Tuffs of Black Creek (Tmtb)	Dacitic(?) pumiceous ash-flow tuff	Pumice, dacitic(?) lithic fragments, pl, opx(?)	Very fine-grained ash	Pumice, ash→devitrified glass; opx(?)→smectites.
Andesitic lavas of Moss Mountain (Tma/Tmv)	Andesite  Dacite  Basaltic andesite	Pl+opx+cpx, pl+opx, pl+cpx Pl+opx, pl+opx+minor hb, pl Pl+cpx+ol, pl+cpx	Intergranular, intersertal, hyalophitic Intersertal, hyalophitic  Intergranular	Opx→nontronite/smectite; hb→Mg+cpx(?); hb→nontronite/smectite; ol→iddingsite; glass→nontronite/smectite.
Basaltic lavas of Koch Mountain (Tmk)	Basalt  Basaltic andesite	Ol+pl, ol Ol+pl, ol+cpx+pl	Intergranular, crude trachytic, vesicular Intergranular, crude trachytic, vesicular	Ol→iddingsite+smectite/saponite; glass→smectite/saponite.
Basaltic lavas of Tumblebug Creek (Tmb/Tmbv)	Basalt	Ol, ol+cpx, ol+cpx+pl	Intergranular, dikty-taxitic, vesicular	Ol→iddingsite.
Oligocene-Miocene lavas, undifferentiated (Toml/Tomv)	Rhyodacite  Dacite  Andesite  Basaltic andesite	Aphyric, pl, pl+hb, pl+qtz+hb, pl+qtz Aphyric, pl, pl+qtz, pl+qtz+hb  Pl+opx, pl, pl+opx+cpx, pl+cpx+ol Pl, pl+cpx+ol, pl+cpx	Vitrophyric, aphyric, banded, hyalophitic Pilotaxitic, intersertal, hyalophitic, amygdaloidal  Intersertal, hyalophitic, intergranular, amygdaloidal Intergranular	Hb→cpx(?) + mg; hb→smectite/saponite; opx→smectite/saponite; glass→smectite/saponite; ol→iddingsite+smectite/saponite; calcite replacements; Fe-staining.
Oligocene-Miocene rhyodacitic lavas (Tomr)	Rhyolite(?), rhyodacite, also includes lavas very similar to unit Toml	Aphyric	Aphyric, vitreous, banded	Some Fe-staining.



others (1964) and Kays (1970) and the Breitenbush formation of White (1980a) and Hammond and others (1980). They are also equivalent to the tuffs of Cougar Reservoir (Priest and Woller, Chapter 4) and Oligocene and lower Miocene tuffs and lavas, undifferentiated (Woller and Priest, Chapter 5).

Lavas similar to those of the Oligocene-Miocene lavas, undifferentiated, crop out within the unit mapped as Oligocene-Miocene rhyodacitic lavas, which should therefore be considered a local rhyodacite- and rhyolite(?) -dominated sequence within the more widespread Oligocene-Miocene lavas, undifferentiated. The authors could not always map the two units separately at this map scale.

Peck and others (1964) suggested a maximum thickness for the Little Butte Volcanic Series of approximately 4,575 m (15,000 ft) in the vicinity of the North Umpqua drainage basin. A measured section approximately 1,525 m (5,000 ft) thick was described by Kays (1970) from the North Umpqua River, about 30 km (18 mi) southwest of the Swift Creek area.

**Oligocene-Miocene lavas, undifferentiated (unit Toml/Tomv):** Oligocene-Miocene lavas, undifferentiated, crop out at low elevations along Salt Creek and west of Groundhog Creek, where they are the predominant rock unit. The base of the unit is not exposed in the map area. Flows are mapped as unit Toml, plugs as unit Tomv.

These rocks range in composition from basaltic andesite to rhyolite, but dacite and rhyodacite are probably the most common rock types exposed within the study area. Yellow-green, lithic-fragment-rich tuffs, very similar to rocks at Lookout Point (Oligocene and lower Miocene tuffs and lavas, undifferentiated, Chapter 5) and Cougar Reservoir tuffs of Cougar Reservoir (Chapter 4) also occur, but they are much less common than in the Cougar and Lookout Point areas (see Chapters 4 and 5). Some interbedded sediments are also included in the Oligocene-Miocene lavas, undifferentiated.

Almost all of the rocks in this unit are altered. Secondary fractures, shears, and cavities are commonly filled with silica, calcite, celadonite, and/or zeolites. Staining is also common. In thin section, these rocks usually contain nontronite or saponite (after phenocryst and/or groundmass phases), celadonite, iron staining, and/or calcite replacement.

Oligocene-Miocene lavas, undifferentiated, within the map area have not been dated. Several miles to the west of the map area, a dacite plug of an equivalent unit was K-Ar dated at  $21.3 \pm 1.0$  m.y. B.P. (Brown and others, 1980b). This sample was slightly altered (celadonite, saponite, calcite, quartz fillings), and the calculated age may have been low because of the loss of radiogenic argon. In the Lookout Point area (Chapter 5), another equivalent lava was dated at  $24.7 \pm 2.0$  m.y. B.P., but that sample was also subjected to low-grade alteration. Five samples of a younger overlying unit (the basaltic lavas of Tumblebug Creek) yielded dates ranging from 17.0 to 13.1 m.y. B.P. (see later discussion).

**Oligocene-Miocene rhyodacitic lavas (unit Tomr):** Rhyodacitic to rhyolitic(?) lava flows occur on the steep south and southeast slopes of Mount David Douglas. The sequence may be as much as 305 m (1,000 ft) thick, but accurate determinations of the total thickness are difficult because of (1) intracanyon Quaternary lavas on the south side of Mount David Douglas that hide parts of the sequence, (2) lithologic similarity between interbedded lavas and those mapped elsewhere as Oligocene-Miocene lavas, undifferentiated, and (3) masking by landslides and colluvium. The Oligocene-Miocene rhyodacitic lavas do not crop out across Salt Creek from their principal occurrence near Mount David Douglas, indicating that Salt Creek may be following the margin of their outcrop area.

The rhyodacites and rhyolites(?) of this unit are typically

buff to pink and aphyric. Flow banding is common, and occasional obsidian flows are present.

Three samples were chemically analyzed for this study, and all are classified as rhyodacite according to the criteria of Chapter 2. The analyses are tabulated in Appendix B, Table B.5.

## Volcanic rocks of the late Western Cascade episode

**Introduction:** Within the map area, rocks of the late Western Cascade episode include the basaltic lavas of Tumblebug Creek, the basaltic lavas of Koch Mountain, and the andesitic lavas of Moss Mountain. They are equivalent to the Sardine series of Thayer (1939), the Sardine Formation of Peck and others (1964), the Sardine Formation and Elk Lake formation of White (1980a), the lavas of Walker Creek (Priest and Woller, Chapter 4), and Miocene andesitic lavas (Woller and Priest, Chapter 5). They are partially equivalent to the Outerson basalt of Hammond and others (1980).

**Basaltic lavas of Tumblebug Creek (unit Tmb/Tmbv):** The basaltic lavas of Tumblebug Creek are best exposed on the mountainsides west of Tumblebug Creek. They are fresh, gray to black, and compact, although a few slightly diktytaxitic olivine-bearing basalts and basaltic andesites also occur. Flows are mapped as unit Tmb; vents and plugs are mapped as unit Tmbv.

Several vents were found for these lavas. Many originated in the vicinity of a plug located in sec. 2, T. 24 S., R. 4 E. (extreme lower left of map on Plate 3). The basaltic lavas of Tumblebug Creek occurring on lower Bear Mountain, the lower portions of Baboon and Noisy Creeks, and the upper Willamette River drainage dip away from this plug. Other vents are present in the upper Juniper Ridge area and near Lighthouse Rock. The Juniper Ridge vent erupted basaltic andesite lavas which were somewhat more plagioclase-phyric (up to 10 percent) than the rest of the unit. Some palagonite tuff and thin air-fall tuff, as well as a small outcrop of a welded ash flow which could not be traced, are also associated with this vent. The attitudes of the flows originating in the vicinity of upper Juniper Ridge are locally steeply inclined near the source plug. However, in the upper Baboon Creek area, they dip to the north at approximately the same attitude as the flows below, which probably originated from the Tumblebug Creek source.

Five K-Ar dates were obtained on the basaltic lavas of Tumblebug Creek for this report. A fresh basalt at the base of Bear Mountain, stratigraphically low in the exposed sequence, was dated at  $17.0 \pm 0.9$  m.y. B.P. (0.66 percent K, 28 percent radiogenic  $Ar^{40}$ ). A sample even lower in the section was dated at  $14.1 \pm 0.8$  m.y. B.P. (0.80 percent K, 26 percent radiogenic  $Ar^{40}$ ), but this date is questionable because of low-grade alteration. A sample taken near the top of the ridge west of Tumblebug Creek was dated at  $15.6 \pm 0.6$  m.y. B.P. (1.10 percent K, 47 percent radiogenic  $Ar^{40}$ ). Two flows were dated in the Baboon Creek area, one low in the section, the other high. The upper dated flow originated from the Juniper Ridge source previously mentioned. The lower flow was dated at  $13.5 \pm 1.1$  m.y. B.P. (0.89 percent K, 18 percent radiogenic  $Ar^{40}$ ), the upper flow at  $13.1 \pm 0.6$  m.y. B.P. (0.87 percent K, 32 percent radiogenic  $Ar^{40}$ ). These dates indicate that the basaltic lavas of Tumblebug Creek were being erupted between 17 to 13 m.y. B.P.

The basaltic lavas of Tumblebug Creek dip at approximately  $15^\circ$  to the north and northeast below a thick sequence of the andesitic lavas of Moss Mountain.

**Basaltic lavas of Koch Mountain (unit Tmk):** The basaltic lavas of Koch Mountain are best exposed north of

Spirit Lake along U.S. Forest Service (USFS) Road 2422 and along an unnamed creek on the north side of the Black Creek canyon in sec. 25, T. 21 S., R. 5 E.

The basaltic lavas of Koch Mountain are olivine basalts and basaltic andesites which are gray when fresh and reddish brown when weathered. They are typically fine grained, with 1 to 3 percent highly iddingsitized olivine as the only phenocryst mineral. Most flows are compact, but a few are diktytaxitic. Nearly all possess moderate to strong alteration of the groundmass and olivine to smectitic clays (probably nontronite/saponite). A few flows contain zeolites and/or amygdaloidal textures. Individual flows are highly variable in thickness, ranging from approximately 1 to 1½ m (3 to 4 ft) up to 38 m (125 ft). In one 120-m (400-ft)-thick section on the north side of Black Creek canyon, 25 thin flows are exposed, each consisting mostly of autobreccia with a thin, 1- to 2-m (3- to 6-ft)-thick massive central section.

The basaltic lavas of Koch Mountain are at least 593 m (1,945 ft) thick. The total thickness is unknown, as the base of the unit is not exposed in the Waldo Lake quadrangle. A maximum thickness of 781 m (2,560 ft) can be inferred, however, from the data obtained in the Black Creek drill hole (sec. 16 Ad, T. 21 S., R. 5 E.). That hole, collared at an elevation of 830 m (2,720 ft), encountered only andesitic lavas of Moss Mountain (see section below) to a depth of 91 m (300 ft), where the contact with the older Oligocene-Miocene lavas, undifferentiated, was penetrated.

Magnetic polarities were measured on the basaltic lavas of Koch Mountain on the north side of Black Creek canyon in sec. 25. All flows from an elevation of 1,600 m (5,245 ft) (the contact with the overlying lavas of the early High Cascade episode) down to an elevation of 1,205 m (3,950 ft) possess reversed polarities. A flow at 1,177 m (3,860 ft) is weakly reversed, and a flow at 848 m (2,780 ft) possesses normal polarity.

Five samples from the section on the north side of Black Creek (sec. 25) were chemically analyzed. Only one of the samples possesses a silica content of less than 53 percent (recalculated volatile-free), the nominal division between basalts and basaltic andesites (see Chapter 2). Silica contents vary from 52.6 to 55.0 percent, with the higher silica contents occurring at the bottom of the section. Chemical data are tabulated in Appendix B, Table B.5.

No K-Ar dates of the basaltic lavas of Koch Mountain are available. They are, however, overlain by the andesitic lavas of Moss Mountain. Just north of the map area on USFS Road 2422 on Koch Mountain, the andesites appear to have flowed into canyons eroded into the basalts. These relationships indicate that the basaltic lavas of Koch Mountain are equivalent to the basaltic rocks of Tumblebug Creek.

The basalts of Koch Mountain are, in places, directly overlain by basalt flows of the early High Cascade episode. In the two locations where this contact was observed, it was marked by a thin (approximately 1.5-m [5-ft]-thick) palagonite bed.

#### **Andesitic lavas of Moss Mountain (unit Tma/Tmv):**

The andesitic lavas of Moss Mountain, which are plagioclase-phyric basaltic andesites, andesites, and dacites, are mapped as unit Tma. Vents and plugs are mapped as unit Tmv. The plagioclase phenocryst content of these flows averages 20 percent and ranges from 5 to 45 percent. The predominant rock type is two-pyroxene andesite. At Moss Mountain, the lithology grades from two-pyroxene andesite at the bottom of the exposed sequence to olivine-clinopyroxene basaltic andesite at the top. Near Verdun Rock, many hornblende- and/or orthopyroxene-bearing dacites occur. The lower members of the Moss Mountain lavas are generally hyalophitic or

intersertal. The degree of crystallization increases upwards in the section, culminating in intergranular textures near the top of the sequence. (See Table 6.2 for more on the petrography of these flows.)

Attitudes measured on the andesitic lavas of Moss Mountain vary throughout the map area, indicating different source areas for many of the sequences. Near Judd Mountain, the flows dip gently to the north at approximately 5°, but at Moss Mountain, the top of the sequence dips southward at approximately 20°. The steep dip of this latter thin-bedded sequence results from its close proximity to its vent.

A flow near the top of Moss Mountain was dated at  $17.3 \pm 0.8$  m.y. B.P. (0.67 percent K, 38 percent radiogenic Ar<sup>40</sup>). This date is not compatible with five younger dates obtained on the underlying basaltic lavas of Tumblebug Creek. The Moss Mountain sample appeared very fresh, although about 10 percent of the plagioclase phenocrysts contained minor minute inclusions of glass and/or smectite. The incompatibility of this date with the dates of stratigraphically lower flows may be due to (1) excess radiogenic argon, or (2) inaccurately measured potassium content. Most of the samples from the basaltic lavas of Tumblebug Creek which were dated have higher potassium contents than the sample from the andesitic lava of Moss Mountain, so an error in the potassium content is probably the most likely reason for the discrepancy.

Andesitic lavas of Moss Mountain mapped in this study include the older Miocene volcanoclastic sediments and lavas of Woller (1982) as well as the andesitic lavas of Moss Mountain of that same study.

**Tuffs of Black Creek (unit Tmtb):** The tuffs of Black Creek are very poorly exposed on three terrace benches which lie at elevations of between 1,343 and 1,464 m (4,400 and 4,800 ft) in upper Black Creek. The tuffs consist of dacitic(?) pumiceous ash-flow tuffs, poorly indurated fine-grained tuffs, pumice falls and flows, and rare, thin, two-pyroxene andesite flows, interbedded locally within the tuffs.

The dacitic(?) pumiceous ash-flow tuffs are gray when weathered and buff to pink when fresh. They are well indurated but unwelded and contain nearly equal amounts of pumice and dark-gray dacitic(?) lithic fragments with subordinate plagioclase crystals. A summary of thin-section data is presented in Table 6.2.

The total thickness of the tuffs of Black Creek may be as much as 111 m (365 ft). Generally, the only good exposures of this unit occur in the beds of the streams which flow across the terrace benches. A break in slope at about the 1,464-m (4,800-ft) elevation may indicate the presence of the uppermost 20 m (66 ft) of ash-flow tuff along the south side of Black Creek, though no outcrops were found at these locations.

The tuffs of Black Creek were not dated. At two of the three locations where they were encountered, they were overlain by two-pyroxene andesite flows. Along Black Creek, they are clearly part of the upper portion of the andesites of Moss Mountain.

#### **Volcanic rocks of the early and late High Cascade episodes**

**Introduction:** The volcanic rocks of the early and late High Cascade episodes are collectively equivalent to the volcanic rocks of the High Cascade Range and Boring Lava of Peck and others (1964).

The flows of these episodes are primarily olivine-bearing basalts, basaltic andesites, and low-silica andesites. These lavas are generally fresh and unaltered unless they have been affected by shearing or faulting. The authors were unable to discern any petrographic or geochemical characteristics that

enabled them to differentiate between the lavas of the early and late High Cascade episodes other than, in some cases, the presence of slight alteration, usually of the olivine phenocrysts. However, many lavas of the early High Cascade episode appear just as pristine as the flows of the late High Cascade episode.

Assignment of flows to their proper episodes in the Waldo Lake-Swift Creek area therefore depends in large part on the recognition of their field relationships, in particular, their ages relative to the uplift of the Western Cascades and the resulting unconformity. As discussed below and in Chapter 2, the uplift of the Western Cascades occurred about 4 m.y. B.P.

The informal nomenclature described and used in Chapter 2 to identify episodes of Western Cascade volcanism is useful primarily in the Western Cascade physiographic province. The Waldo Lake-Swift Creek area, however, extends into the neighboring High Cascade physiographic province in the eastern half of the study area. The unconformity between lavas of the early and late High Cascade episodes, which serves to distinguish the two units in the Western Cascade physiographic province, becomes less useful in the High Cascades. In the High Cascade province, many lavas of the late High Cascade episode conformably(?) overlie lavas of the early High Cascade episode; any unconformity, if it does exist in this area, is very difficult to identify. Therefore, in some areas of the map, sequences of High Cascade lavas which could not be definitively assigned to either the early or late High Cascade episodes are mapped as an undifferentiated unit, the upper Tertiary-Quaternary lavas, undifferentiated.

**Miocene-Pliocene basaltic lavas (unit Tpb/Tpv):** Lavas of the early High Cascade episode are here mapped as Miocene-Pliocene basaltic lavas. Flows are mapped as unit Tpb; vents and plugs are mapped as unit Tpv. These units are distinguished in this study by two criteria: (1) they cap ridges in the Western Cascade province; or (2) they possess K-Ar ages, or are associated with lavas that possess ages, older than 4 m.y. In the transition zone between the Western and High Cascade physiographic provinces, the identification of these lavas frequently hinges on criterion 2.

Rocks of this unit are equivalent to the lavas of Tipsoo Butte (Priest and Woller, Chapter 4) and the Outerson formation of White (1980a) and the Outerson basalt of Hammond and others (1980) and partially equivalent to the Outerson volcanics of Thayer (1939). Vent areas were found at several places in the study area, including Wolf Mountain and Bear Mountain.

One of the basal flows just west of Hemlock Butte was dated at  $5.56 \pm 0.34$  m.y. B.P. (0.90 percent K, 24 percent radiogenic  $Ar^{40}$ ). This flow directly overlies a flow of andesitic lava of Moss Mountain. A second K-Ar date of  $5.53 \pm 0.41$  m.y. B.P. (0.94 percent K, 19 percent radiogenic  $Ar^{40}$ ) was obtained from a flow from near the top of the section near Pinto Mountain. A third K-Ar date from near the top of Bear Mountain was  $4.32 \pm 0.4$  m.y. B.P. (1.25 percent K, 15 percent radiogenic  $Ar^{40}$ ).

**Pleistocene basaltic lavas (unit QTb/QTv):** Volcanic rocks of the late High Cascade episode are here mapped as Pleistocene basaltic lavas. Flows are mapped as unit QTb and vents and plugs as unit QTv. In the Waldo Lake-Swift Creek area, volcanic rocks of the High Cascade episode are mapped as Pleistocene basaltic lavas if they meet any of the following criteria: (1) the lavas flowed into canyons within the youthful (dissected) topography of the Western Cascades or are equivalent or younger than the intracanyon flows; (2) the lavas are obviously Pleistocene or younger, based on surficial flow morphology or their relationship to glacial features; or (3) the lavas are associated with lavas younger than 2 m.y. B.P., as

determined by K-Ar method of absolute dating (no K-Ar dates in the map area were obtained in the 4- to 2-m.y. B.P. interval). If intracanyon lava flows began to appear in this area of the Western Cascade Range at the same time as they did farther north in the Horse Creek-McKenzie River area (4 to 3 m.y. B.P. [see Chapter 2 for the discussion of dates of intracanyon lavas in that area]), then lavas as old as middle Pliocene may also be included in this unit (see criterion 1 above).

Pleistocene basaltic lavas are equivalent to the High Cascade lavas of White (1980a); the Minto lavas, Battle Ax lavas, Olallie lavas, and Santiam basalts of Thayer (1939); and the older and younger High Cascade basalts and volcanic deposits of Mount Jefferson of Hammond and others (1980).

Pleistocene basaltic lavas dominate large areas of the eastern half of the study area. Diamond Peak is a young composite cone whose lavas cover many square kilometers. Its Tertiary base is exposed on its southwest side. Mount Yoran, Lakeview Mountain, Fuji Mountain, and Cupit Mary Mountain are other major vents.

The olivine-phyric basalts and basaltic andesites of the Pleistocene basaltic lavas are very fresh, almost never showing any alteration. Also included in the unit are palagonitic hyaloclastites and cinder deposits as well as occasional interbedded sediments.

The authors have dated six flows from this unit. The oldest date,  $1.98 \pm 0.25$  m.y. B.P. (0.71 percent K, 9 percent radiogenic  $Ar^{40}$ ), was obtained from an intracanyon lava flow located near the confluence of Pinto and Wolf Creeks (elevation 1,128 m [3,700 ft]).

**Upper Tertiary-Quaternary lavas, undifferentiated (unit QTv/QTuv):** Lavas and sequences of lavas, vents, and plugs of the High Cascade episode which fit neither the early High Cascade nor the late High Cascade recognition criteria listed above are here mapped as upper Tertiary-Quaternary lavas, undifferentiated. The ages of these units may be as old as late Miocene and as young as late Pleistocene. The difficulty of locating the unconformity, if it exists, in the eastern part of the map area has already been discussed.

**Holocene Mazama pumice-fall deposit:** The youngest volcanic unit exposed in the Waldo Lake-Swift Creek area is a thin dacitic air-fall tuff believed to have originated from the Mount Mazama eruption  $6,845 \pm 50$  C<sup>14</sup> years ago (Bacon, 1983a). It mantles the landscape and, if shown on the map, would obscure important bedrock relationships. It is unconsolidated and yellow and appears to be bedded where undisturbed. Voids occur between the lapilli- to coarse-ashed-sized pumice. No fine ash or block-sized fragments were found.

The chemistry of the pumice is given in Appendix B, Table B.4 (field no. P-302, no. 88). The high water content casts doubt on the accuracy of the analysis and perhaps explains the discrepancies between this analysis and other published analyses of Mazama ash. The phenocryst assemblage (e.g., the presence of hornblende phenocrysts) and lateral continuity with known Mazama ash deposits, however, support a Mount Mazama source.

## STRUCTURE

### Introduction

Faulting in the Waldo Lake-Swift Creek area follows northwesterly, northeasterly, and northerly trends.

### Northwest-trending faults

Northwest-trending faults mapped in this report, when compared to the northeasterly and northerly trends, are few in number. On the south side of Wolf Mountain, a northwesterly



trending fault displaces andesitic lavas of Moss Mountain approximately 20 m (66 ft). This fault could not be traced.

### **Northeast-trending faults**

A northeast-trending fault cuts through the Pinto Mountain-Pinto Creek area. On Pinto Mountain, a sequence of lavas of the early High Cascade episode is downdropped to the southeast by approximately 152 m (500 ft). Alteration along the fault is locally extensive, consisting of bleaching, brecciation, silicification, and/or pyritization. The fault could not be traced southwest of Hemlock Butte, where Swift Creek flows on a course nearly parallel to that of the fault. Offset across Swift Creek could not be proved, but a moderately thick sequence of Miocene-Pliocene basaltic lavas found on Bear Mountain are not present at Moss Mountain or eastern Juniper Ridge. This fault cuts a flow dated at  $5.53 \pm 0.41$  m.y. B.P.

Another northeast-trending fault with down-to-the-southeast movement occurs just north of the State Highway 58 tunnel. Oligocene-Miocene rhyodacitic flows are juxtaposed against sheared and altered High Cascade lavas. The amount of displacement on this fault may be substantial. The fault is buried by lavas of the late High Cascade episode from Fuji Mountain on the southeast side of Fuji Meadow, which is a structural high of andesitic lavas of Moss Mountain.

### **North-trending faults**

**Groundhog Creek fault:** The existence of a large north-trending fault is inferred in the extreme western portion of the map area. The course of the fault follows the South Fork of Groundhog Creek and passes through Shady Gap and Bunchgrass Ridge to the north. Several extensive landslides cover the trace of the fault for most of its length within the map area. The fault is inferred to have normal displacement down to the east.

The fault is most evident where it crosses Bunchgrass Ridge just north of the northern map boundary of Plate 3. Here the bottom of the andesitic lavas of Moss Mountain is juxtaposed with the top of the same map unit across the fault. The displacement at this location is approximately 244 m (800 ft), based on the offset of the lower contact of the andesitic lavas of Moss Mountain.

There may be greater displacement in the Groundhog Creek and Shady Gap areas. At Groundhog Creek, greater than 610 m (2,000 ft) of flows of the late Western Cascade episode occur on the east side of the inferred fault but are absent across the fault to the west. At Shady Gap, which is a low saddle between Coyote Mountain and Cougar Mountain (see Figure 6.1), a similar situation exists. A thick sequence of rocks of the late Western Cascade and early High Cascade episodes is present at Coyote Mountain but is absent from Cougar Mountain. Estimation of the displacement of the fault at Shady Gap is complicated by the locally great relief on the unconformable contact between the Oligocene-Miocene lavas, undifferentiated, and the andesitic lavas of Moss Mountain. However, many of the flows forming the thick pile of the andesitic lavas of Moss Mountain present at Coyote Mountain on the east side probably originated from a source west of the fault, based on the preservation of initial dips. Neither the source nor the andesitic sequence were found west of Shady Gap. There, a flow of the late(?) High Cascade episode has capped Oligocene-Miocene lavas, undifferentiated, at Cougar Mountain. Erosion of the uplifted west side of the fault has probably caused the absence of the andesitic lavas of Moss Mountain from the west sides of Groundhog Creek and Shady Gap.

**Age of Groundhog Creek fault:** The Groundhog Creek

fault cuts upper flows of the andesitic lavas of Moss Mountain at Bunchgrass Ridge. At this location, numerous north-south dikes lithologically similar to rocks of the late Western Cascade episode intrude the downthrown east side of the fault. The dikes parallel the fault, suggesting either that they were emplaced in the same stress field that produced the fault or that they were emplaced subsequent to the onset of faulting or fracturing. Either case suggests that faulting may have occurred during late Western Cascade time.

There is no direct evidence that the Groundhog Creek fault affects lavas of High Cascade age. The absence of lavas of the early High Cascade episode on Bunchgrass Ridge west of the structure suggests that these flows were either uplifted and eroded away on the west side of the fault or blocked from westward flow by the east-facing fault scarp. It is also possible that, because the exposed sequence of early High Cascade age is thin in this locality, the lavas never reached the Groundhog Creek fault.

Along Groundhog Creek, the topographic expression of the fault-line scarp can be classified as obsequent, that is, topographically reversed. The presence of a flow of probable late High Cascade age capping Cougar Mountain suggests that the topographic reversal had occurred by late High Cascade time. Therefore, on the basis of the available evidence, we hypothesize that the Groundhog Creek fault is younger than the upper andesitic lavas of Moss Mountain at Bunchgrass Ridge. The fault may or may not affect flows of the early High Cascade episode at the same locality and is probably pre-Quaternary in age.

**Waldo Lake fault:** The presence of a major north-south trending fault that cuts flows of the early High Cascade episode is inferred in the Waldo Lake area. Quaternary flows from the Twins just east of the map area apparently overlap the base of the inferred fault scarp. This structure is analyzed in detail below in the discussion of the Western Cascade-High Cascade boundary.

The lineament along the west flank of Lakeview and Red-top Mountains is possibly an extension of the Waldo Lake fault. Young lavas originating from Diamond Peak about this "scarp" from the west. This feature is also discussed below.

## **DISCUSSION**

### **Eugene-Denio lineament**

There has been considerable speculation in the literature concerning the nature of the Eugene-Denio lineament, a prominent northwest-trending lineament extending from Eugene, Oregon, to Denio, Nevada. Within the Waldo Lake-Swift Creek area, the lineament is expressed in the parallel northwest-trending drainages of Hills Creek and Salt Creek (Lawrence, 1976; Kienle and others, 1981; see Figure 6.1).

Lawrence (1976) proposed that the Eugene-Denio lineament was a right-lateral wrench structure and postulated that it, along with the Brothers fault zone farther north, was one of the bounding structures of the Basin and Range physiographic province. Lawrence cited a 10- to 20-km (6- to 12-mi) offset on the axis of the High Cascade province as evidence of dextral movement.

Brown and others (1980b) found no evidence of lateral displacement along the lineament in their reconnaissance mapping of the Known Geothermal Resource Area (KGRA) west of Willamette Pass. Couch (1979) and Connard (1980) reported that across the lineament there was a right-lateral offset of short-wavelength magnetic anomalies associated with the High Cascades, but Couch (1979) and Pitts (1979) reported a left-lateral sense on residual gravity anomalies in the same area. Woller and Priest (Chapter 5) showed that at

Lookout Point Reservoir no substantial movement had occurred during the last 22 m.y.

Within the map area, the authors found no evidence of dextral movement along the Eugene-Denio trend. Small northwest-trending shears and faults of relatively minor vertical displacement (less than 50 m [164 ft]) were found, but they do not comprise a distinct northwest-trending major fault zone.

The hypothesized offset on the High Cascade volcanic axis presupposes that the large composite cones are all centered on the axis of the High Cascade province. Detailed mapping, however, indicates that Diamond Peak sits on a highland of Tertiary rocks located at the eastern edge of the uplifted Western Cascade block. Other large vents of late High Cascade age in the Waldo Lake area, such as Mount Yoran, Fuji Mountain, and Cupit Mary Mountain, are also located along the eastern margin of the Western Cascades block, indicating that across the Eugene-Denio lineament there is no offset of the eastern boundary of the Western Cascade Range and, by inference, no offset of the High Cascade Range.

### Western Cascade-High Cascade transition zone

The nature of the Western Cascade-High Cascade transition zone has also been a subject of considerable discussion. From studies in the Mount Hood (Beeson and others, in preparation; Woller and Anderson, unpublished mapping, 1981; Williams and others, 1982), Breitenbush (White, 1980a), Belknap-Foley (Brown and others, 1980b; Avramenko, 1981; Flaherty, 1981; Taylor, 1981), Green Ridge (Hales, 1975; Taylor, 1981), Walker Rim (Walker, 1977; MacLeod, unpublished mapping, 1981), Diamond Lake (Barnes, 1978), Lake of the Woods (Maynard, 1974; Smith and others, 1982), and Klamath Lake (Walker, 1977) areas, there is considerable evidence that the High Cascade province may be bounded by a system of predominantly north-south faults.

The authors have found down-to-the-east and -southeast faults that are apparently related to the uplift of the Western Cascade province relative to the High Cascade province. At Pinto Mountain, one fault is younger than 5 m.y., an age that is in good accord with the age of faulting at Belknap-Foley (see discussion in Chapter 2). The Groundhog Creek fault appears to be an analogue of the Cougar Reservoir fault discussed in Chapter 4.

### Comparison of Groundhog Creek and Cougar Reservoir faults

The similarities between the Groundhog Creek fault and the fault at Cougar Reservoir (see Chapter 4) are striking. Both the Cougar and Groundhog fault zones are located at approximately the same longitude. Both may have substantial displacement. The Cougar fault has a minimum displacement of 366 m (1,200 ft), but one of the viable hypotheses led to a calculated displacement of greater than 1,033 m (3,388 ft) (see discussion in Chapter 4). At Shady Gap, approximately 450 m (1,476 ft) of andesites apparently have been removed from the west side of the fault. Both faults are associated with narrow bands of contiguous residual gravity lows (Couch and others, 1982a,b). Couch and others (1982a) interpreted this trough to be a major fracture and fault breccia zone which extends from the Columbia River to northern California. They estimated that vertical displacements of up to 2 to 3 km (1 to 2 mi) occurred along the zone and suggested that this fracture and fault zone is the western margin of a Cascade graben. Other similarities between the Groundhog Creek and Cougar Reservoir faults include their association with the 100-mW/m<sup>2</sup> contour of the heat-flow transition zone (Black and others, Chapter 7) and their proximity to thermal springs

(Groundhog Creek fault to McCredie Hot Springs, Cougar Reservoir fault to Terwilliger Hot Springs).

### Western Cascade-High Cascade boundary

For purposes of discussion we have constructed a nearly north-south hypothetical line that coincides with the easternmost north-south fault on Plate 3 and that runs through the two deepest parts of Waldo Lake, a point approximately 1 km (½ mi) east of the easternmost exposure of rocks of the late Western Cascade episode in Salt Creek, and through the linear portions of Whitefish and Trapper Creeks. This line is called the "hypothetical line" in the following discussion.

Three cross sections across the hypothetical line at Black Creek-Waldo Lake (line A-A', Plate 3), Salt Creek (line B-B'), and Diamond Peak-Redtop Mountain (line C-C') are used in the following discussion to examine the geologic and geomorphic evidence for large-scale faulting. In subsequent sections, the residual gravity contours across the hypothetical line in the same areas are discussed.

### Black Creek-Waldo Lake

In the Black Creek-Waldo Lake vicinity, the hypothetical line approximates the boundary between the deeply dissected terrane of the Western Cascades and the poorly-drained structural platform to the east (see map and cross section A-A', Plate 3). The headwall of Black Creek, a feature at least partially due to glaciation, is composed of andesites and basalts of the late Western Cascade episode. It is capped by undated High Cascade flows.

The Twins, a young, symmetrical Quaternary cone located 5 km (3 mi) due east of Waldo Lake, has produced lavas that have filled in the east side of the lake. The smooth symmetrical shape of the Twins and the accordance of the bathymetric contours with the surficial contours indicate that the Twins cone was the source of the flows underlying the east side of Waldo Lake. The exact age of the Twins is not known. The Twins' unglaciated shape may be a function of the rain shadow effect of the Cascades rather than a function of a possible very young age for the cone. It is interesting to note that while the "front line" of peaks on the crest line which are most exposed to weather from the west (Diamond Peak, Fuji Mountain, Mount Yoran) are heavily dissected by glaciation, many of those to the east are only lightly affected.

The origins of Waldo Lake and many other High Cascade lakes are commonly credited to glaciation. However, the bathymetry of Waldo Lake (Figure 6.2) makes the glacial origin theory of Waldo Lake problematical. It could not have been formed by glaciers advancing from the east, because glaciers gouge (and therefore steepen) the channel on the side toward the source of the ice, and abrade (and hence reduce the grade of the slope) on the "downstream" side. It is unlikely that Waldo Lake was formed by eastward-moving glaciers, because (1) there is no obvious source for an eastward-moving glacier to the west of Waldo Lake, and (2) the headwall of Black Creek suggests movement of glaciers in a westward course in that drainage. The reentrants on the steep west side of Waldo Lake may have been east-facing stream headwaters or glacial cirques, but no morainal deposits are evident. If glaciers moved into the Waldo Lake area from the north or south, they would have formed a U-shaped valley with smooth margins. The west side of Waldo Lake shows no evidence of smoothing nor evidence of any U-shape.

Therefore, it is more likely that the Twins formed after the development of a deep basin on the east side of the Waldo Lake escarpment. The Waldo Lake depression must have been much deeper at one time. The bathymetry of Waldo Lake shows that the two deepest depressions lie in a north-south

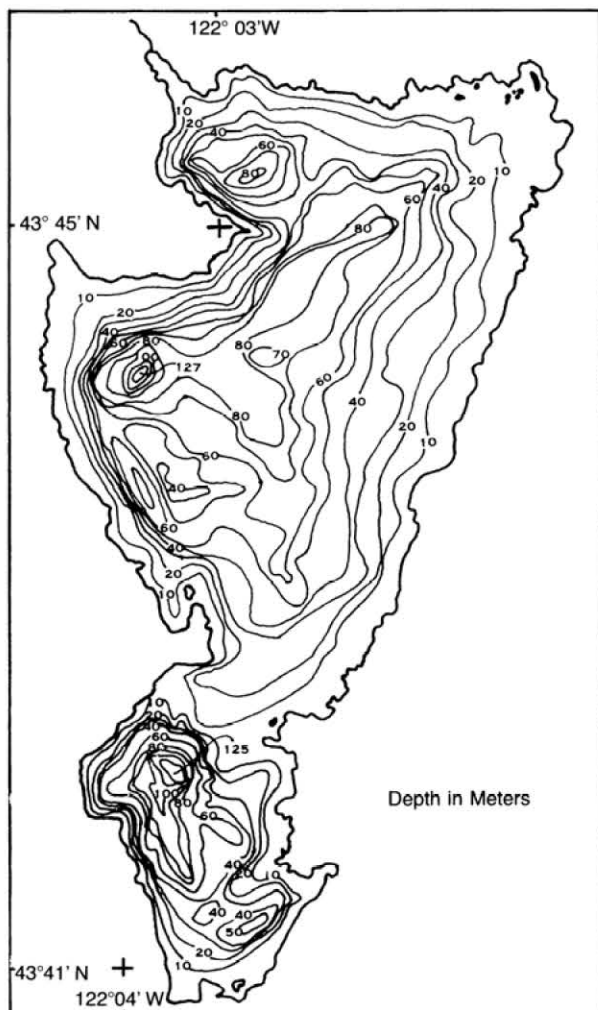


Figure 6.2. Map showing the bathymetry of Waldo Lake (source: U.S. Forest Service). Contours show depth in meters.

line along the west side of the lake. Therefore, it appears that Quaternary, west-flowing lavas are abutting a north-south highland of Western Cascade flows in this vicinity. The north-south highland of older (Tertiary) rocks extends 7.5 km (4.5 mi) north of the map boundary. Younger flows appear to abut the east side of the highland in that locality as well. A breach in the north-south highland, at 43°45.0' N. latitude, 122°5.0' W. longitude apparently has prevented the overtopping of the highland by lavas from the east. Flows of the late High Cascade episode are clearly present at the bottom of the breach.

The length, linearity, and geological relations of this north-south highland support the hypothesis that it is a fault-line scarp of a major fault with displacement down to the east.

### Salt Creek

The change in topographic character between the Western Cascade and High Cascade provinces is more subtle and gradual in the Salt Creek drainage. Flows of the late Western Cascade episode are present in this area as far east as 122°4.6' W. longitude. (In the Black Creek area, these older rocks are exposed as far east as 122°4.9' W. longitude.) Just east of these outcrops, Quaternary flows and vents bury any structure that

may be present (see map and cross section B-B', Plate 3).

East of the study area, most of the volcanoes east of the above-mentioned hypothetical line are very similar to the Twins in that they are symmetrical and essentially undissected by glaciation or stream erosion. These young cones (Maiden Peak [elevation 2,384 m (7,818 ft), relief 1,044 m (3,422 ft)], Hamner Butte [elevation 2,165 m (7,100 ft), relief 827 m (2,711 ft)], and Davis Mountain [elevation 2,024 m (6,635 ft), relief 685 m (2,246 ft)]) rise from a base of other Quaternary lavas. Flows of the late Western Cascade episode are exposed at the 1,525-m (5,000-ft) elevation west of the hypothetical line, and the divide through Willamette Pass is at an elevation of 1,563 m (5,126 ft).

This suggests that the north-south Tertiary highland immediately west of the hypothetical line at Waldo Lake continues southward across the Salt Creek drainage. An alternative hypothesis, which is permissible within the constraints of the data, is that young lavas of the High Cascade episode are onlapping rocks of the older Western Cascade episode to the west without structural control.

### Diamond Peak-Redtop Mountain

Diamond Peak is a Quaternary composite cone that sits atop a structural high of rocks of the late Western Cascade and early High Cascade episodes. Flows of the early High Cascade episode are found at 1,830 m (6,000 ft) on the west side of Diamond Peak. The top of Diamond Peak is at 2,667 m (8,744 ft), indicating that the thickness of flows of the late High Cascade episode on Diamond Peak is probably not greater than 836 m (2,742 ft) (see map and cross section C-C', Plate 3).

East of Diamond Peak, Redtop and Lakeview Mountains reach elevations of 2,155 m (7,065 ft). The exposed superstructure of Redtop-Lakeview Mountain (relief 630 m [2,065 ft]), which is composed entirely of High Cascade lavas (Sherrod and others, in press), has been heavily glaciated. The Tertiary base of the Redtop-Lakeview Mountain escarpment is not exposed (Sherrod and others, in press). It is clearly older than the youngest activity at Diamond Peak, as flows from Diamond Peak wrap around the bases of these mountains. The young flows from Diamond Peak about the west-facing side of the escarpment along Trapper and Whitefish Creeks. On aerial photographs, the north-south lineament along those creeks suggests the presence of a buried structure.

The west-facing Redtop Mountain escarpment is probably the result of eastward-moving glaciers from Diamond Peak which gouged out a valley in front of the escarpment. A similar situation occurs on the east side of Mount Jefferson to the north, where a west-facing escarpment was created at Bald Peter Ridge (Hales, 1975). The linear north-south boundary of the Redtop Mountain escarpment suggests that a north-south structural zone of weakness may have localized the glaciers.

### Residual gravity studies

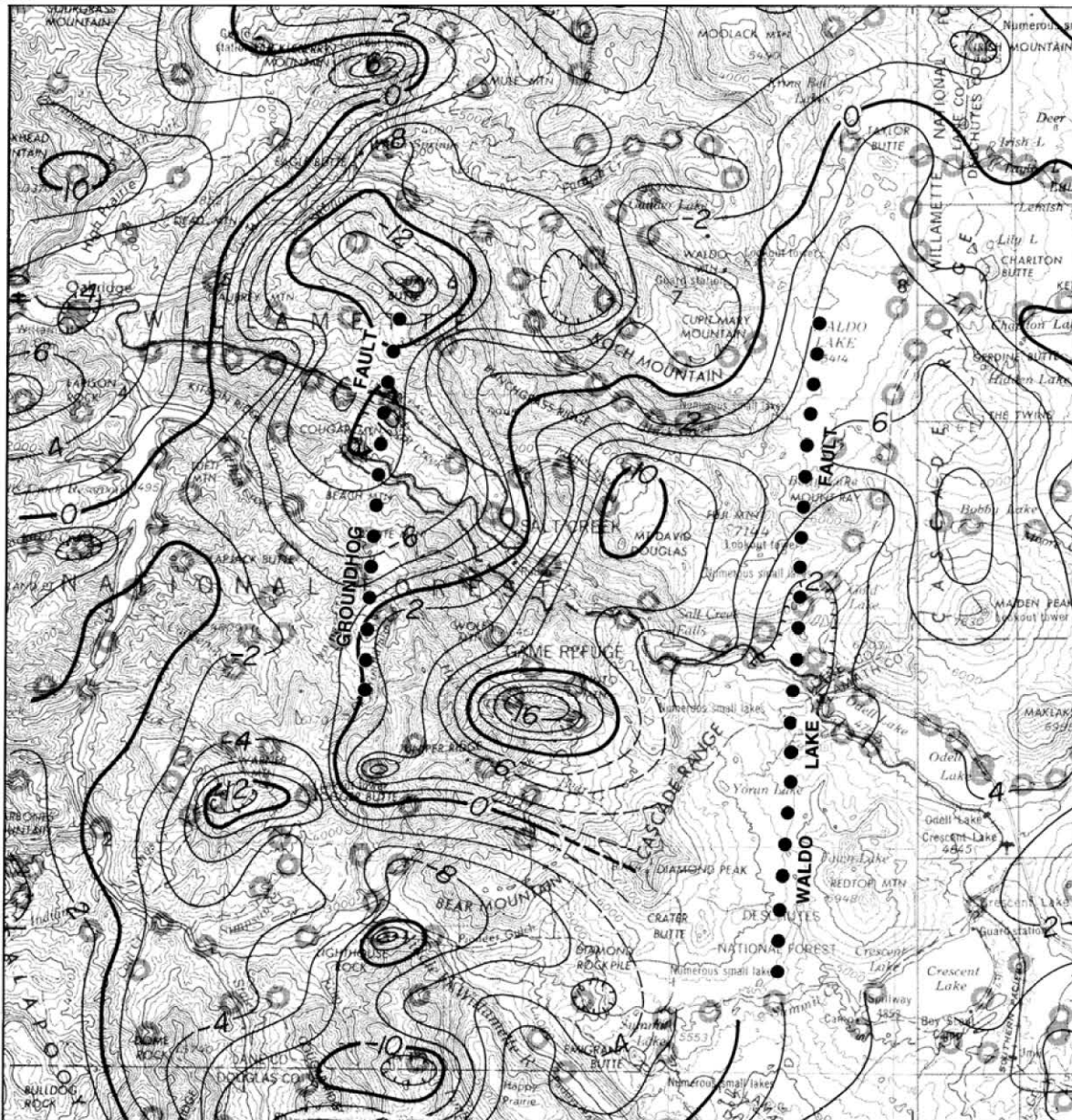
Residual gravity studies (see Figure 6.3) by Couch and others (1982a,b) show the same gravity signature at all three of the localities just discussed above. At Black Creek-Waldo Lake, the residual gravity increases in value from -2 mgal on the west side of the hypothetical line to +4 mgal on the east side. At Salt Creek, values on the east limb of a gravity trough rise from under +2 mgal to over +4 mgal. The high gravity of the west limb of the trough is due to major andesitic volcanic centers of the late Western Cascade episode at Moss Mountain and Mount David Douglas. There is a gap in gravity data between Diamond Peak and Redtop-Lakeview Mountains, but just south of the data gap, the residual gravity values change from -2 mgal on the west to +4 mgal on the east.



122° 30'

122° 15'

122° 00'



43° 45'

43° 30'

122° 30'

Base map by U.S. Geological Survey —  
reduced version of Roseburg, Crescent, Salem,  
Bend, 1:250,000 Scale Map  
Topographic contour interval 200 ft with  
supplementary contours at 100-ft intervals  
TRANSVERSE MERCATOR PROJECTION

SCALE  
5 0 5 MILE

Gravity Anomaly Contour Interval 2 Milligals  
Gravity stations are shown as open circles

Estimated uncertainty in  
measurements 1.0 milligal  
Theoretical gravity: IGF (1930)  
Reduction density 2.43 g/cc  
Regional components greater  
than 90 km are removed

122° 00'

Prepared by R.W. Couch, G.S. Pitts,  
M. Gemperle, C. Veen, and D. Braman

GEOPHYSICS GROUP,  
OREGON STATE UNIVERSITY  
November 1981

Figure 6.3. Residual gravity anomaly map of the area covered by the geologic map on Plate 3 (modified from Couch and others, 1982b). Locations of Groundhog Creek (left) and Waldo Lake (right) faults shown. Gravity anomaly contour interval=2 mgal. Gravity stations shown as circles. Topographic contour interval=200 ft, with supplementary 100-ft intervals. Estimated uncertainty in measurements=1.0 mgal. Theoretical gravity=IGF (1930). Reduction density=2.43 g/cm<sup>3</sup>. Regional components greater than 90 km are removed.

The increase in values of the residual gravity anomaly across the hypothetical line is probably the result of a thick sequence of High Cascade basalts east of the line. The steep slope of the gravity gradients across the hypothetical line argues for an equally sharp change in the thickness of High Cascade basalts across the hypothetical line.

This same residual gravity contour lineament and gradient can be traced northward into the Belknap-Foley area, where large-scale, down-to-the-east normal faulting is well documented (Brown and others, 1980a; Taylor, 1980, 1981; Flaherty, 1981; Avramenko, 1981; Priest and Woller, unpublished mapping, 1980). In the Belknap-Foley area, the amplitude of the residual gravity anomaly increases from  $-5$  mgal to  $+10$  mgal from Frissel Point to Sims Butte, and from  $-1$  mgal to  $+6$  mgal from Horse Creek to the Husband and Nosh Lake. The eastward increase in values of the residual gravity anomaly in both of these localities within the Belknap-Foley area probably reflects the thick pile of dense High Cascade rocks east of the down-to-the-east normal faults mapped by the researchers named above.

The geologic structures, heat flow, and residual gravity anomalies in the Waldo Lake-Swift Creek area correspond closely to those of the Cougar Reservoir-Belknap-Foley area. The similarities of the Groundhog Creek and Cougar Reservoir fault have already been discussed. The residual gravity anomalies display the same pattern across the Cougar Reservoir and Groundhog Creek fault zones and across the Belknap-Foley and Waldo Lake-Black Creek structures. Heat-flow patterns, which are discussed more completely in Chapter 7, also show the same increasing signature from west to east across the structures of both the Cougar-Belknap-Foley and Waldo Lake-Swift Creek areas.

The linearity and continuity of the geologic structures and geophysical anomalies in both areas deserve emphasis. The consistent north-south trends of the major fault zones at nearly the same longitudes, the continuous gravity troughs and lineations in the two areas at nearly the same longitudes, and the location of the heat-flow transition on the nearly identical north-south trend suggest that regional tectonic forces are affecting geological and geophysical processes in a regional, systematic way.

### **Western Cascade-High Cascade boundary: Conclusions**

From the evidence presented above, the authors postulate that there is a north-south fault along the west side of Waldo Lake. This conclusion is based on the following lines of evidence: (1) the bathymetry of Waldo Lake suggests that it is unlikely that the east-facing Waldo Lake scarp is the product of glacial erosion; (2) there is a thick sequence of High Cascade

lavas east but not west of the east-facing scarp; (3) the total length of linear highland of older rocks on the west side of Waldo Lake is 14.5 km (9 mi) from the southern Waldo Lake depression into the Chucksney Mountain quadrangle to the north; and (4) the residual gravity data of Couch and others (1982a,b) show an increase of gravity across a north-south line correlative with the proposed Waldo Lake fault. Although we cannot show a direct offset across the fault zone, the evidence supports the inference of major north-south, down-to-the-east faulting in this area.

The case is less clear in the Salt Creek and Diamond Peak-Redtop Mountain areas. Evidence that supports a southward continuation of the proposed north-south Waldo Lake fault into these two areas includes the following: (1) rocks of the late Western Cascade episode disappear east of the proposed fault, whereas they dominate the geology west of it; (2) gravity signatures are similar to those at Belknap-Foley and Waldo Lake-Black Creek; and (3) geomorphology of the area shows a consistent change in character across the proposed fault.

Alternatively, arguments against the proposed fault south of Waldo Lake are as follows: (1) no zone of faulting is evident in the Salt Creek area; (2) lavas from the young volcanoes centered east of the proposed fault may be simply onlapping the older topography to the west, as suggested by the elevations of many of the youngest cones which are higher than the topography to the west; and (3) broad upwarping rather than block faulting of the Western Cascade Range may be responsible for the greater dissection of that province by erosional and glacial processes.

Therefore, in the Salt Creek and Diamond Peak-Redtop Mountain areas, we can only conclude that faulting is one of several viable hypotheses that may explain the Western Cascade-High Cascade boundary.

### **Age of uplift of the Western Cascades**

The oldest K-Ar date on an intracanyon flow of the late High Cascade episode is  $1.98 \pm 0.25$  m.y. B.P. The youngest date obtained on ridge-capping rocks of the early High Cascade episode is  $4.32 \pm 0.40$  m.y. B.P. Therefore, the onset of Western Cascade uplift began during the interval between the two dates.

It is unfortunate that the intracanyon flow of the late High Cascade episode high on the south side of Mount David Douglas has not been dated. This flow may be one of the oldest lavas of the late High Cascade episode in the Waldo Lake area. This flow crops out over 610 m (2,000 ft) above Salt Creek. Dates from this flow and remnants of similar flows of the late High Cascade episode remaining on the walls of Salt Creek and the upper portions of Black Creek could provide valuable information on the timing and rate of uplift of the Western Cascades.

## CHAPTER 7. HEAT FLOW IN THE OREGON CASCADES

By Gerald L. Black, Oregon Department of Geology and Mineral Industries, and David D. Blackwell and John L. Steele, Department of Geological Sciences, Southern Methodist University, Dallas, Texas

### ABSTRACT

Heat-flow data from 170 holes, most of them located in the Willamette Valley, Western Cascade, and High Cascade physiographic provinces, are tabulated. The data indicate that a zone of low heat flow averaging  $43 \pm 1$  mW/m<sup>2</sup> occupies the Willamette Valley province and most of the Western Cascade province. A zone of higher heat flow averaging  $104 \pm 9$  mW/m<sup>2</sup> occupies the High Cascade province and extends about 10 km (6 mi) into the Western Cascade province. The transition between the two zones is very narrow, averaging less than 10 km (6 mi) in width throughout most of its length in Oregon. Heat flow in the Willamette Valley and Western Cascade provinces is primarily conductive.

In the High Cascade province, high lateral permeability makes the measurement of meaningful heat-flow values virtually impossible at depths of less than 300 m (984 ft). A 25-mgal negative gravity anomaly which is superimposed on a regional negative trend occurs at the heat-flow transition zone. Thermal modeling of the heat-flow data and gravity modeling indicate that temperatures as high as 700° C may underlie the High Cascade province and that it is possible that molten rock underlies large portions of the high heat-flow zone. Three conceptual models that may explain the origin of the north-south line of hot springs paralleling the High Cascade-Western Cascade boundary are described. Finally, numerical estimates for the geothermal potential of the Cascade Range of Oregon are made. The estimates are based on the heat-flow data base and thermal modeling.

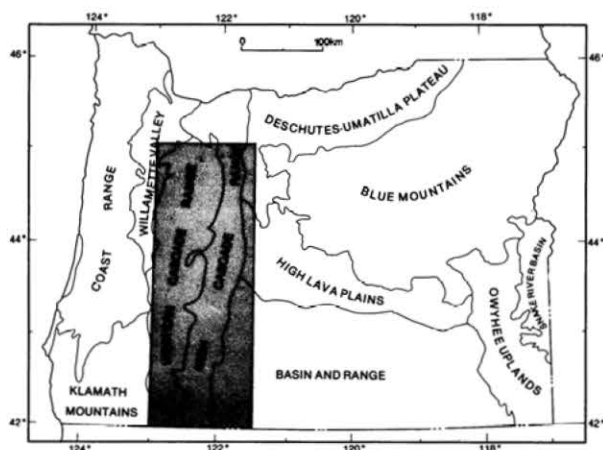


Figure 7.1. Map showing the physiographic provinces of Oregon (after Dicken, 1950). Area discussed in this paper is outlined in black.

### INTRODUCTION

The Cascade Range in Oregon is separated into two physiographic provinces: (1) the Western Cascades, composed of Oligocene to upper Miocene flows, epiclastic deposits, and pyroclastic rocks; and (2) the High Cascades, composed primarily of Pliocene to Holocene lava flows (Figure 7.1). The High Cascade province lies east of the Western Cascades and includes the prominent composite volcanic cones which characterize the Cascade Range (e.g., Mount Hood, Mount Jefferson, Three Sisters, and Crater Lake).

In this report only that portion of the Cascade Range south of the Clackamas River (approximately 45°05' N. latitude) will be discussed. The region north of the Clackamas River in the vicinity of the Mount Hood volcano has been discussed in detail by Blackwell and others (1978), Blackwell and Steele (1979), and Steele and others (1982).

Heat-flow data for 170 holes in the region bounded by longitudes 121°30' and 123°00', the California-Oregon border, and latitude 45°05' N. (the rectangle indicated on Figure 7.1) are summarized in Appendix D. Physiographic provinces included within the study area and their abbreviations as used in Appendix D are parts of the Basin and Range (BR), High Lava Plain (HL), Deschutes-Umatilla Plateau (DU), High Cascade Range (HC), Western Cascade Range (WC), Willamette Valley (WV), and Klamath Mountain (KM) physiographic provinces (Figure 7.1). Although heat-flow data from the Klamath Falls region are included in Appendix D for completeness, that area is not discussed in this report.

Also listed in Appendix D are the hole location, both by township, range, and section and by latitude and longitude; an abbreviation for the physiographic province in which the hole is found; the hole name and date of logging used for calculation of the temperature gradient; an abbreviation for hole type; collar elevation; hole depth; the depth interval over which the temperature gradient was calculated; the average thermal conductivity; the uncorrected and corrected temperature gradients; corrected heat flow; evaluation of heat-flow quality; and a brief lithologic summary. Hole locations are given to the nearest quarter-quarter or quarter-quarter-quarter section using a system in which the northeast, northwest, southwest, and southeast quarters are assigned the letters A, B, C, D, respectively. The hole is first located to the nearest quarter section, then the nearest quarter-quarter section, and finally the nearest quarter-quarter-quarter section (see Appendix C). For example, a hole located in the northeast quarter of the southwest quarter of sec. 2 would be listed in the table as 2Ca. The abbreviations for physiographic provinces are as given previously except that the abbreviation WH is used for those holes located near the Western Cascade-High Cascade boundary. Hole types include water wells (WW), oil and gas prospects (OW), temperature-gradient holes (TG), damsite-foundation studies (FS), and mineral-exploration holes (ME).



All calculations of thermal conductivity, corrected and uncorrected temperature gradients, and corrected heat flow were performed under the direction of David D. Blackwell at Southern Methodist University. Thermal conductivities were measured on equipment similar to that described by Roy and others (1968). When possible, thermal conductivities were measured on core samples; but inasmuch as cores were only rarely available, conductivities were usually determined from cuttings using the technique of Sass and others (1971).

When cuttings are used to measure thermal conductivity, porosities must be estimated. Typical values vary from 25 to 35 percent for unconsolidated sediments and semiconsolidated sedimentary rocks to 5 to 10 percent for volcanic rocks (Blackwell and others, 1982). Where several cuttings samples were available from a single hole, the results were averaged, and the mean thermal conductivity, followed by the standard error in parentheses, is listed in Appendix D. Thermal conductivity values from Appendix D which are in parentheses are either assumed values based on measurements of typical lithologies in the area or are based on measurements of only one or two cuttings samples from the hole.

For any hole which penetrated basalts of the Columbia River Basalt Group, a thermal conductivity of  $1.59 \text{ W}/(\text{m}^\circ\text{K})$  was assumed. Though the scatter is large, this is the mean of many measurements made on these rocks from Oregon and Washington (Blackwell and others, 1982).

The uncorrected temperature gradients result from a least-squares fit to the raw temperature-depth data over the depth interval shown. Standard errors are given in parentheses below the gradient. The corrected temperature gradients have been corrected for the effects of topography using the method of Blackwell and others (1980). Corrected heat flow in  $\text{mW}/\text{m}^2$  is the product of thermal conductivity and the terrain-corrected temperature gradient.

The heat-flow quality is a semiquantitative assessment of the reliability of the heat-flow determination. "A" quality determinations are considered to be  $\pm 5$  percent, "B" are  $\pm 10$  percent, "C" are  $\pm 25$  percent, and "D" values are of uncertain reliability (Blackwell and others, 1982). An "X" indicates that the temperature-depth data are not suitable for heat-flow determinations, usually because of large-scale aquifer effects. Most of the problems in calculating heat flow are due to uncertainties regarding the thermal conductivity (Blackwell and others, 1982), though occasionally problems result from making terrain corrections in areas of unusually complex topography.

Nearly all of the data in Appendix D are either unpublished or have been published only in open-file reports. Sources of published data are Bowen (1975), Hull and others (1976, 1977, 1978), Youngquist (1980), Brown and others (1980a,b), Blackwell and others (1982), and Mase and others (1982).

## DATA COLLECTION

The collection of heat-flow data in the Cascade Range of Oregon is an on-going process that began on a large scale in 1976. In that year, an extensive effort was made to locate and log existing holes (mostly domestic water wells) in the Western Cascade and Willamette Valley physiographic provinces (Figure 7.1). The holes were located primarily along the drainages of the Santiam River, McKenzie River, and Middle Fork of the Willamette River. A 16-hole drilling program was also completed in 1976 along the Western Cascade-High Cascade boundary, with most of the holes located near the hot

springs (i.e., Austin, Bagby, Breitenbush, Belknap, Foley, and McCredie Hot Springs) that occur in an approximate north-south line along the boundary. Where possible, the holes were drilled to a depth of 152 m (500 ft). In 1977, the emphasis was on the collection of data from existing wells in the High Lava Plain and Deschutes-Umatilla Plateau provinces along the eastern margin of the High Cascades; in 1978, extensive drilling was carried out in the vicinity of Mount Hood. In 1977, some data were also collected from existing wells in the southern Oregon Cascades near Medford and Ashland. In 1979-1980, the emphasis was again on the drilling of temperature-gradient holes. In 1979, six deep holes (up to 600 m [1,968 ft]) were drilled along the western margin of the High Cascades under the auspices of the Eugene Water and Electric Board (EWEB) to test the geothermal significance of geophysical anomalies (Youngquist, 1980). In 1979-1980, 21 temperature-gradient holes were drilled by the Oregon Department of Geology and Mineral Industries. Most of these holes were again located near the boundary between the High Cascade and Western Cascade physiographic provinces, but three holes were sited on Green Ridge along the east side of the central High Cascades. The objective of the 1979-1980 drilling program was to test in the northern and central Cascades the heat-flow model of the Cascade Range that was developed by Blackwell and others (1978) from the data collected in 1976-1977. In 1981, heat-flow data were collected from existing wells in the southern Oregon Cascades in an attempt to increase the data base in that area.

In addition to the above efforts, the U.S. Geological Survey (USGS) published an extensive data set for the Cascade Range of northern California. Included in the data set was information on three heat-flow holes drilled in the Klamath Mountain province of southern Oregon (Mase and others, 1982). The data from one of the holes are included in Appendix D.

## CASCADE HEAT FLOW

The nature of the regional heat flow in the Cascade Range of Oregon was first discussed by Blackwell and others (1978) and later amplified by Blackwell and others (1982). The single most striking feature of the regional heat flow is a rapid increase from values on the order of  $40 \text{ mW}/\text{m}^2$  in the Willamette Valley and Western Cascade provinces to values of greater than  $100 \text{ mW}/\text{m}^2$  in the eastern part of the Western Cascade and the High Cascade provinces (Figure 7.2). The transition from lower to higher heat flow is very abrupt, taking place over a lateral distance of less than 20 km (12 mi) in those portions of the northern and central Cascades for which detailed data are available (Blackwell and others, 1978, 1982).

The transition from average to high heat flow takes place approximately 10 km (6 mi) west of the mean physiographic boundary between the High Cascades and Western Cascades (Blackwell and others, 1982). The geographic boundary is very irregular because the nearly horizontal rocks of the early High Cascade episode (lavas between 9 and 4 m.y. B.P., according to Priest and others, Chapter 2) cap ridges formed mostly of Western Cascade rock. Topographic effects thus result in a very complicated boundary. The boundary is also characterized by a nearly north-south line of hot springs which typically occur in Western Cascade rocks or in High Cascade rocks just inside the boundary with the Western Cascades. The origin of the hot springs is of interest with respect to the geothermal potential of the region and is discussed in more detail in a later section.

## WESTERN CASCADE-WILLAMETTE VALLEY HEAT FLOW

Heat-flow data from the Western Cascades (west of the transition to higher heat flow) and the adjoining Willamette Valley province are very uniform. The average value for the two provinces is  $43 \pm 1$  mW/m<sup>2</sup>, and the average gradient is  $30 \pm 1^\circ$  C/km (Blackwell and others, 1982). Typical gradients range from  $25^\circ$ - $35^\circ$  C/km.

As has been mentioned previously, most of the data from this area were collected from existing water wells located near developments in the drainages of major streams. Water wells generally represent a "worst case" situation for the collection of heat-flow data, because there is no control over the way in which the well is finished, and intraborehole fluid movements can make the interpretation of temperature-depth curves difficult. However, this lack of control turned out not to be a problem in this region. The heat-flow regime is conductive, and linear temperature-depth relationships are the rule. Pervasive alteration of the Western Cascade volcanic and volcanoclastic rocks to clays and zeolites effectively "seals" the rocks and results in low permeability. Only rarely was there a problem with intraborehole fluid movement, and there was no evidence of regional aquifer effects (Blackwell and others, 1982).

## HIGH CASCADE HEAT FLOW

Heat-flow values obtained from shallow drill holes (i.e., less than 300 m [984 ft]) in the High Cascade provinces of Oregon and California (Mase and others, 1982) are typically anomalously low. The effect is regional and apparently results from the high permeability existing at the flow contacts of the young volcanic rocks. The high permeability, coupled with high precipitation in the region, results in the rapid downward percolation and lateral flow of rainfall and snow melt, effectively washing away heat from deeper in the crust. The upper 300 m (984 ft) of the crust is transparent with respect to heat flow, and the effective surface of the earth with respect to heat flow lies at a depth of about 300 m (984 ft) (Blackwell and others, 1982) in this province. This pattern is exemplified by hole T12S/R7E/9Da (Youngquist, 1980), which is isothermal to a depth of 300 m (984 ft) but which possesses a temperature gradient and heat-flow value below that depth typical of those found in the higher heat-flow portions of the transition zone (see following section).

The above is true only for the youngest rocks in the High Cascades. In the upper Miocene volcanic rocks of the early High Cascade episode (Chapter 2), alteration has reduced permeability so that in places conductive temperature gradients can be measured in holes 100-150 m (328-492 ft) deep. A good example is hole T12S/R9E/1Bcd (Appendix D), a 152-m (500-ft) temperature-gradient test drilled in basalt of the early High Cascade episode. The temperature-depth curve is linear, indicating conductive heat flow, with an uncorrected gradient of  $79.2^\circ \pm 1.5^\circ$  C/km.

## WESTERN CASCADE-HIGH CASCADE BOUNDARY REGION

Those holes in Appendix D which have been assigned a province code of WH are located in or near the boundary between the High Cascades and Western Cascades. As most of the holes were drilled specifically for heat-flow purposes, nearly all of them were cored in the more highly altered rocks of Western Cascade or early High Cascade age, and care was taken to grout the holes in order to prevent intraborehole

fluid movement.

Temperature-depth curves from most of the holes in this region are linear, and the heat flow is basically conductive except in the immediate vicinity of some of the hot springs where geothermal systems are obviously in operation (e.g., holes T6S/R7E/21Cd; T6S/R7E/30Bb; T9S/R7E/20Aa, -20Ac, -2Ad; and T17S/R5E/20Ba). Even in these geothermal areas, holes as close as 1 km (0.6 mi) to the hot springs frequently showed no anomalous heat flow (e.g., holes near Wall Creek, Terwilliger, and Belknap Hot Springs).

The mean heat flow east of the transition to higher heat flow is  $104 \pm 9$  mW/m<sup>2</sup>, and the mean gradient is  $66^\circ \pm 7^\circ$  C/km (Blackwell and others, 1978, 1982). The means were derived from data obtained during the 1976 drilling program, though it should be noted that data from those holes located in obvious geothermal systems were excluded from the calculations. Most of the holes in the 1976 study were located within 1 to 5 km (0.6 to 3 mi) of hot springs (i.e., Austin, Bagby, Breitenbush, Belknap, Foley, and McCredie Hot Springs), so that there was some concern that the data might be prejudiced. We concluded, however, that the very uniform values of terrain-corrected heat flow and temperature gradient indicate that the nearness of the springs has no general effect (Blackwell and others, 1982). The 1979-1980 drilling program was designed to address this potential problem. In general, drill sites were selected that filled in gaps between previous values, were not located near obvious hot springs, were located east of the suspected transition to higher heat flow, and were cored in rock types (i.e., Western Cascade and lower High Cascade rocks) in which heat flow was typically conductive.

The results of the 1979-1980 drilling program (Appendix D; Figure 7.2) confirm, in the central and northern Cascades, the rapid increase in heat-flow values from approximately 40 mW/m<sup>2</sup> in the Western Cascades to values on the order of 100 mW/m<sup>2</sup> east of the transition zone. In the south-central Cascades between latitudes  $42^\circ 45'$  and  $43^\circ 30'$ , where there is only one heat-flow point associated with the transition zone, an adequate data base is clearly lacking; in the extreme southern Cascades, there is inadequate information to accurately constrain the position of the 100-mW/m<sup>2</sup> contour, although the position of the 60-mW/m<sup>2</sup> contour is adequately controlled by a combination of data from domestic water wells and data from the Cascade Range in northern California.

In the southern portion of the Cascades, nearly all of the heat-flow values are based on temperature gradients measured in domestic water wells. For many of these holes, accurate terrain corrections and thermal-conductivity measurements have not yet been completed so that the estimated plotted heat-flow values are subject to large error.

## INTERPRETATION OF HEAT-FLOW TRANSITION ZONE

The east-west cross sections of Figure 7.3 extend from the center of the High Cascade province, through the Western Cascades, and into the Willamette Valley province. Plotted are values for corrected temperature gradient and heat flow. The zero line is the 100-mW/m<sup>2</sup> heat-flow contour (Figure 7.2) which is located about 10 km (6 mi) west of the mean position of the physiographic boundary between the Western and High Cascade provinces (Blackwell and others, 1982).

Also shown (relative to the 100-mW/m<sup>2</sup> contour) are the positions of the hot springs associated with the boundary and the line of young Quaternary volcanoes which make up the youngest part of the High Cascade province. Other versions of Figure 7.3 have appeared in Blackwell and others (1978), Blackwell and Steele (1979), and Blackwell and others (1982).

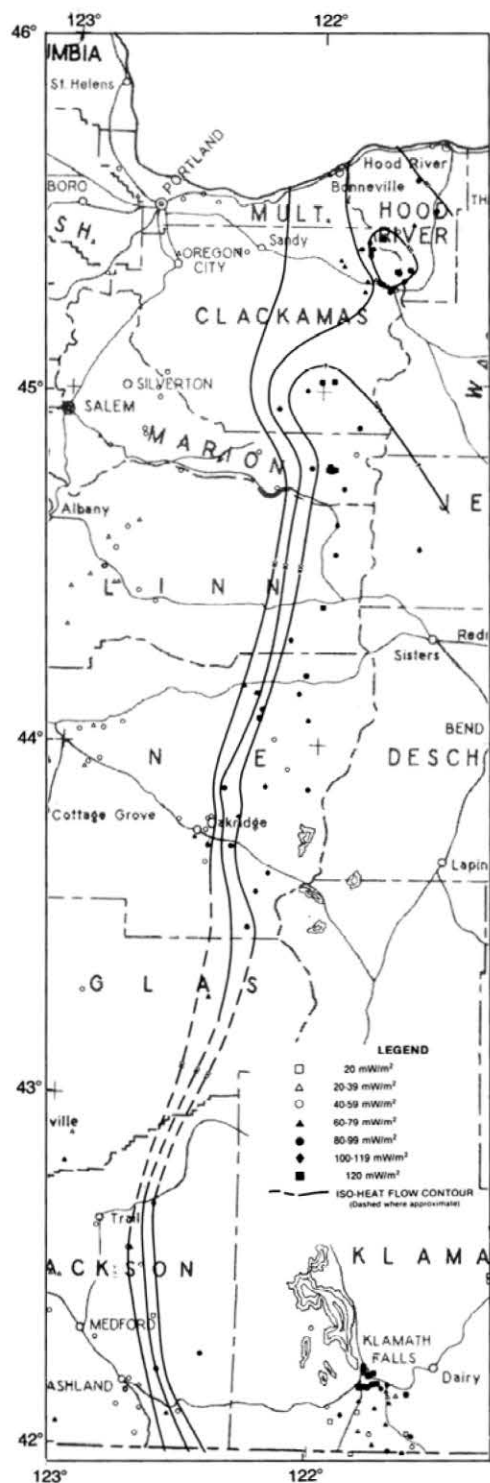


Figure 7.2. Map showing heat flow in the Cascade Range of Oregon. Contour interval =  $20 \text{ mW/m}^2$ .

Figure 7.3 has been modified from Blackwell and others (1982) by the addition of heat-flow data obtained during the 1979-1980 DOGAMI drilling program and the 1979 EWEB drilling program (Youngquist, 1980).

For most of the length of the Cascade Range, the data from Figures 7.2 and 7.3 clearly demonstrate the rapid increase in heat flow from very uniform values on the order of  $40 \text{ mW/m}^2$  in the Willamette Valley and Western Cascades to values around  $100 \text{ mW/m}^2$  east of the transition zone.

North of the Clackamas River, however, the nature of the transition zone changes. Although the relative position of the transition remains intact, the amplitude of the variation is lower, ranging from about  $30 \text{ mW/m}^2$  on the west to  $80 \text{ mW/m}^2$  on the east. For this portion of the Cascade Range in Oregon and Washington, heat-flow values in excess of  $100 \text{ mW/m}^2$  are found only in "spot," or local, anomalies associated with the young composite volcanoes making up the High Cascade peaks (Blackwell, personal communication, 1982). The change in heat-flow pattern at the Clackamas River corresponds to a marked decrease in the volume of basaltic volcanism north of the Clackamas River (Priest, 1982; Priest and others, Chapter 2).

South of the Clackamas River the transition zone is very narrow. It averages about  $10 \text{ km}$  ( $6 \text{ mi}$ ) or less in width in areas where there are adequate data to constrain it, and nowhere is it known to exceed  $20 \text{ km}$  ( $12 \text{ mi}$ ) in width. The uniformity from north to south indicates that crustal conditions beneath the zone are similar throughout the length of the study area (Blackwell and others, 1982).

Heat-flow studies by the U.S. Geological Survey have verified the existence of a transition from lower to higher heat flow in the Cascade Range of northern California. There, the position of the  $60 \text{ mW/m}^2$  contour has been determined fairly accurately, but the presence of a heat-flow high with a magnitude on the order of  $100 \text{ mW/m}^2$  has not been verified, probably due to the masking effects of hydrothermal circulation in the porous young volcanic rocks of the High Cascades (Mase and others, 1982).

A temperature profile is also shown in Figure 7.3. It is based on the heat-flow profile and was obtained by the method of continuation of heat-flow data described by Brott and others (1981). Constant thermal conductivity and steady-state conditions were assumed in the construction of the model (Blackwell and others, 1982). The first assumption is reasonable for the mafic rocks found in the Cascades, whereas the second, though not completely valid, leads to results that do not differ significantly from those obtained using transient models for the depth range shown (Blackwell and others, 1982). The assumptions involved in the construction of Figure 7.3 are discussed in more detail by Blackwell and others (1982).

The temperature profile of Figure 7.3 implies high temperatures at shallow depths east of the  $100 \text{ mW/m}^2$  contour (approximately  $10 \text{ km}$  [ $6 \text{ mi}$ ] west of the physiographic boundary). Inasmuch as any one of the isotherms can satisfy the heat-flow anomaly, the temperature does not necessarily have to reach  $700^\circ \text{C}$ . The profile does, however, indicate the presence of an intense heat source at relative shallow levels in the crust (Blackwell and others, 1982).

Further support for the above thermal model comes from depth to Curie-point isotherm calculations of Connard (1980) and McLain (1981). Using a Curie-point temperature of  $580^\circ \text{C}$ , Connard (1980) calculated a depth to the Curie-point isotherm of  $6$  to  $9 \text{ km}$  ( $3.6$  to  $5.4 \text{ mi}$ ) below sea level beneath much of central Cascades between latitudes  $43^\circ 00'$  and  $44^\circ 00'$ . McLain (1981), working in the southern Cascades and using the same Curie-point temperature, calculated a depth to the



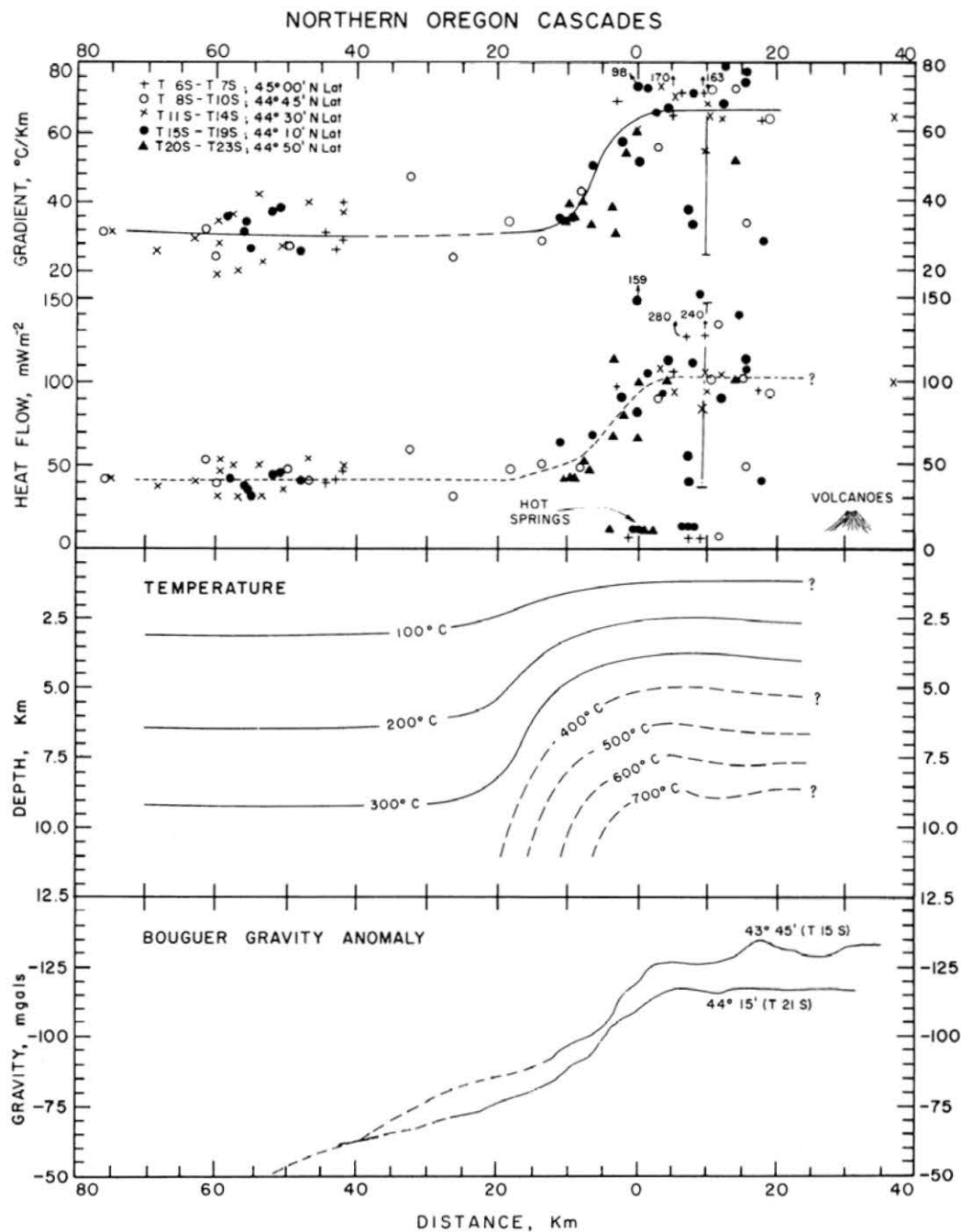


Figure 7.3. Geothermal gradient, heat flow, interpreted crustal temperatures, and regional Bouguer gravity for the western part of the northern Oregon Cascade Range (gravity data are from Couch and Baker, 1977). Heat-flow data between latitudes 43° 15' N. and 45° 05' N. are projected onto the profile. The zero distance reference is the 100-mW/m²-heat-flow contour line (modified from Blackwell and others, 1982).

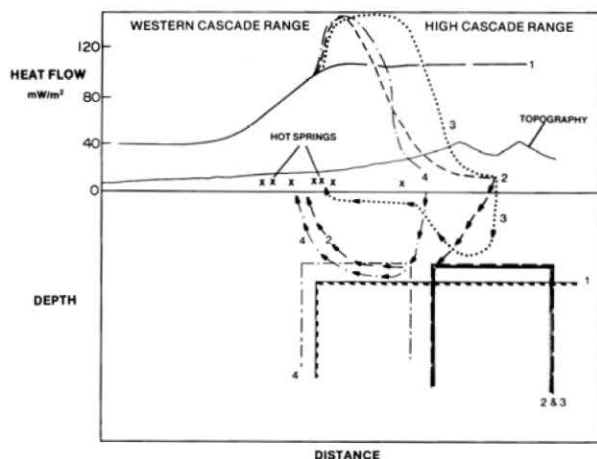


Figure 7.4. Several models of the relationship of hot springs to the heat-flow transition observed at the Western Cascade Range-High Cascade Range boundary. Four curves are shown, with three different variations in fluid circulation. In curve 1, the observed conductive anomaly (see Figure 7.3) is shown. In the other three models, the hot-spring anomalies are interpreted in terms of various controls on water circulation (see text) (from Blackwell and others, 1982).

Curie-point isotherm of 4 to 6 km (2.4 to 3.6 mi) below sea level in the Klamath Falls-Mount McLoughlin area and 5 to 7 km (3 to 4.2 mi) below sea level in the vicinity of Crater Lake. In the intervening areas of the southern Cascades, the depth to the Curie-point isotherm was 6 to 14 km (3.6 to 8.4 mi) below sea level.

Also shown on Figure 7.3 are two Bouguer gravity profiles which were constructed from the data of Couch and Baker (1977) and Berg and Thiruvathukul (1967). A negative gravity anomaly of 25 mgal is superimposed on background values which decrease eastward toward the crest of the High Cascades.

The 25-mgal anomaly is regional in extent and occurs at the heat-flow transition zone. Blackwell and others (1982) offered four possible explanations for its occurrence: (1) the change in gravity is associated with the same phenomenon which causes the change in heat flow; (2) the gravity gradient corresponds to a western boundary of the proposed High Cascade graben (Allen, 1966), and the presence to the east of low-density volcanic rocks; (3) the anomaly is fortuitously coincidental with the heat-flow boundary, and it reflects a change in the density structure of the crust; and (4) a local negative anomaly is superimposed on the regional trend (Couch, 1979).

Blackwell and others (1982) examined several density models to investigate the above possibilities. They concluded that thermal expansion alone could not account for the gravity anomaly and that the presence of molten material or a change of rock type at depth is required to explain it. Although realizing that large-scale intrusives or normal faulting could generate density differences at levels shallow enough to generate the observed profiles, they preferred a model requiring the presence of molten material at depth because of the close correspondence between the gravity and heat-flow anomalies, and they interpreted the gravity data to indicate the presence of a large zone of partially molten material residing in the upper part of the crust beneath the High Cascades and extending about 10 km (6 mi) west of the High Cascade-Western Cas-

cade boundary.

Although the above hypothesis would explain the coincidence of the gravity and heat-flow anomalies, several geologic questions concerning the model remain to be answered. The molten material must be either mantle-derived magma or partially melted upper crustal material. Most of the volume of late High Cascade volcanism is of basaltic to basaltic andesite composition (Priest and others, Chapter 2), which does not usually form large intrusive bodies. If the molten material is composed of partially melted rocks of the early and/or late Western Cascade episodes, it should be silicic in composition. Lavas of silicic composition have not reached the surface in high quantities in the High Cascade province. It also seems likely that if molten material underlies the High Cascades at relatively shallow depths, recent volcanic eruptions should be more frequent than they have been in the recent geologic past. The answers to these questions and the ultimate validity of the partial melting model must await the completion of deep drilling in the High Cascade province.

## ORIGIN OF HOT SPRINGS

A line of hot springs which appear to be associated with the heat-flow transition zone parallels the Western Cascade-High Cascade physiographic boundary. Figure 7.4, taken from Blackwell and others (1982), shows several conceptual models which could explain the existence of the springs. Also included are heat-flow profiles which would result from each of the models. The first (curve 1, Figure 7.4) shows the regional background conductive heat flow. The regional heat flow is assumed to be due to a crustal source underlying the entire High Cascade Range. The other three models (curves 2, 3, and 4) include convective heat transfer. The heat-flow curves for these models show the convective heat flow from the hot springs superimposed on the regional conductive anomaly. In all cases the hot springs result from the deep circulation of meteoric water, assumed to be from east to west, driven primarily by elevation differences between the High Cascades and the stream valleys in which the hot springs issue (Blackwell and others, 1982).

The models differ in the location of the source providing the heat and/or the circulation path of the fluid. In model 2, the water circulates to a depth greater than 2 km (1.2 mi) and comes up directly beneath the hot springs; in model 3 the water circulates essentially vertically downward beneath the volcano, then rises rapidly to relatively shallow depths and flows laterally along permeable horizons to emerge at the hot springs. In both of these models, the heat source underlies the central portion of the High Cascade Range. In model 4, the heat source responsible for the hot springs is confined to a narrow band along the physiographic boundary. It could be a shallow heat source offset from the axis of the High Cascades, or alternatively the hot springs could be localized by fractures in intrusives buried beneath the physiographic boundary or by proposed graben-bounding normal faults.

In the model for Cascade heat flow favored by Blackwell and others (1982), the entire region of the Cascades east of the transition zone has a background heat flow on the order of 100 mW/m<sup>2</sup> resulting from a zone of partially molten material lying at a depth of approximately 10 km (6 mi). Magmatic temperatures at shallower depths probably occur only directly beneath active Quaternary volcanoes. This model is exemplified by curve 1 of Figure 7.4. Hot springs and local heat flow anomalies with values much above or below 100 mW/m<sup>2</sup> are probably related to ground-water convection. Local heat-flow anomalies, with or without associated hot springs, could possess heat-flow profiles similar to those of models 2-4, Fig-

ure 7.4. Combinations of the models are likely to occur at any given locality.

While the hot springs that occur in the Cascades certainly result from convective processes, the specific mechanism operative at any given spring is unknown. The nature of vertical and horizontal permeability at depth is also largely unknown. It is likely to be highly complex and probably varies from location to location. The types of reservoir rock that might occur in the Central Range are discussed by Priest (Chapter 8).

Although the specific details of the convective systems operative at any given spring are unknown, it is obvious that the positions of several of the Cascade hot springs are controlled by normal faults with down-to-the-east displacement. In the central Cascades near Belknap Hot Springs, Brown and others (1980) mapped north-northeast-trending normal faults which clearly control the location of that hot spring and another smaller spring (Bigelow Hot Spring) to the north. The position of Terwilliger Hot Springs appears to be controlled by the nearly north-south-trending Cougar Reservoir fault (see Priest and Woller, Chapter 4 and Plate 2, this report). Farther south, in the Waldo Lake-Swift Creek area, the location of McCredie Hot Springs appears to be controlled by the north-south trending Groundhog Creek fault (see Woller and Black, Chapter 6, this report). A heat-flow profile across these springs could be similar to that of model 4, Figure 7.4.

To summarize, the Cascade hot springs are the result of convective processes, the precise nature of which is unknown. Three possible models for the hot springs are shown in Figure 7.4. Any given spring could result from any one, or any combination, of the three models. The locations of several of the springs are controlled by north-south-trending normal faults. It may be that, as more detailed geologic mapping becomes available, the locations of all of the Cascade hot springs will be found to be fault controlled.

## GEOTHERMAL POTENTIAL OF THE CASCADES

The data set for the Cascade Range of Oregon clearly represents a subduction-zone heat-flow pattern (Blackwell and others, 1982). The linear band of uniform low heat flow, separated by a narrow transition zone from a zone of much higher heat flow, is characteristic. The low-heat-flow zone is caused by the subducting slab, which acts as a heat sink until it reaches depths of 100 to 150 km (60 to 90 mi), while the high-heat-flow zone is due to magmatic processes which generate the volcanic arc. A detailed discussion of the plate-tectonic implications inherent in the Oregon data set can be found in Blackwell and others (1982).

The data contained in this report and the above considerations indicate that the geothermal potential of the Western Cascade Range west of the transition zone (and of other provinces of Oregon farther to the west) is limited. Typical gradients are only 25° to 35° C/km (Blackwell and others, 1978), so that temperatures above 50° C, the minimum temperature for the direct use of geothermal waters in space-heating applications, will not occur shallower than 1 km (0.6 mi). The low gradients do not rule out, of course, the use of lower temperature fluids (down to 10° C) in agricultural, aquacultural, and heat-pump applications. A further hindrance to geothermal exploitation in the Western Cascades is the relative impermeability of the rocks, which may make the utilization of the resource impractical.

The prospects for the exploitation of geothermal energy in the High Cascade Range are considerably more promising. It has been shown that the heat-flow transition zone is due to

regional crustal effects rather than local upper crustal effects, and temperature modeling (Figure 7.3) has indicated the possibility of a zone of partial melting at a depth of 10 km (6 mi) (Blackwell and others, 1978, 1982). The regional temperature gradient east of the transition zone is 66° C/km (Figure 7.3), so that the circulation of ground water to depths of 5 km (3 mi) could produce temperatures on the order of 300° C.

Inasmuch as volcanic arcs represent major geothermal provinces and are already the sites of power-generating facilities at other places in the world, it seems likely that the Oregon Cascade Range possesses significant potential for the generation of electricity from geothermal fluids. One of the problems with this analogy is the absence of evidence for large high-temperature hydrothermal systems in the High Cascade Range. The comparative lack of surface manifestations, as has been mentioned previously, is probably due to the masking effect of cold ground-water flow in permeable young volcanic rocks. Another possibility is that there is insufficient heat stored in the shallow parts of the volcanic carapaces of the large composite volcanoes to significantly heat up the ground water (Blackwell and others, 1982). Whatever the reason, the lack of surface manifestations does not necessarily imply the nonexistence of geothermal resources. In the Western Cascades, where thermal conditions prior to 6 m.y. B.P. were probably similar to those of the High Cascades of today (Blackwell and others, 1982), there is ample evidence of hydrothermal circulation in the form of exposed plutons and surrounding large areas of altered country rock (Peck and others, 1964). Using oxygen-isotope data, Taylor (1971) found evidence for extensive interaction of shallow magma chambers with ground-water systems. This evidence in an extinct volcanic arc so clearly related to the present-day active volcanic arc suggests the presence of similar systems beneath the High Cascades.

Further evidence for the existence of high-temperature geothermal systems beneath the High Cascades comes from deep drill holes at three different localities. In the Meager Creek Geothermal Area, located on the extension of the Cascade Range in British Columbia, Canada, drill hole M7 encountered a bottom-hole temperature of 202.2° C at a depth of 367 m (1,204 ft). The temperature gradient at the bottom of the hole was 330° C/km (Fairbank and others, 1981). At Newberry volcano, located in the central portion of the Oregon Cascades, a 930-m (3,050-ft) hole completed by the USGS in 1981 encountered a bottom-hole temperature of 265° C (Sammel, 1981). Finally, at Mount Lassen, in the Cascade Range of northern California, drill hole Walker "O" No. 1, encountered a temperature of 176° C at a depth of 610 m (2,001 ft). In this last hole, there was a reversal in the temperature-depth curve below 731 m (2,398 ft), and the bottom-hole temperature was 124° C at a depth of 1,222 m (4,008 ft) (Beall, 1981). These three holes clearly demonstrate the presence of temperatures adequate for the generation of electrical energy beneath the High Cascades at major volcanic centers. The demonstration of high temperature beneath the Cascade chain as a whole must await the completion of a deep (2- to 3-km [1.2- to 1.8-mi]) drill hole in the High Cascade province between the major volcanic vents.

The data in Table 7.1 represent an attempt to estimate the geothermal electrical-generation potential of the Cascade Range using the methods of Brook and others (1979). In performing the calculations, two assumptions are made concerning the recoverability of electrical energy from geothermal resources. First, a minimum temperature of 150° C is required for the generation of electricity from geothermal fluids; and second, the maximum depth from which geothermal fluids can be recovered is 3 km (1.8 mi). The first assumption is con-



Table 7.1. *Estimates of the electrical generation potential of the Oregon Cascade Range*

Estimate	Reservoir volume (km <sup>3</sup> )	Mean reservoir temperature (°C)	Reservoir thermal energy (x10 <sup>18</sup> joules)	Electrical energy (MWe for 30 yrs)
1	35,948	190	16,985	401,760
2	33,465	190	15,812	374,000
3	222	190	105	2,485

vative, as it ignores generation schemes (e.g., binary cycles) which can generate electricity from fluids at temperatures substantially less than 150° C. It is used to simplify the comparison of estimates between this report and USGS Circular 790 (Brook and others, 1979), which uses the same assumption. The second assumption is more valid, as 3 km (1.8 mi) represents the maximum depth of production wells drilled in various geothermal areas around the world (Brook and others, 1979).

In order to estimate the electrical-generation potential of the Cascade Range in Oregon, estimates must be obtained for mean reservoir temperature and reservoir volume. Temperature estimates can be derived from the temperature profile of Figure 7.3, the derivation of which was discussed previously. The depth to the 150°-C isotherm is 1.75 km (1.05 mi), and the temperature at 3 km (1.8 mi) is estimated to be 230° C, yielding a mean reservoir temperature of 190° C and a reservoir thickness of 1.25 km (0.75 mi).

Estimate 1 (Table 7.1) assumes that the entire area of the Cascade Range bounded by the California-Oregon border, longitude 121°30', the 100-mW/m<sup>2</sup> contour (Plate 7), and the Clackamas River lineament is underlain by a reservoir 1.25 km (0.75 mi) thick. Included within this estimate are some areas which are definitely not available for geothermal development (e.g., Crater Lake National Park, Warm Springs Indian Reservation, and the various wilderness areas). In estimate 2 (Table 7.1) these areas have been excluded from the calculations.

Inherent in the calculations of Table 7.1 is the assumption that, due to nonideal reservoir behavior, only 25 percent of the reservoir thermal energy is recoverable at the wellhead. Limited experience in the vicinity of Mount Hood indicates that

this estimate may be high. Drill hole Old Maid Flat 7A (T.D. 1,839 m [6,028 ft]) produced a total of less than 4 liters (1 gallon) per minute from the thermal zone in the bottom 915 m (3,001 ft) of the well (Priest and others, 1982). Though Old Maid Flat 7A bottomed in Western Cascade rocks, which are known from experience to be relatively impermeable, similar conditions may exist at depth beneath the High Cascades due to the alteration of volcanic rocks. To account for this possibility, estimate 3 (Table 7.1) was prepared. In this estimate, permeability was assumed to be present only as fracture permeability in a 100-m (330-ft)-wide zone associated with north-south lineations. The total length of north-south lineations in the Cascade Range was derived from maps by Venkatakrishnan and others (1980) and Kienle and others (1981). The 100-m (330-ft) width is an arbitrary value based on observations of north-trending faults in the Belknap Hot Springs and Cougar Reservoir (Priest, personal communication, 1982) areas of the central Cascades, and north-south lineations were used because they were judged to have the highest probability of remaining open in the state of essentially north-south compression that exists in the Cascades at the present time (Venkatakrishnan and others, 1980).

Estimate 3 was prepared as a sort of worst-case estimate for the theoretical potential of the Cascades. A stratigraphic reservoir (again 1.25 km [0.75 mi] in thickness) covering an area of only 178 km<sup>2</sup> (68.7 mi<sup>2</sup>) would produce the same amount of theoretical potential that the fault model does. By comparison, the total power capacity of The Geysers is rated at 1,610 MW over an area of 60 to 120 km<sup>2</sup> (23 to 46 mi<sup>2</sup>) (Brook and others, 1979).

The estimates of Table 7.1 are based solely upon the conductive heat-flow anomaly underlying the Cascade Range east of the transition zone. Estimates for known (e.g., Austin and Breitenbush Hot Springs) or undiscovered hydrothermal systems masked by cool ground water are not included, nor are estimates of residual heat remaining in igneous related systems (Smith and Shaw, 1979).

As can be seen in estimate 1 of Table 7.1, there is a tremendous amount of thermal energy contained in the rocks east of the transition zone. The high heat flow, coupled with high background temperature gradients and the evidence for recent volcanism, provides strong inducement for continued exploration in the Cascade Range of Oregon.

## CHAPTER 8. GEOTHERMAL EXPLORATION IN THE CENTRAL OREGON CASCADE RANGE

By George R. Priest,  
*Oregon Department of Geology and Mineral Industries*

### ABSTRACT

Exploration in the central Oregon Cascades should be focused within the High Cascade heat-flow anomaly. In the volcanic rocks of the Western Cascade episode, geothermal aquifers are most likely to occur where thick sections of brittle intrusive or holocrystalline flow rock have been recently fractured by tectonic deformation. In the younger rocks of the High Cascade episode, exploration should be focused on unusually thick sequences within large grabens or calderas; the Waldo Lake-Lookout Mountain area and High Cascade province 20 km (12 mi) north of Breitenbush Hot Springs are probable examples. Areas of youthful silicic volcanism, such as Mount Jefferson, Crater Lake, and South Sister, are particularly attractive targets, because they may be underlain by shallow plutonic heat sources. A high priority target is the silicic highland around the Three Sisters. Because most of this area is in the Three Sisters Wilderness, however, the only portion that may be exploited is in the Devils Lake-Sparks Lake area.

### INTRODUCTION

This paper presents some guidelines and targets for geothermal exploration in the central Oregon Cascade Range. A brief summary of known central Oregon Cascade hydrothermal systems and probable heat sources is followed by general discussions of the hydrology and types of aquifers which typically occur in hydrothermal systems of volcanic terranes. Available drilling data concerning probable reservoir characteristics of Cascade rock units are covered in the general discussion of geothermal aquifers. Exploration targets and techniques are recommended for the central Oregon Cascade Range. The recommendations are based on the general discussions of the entire range and on comparisons with other similar areas.

### KNOWN HYDROTHERMAL SYSTEMS IN THE CENTRAL OREGON CASCADE RANGE

Fifteen thermal springs with temperatures above 20° C are known in the Oregon Cascade physiographic province (Figure 8.1). Most of the springs are concentrated in deep valleys along the eastern margin of the Western Cascade Range. The thermal springs in the central Oregon Cascades are moderately saline NaCl waters (Mariner and others, 1980).

The hottest springs are all in the north-central portion of the Western Cascade Range, adjacent to the High Cascade Range. From north to south, the springs closest to the High Cascades are Austin (Carey) Hot Springs (86° C), Breitenbush Hot Springs (92° C), Bigelow Hot Springs (61° C),

Belknap Hot Springs (86.7° C), and Foley Hot Springs (80.6° C) (Mariner and others, 1980). In this paper, this line of springs is referred to as the Austin-Belknap belt. These springs have estimated reservoir temperatures of between 99° C and 125° C, based on various chemical geothermometers calculated from the concentrations of Na, K, Ca, Mg, and Si (Brook and others, 1979). The sulfate-oxygen isotope geothermometer gives estimated reservoir temperatures of 181° C for Austin Hot Springs, 176° to 195° C for Breitenbush Hot Springs, and 148° C for Belknap Hot Springs (Brook and others, 1979; Mariner and others, 1980).

The higher reservoir temperatures estimated by the sulfate-oxygen isotope geothermometer are important, because, if accurate, they indicate that the Austin and Breitenbush hydrothermal systems may be potential producers of electricity from high-temperature (more than 150° C) fluids. McKenzie and Truesdell (1977) presented evidence from various geothermal fields indicating that the sulfate-oxygen isotope method yields very reliable estimates of reservoir temperature. In a study of Yellowstone Park, they found that, as in the Cascade springs, the Na-K-Ca-Mg geothermometers gave lower estimated reservoir temperatures. They found that, for the Yellowstone caldera, the sulfate-water system was in close agreement with carbon-isotopic and enthalpy-chloride estimates. McKenzie and Truesdell (1977) concluded that, in the case of Yellowstone, the sulfate-water system may be a better indication of the temperatures of deepest reservoirs than estimates by the standard chemical geothermometers. They attributed the efficacy of the technique to the rate of exchange of oxygen isotopes between sulfate and water. The exchange rate is fast enough to ensure equilibration within deep geothermal reservoirs but slow enough to be little affected by re-equilibration during ascent of thermal water to hot springs at the surface.

In addition to the above boiling or near-boiling hot springs, a number of warm springs occur at somewhat greater distances west of the central High Cascades. The main warm springs are, from north to south: Bagby Hot Springs (52° C), Terwilliger Hot Springs (42° C), Wall Creek Warm Springs (41° C), McCredie Hot Springs (73° C), Kitson Hot Springs (43° C), and Umpqua Hot Springs (47° C) (Oregon Department of Geology and Mineral Industries, 1982). This line of springs is referred to in this paper as the Bagby-McCredie belt.

In addition to the above springs, three warm springs have been reported in the central High Cascade province: (1) Summit Lake Warm Spring (Oregon Department of Geology and Mineral Industries, 1982); (2) warm springs at the bottom of Crater Lake (Williams and von Herzen, 1982); and (3) a warm spring reported, but not verified, 2 km (1.2 mi) north of Devils Lake near the South Sister. Hikers in the central High Cascades area have reported that numerous High Cascade springs do not freeze in winter, but none of these springs have so far

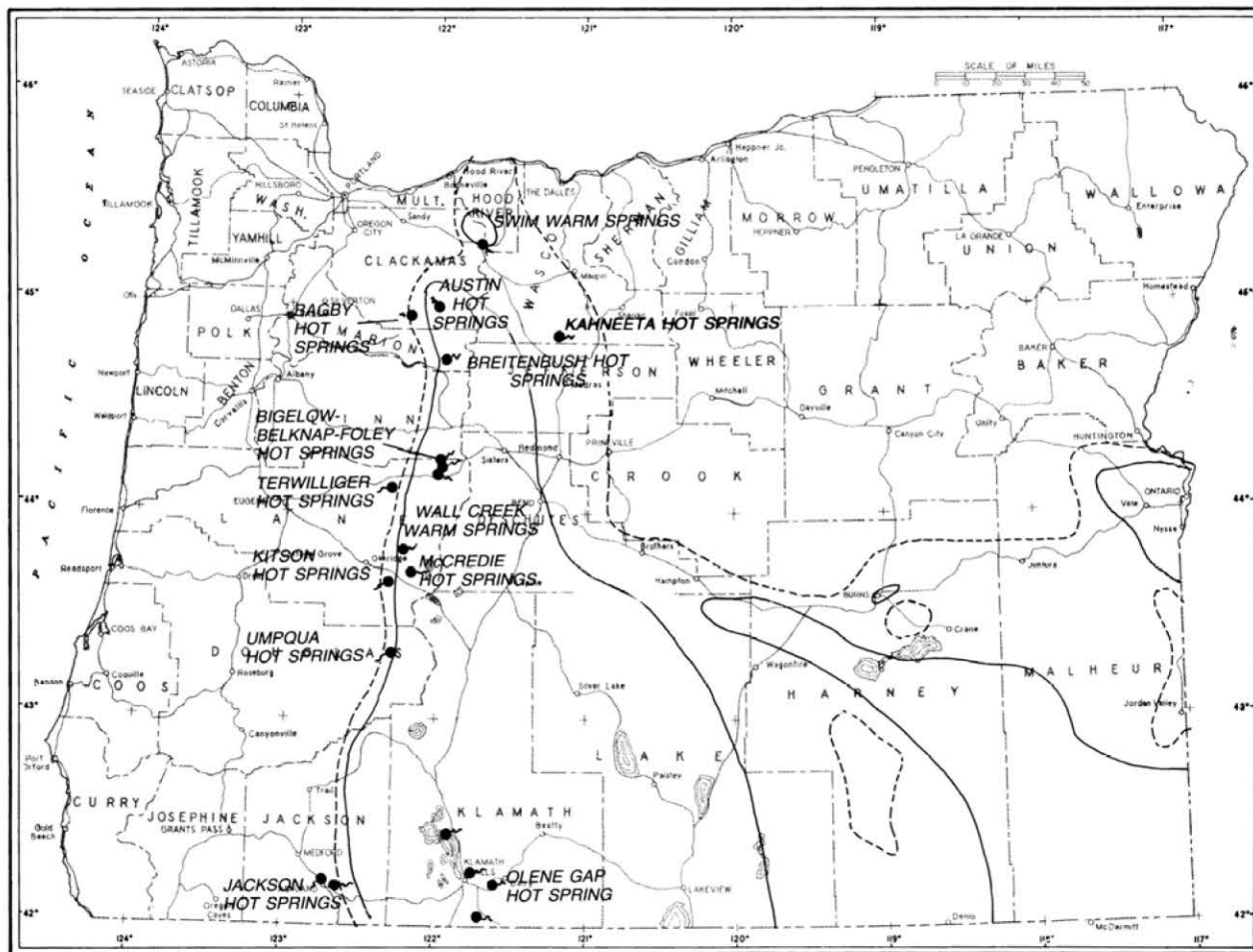


Figure 8.1. Thermal springs in and adjacent to the Oregon Cascade Range. Solid lines are the 100-mW/m<sup>2</sup> heat-flow contour; dashed lines are the 80-mW/m<sup>2</sup> contour of Blackwell and others (1978) and Black and others (this volume).

been sampled and verified by scientific observers. An infrared survey or a winter aerial survey of the High Cascade Range might reveal more of these warm springs.

Where chemical analyses are available, the warm springs in the central Western Cascade Range generally give lower calculated reservoir temperatures than the hot springs closer to the High Cascade Range. No chemical data are available for the three reported warm springs within the High Cascades, but Na-K-Ca-Mg data give estimated reservoir temperatures of between about 71° and 126° C for the warm springs in the Western Cascades.

For a detailed discussion of the relationship of the hot springs to the regional heat flow, the reader is referred to Chapter 7, Figure 7.4, and Blackwell and others (1978, 1982). Blackwell and others (1982) concluded that much of the Cascade heat-flow high shown in Figure 7.2 is caused by a zone of partial melting at a depth of about 10 km (6 mi) that extends across the High Cascade Range into the edge of the Western Cascade Range. They explained the hot-spring belt as the product of local convective circulation within this overall province of high conductive heat flow. The Bagby-McCredie warm-spring belt could, in this model, have lower temperature springs than the Austin-Belknap belt, because the former lies on the outer margin of the conductive heat-flow anomaly. The

conductive heat-flow model, which is now constrained chiefly by shallow (100-700 m [328-2,296 ft]) data, needs to be tested by deep (1-3 km [0.6-1.8 mi]) drilling in both the High Cascades and Western Cascades.

The absence of significant hot springs in the central Oregon High Cascade Range is discussed in the next section. Possible hydrologic analogues of High Cascade hydrothermal systems are also discussed.

## HYDROLOGY OF GEOTHERMAL SYSTEMS IN VOLCANIC TERRANES

## Introduction

Healy (1976), drawing on his experience in New Zealand and southeast Asia, gave a good summary of hydrologic factors which control the development of geothermal systems. The following discussion summarizes his observations.

### Problems with the “reservoir” concept

Because volumes of permeable rock saturated by hot water and/or steam have been outlined by drilling in various geothermal fields, these resources have often been termed "reservoirs" in analogy to oil and gas reservoirs. Unlike oil and gas reservoirs, however, geothermal resources are not confined to



a static "reservoir." Hydrothermal systems are flows of hot water or steam, chiefly of meteoric origin, and should be considered dynamic aquifers rather than static reservoirs. Several important concepts follow from this fundamental observation:

1. Hot-water systems can be modeled by standard hydrologic techniques.
2. The systems are recharged by meteoric water and are thus, to some extent, renewable.
3. Most systems are active flows of hot water or steam. This partially explains the behavior of the Wairakei, New Zealand, hydrothermal system during an increase in production. Healy (1976) observed that "while production was being increased in the Wairakei field, temperatures declined because of flashing of boiling water as water level and pressure fell. At the same time, recharge by water at temperatures possibly higher than before increased (Bolton, 1970). As conditions stabilize, further decrease in temperature and loss of stored heat should eventually cease, unless production is increased again or temperature or recharge water declines. Recharge is now practically the only source of heat." The recharge of hot water to the Wairakei reservoir "has been estimated to be about 4.5 times the original natural inflow, indicating an increase of at least 3 times resulting from lowered pressures induced in the field by production."

The above-mentioned behavior of the Wairakei field during production is an excellent example of the dynamic nature of geothermal systems. The Wairakei "reservoir" originally outlined by drilling was long ago exhausted, but production continues from unknown hydrologically connected aquifers. The system is also probably recharged by new meteoric water.

The complexities introduced by the dynamic nature of hydrothermal systems make it exceedingly difficult to apply standard oil and gas reservoir estimation techniques to geothermal resources. These limitations should be borne in mind when utilizing electrical power estimates like those of Black and others (Chapter 7).

### **Large-scale hot-water hydrothermal systems not associated with a single volcano**

The Yellowstone and Wairakei geothermal systems were cited by Healy (1976) as examples of this type of hydrothermal system. He inferred that these hydrothermal systems are heated by a widespread heat source or sources at depth with circulation governed by intermediate or regional ground-water flow. Large hot-water systems of this kind are commonly found in large-scale volcano-tectonic depressions like the Taupo volcanic zone and the extensive Yellowstone caldera system. The surface thermal manifestations may be far removed from any active volcano.

These systems are characterized by lateral flow of thermal water over great distances in permeable stratigraphic layers (see the later discussion on reservoir rocks in New Zealand). The effect of this circulation pattern is to utilize meteoric water from a large area to sweep up and concentrate conductive heat into a discreet zone or aquifer.

In areas of low rainfall, poor permeability, or deep ground-water table, the movement of ground water can be greatly restricted, and heat may be largely dissipated by conduction. These conditions of limited water supply can lead to the development of vapor-dominated geothermal systems if a strong heat source is present. This type of vapor-dominated system usually occurs at high altitude.

### **Geothermal fields associated with specific volcanoes**

These hydrothermal systems are intimately associated with individual subvolcanic plutons at andesitic, dacitic, and basaltic volcanoes. Examples of these systems are commonly found in the circum-Pacific belt of Quaternary volcanoes in Japan, the Philippines, Indonesia, Chile, and Central America. Vapor-dominated conditions in association with fumaroles and acid sulfate waters often prevail at high altitudes on these volcanoes. At lower levels, hot water flows outward around the base of the volcanoes.

Hakone volcano, Japan, is a good example of this type of hydrothermal system in a long-lived active andesitic volcanic center. Hakone volcano consists of a large composite cone sitting within a 11-km (6.6-mi)-wide depression formed by two overlapping Pleistocene calderas (Kuno, 1950; Kuno and others, 1970; Oki and Hirano, 1974). Wells drilled adjacent to fumaroles on the central cone have encountered a superficial zone of sulfate water. This zone is separated from a major NaCl-rich aquifer at several hundred meters depth by a shallow steam zone (Oki and Hirano, 1970).

In their hydrologic model of Hakone volcano, Oki and Hirano (1974) postulated that dense volcanic steam (450°-480° C) bearing several percent of NaCl ascends from the roots of the volcano and mixes with bicarbonate-sulfate meteoric water at depths ranging from 4 km (2.4 mi) up to the surface. The mixed water constitutes a hot water-dominated hydrothermal system which undergoes secondary boiling and repeated condensation in the volcanic edifice. This repeated vaporization and condensation concentrates volatile components such as hydrogen sulfide and carbon dioxide in the gas phase which appear as solfataric emissions.

One very important aspect of the Japanese geothermal systems which may be highly relevant to the High Cascade Range hydrology is what Oki and Hirano (1974) called the "hot eye and cold eyelid" concept. They noted that young composite cones like Mount Fuji and Asama, which are composed of thick piles of volcanic material, do not have surface hydrothermal activity because the thick edifices act as a "cold eyelid" of rapidly infiltrating meteoric water covering the "hot eye" of the deeper hydrothermal system. Hakone has abundant surface hydrothermal activity because it has a very strong flow of deep hydrothermal fluids which allows the hot waters to ascend high enough in the cone to create local vapor-dominated areas. In areas of less vigorous deep hydrothermal activity, the "hot eye" can be closed by invasion of the waters of the "cold eyelid." Hakone was thought to be particularly favorable for deep hydrothermal circulation, because it, unlike the adjacent youthful composite cones, sits in a deeply dissected caldera.

The "cold eyelid" effect obscures the high-temperature hydrothermal system at Newberry caldera (Sammel, 1981). Newberry does, however, have some surface fumaroles and fumarole-related hot springs. At Newberry, the high horizontal permeability and low vertical permeability of many of the shallow intracaldera strata allow horizontal aquifers to wash away the heat without setting up a large-scale vertical convection system (Sammel, 1981; MacLeod and Sammel, 1982).

### **Applications to the central High Cascade Range**

The presence of numerous central-vent-type composite cones in the High Cascade Range suggests that the isolated-volcano model may apply to many areas. Absence of large, surface thermal manifestations in central High Cascade volcanoes implies that the "cold eyelid" effect of the permeable

carapaces has either covered or overwhelmed the deep high-temperature geothermal systems. A possible exception may be Crater Lake, which has thermal springs in the caldera (Williams and von Herzen, 1982).

The series of hot and warm springs along the western margin of the High Cascade Range is far removed from the obvious heat sources in the volcanic arc, suggesting that the large-scale circulation model may also apply. If this is the case, then by analogy with the New Zealand fields, one would predict that large stratigraphic aquifers which can conduct thermal water away from the subvolcanic heat sources must be present at depth. Possible stratigraphic aquifers of this kind are examined in the next section.

## POTENTIAL RESERVOIR ROCKS FOR HYDROTHERMAL CIRCULATION

### Introduction

Little is known about the geothermal reservoir characteristics of the volcanic rocks of the Cascades, especially under hydrothermal conditions in the 200° to 300° C range. Some of the more important data from the Cascade Range and adjacent areas are summarized below along with relevant examples from geothermal areas in other parts of the world.

### Drilling at Old Maid Flat near Mount Hood

Two deep test wells at Old Maid Flat near Mount Hood — one 1,200 m (3,936 ft) deep (OMF-1) and the other 1,837 m (6,025 ft) (OMF-7A) — encountered no significant thermal fluids, even though both penetrated fractured flows of the Columbia River Basalt Group (Priest and others, 1982a). Diamond core from OMF-7A showed that the basalts have closely spaced open fractures and that microquartz diorites in the well may also have some partially open fractures (Priest and others, 1982a). The Old Maid Flat rocks with the least permeability are Miocene and older andesite to dacite debris flows, flow breccias, and volcanoclastic rocks (Priest and others, 1982a). Priest and others (1982a) concluded that the presence of metastable volcanic phases such as glass in the andesites and dacites rendered them chemically reactive and subject to self sealing. Where adequate fluids are present, glassy volcanic rocks have been shown to be particularly subject to self sealing (e.g., Keith and others, 1978).

Volcanic rocks over most of the length of the Old Maid Flat 7A well have been subjected to laumontite-grade (zeolite-facies) metamorphism at temperatures of 120° to 205° C (Holdaway and Bussey, 1982). Holdaway and Bussey (1982) estimated that greenstones (greenschist-facies) encountered in the last 130 m (426 ft) of the well were once at 300 ± 50° C. The bottom-hole temperature was about 119° C (Priest and others, 1982a).

Priest and others (1982a) concluded that potentially permeable tholeiitic basalts and intrusive rocks in the OMF-7A and OMF-1 wells have been prevented from receiving meteoric water by interbedded impermeable volcanic rocks. They further concluded that a nearby northwest-trending normal fault with hundreds of feet of displacement was not able to conduct ground water to the permeable stratigraphic layers in the thermal zone. They inferred that the fault was late Pliocene in age, although Robison and others (1982) showed, in a later map, an extension of the fault cutting Holocene and Pleistocene lavas of Mount Hood. This fault, in spite of its large displacement and youthful age, apparently did not create enough permeability to generate a large-scale low-temperature geothermal system. This may not mean that a similar fault in areas with higher temperature metamorphic assemblages could not create permeability, but it does show that fractured rocks around a fault zone in chemically reactive

andesitic to dacitic debris flows may not always be able to conduct large quantities of meteoric water in areas of laumontite-grade metamorphism.

### Drilling at the Pucci Chairlift site, Mount Hood

The 1,220-m (4,002-ft)-deep Pucci hole was drilled by the U.S. Geological Survey (USGS) on the south flank of Mount Hood. The hole had a maximum temperature of about 80° C, and after penetrating the young Mount Hood sequence, encountered laumontite-grade metamorphosed, upper Miocene andesitic rocks below 731 m (2,398 ft) (Robison and others, 1981; Gannett and Bargar, 1981). Geophysical logs of Robison and others (1981) suggest that the rocks from 942 to 1,039 m (3,090 to 3,408 ft) in the well were highly fractured (Gannett and Bargar, 1981). A flow test yielded 416 liters (110 gallons) per minute of warm water from the lower part of the well (Keith and Causey, 1982).

The rocks in the lower part of the Pucci well are similar to the altered andesites and dacites found to be impermeable at Old Maid Flat. The fractured nature of the Pucci rocks relative to the Old Maid Flat andesites and dacites probably accounts for the higher permeability.

Drilling through the youthful Mount Hood rocks posed a serious drilling problem, because of the tendency of those rocks to cave into the drill hole (Robison, personal communication, 1981). Similar very difficult drilling conditions appear to prevail in other youthful volcanic rocks throughout the High Cascade Range (e.g., see Youngquist, 1980).

### Shallow drill holes around Mount Hood

Temperature gradients in shallow (less than 500-m [1,640-ft]-deep) drill holes in the Mount Hood area were disturbed by active ground-water circulation in fractured Miocene intrusives and post-Miocene volcanic rocks (e.g., Steele and others, 1982). The gradients were infrequently disturbed by ground-water circulation in Miocene and older volcanic rocks, owing to the impermeable nature of the older, altered rocks (Steele and others, 1982). The apparent permeability of the fractured intrusive rocks, in spite of their age, may indicate that those rocks could be good reservoir rocks at depth. Results of deep test drilling in fractured intrusive rocks are summarized in the next section.

### Drilling at Meager Creek, British Columbia

The Meager Creek geothermal system occurs chiefly within fractured and faulted Cretaceous quartz diorite (Fairbank and others, 1981). Faults and parallel fractures act as the major controls of hydrothermal fluids in the 200° to 250° C range (Fairbank and others, 1981; informal communication from project geologist, 1983). The Meager Creek fault, which is described as a "relatively young extensional feature" with "about 500 m (1,640 ft) of normal dip-slip movement possibly related to subsidence" is, with associated parallel fractures, a major control on the reservoir configuration (Fairbank and others, 1981).

The observations at Meager Creek are in harmony with the previously discussed finding at Mount Hood that fractured intrusive rocks can allow active fluid circulation. The Meager Creek data allow that generalization to be extended to fluids at high temperature.

Drilling in the fractured plutonic rocks at Meager Creek has not been completely successful at delineating adequate fluids, and some difficult drilling conditions have been encountered (informal communication from project geologist, 1983). Difficult drilling conditions and somewhat erratic and unpredictable fluid production have also been reported in similar intrusive rocks near the Cuernos volcano in the Philippines (McNitt and others, 1983).

The next section demonstrates that basal conglomerates and weathered horizons developed at surfaces of unconformity on old crystalline basement rocks may also serve as aquifers.

### **Zunil geothermal field, western Guatemala—comparison to Ashland, Oregon**

In the Zunil area, hydrothermal fluids at temperatures in excess of 280° C flow upward within an inclined conglomeratic layer and in underlying weathered and fractured granodiorite (Bethancourt and Dominco, 1982). Overlying volcanic rocks, which consist of 300 to 400 m (984 to 1,312 ft) of Tertiary andesite flows overlain by 500 to 600 m (1,640 to 1,968 ft) of Quaternary rhyodacitic to dacitic lavas and pyroclastic rocks, act as an impermeable cap on this aquifer (Bethancourt and Dominco, 1982). The area is apparently only weakly affected by tectonic deformation which has created fracture permeability in the volcanic rocks of the Cerro Quemado-Volcan Santa Maria volcanic axis where the hot fluids originated (Bethancourt and Dominco, 1982).

This system resembles the circulation system at Ashland, Oregon, where low-temperature (22°–44° C) fluids migrate up the unconformity separating the Ashland pluton from overlying impermeable sedimentary rocks (Black and others, 1983). If the source of the Ashland fluids is analogous to the Zunil source, the fluids may be infiltrating down into this aquifer in warmer, more fractured areas of the Cascade Range to the east.

### **Shallow drilling in the central Cascade Range, Oregon**

The writer and other workers in the central Oregon Cascade Range have, in the course of drilling and logging temperature-gradient holes, noted that a general correlation exists between the age of volcanic rocks and their permeability. In general, drill holes in lavas and breccias younger than about 10 m.y. tend to encounter numerous rapidly circulating aquifers and have nonconductive temperature-depth profiles (e.g., Blackwell and others, 1978; Youngquist, 1980). Older rocks tend to have fewer aquifers and commonly display conductive temperature gradients.

The correlation of permeability with age is more a function of alteration than any other factor. The older rocks, especially those with abundant metastable phases such as glass, are generally, though not always, more altered than the younger volcanic rocks. The alteration process causes the deposition of clays, quartz, calcite, and other minerals into pores and fractures, reducing permeability. Alteration is chiefly a function of depth of burial and proximity to hydrothermal systems. The probability that rocks will have been deeply buried and exposed to hydrothermal systems is naturally higher in older rocks, although youthful volcanic rocks adjacent to shallow plutonic bodies also suffer severe alteration.

Altered Oligocene tuffaceous rocks are particularly impermeable and generally yield conductive temperature gradients. Fractured holocrystalline lavas within altered tuffaceous rocks can, however, retain significant permeability, as demonstrated by the large aquifer encountered in the Terwilliger Hot Springs drill hole (see Chapter 4). This probably means that other fractured holocrystalline lavas throughout the Cascades could also retain significant permeability under low-grade metamorphic conditions.

### **Evidence of permeability from geophysical data in the Cascade Range**

Couch and others (1982) inferred from seismic refraction

and gravity data that High Cascade rocks, including units of the early High Cascade episode, are of substantially lower density (2.27 g/cm<sup>3</sup>) than the underlying older volcanic rocks (2.60 g/cm<sup>3</sup>). As explained in Chapter 2, the older Western Cascade rocks tend to be more silicic than rocks of the early and late High Cascade episodes. Silicic rocks should be less dense than mafic rocks, so it follows that the lower density of the High Cascade sequence is a function of some factor other than chemical composition. The most plausible factor is porosity. The younger rocks are probably less compacted and less sealed by alteration minerals than rocks of the Western Cascade episode of volcanism. The higher porosity of the High Cascade sequence may mean that it also has higher overall permeability than the older rocks. In a calculated section across the northern Oregon Cascade Range 20 km (12 mi) north of Breitenbush Hot Springs, Couch and others found that low-density (2.27 g/cm<sup>3</sup>) rocks extend down to as much as 3-km (1.8-mi) depth in the western margin of the High Cascade province. A similar calculated section through the southern Cascade Range showed a similar, albeit thinner, block of low-density material in the Klamath graben east of the Cascade Range (Couch and others, 1982a). In both areas, the most reasonable geological interpretation is that the low-density blocks are bounded on the east and west sides by major faults. Couch and others (1982a) inferred that similar faults bound the High Cascade Range throughout the central Oregon Cascades.

Calderas are also possible repositories for great thicknesses of low-density, possibly permeable pyroclastic and epiclastic material. The following sections examine the possibility of calderas in the Cascades and look at the data from Newberry caldera.

### **Evidence of unmapped calderas in the central High Cascade province**

Extensive ash flows from High Cascade source areas occur in the Deschutes Formation and in overlying sequences of the late High Cascade episode of the Deschutes Basin (Taylor, 1980). In other areas of ash-flow volcanism, (e.g., Newberry and Crater Lake calderas), cauldron subsidence commonly accompanies ash-flow eruption. Similarly, Deschutes Formation calderas and younger calderas may be largely obscured by Quaternary lava flows of the late High Cascade episode. It is thus possible that unmapped calderas similar to the calderas at Crater Lake and Newberry underlie the central High Cascade province.

A large circular gravity low south of the Three Sisters in the Lookout Mountain area may be a large zone of cauldron subsidence (Couch and others, 1982a). This area and other areas beneath the central High Cascade Range may be underlain by extensive, possibly permeable, pyroclastic and epiclastic caldera-fill deposits. Caldera margins in these areas may contain fractured rocks adjacent to ring faults as well as permeable caldera-wall facies of caldera-fill deposits (see Nigorioka geothermal field below). The central caldera-fill deposits may also contain permeable strata and fault zones (see Baca geothermal field below).

### **Exploration at Newberry caldera**

Hydrothermally altered volcanic rocks were recovered in the diamond core from the 932-m (3,057-ft)-deep Newberry 2 drill hole at Newberry caldera (MacLeod and Sammel, 1982). The bottom-hole temperature was about 265° C (Sammel, 1981). In the lower part of the well, volcanic breccias interstratified with more compact lavas were altered to "clay minerals, quartz, carbonates, epidote, chlorite, and sulfides" (MacLeod and Sammel, 1982). Below about 758 m (2,486 ft),



the Newberry 2 well was in the 150° to 265° C range and encountered chiefly basalt and basaltic andesite (MacLeod and Sammel, 1982). There were few permeable zones below 758 m (2,486 ft), although gas was encountered in hydrothermally altered strata (MacLeod and Sammel, 1982), and a 2-m (6.6-ft) zone in the bottom of the well produced steam from formation fluids (Sammel, 1981; Sammel, personal communication, 1983). MacLeod and Sammel (1982) concluded that, whereas there is lateral permeability in numerous zones within Newberry caldera, vertical permeability is low and is probably restricted to faults, ring fractures, or brecciated intrusion conduits. Similar low vertical permeabilities were found at the Long Valley caldera (Sorey and others, 1978). MacLeod and Sammel (1982) postulated that lateral flow of fluids may be restricted to permeable strata with good hydraulic connections to fluid-bearing vertical fracture zones. They concluded that older pre-Newberry rocks, here intruded at depth, may be more likely to harbor large-scale hydrothermal convection systems than the younger rocks of the caldera block.

A soil-mercury survey completed by the Oregon Department of Geology and Mineral Industries identified areas of anomalous soil mercury paralleling ring fractures and a north-east-trending fissure/fault system on the southeast flank of the volcano (Priest and others, in press). These anomalies could mean that a major hydrothermal system lies partly outside the caldera in this fissure/fault zone (Priest and others, in press). A fissure/fault-controlled reservoir is described in the next section.

### East Rift of Kilauea volcano, Hawaii

A 1,960-m (6,429-ft)-deep drill hole on the East Rift of Kilauea volcano encountered 300° C fluids in heavily fractured, altered submarine basalt flows (Furumoto, 1978). The fluids were chiefly in a permeable zone at 1,200 m (3,936 ft) in a sequence of pillow lavas (Furumoto, 1978) with montmorillonite, pyrite, quartz, chlorite, calcite, anhydrite, and heulandite alteration (Fan, 1978). A permeable zone also occurred at 1,900 m (6,232 ft) in similar rocks with actinolite, chlorite, quartz, hematite, pyrite, calcite, and anhydrite alteration (Fan, 1978; Furumoto, 1978).

The pillow lavas were impermeable, except where cut by fractures related to expansion and growth of a basaltic dike complex which underlies the reservoir (Furumoto, 1978). Fractures were sealed with alteration minerals between 675 and 1,000 m (2,214 and 3,289 ft) (between about 170° and 240° C) (Furumoto, 1978). Open and partially open fractures which were encountered below about 1,000 m (3,280 ft) are thought to have been created by tensional stresses in the fissure zone and by brittle fracturing of hot rocks when contacted by ground water (Furumoto, 1978). The low salinity of the hydrothermal water indicates that it is meteoric water which infiltrated into the area (Furumoto, 1978).

In view of (1) the importance of vertical fracture zones for providing conduits for circulation and interconnection of aquifers at Newberry and (2) the essential role of fracturing in otherwise impermeable units at Kilauea, the discussion in the next section examines the evidence for fault-controlled circulation in the Cascades.

### Correlation of thermal springs and faulting in the Oregon Cascade Range

There is a good correlation between many thermal springs and fault zones in the Oregon Cascades. Bagby Hot Springs is located on a N. 80° W.-trending fault (Dyhrman, 1975). The Breitenbush Hot Springs "issue from fractures, or faults, and contacts of basalt dikes cutting Breitenbush Tuff" (Ham-

mond and others, 1980). Bigelow and Belknap Hot Springs are closely associated with a major north-south fault which experienced offset between 5 and 4 m.y. B.P. (see Brown and others, 1980a; Flaherty, 1981). Small northwest-trending shears and fractures are associated with both Terwilliger Hot Springs (Chapter 4) and with Foley Hot Springs (unpublished mapping of Priest, 1980). Both Terwilliger and Foley Hot Springs are very close to major north-south faults (Chapter 4; Flaherty, 1981). McCredie Hot Springs is located adjacent to the Groundhog Creek fault, a major north-south fault (Woller and Black, Chapter 6).

The association of many of the Cascade hot springs with faults should come as no surprise. It is well known that hydrothermal systems are very commonly controlled by faults in volcanic terrane throughout the Basin and Range province of Oregon. The Klamath Falls hot springs area is a typical example (see Sammel, 1980). Fracture zones adjacent to major faults in the Oregon Cascades appear to provide fracture permeability in a variety of different volcanic rock types including, from the evidence at Breitenbush (Hammond and others, 1980), altered tuffaceous rocks.

While fault zones appear to serve as important conduits for vertical transfer of fluids, it is difficult to imagine a large reservoir of hydrothermal fluid in a fault. Intuition suggests that large laterally continuous aquifers seem to offer more reservoir capacity than narrow fault/fracture zones. The next several sections examine some stratigraphic aquifers in other parts of the world. One important observation to keep in mind is the large number of the following examples which are located in calderas and large volcano-tectonic grabens.

### Drilling at Long Valley caldera, California

A caldera 29 km long and 15 km wide (17.4 mi long and 9 mi wide) in the Long Valley area was formed in response to eruption of about 600 km<sup>3</sup> (144 mi<sup>3</sup>) of rhyolitic ash-flow tuff (the Bishop Tuff) about 0.7 m.y. ago (Bailey and others, 1976). Volcanic activity has continued into Holocene time (Bailey and others, 1976).

Drilling and hydrologic analysis of the geothermal system at Long Valley were completed by Sorey and others (1978). They found that, in the caldera fill, permeable zones were confined to volcanic flows and thin sandy zones, with one well intercepting high permeability in a faulted, altered rhyolite. Hydrothermally altered layers tended to have a very low permeability and were inferred to be barriers to upward-convecting deep geothermal waters. In their conceptual model of the geothermal system, Sorey and others (1978) inferred that, below the caldera fill, the deep hydrothermal system is confined to "fractured, welded Bishop Tuff and underlying basement rocks." They assumed that the rocks were altered, but that permeable flow channels were maintained by "tectonic activity or successive invasion of unaltered rock by hydrothermal fluids." This model hypothesizes that stratigraphic permeability lost through silicification and other alteration processes could be continually restored by tectonic reupturing of brittle, altered rocks.

### Drilling in the Baca geothermal area, Valles caldera, New Mexico

Like the Long Valley caldera, the large Valles caldera was formed by voluminous eruption of rhyolitic ash-flow tuff during the Pleistocene (Smith and Bailey, 1968). Fumarolic and hot-spring activity attest to continuing high heat flow and active hydrothermal circulation in the area.

Union Oil Company of California discovered temperatures of up to 341° C (Kerr, 1982; Molloy, 1982) and fluids with base temperatures in excess of 260° C in the west-central

part of the caldera (Dondanville, 1978). Production was obtained from "fractures in the pumicey basal 305 m (1,000 ft) of Bandelier Tuff" (Dondanville, 1978). Hulen and Nielson's (1982) analysis of the well data disclosed that "permeable nonwelded tuffs and tuffaceous sandstones of the Bandelier Tuff appear to be prominent fluid flow channels." Molloy (1982) noted that the permeable units were "tuffaceous sandstones and sand-sized tuff beds." Many fluid entries were correlated with faults and fracture zones (Hulen and Nielson, 1982), but fault interception was not sufficient in itself to ensure production (Molloy, 1982). The stratigraphic aquifers of tuff and tuffaceous sandstone were apparently not part of the Union Oil drilling model, even though they accounted for 12 of 23 steam or hot-water entries encountered (Molloy, 1982). According to Molloy (1982), more emphasis on these tuffaceous aquifers and on intersecting faults, fissures, and units with extensive cooling joints would have greatly increased the success rate of the drilling program.

As yet, the nature of the permeability in the tuffaceous sandstone has not been determined. Hulen and Nielson (1982) postulated that original intergranular permeability may be locally eliminated by interstitial deposition of alteration minerals. In that case, permeability might be caused by the fracturing processes hypothesized by Sorey and others (1978) for the Long Valley geothermal system (Hulen and Nielson, 1982). "Alternatively, original intergranular permeability may be increased by hydrothermal dissolution of unstable framework grains and cement, as documented for deep sandstone aquifers of the Cerro Prieto geothermal field (Lyons and van de Kamp, 1980)" (Hulen and Nielson, 1982).

Thus far, difficult drilling conditions and poorly understood reservoir conditions have combined to prevent confirmation of steam sufficient to power a proposed 50-MW power plant at Baca (Kerr, 1982). The fluids in the Baca reservoir were under less hydrostatic pressure than commonly used drilling muds (Kerr, 1982). This underpressured condition and the high temperatures prevented use of standard drilling muds in thermal zones, because muds could penetrate the productive horizons and bake to an impermeable plug. Using special low-density drilling fluids caused the following severe drilling problems: "Drill pipe corroded, stuck, or twisted off in the hole; drill-hole sides collapsed; and drilling fluids disappeared into unmapped permeable rock formations" (Kerr, 1982). A Lawrence Berkeley review team concluded that, because of low hydrostatic pressure and low permeability, the transmissivity at Baca is "ten times smaller than at successfully developed fields such as the Geysers in California" (Kerr, 1982). If this conclusion is valid, it may have serious implications for development of other caldera-related geothermal reservoirs such as Newberry caldera. Indeed, numerous drilling problems were encountered in the preliminary exploration at Newberry caldera (Sammel, 1981; MacLeod and Sammel, 1982).

### **Nigorikawa geothermal field, Hokkaido, north-eastern Japan**

The Nigorikawa geothermal field is in a 3-km (1.8-mi)-wide Quaternary caldera filled with volcanoclastic rocks and an underlying "tuff breccia which is fall-back in origin" (Ide, 1982). A caldera-wall facies of the caldera-fill deposits consists of "a few tens of meters of breccia and tuff breccia containing many accidental large blocks derived from the country rocks" (Ide, 1982). The country rocks are a pre-Tertiary sequence of slate, chert, limestone, and andesitic tuff and overlying Miocene andesitic lavas and volcanoclastic rocks (Ide, 1982).

Fluids of more than 240° C temperature (270° C maximum) have been found at 2,000-m (6,560-ft) depth in the

caldera-wall facies of the caldera-fill deposits and within limestone interbeds and pre-Tertiary faults in the walls of the caldera, and drilling has confirmed sufficient resources for a 50-MW power plant (Ide, 1982). Landslide breccias and talus deposits which probably occur along the walls of partially infilled calderas such as the Newberry and Crater Lake calderas could be analogues of the caldera-wall facies at Nigorikawa.

### **Geothermal areas at north-central Kyushu, southwestern Japan**

The Otaki-Yunotani geothermal areas lie in a major Pleistocene tectonic depression 30 to 40 km (18 to 24 mi) wide and 150 km (90 mi) long on the island of Kyushu, Japan (Yamasaki and Hayashi, 1976). The depression is filled with a thick sequence of Quaternary andesitic to rhyolitic volcanic and epiclastic rocks (Yamasaki and Hayashi, 1976).

Geothermal areas at Kyushu are associated with numerous Holocene volcanic centers, especially calderas and dome complexes, distributed throughout the area. Hydrothermal fluids at about 200° C are produced from 500- to 1,500-m (1,640- to 4,920-ft)-deep wells drilled into Pleistocene volcanic rocks. The main producing horizon is the Hohi Series, a lower Pleistocene stack of pyroxene andesite lavas and associated pyroclastic rocks (Yamasaki and Hayashi, 1976). "Tuff breccias" within the Hohi sequence appear to be the main reservoir in the Otake geothermal area (Yamasaki and Hayashi, 1976). In the Yunotani geothermal field, fluids apparently rise out of the Hohi Series along a fault and spread out into overlying sedimentary and volcanic rocks (Parmentier and Hayashi, 1981). Production of dry steam at Yunotani occurs from fractured volcanic rocks in this fault (Parmentier and Hayashi, 1981). In observations regarding the geothermal fields of Japan and other volcanic areas associated with tectonic depressions, Yamasaki and Hayashi (1976) pointed out the following: (1) "Permeable formations such as tuffs, tuff breccias, and so on constitute aquifers for the areas, and impermeable lavas, welded tuffs, and so on, act as capping [units]"; (2) promising geothermal targets are faults bordering these tectonic depressions and fault intersections with the border faults; and (3) areas of silicic volcanic intrusion and calderas are sites of unusual permeability caused by fissuring and faulting.

### **New Zealand geothermal areas**

The New Zealand geothermal fields at Broadlands and Wairakei produce fluids of about 265° C from faults and stratigraphic horizons in a terrane of predominantly silicic volcanic and epiclastic rocks which are fill in a large volcanotectonic depression. New Zealand is one of the world's largest producers of electricity from hot-water-dominated geothermal systems.

In an excellent review of controls of reservoir permeability, Grindley and Brown (1976), citing examples chiefly from New Zealand, described the following types of hydrothermal aquifers in volcanic terranes:

1. The best aquifers are in volcanoclastic rocks composed of porous rhyolitic pumice capped by impermeable siltstones. This type of aquifer at Wairakei and Broadlands has porosities between 20 and 40 percent and wet densities between 1.8 and 2.2 g/cm<sup>3</sup>. Deposits of this kind, where they are over about 200 m (656 ft) thick, over 200° C, and shielded from downward influxes of cool meteoric water, are excellent reservoirs for water-dominated geothermal fluids.
2. They considered that the volcanoclastic aquifers were superior to aquifers controlled by primary volcanic faults, fractures, and vesicles (e.g., cooling joints, frac-

tures and faults produced during intrusion and cauldron subsidence, and scoriaceous zones of lavas). Primary jointing in andesites, ignimbrites, and basalts were thought to provide particularly unreliable permeability unless enhanced by "secondary fracturing." All of the above "primary fractures" were considered relatively shortlived, owing to self-sealing effects of hydrothermal alteration.

3. Two major types of "secondary fracturing" were recognized as particularly important for permeability in New Zealand fields, where deeply buried (over 1.5 km [0.9 mi]) volcanoclastic and volcanic units have lost primary fracture or intergranular permeability:
  - a. Open fault zones— About half of the production from both the Wairakei and Broadlands fields comes from active normal to oblique-slip fault zones dipping 75° to 85° which have open spaces along the slip face. Faulted andesites were found to be particularly productive, especially at fault intersections.
  - b. Hydraulic fracturing— Fissures can be developed by hydraulic fracturing adjacent to faults and aquicludes. "Where fluids are prevented from reaching the surface, either by self sealing at the top of a dormant fault or below an aquiclude, pore pressures will increase." This pressure often exceeds the strength of the rocks, producing a hydraulic fracture. These fractures are commonly found as anomalously wide, silicified breccia zones along normal faults and are thought to be common on the outer margins of silicic plutons undergoing retrograde boiling.

## Summary

Types of reservoir rocks which are known to contain significant fluids and/or permeability in volcanic terranes include the following:

1. Fractured intrusive rocks and brecciated intrusion conduits.
2. Fractured, brittle volcanic rocks which have not been extensively altered (e.g., many Cascade sequences which are younger than about 10 m.y.)
3. Fractured holocrystalline lavas, even where altered by zeolite-facies metamorphism.
4. A variety of volcanic rocks, including highly altered rocks, which are adjacent to major faults and associated tectonic joint systems.
5. Caldera-wall facies of caldera-fill deposits.
6. Nonwelded tuffs and tuffaceous sandstones.
7. Conglomerates and weathered zones developed at surfaces of unconformity on old crystalline basement rocks below a volcanic or sedimentary pile.

The best reservoir rocks are strata with high intergranular permeability and porosity. Nonwelded tuffs and coarse epiclastic rocks, where not sealed by deposition of alteration minerals, are the best targets.

Rocks with only various types of fracture permeability are less desirable drilling targets, because the presence of this type of permeability is much more difficult to predict, and fractures may not always interconnect.

When drilling to great depth (greater than 1.5 km [0.9 mi]), intergranular permeability commonly decreases sharply because of compaction and metamorphic reactions. Under these conditions, it is particularly important to aim drilling at areas of high fracture permeability such as faults, even if strata with possible intergranular permeability are present.

Where units with high intergranular permeability are rare

or absent in layered volcanic terrane, it is critical that exploration be focused on areas cut by extensive vertical fractures and faults. Vertical fracture permeability is necessary in such areas to establish large-scale hydrothermal convection, because layered volcanic terranes can have very poor vertical permeability even when individual horizontal units are permeable. In addition to tectonic faults, faults caused by intrusive bodies and associated brecciated intrusion conduits can provide excellent vertical pathways, as can the caldera-wall facies of caldera-fill deposits.

The same tectonic and intrusive forces which create vertical fracture permeability can promote secondary fracture permeability in layered, otherwise impermeable volcanic rocks, if the rocks are brittle. Brittle holocrystalline lavas and units altered to brittle metamorphic assemblages are particularly prone to secondary fracturing during folding and faulting.

## Applications to the central Cascade Range

**Units of the early Western Cascade episode:** These rocks, which are dominated by glass-rich pyroclastic and epiclastic units, are probably largely sealed by alteration minerals except where fractured holocrystalline lavas are present or where large, youthful faults or youthful intrusions have created fracture permeability. Where they are located in faulted areas of high heat flow, early Western Cascade volcanic centers may be the best drilling targets. A larger ratio of holocrystalline intrusive rocks and lavas relative to altered tuff may be present at volcanic centers. A high proportion of these brittle rocks will enhance the effects of tectonic fracturing.

**Units of the late Western Cascade episode:** These rocks are predominately lavas of mafic to intermediate composition, although dacitic tuffs, particularly nonwelded tuffs, and hyaloclastic units are interbedded in many sections (see Chapters 3 and 4). The nonwelded tuffs and interflow zones of the lavas may provide stratigraphic aquifers, where not sealed by alteration minerals. Areas of heavy tectonic fracturing may locally produce subhorizontal aquifers in the brittle lavas. Mafic glasses are probably sealed by alteration minerals. Deeply buried Miocene dacitic debris flows and autobreccias are commonly also tightly sealed with secondary alteration minerals.

In order to take advantage of the voluminous, easily fractured brittle lavas in sequences of late Western Cascade age, it would be wise to drill close to zones of tectonic fracturing. Volcanic and intrusive centers in areas of high heat flow are good targets for the same reasons outlined above for rocks of the early Western Cascade episode.

**Units of the High Cascade episode:** High Cascade rocks are generally less than 9 m.y. old and are composed chiefly of mafic lavas, although some intermediate to silicic rocks also occur throughout the sequence (see Chapter 2). Previously mentioned drilling and geophysical data on these rocks indicate that they may be substantially less altered and more permeable than Western Cascade rocks. Geophysical data from the northern Oregon High Cascades indicated that, where downdropped by faults, sections up to 3 km (1.8 mi) thick of these permeable High Cascade rocks may be locally present. Sections this thick could extend into very hot parts of the crust, and faults associated with the downdropped blocks could create additional fracture permeability.

Tuffaceous sandstone and nonwelded tuff are among the most favorable stratigraphic targets at Baca and Wairakei. As previously discussed, rocks of this kind in the High Cascades are probably interbedded in rocks of the early High Cascade episode and, to a lesser extent, in rocks of the late High Cascade episode.

Unmapped calderas related to ash-flow eruptions that



occurred in early and late High Cascade time may also be present beneath the central Oregon High Cascade Range. These calderas may offer geothermal reservoir rocks in the form of caldera-wall facies of caldera-fill deposits, tuffaceous sands and nonwelded tuff within the caldera fill, and numerous faults and fractures associated with caldera formation and subvolcanic intrusion. Geophysical evidence was presented which supports the existence of a large area of cauldron subsidence south of the Three Sisters in the Lookout Mountain area.

Scoriaceous zones, autobreccias, cinders, and other highly fractured stratigraphic layers within the High Cascade sequence should be good aquifers, especially where additionally fractured at fissure or fault zones. Volcanic vent alignments and mapped faults and fissures may be good drilling targets for fractured reservoirs throughout the High Cascade sequence. Particular attention should be paid to intersecting faults and volcanic vent alignments. Specific structural zones which may be highly permeable and which probably lie within the High Cascade heat-flow anomaly are the following:

1. The Green Ridge-Tumalo fault-Newberry caldera-Walker Rim zone.
2. The upper McKenzie River-Horse Creek-Waldo Lake zone.
3. Volcanic vent alignments associated with the Collier Cone-Sand Mountain-Belknap Crater area, Three Sisters area, Lookout Mountain area, and the Mount Jefferson-Olallie Butte area.

## POSSIBLE SHALLOW PLUTONIC BODIES

Many of the previously discussed geothermal systems were associated with volcanic rocks with high silica contents (e.g., the New Zealand systems). Smith and Shaw (1973) also noted that the presence of young siliceous volcanic rocks is an important guide to areas with geothermal resource potential.

The correlation of geothermal systems with high-silica volcanic rocks is probably a function of the tendency of high-silica magmas to form shallow crustal plutonic bodies. Siliceous magmas probably have a tendency to remain and accumulate in the crust, rather than to erupt, for the following reasons:

1. The high viscosity of these magmas makes it difficult for them to travel rapidly to the surface. Siliceous magmas probably travel slowly upward and thus have more time to cool during intrusion than less viscous magmas such as basalt.
2. Siliceous magmas have lower temperatures than more mafic magmas, and many of them may be partial melts of crustal rocks, and thus not far above their solidus temperatures. Even slight cooling of a near-solidus magma will cause solidification. Low-temperature magmas also have little thermal energy for melting and stopping their way to the surface.
3. Many siliceous magmas are hydrous. When they rise to shallow levels,  $H_2O$  is exsolved, raising the crystallization temperature and thus causing the melt to solidify before reaching the surface.

In order to evaluate the compositions of magma which have in the past formed shallow plutonic bodies, the compositions of some of the largest plutons of the Oregon Western Cascade Range were examined. Table 8.1 lists some compositions of intrusives from hypabyssal plutons and the youngest lavas from nearby High Cascade volcanoes. The compositions of the plutons are in general no more siliceous than the nearby cones, and many of the intrusives (e.g., the Little North Santiam and Blue River plutons) have generated widespread

hydrothermal alteration aureoles.

The above data suggest that youthful High Cascade volcanoes with intermediate to silicic compositions may be underlain by shallow plutonic bodies and associated hydrothermal systems. Mount Hood (Wise, 1969), Mount Jefferson (Sutton, 1974), the South Sister and surrounding silicic vents (Taylor, 1980), and Crater Lake (Williams, 1942) are some examples of volcanoes with relatively silicic volcanic edifices. The silicic volcanic highland associated with the South Sister, one of the largest and most silicic Holocene volcanic centers in the Cascades, appears to have considerable geothermal potential. Because most of the area is in the Three Sisters Wilderness, the only portion that may be exploited is in the Devils Lake-Sparks Lake area.

In spite of the above permissive evidence for shallow intrusions in the High Cascades, teleseismic exploration in the province has been singularly unsuccessful in locating any large (diameter of 5 km [3 mi] or more), currently molten plutonic bodies (Iyer and others, 1982). The teleseismic surveys do indicate that there is a very broad area of low seismic velocity associated with the lower crust and upper mantle under the High Cascade heat-flow anomaly (Iyer and others, 1982). Iyer and others (1982) interpreted this deep layer of low-velocity material as "due to the presence of hot rock and pockets of magma." They concluded that there may be pockets of magma smaller than 5 km (3 mi) in diameter under the Cascade volcanoes, but high-resolution seismic techniques will be needed to locate them.

The caldera at Crater Lake is compelling evidence that plutonic bodies have intruded to very shallow levels in the crust in the High Cascades. Detailed seismic and heat-flow studies around sites of Holocene andesitic to rhyodacitic volcanism are needed to find the small shallow plutons which may be present.

## IMPLICATIONS OF THE PROPOSED TECTONIC MODEL FOR EXPLORATION

Priest and others (Chapter 2) concluded that the central Western Cascade Range had rotated across the main zone of magma generation under the High Cascade Range in response to Basin and Range spreading. They postulated that the rotation and extension was episodic with the last major episode of extension occurring between 4 and 5 m.y. ago. The last episode was accompanied by uplift of the Western Cascade Range relative to the area now occupied by the High Cascade volcanic pile. In many places, regional north-south faults separate the uplifted Western Cascade block from the High Cascade province, and it was concluded that these faults are probably localized by the boundary between the cooler, more rigid Western Cascade crust and the hotter, more plastic High Cascade crust.

The above model implies that deep heat flow is much higher in areas on and east of the regional north-south fault system separating the Western Cascade and High Cascade Ranges than it is in areas west of these faults. The implications of this model for exploration are obvious.

## CONCLUSIONS AND RECOMMENDATIONS

The central Oregon Cascade Range has all of the ingredients for the creation of major hydrothermal circulation systems. The following list summarizes some of these factors:

1. Heat flow is probably 100 mW/m<sup>2</sup> or more over all of the central Oregon High Cascade Range as well as in areas adjacent to the range (see Chapter 7).
2. Permeable volcanic rocks, including potentially highly

Table 8.1. Analyses of late-stage High Cascade volcanic rocks from Mount Hood, Mount Jefferson, and the South Sister compared to nearby hypabyssal plutonic rocks. All values in weight percent

Reference	Wise (1969)					Olson (1978)
General unit	Mount Hood					Late Western Cascade pluton near Mount Jefferson
Specific unit	Still Creek intrusion (average comp.)	Laurel Hill intrusion (average comp.)	Crater Rock lava	Steel Cliff lava (average comp.)	Barrett Spur lava	Little North Santiam pluton (average comp.)
SiO <sub>2</sub>	57.5	63.5	62.05	61.85	61.07	65.50
TiO <sub>2</sub>	0.87	0.82	0.74	0.74	0.80	0.61
Al <sub>2</sub> O <sub>3</sub>	14.6	14.5	16.83	17.04	16.96	15.65
Fe <sub>2</sub> O <sub>3</sub>	3.70	2.5	2.90	2.41	2.48	1.63
FeO	3.54	2.94	2.75	3.15	3.09	2.79
MnO	0.24	0.04	0.08	0.13	0.08	—
MgO	3.12	1.45	2.25	2.41	2.30	1.86
CaO	6.7	4.3	5.60	5.75	5.86	4.10
Na <sub>2</sub> O	3.78	4.17	4.22	4.42	4.28	3.84
K <sub>2</sub> O	1.13	3.06	1.55	1.41	1.79	3.01
Volatiles	4.4	3.4	0.77	0.59	1.02	0.69
P <sub>2</sub> O <sub>5</sub>	0.17	0.13	0.17	0.16	0.22	0.23
Total	99.75	100.08	99.91	100.06	99.95	99.95

Table 8.1. Analyses of late-stage High Cascade volcanic rocks from Mount Hood, Mount Jefferson, and the South Sister compared to nearby hypabyssal plutonic rocks—continued

Reference	Sutton (1974)			Wozniak (1982)	Storch (1978)
General unit	Uppermost Mount Jefferson lavas			Uppermost silicic South Sister lavas	Plutons near South Sister
Specific unit	Goats Peak hornblende dacite	North complex	Topmost peak	Holocene rhyodacite (average comp.)	Intrusives in Blue River district
SiO <sub>2</sub>	67.48	64.29	60.66	73.30	62.30-68.40
TiO <sub>2</sub>	0.46	0.61	0.81	0.33	0.45- 1.00
Al <sub>2</sub> O <sub>3</sub>	15.32	16.59	17.70	14.60	15.60-16.80
Fe <sub>2</sub> O <sub>3</sub>	2.77	1.74	4.19	—	—
FeO	0.56	2.57	1.53	1.70	3.40- 6.80
MnO	0.07	0.00	0.09	—	—
MgO	1.25	1.67	2.85	0.40	1.50- 3.40
CaO	3.08	4.36	5.75	1.90	2.80- 3.90
Na <sub>2</sub> O	5.06	5.00	4.25	4.80	3.30- 3.80
K <sub>2</sub> O	1.70	1.49	1.12	3.36	2.05- 3.35
Volatiles	—	—	1.00	—	—
P <sub>2</sub> O <sub>5</sub>	0.35	0.15	0.24	—	—
Total	98.10	98.47	100.19	100.39	91.40-107.45

permeable nonwelded tuffs and volcanoclastic sandstones are present. Units of the early High Cascade episode may have a particularly large number of these tuffaceous interbeds.

3. Numerous Holocene volcanic centers which may be underlain by shallow plutonic heat sources are present. Volcanoes with relatively silicic compositions, such as Mount Jefferson, South Sister, and Crater Lake, are most likely to have shallow plutonic bodies. The Quaternary silicic highland described by Taylor (1980) in the Three Sisters area is a particularly attractive target. A portion of this highland lies outside of wilderness areas at Devils Lake south of the South Sister.
4. Major faults and volcanic fissure zones are abundant, particularly on the margins of the High Cascade Range. The McKenzie River-Horse Creek-Waldo Lake and Green Ridge-Tumalo-Newberry caldera-Walker Rim zones are particularly worthy of attention, as are the numerous volcanic center alignments within the High Cascade province.
5. Great thicknesses of low-density, highly porous, and permeable volcanic rock may be locally present in tectonic grabens and in calderas. The Lookout Mountain gravity low may be an area of this kind. The High Cascade province east of the upper Clackamas River is another possible example (Couch and others, 1982a).
6. Hot springs occur in a regular belt within the western part of the High Cascade heat-flow anomaly within a zone of faults. This may mean that fluids are leaking upward in vertical fracture zones from regional aquifers at depth. The Austin, Breitenbush, and Belknap-Foley hot spring areas have the hottest springs.

Negative attributes of the Oregon Cascade geologic setting are also of concern. Some of these are listed below:

1. With the exception of fumaroles at Mount Hood and warm springs at Mount Hood and Crater Lake, the Oregon High Cascade Range, particularly the central High Cascades, is conspicuously lacking in hot springs and fumaroles. This could mean that the subvolcanic heat sources have been overwhelmed by influxes of cold meteoric water.
2. Much of the Holocene volcanic activity has been mafic rather than silicic. Mafic volcanism in continental areas is seldom associated with large, high-level plutonic bodies.
3. Over large areas of the Cascade Range, drilling to great depth (i.e., over 1.5 km [0.9 mi]) is likely to encounter altered rocks of the Western Cascade episode of volcanism. Unless fractured by relatively young volcanic or

tectonic processes, these rocks are likely to have low permeability.

4. Drilling in High Cascade rocks has proven to be difficult and expensive. Even when finally drilled, shallow (less than 600-m [1,968-ft]-deep) temperature-gradient holes in thick High Cascade sequences seldom give good measures of deep heat flow because of highly active circulation of cool ground water. This often necessitates drilling to depths greater than 600 m (1,968 ft) at the initial prospecting stage — a very expensive and risky exploration technique. When drilling in High Cascade terrane, every effort should be made to locate prospect holes at the lowest possible elevation in order to try to drill as cheaply as possible through the vadose zone into the regional ground-water table. Alternatively, islands of older, altered rock may give good shallow-temperature data, even at higher elevations.

One of the above negative attributes may actually prove to be an asset in the right structural setting. The general impermeability of many of the Western Cascade rocks may, where they are faulted against younger permeable units, cause them to act as barriers which can force laterally circulating hydrothermal fluids upward in vertical fractures. Likewise, blocks of western Cascade rock might block High Cascade ground water from draining rapidly off into lower elevations. This could allow the water to remain in extended contact with potentially hot rocks along the High Cascade axis.

Additional seismic refraction and gravity surveys should be completed in the High Cascade Range to find thick sections of low-density High Cascade rock juxtaposed against Western Cascade blocks. Particularly promising targets for this type of exploration are the Waldo Lake area (see Chapter 6) and the Lookout Mountain gravity low east of Waldo Lake. The lateral extent of the thick section of low-density material already documented by Couch and others (1982a) east of the Clackamas River should also be investigated to see if it extends into the Mount Jefferson-Three Sisters area.

Many geothermal aquifers in volcanic terranes in other parts of the world have been directly located by electrical techniques such as resistivity surveys. Soil-mercury surveys can also outline areas underlain by hydrothermal systems (Matlick and Buseck, 1976). After defining attractive structures by geologic mapping and by the previously discussed geophysical techniques, detailed soil and electrical surveys can find which parts of the structures actually have fluids. These relatively low-cost surface surveys can focus expensive drilling on the most productive locations. The surface-survey step is particularly critical in the High Cascade Range, where drilling costs tend to be very high.



Page 88 is blank

## REFERENCES

- Allen, J.E., 1966, The Cascade Range volcano-tectonic depression of Oregon, in Lunar Geological Field Conference, Bend, Oregon, August 1965, Transactions: Oregon Department of Geology and Mineral Industries, in cooperation with Oregon Division of Planning and Development, p. 21-23.
- Anderson, J.L., 1978, The stratigraphy and structure of the Columbia River basalt in the Clackamas River drainage: Portland, Oreg., Portland State University master's thesis, 136 p.
- Armentrout, J.M., 1981, Correlation and ages of Cenozoic chronostratigraphic units in Oregon and Washington, in Armentrout, J.M., ed., Pacific Northwest Cenozoic biostratigraphy: Boulder, Colo., Geological Society of America Special Paper 184, p. 137-148.
- Armstrong, R.L., Taylor, E.M., Hales, P.O., and Parker, D.J., 1975, K-Ar dates for volcanic rocks, central Cascade Range of Oregon: *Isochron/West*, no. 13, p. 5-10.
- Atwater, T., 1970, Implications of plate tectonics for the Cenozoic tectonic evolution of western North America: *Geological Society of America Bulletin*, v. 81, no. 12, p. 3513-3535.
- Atwater, T., and Molnar, P., 1973, Relative motion of the Pacific and North American plates deduced from sea-floor spreading in the Atlantic, Indian, and South Pacific Oceans, in Kovach, R.L., and Nur, A., eds., Tectonic problems of the San Andreas fault system, Conference Proceedings: Stanford, Calif., Stanford University Publications, Geological Sciences, v. 13, p. 136-148.
- Avramenko, W., 1981, Volcanism and structure in the vicinity of Echo Mountain, central Oregon Cascade Range: Eugene, Oreg., University of Oregon master's thesis, 156 p.
- Bacon, C.R., 1983a, Possible relations between magmatism, rates of extension, and the state of stress in the crust [abs.]: *Geological Society of America Abstracts with Programs*, v. 15, no. 5, p. 288.
- 1983b, The precursory and climactic eruptions of Mount Mazama and collapse of Crater Lake caldera, Oregon [abs.]: *Geological Society of America Abstracts with Program*, v. 15, no. 5, p. 330.
- [in press], Eruption history of Mount Mazama, Cascade Range, U.S.A.: *Journal of Volcanology and Geothermal Research*.
- Bailey, R.A., Dalrymple, G.B., and Lanphere, M.A., 1976, Volcanism, structure, and geochronology of Long Valley caldera, Mono County, California: *Journal of Geophysical Research*, v. 81, no. 5, p. 725-744.
- Baldwin, E.M., 1981, *Geology of Oregon* (3rd ed.): Dubuque, Iowa, Kendall/Hunt, 170 p.
- Barnes, C.G., 1978, The geology of the Mount Bailey area, Oregon: Eugene, Oreg., University of Oregon master's thesis, 123 p.
- Beall, J.J., 1981, A hydrologic model based on deep test data from the Walker "O" No. 1 well, Terminal Geyser, California: *Geothermal Resources Council Transactions*, v. 5, p. 153-156.
- Beaulieu, J.D., 1974, Geologic hazards of the Bull Run Watershed, Multnomah and Clackamas Counties, Oregon: Oregon Department of Geology and Mineral Industries Bulletin 82, 77 p.
- 1977, Geologic hazards of parts of northern Hood River, Wasco, and Sherman Counties, Oregon: Oregon Department of Geology and Mineral Industries Bulletin 91, 95 p.
- Beeson, M.H., and Moran, M.R., 1979, Stratigraphy and structure of the Columbia River Basalt Group in the Cascade Range, Oregon, in Hull, D.A., investigator, and Riccio, J.F., ed., 1979, Geothermal resource assessment of Mount Hood: Oregon Department of Geology and Mineral Industries Open-File Report O-79-8, p. 5-77.
- Beeson, M.H., Moran, M.R., Anderson, J.L., and Vogt, B.F., 1982, The relationship of the Columbia River Basalt Group to the geothermal potential of the Mount Hood area, Oregon, in Priest, G.R., and Vogt, B.F., eds., *Geology and geothermal resources of the Mount Hood area, Oregon*: Oregon Department of Geology and Mineral Industries Special Paper 14, p. 43-46.
- [in preparation], Stratigraphy and structure of the Columbia River Basalt Group in the Cascade Range, Oregon.
- Berg, J.W., and Thiruvathukal, J.V., 1967, Complete Bouguer gravity anomaly map of Oregon, in Oregon Department of Geology and Mineral Industries, Gravity maps of Oregon (onshore and offshore): Oregon Department of Geology and Mineral Industries Geological Map Series GMS-4b.
- Bethancourt, H.R., and Dominco, E., 1982, Characteristics of the Zunil geothermal field, western Guatemala: *Geothermal Resources Council Transactions*, v. 6, p. 241-244.
- Black, G.L., 1982, An estimate of the geothermal potential of Newberry volcano, Oregon: Oregon Department of Geology and Mineral Industries, Oregon Geology, v. 44, no. 4, p. 44-46; and A revision to the estimate: Oregon Geology, v. 44, no. 5, p. 57.
- Black, G.L., Elliott, M., D'Allura, J., and Purdom, W., 1983, Results of a geothermal resource assessment of the Ashland, Oregon, area, Jackson County: Oregon Department of Geology and Mineral Industries, Oregon Geology, v. 45, no. 5, p. 51-55.
- Blackwell, D.D., Bowen, R.G., Hull, D.A., Riccio, J.F., and Steele, J.L., 1982, Heat flow, arc volcanism, and subduction in northern Oregon: *Journal of Geophysical Research*, v. 87, no. B10, p. 8735-8754.
- Blackwell, D.D., Bowen, R.G., and Schuster, J.E., 1973, Heat flow and Cenozoic tectonic history of the northwestern United States [abs.]: *Geological Society of America Abstracts with Programs*, v. 5, no. 1, p. 12-13.
- Blackwell, D.D., Hull, D.A., Bowen, R.G., and Steele, J.L., 1978, Heat flow of Oregon: Oregon Department of Geology and Mineral Industries Special Paper 4, 42 p.
- Blackwell, D.D., and Steele, J.L., 1979, Heat flow modeling of the Mount Hood volcano, Oregon, in Hull, D.A., investigator, and Riccio, J.F., ed., *Geothermal resource assessment of Mount Hood*:

- Oregon Department of Geology and Mineral Industries Open-File Report O-79-8, p. 190-264.
- Blackwell, D.D., Steele, J.L., and Brott, C.A., 1980, The terrain effect on terrestrial heat flow: *Journal of Geophysical Research*, v. 85, no. B9, p. 4757-4772.
- Bolton, R.S., 1970, The behaviour of the Wairakei geothermal field during exploitation: *Geothermics*, Special Issue 2, v. 2, pt. 2, p. 1426-1439.
- Bowen, R.G., 1975, Geothermal gradient data: Oregon Department of Geology and Mineral Industries Open-File Report O-75-3, 114 p.
- Bowen, R.G., Peterson, N.V., and Riccio, J.F., 1978, Low- to intermediate-temperature thermal springs and wells in Oregon: Oregon Department of Geology and Mineral Industries Geological Map Series GMS-10, scale 1:1,000,000.
- Brook, C.A., Mariner, R.H., Mabey, D.R., Swanson, J.R., Gufanti, M., and Muffler, L.J.P., 1979, Hydrothermal convection systems with reservoir temperatures  $\geq 90^{\circ}\text{C}$ , in Muffler, L.J.P., ed., *Assessment of geothermal resources of the United States—1978*: U.S. Geological Survey Circular 790, p. 18-85.
- Brott, C.A., Blackwell, D.D., and Morgan, P., 1981, Continuation of heat flow data: A method to construct isotherms in geothermal areas: *Geophysics*, v. 46, no. 12, p. 1732-1744.
- Brown, D.E., McLean, G.D., Priest, G.R., Woller, N.M., and Black, G.L., 1980a, Preliminary geology and geothermal resource potential of the Belknap-Foley area, Oregon: Oregon Department of Geology and Mineral Industries Open-File Report O-80-2, 58 p.
- Brown, D.E., McLean, G.D., Woller, N.M., and Black, G.L., 1980b, Preliminary geology and geothermal resource potential of the Willamette Pass area, Oregon: Oregon Department of Geology and Mineral Industries Open-File Report O-80-3, 65 p.
- Brown, R.E., 1941, The geology and petrography of the Mount Washington area, Oregon: New Haven, Conn., Yale University master's thesis, 139 p.
- Bunker, R.C., Farooqui, S.M., and Thoms, R.E., 1982, K-Ar dates for volcanic rocks associated with Neogene sedimentary deposits in north-central and northeastern Oregon: *Isochron/West*, no. 33, p. 21-22.
- Callaghan, E., 1933, Some features of the volcanic sequence in the Cascade Range in Oregon: *American Geophysical Union 14th Annual Meeting, Transactions*, p. 243-249.
- Callaghan, E., and Buddington, A.F., 1938, Metalliferous mineral deposits of the Cascade Range in Oregon: *U.S. Geological Survey Bulletin* 893, 141 p.
- Carmichael, I.S.E., Turner, F.J., and Verhoogen, J., 1974, *Igneous petrology*: New York, N.Y., McGraw-Hill, 739 p.
- Chaney, R.W., 1938, Ancient forests of Oregon: A study of earth history in western America: *Carnegie Institution of Washington Publication* 501, p. 631-648.
- 1956, The ancient forests of Oregon: Eugene, Ore., Oregon System of Higher Education, Condon Lectures [reprint of 1948 edition], 56 p.
- Chayes, F., 1965, Statistical petrography: *Carnegie Institution of Washington Year Book* 64, p. 153-165.
- 1966, Alkaline and subalkaline basalts: *American Journal of Science*, v. 264, no. 2, p. 128-145.
- Christiansen, R.L., and Lipman, P.W., 1972, Cenozoic volcanism and plate tectonic evolution of the western United States. II. Late Cenozoic: *Royal Society of London Philosophical Transactions, Series A*, v. 271, no. 1213, p. 249-284.
- Clayton, C.M., 1976, *Geology of the Breitenbush Hot Springs area, Cascade Range, Oregon*: Portland, Ore., Portland State University master's thesis, 79 p.
- Connard, G.G., 1980, Analysis of aeromagnetic measurements from the central Oregon Cascades: Corvallis, Ore., Oregon State University master's thesis, 101 p.
- Couch, R.W., 1979, Geophysical investigations of the Cascade Range in central Oregon: U.S. Geological Survey Extramural Geothermal Research Program, Final Report, 95 p.
- Couch, R.W., and Baker, B., 1977, Geophysical investigations of the Cascade Range in central Oregon: U.S. Geological Survey Extramural Geothermal Research Program, Technical Report no. 2, 55 p.
- Couch, R.W., Gemperle, M., and Connard, G.G., 1978, Total field aeromagnetic anomaly map, Cascade Mountain Range, central Oregon: Oregon Department of Geology and Mineral Industries Geological Map Series GMS-9, scale 1:125,000.
- Couch, R.W., Gemperle, M., McLain, W.H., and Connard, G.G., 1981a, Total field aeromagnetic anomaly map, Cascade Mountain Range, southern Oregon: Oregon Department of Geology and Mineral Industries Geological Map Series GMS-17, scale 1:250,000.
- Couch, R.W., and Lowell, R.P., 1971, Earthquakes and seismic energy release in Oregon: Oregon Department of Geology and Mineral Industries, Ore Bin, v. 33, no. 4, p. 61-84.
- Couch, R.W., Pitts, G.S., Braman, D.E., and Gemperle, M., 1981b, Free-air gravity anomaly map and complete Bouguer gravity anomaly map, Cascade Mountain Range, northern Oregon: Oregon Department of Geology and Mineral Industries Geological Map Series GMS-15, scale 1:250,000.
- Couch, R.W., Pitts, G.S., Gemperle, M., Braman, D.E., and Veen, C.A., 1982a, Gravity anomalies in the Cascade Range in Oregon: Structural and thermal implications: Oregon Department of Geology and Mineral Industries Open-File Report O-82-9, 43 p.
- Couch, R.W., Pitts, G.S., Gemperle, M., Veen, C.A., and Braman, D.E., 1982b, Residual gravity maps of the northern, central, and southern Cascade Range, Oregon,  $121^{\circ}00'$  to  $122^{\circ}30'$  W. by  $42^{\circ}00'$  to  $45^{\circ}45'$  N.: Oregon Department of Geology and Mineral Industries Geological Map Series GMS-26, scale 1:250,000.
- Couch, R.W., Pitts, G.S., Veen, C.A., and Gemperle, M., 1981c, Free-air gravity anomaly and complete Bouguer gravity anomaly map, Cascade Mountain Range, southern Oregon: Oregon Department of Geology and Mineral Industries Geological Map Series GMS-16, scale 1:250,000.
- Crandell, D.R., 1980, Recent eruptive history of Mount Hood, Oregon, and potential hazards from future eruptions: *U.S. Geological Survey Bulletin* 1492, 81 p.
- Davie, E.I., II, 1980, The geology and petrology of Three Fingered Jack, a High Cascade volcano in central Oregon: Eugene, Ore., University of Oregon master's thesis, 138 p.
- Davis, G.A., 1981, Late Cenozoic tectonics of the Pacific Northwest with special reference to the Columbia Plateau: Washington Public Power Supply System, Final Safety Analysis Report, Nuclear Project 2, Appendix 2.5 N., revised preliminary draft, 44 p.
- Dicken, S.N., 1950, *Oregon geography*: Eugene, Ore., University of Oregon Cooperative Bookstore, 104 p.



- Dickinson, W.R., 1968, Circum-Pacific andesite types: *Journal of Geophysical Research*, v. 73, no. 6, p. 2261-2269.
- Donato, M.M., 1975, The geology and petrology of a portion of the Ashland pluton, Jackson County, Oregon: Eugene, Oreg., University of Oregon master's thesis, 89 p.
- Dondanville, R.F., 1978, Geologic characteristics of the Valles Caldera geothermal system, New Mexico: *Geothermal Resources Council Transactions*, v. 2, p. 157-160.
- Drake, E.T., 1982, Tectonic evolution of the Oregon continental margin: Oregon Department of Geology and Mineral Industries, *Oregon Geology*, v. 44, no. 2, p. 15-21.
- Dyhrman, R.G., 1975, Geology of the Bagby Hot Springs area, Clackamas and Marion Counties, Oregon: Corvallis, Oreg., Oregon State University master's thesis, 78 p.
- Elliott, M.A., D'Allura, J.A., and Purdom, W.B., 1981, Geology of the City of Ashland and vicinity, Jackson County, Oregon: Oregon Department of Geology and Mineral Industries unpublished report, 15 p.
- Fairbank, B.D., Openshaw, R.W., Souther, J.G., and Stauder, J.J., 1981, Meager Creek Geothermal Project—an exploration case history: *Geothermal Resources Council Bulletin*, v. 10, no. 6, p. 3-7.
- Fan, P., 1978, Mineral assemblages of hydrothermal alterations of basalts from Hawaii: *Geothermal Resources Council Transactions*, v. 2, p. 185-187.
- Fiebelkorn, R.B., Walker, G.W., MacLeod, N.S., McKee, E.H., and Smith, J.G., 1982, Index to K-Ar age determinations for the State of Oregon: U.S. Geological Survey Open-File Report 82-596, 40 p.
- Flaherty, G.M., 1981, The Western Cascade-High Cascade transition in the McKenzie Bridge area, central Oregon Cascade Range: Eugene, Oreg., University of Oregon master's thesis, 178 p.
- Fournier, R.O., 1979, A revised equation for the Na/K geothermometer: *Geothermal Resources Council Transactions*, v. 3, p. 221-224.
- Fournier, R.O., and Rowe, J.J., 1966, Estimation of underground temperatures from the silica content of water from hot springs and wet-steam wells: *American Journal of Science*, v. 264, no. 9, p. 685-697.
- Fournier, R.O., and Truesdell, A.H., 1973, An empirical Na-K-Ca geothermometer for natural waters: *Geochimica et Cosmochimica Acta*, v. 37, no. 5, p. 1255-1275.
- Furumoto, A.S., 1978, The relationship of a geothermal reservoir to the geological structure of the East Rift of Kilauea Volcano, Hawaii: *Geothermal Resources Council Transactions*, v. 2, p. 199-201.
- Gannett, M.W., and Bargar, K.E., 1981, Volcanic stratigraphy and secondary mineralization of USGS Pucci geothermal test well, Mount Hood, Oregon: U.S. Geological Survey Open-File Report 81-1330, 26 p.
- Ganoe, S.J., 1983, Investigation of  $P_n$ -wave propagation in Oregon: Corvallis, Oreg., Oregon State University master's thesis, 97 p.
- Greene, T.H., and Ringwood, A.E., 1968, Genesis of the calc-alkaline igneous rock suite: *Contributions to Mineralogy and Petrology*, v. 18, no. 2, p. 105-162.
- Grindley, G.W., and Browne, P.R.L., 1976, Structural and hydrological factors controlling the permeabilities of some hot-water geothermal fields, in *Second United Nations Symposium on the Development and Use of Geothermal Resources*, San Francisco, California, 1975, Proceedings: Washington, D.C., U.S. Government Printing Office, v. 1, p. 377-386.
- Hales, P.O., 1975, Geology of the Green Ridge area, Whitewater River quadrangle, Oregon: Corvallis, Oreg., Oregon State University master's thesis, 90 p.
- Hammond, P.E., 1979, A tectonic model for evolution of the Cascade Range, in Armentrout, J.M., Cole, M.R., and Terbest, H., Jr., eds., *Cenozoic paleogeography of the western United States: Pacific Coast Paleogeography Symposium No. 3*, Anaheim, Calif., Society of Economic Paleontologists and Mineralogists, Pacific Section, p. 219-237.
- 1980, Reconnaissance geologic map and cross sections of southern Washington Cascade Range, latitude 45°30'-47°15' N., longitude 120°45'-122°22.5' W.: Portland, Oreg., Portland State University Department of Earth Sciences, 31 p., 2 sheets, scale 1:125,000.
- Hammond, P.E., Anderson, J.L., and Manning, K.J., 1980, Guide to the geology of the upper Clackamas and North Santiam Rivers area, northern Oregon Cascade Range, in Oles, K.F., Johnson, J.G., Niem, A.R., and Niem, W.A., eds., *Geologic field trips in western Oregon and southwestern Washington: Oregon Department of Geology and Mineral Industries Bulletin 101*, p. 133-167.
- Hammond, P.E., Geyer, K.M., and Anderson, J.L., 1982, Preliminary geologic map and cross sections of the upper Clackamas and North Santiam Rivers area, northern Oregon Cascade Range: Portland, Oreg., Portland State University Department of Earth Sciences, scale 1:62,500.
- Hart, W.K., 1982, Chemical, geochronologic, and isotopic significance of low-K, high-alumina olivine tholeiite in the northwestern Great Basin, U.S.A.: Cleveland, Ohio, Case Western Reserve University doctoral dissertation, 410 p.
- Hart, W.K., and Mertzman, S.A., 1983, Late Cenozoic volcanic stratigraphy of the Jordan Valley area, southeastern Oregon: Oregon Department of Geology and Mineral Industries, *Oregon Geology*, v. 45, no. 2, p. 15-19.
- Healy, J., 1976, Geothermal fields in zones of recent volcanism, in *Second United Nations Symposium on the Development and Use of Geothermal Resources*, San Francisco, California, 1975, Proceedings: Washington, D.C., U.S. Government Printing Office, v. 1, p. 415-422.
- Hering, C.W., 1981, Geology and petrology of the Yamsay Mountain complex, south-central Oregon: A study of bimodal volcanism: Eugene, Oreg., University of Oregon doctoral dissertation, 194 p.
- Higgins, M.W., 1973, Petrology of Newberry volcano, central Oregon: *Geological Society of America Bulletin*, v. 84, no. 2, p. 455-487.
- Hodge, E.T., 1933, Age of Columbia River and lower canyon [abs.]: *Geological Society of America Bulletin*, v. 44, pt. 1, p. 156-157.
- 1938, Geology of the lower Columbia River: *Geological Society of America Bulletin*, v. 49, no. 6, p. 831-929.
- Holdaway, M.J., and Bussey, S., 1982, Mineralogy of the Old Maid Flat exploratory hole no. 7A, in Priest, G.R., and Vogt, B.F., eds., *Geology and geothermal resources of the Mount Hood area, Oregon: Oregon Department of Geology and Mineral Industries Special Paper 14*, p. 57-76.
- Hulen, J.B., and Nielson, D.L., 1982, Stratigraphic permeability in the Baca geothermal system, Redondo Creek area, Valles Caldera, New Mexico, in *Geothermal Resources Council Transactions*, v. 6, p. 27-30.
- Hull, D.A., Blackwell, D.D., and Black, G.L., 1978, Geothermal gradient data: Oregon Department of Geology and Mineral Industries Open-File Report O-78-4, 187 p.
- Hull, D.A., Blackwell, D.D., Bowen, R.G., Peterson, N.V., and Black, G.L., 1977, Geothermal gradient data: Oregon Department of

- Geology and Mineral Industries Open-File Report O-77-2, 134 p.
- Hull, D.A., Bowen, R.G., Blackwell, D.D., and Peterson, N.V., 1976, Geothermal gradient data, Brothers fault zone, central Oregon: Oregon Department of Geology and Mineral Industries Open-File Report O-76-2, 24 p.
- Hull, D.A., investigator, and Riccio, J.F., ed., 1979, Geothermal resource assessment of Mount Hood: Oregon Department of Geology and Mineral Industries Open-File Report O-79-8, 273 p.
- Ide, T., 1982, Geology in the Nigorikawa geothermal field, Mori-Machi, Hokkaido, Japan, in *Geothermal Resources Council Transactions*, v. 6, p. 31-34.
- Irvine, T.N., and Baragar, W.R.A., 1971, A guide to the chemical classification of the common volcanic rocks: *Canadian Journal of Earth Sciences*, v. 8, no. 5, p. 523-548.
- Iyer, H.M., Rite, A., and Green, S.M., 1982, Search for geothermal heat sources in the Oregon Cascades by means of teleseismic *P*-residual technique [abs.]: Society of Exploration Geophysicists, 52nd Annual Meeting, Dallas, Tex., 1982, Technical Program Abstracts, p. 479-482.
- Jakes, P., and White, A.J.R., 1969, Structure of the Melanesian arcs and correlation with distribution of magma types: *Tectonophysics*, v. 8, no. 3, p. 223-236.
- 1972, Major and trace element abundances in volcanic rocks of orogenic areas: *Geological Society of America Bulletin*, v. 83, no. 1, p. 29-39.
- Jan, M.Q., 1967, Geology of the McKenzie River valley between the South Santiam Highway and the McKenzie Pass Highway, Oregon: Eugene, Ore., University of Oregon master's thesis, 70 p.
- Kays, M.A., 1970, Western Cascades volcanic series, South Umpqua Falls region, Oregon: Oregon Department of Geology and Mineral Industries, Ore Bin, v. 32, no. 5, p. 81-94.
- Keith, T.E.C., and Causey, J.D., 1982, Mineral and geothermal resource potential of the Mount Hood Wilderness, Clackamas and Hood River Counties, Oregon: U.S. Geological Survey Miscellaneous Field Studies Map MF-1379-E, 8 p., scale 1:62,500.
- Keith, T.E.C., White, D.E., and Beeson, M.H., 1978, Hydrothermal alteration and self-sealing in Y-7 and Y-8 drill holes in northern part of Upper Geyser Basin, Yellowstone National Park, Wyoming: U.S. Geological Survey Professional Paper 1054-A, 26 p.
- Kerr, R.A., 1982, Extracting geothermal energy can be hard: *Science*, v. 218, no. 4573, p. 668-669.
- Kienle, C.F., Nelson, C.A., and Lawrence, R.D., 1981, Faults and lineaments of the southern Cascades, Oregon: Oregon Department of Geology and Mineral Industries Special Paper 13, 23 p.
- Kuno, H., 1950, Geology of Hakone volcano and adjacent areas, Part I: *Journal of the Faculty of Science, University of Tokyo*, section 2, v. 7, p. 257-279.
- 1966, Lateral variation of basalt magma type across continental margins and island arcs: *Bulletin Volcanologique*, v. 29, p. 195-222.
- Kuno, H., Oki, Y., Ogino, K., and Hirota, S., 1970, Structure of Hakone caldera as revealed by drilling: *Bulletin Volcanologique*, v. 34, no. 3, p. 713-725.
- Lawrence, R.D., 1976, Strike-slip faulting terminates the Basin and Range province in Oregon: *Geological Society of America Bulletin*, v. 87, no. 6, p. 846-850.
- Lidstrom, J.W., Jr., 1972, A new model for the formation of Crater Lake caldera, Oregon: Corvallis, Ore., Oregon State University doctoral dissertation, 85 p.
- Lutton, R.J., 1962, Geology of the Bohemia mining district, Lane County, Oregon: Tucson, Ariz., University of Arizona doctoral dissertation, 172 p.
- Lux, D.R., 1981, Geochronology, geochemistry, and petrogenesis of basaltic rocks from the Western Cascades, Oregon: Columbus, Ohio, Ohio State University doctoral dissertation, 171 p.
- 1982, K-Ar and  $^{40}\text{Ar}$ - $^{39}\text{Ar}$  ages of mid-Tertiary volcanic rocks from the Western Cascade Range, Oregon: *Isochron/West*, no. 33, p. 27-32.
- Lyons, D.J., and van de Kamp, P.C., 1980, Subsurface geological and geophysical study of the Cerro Prieto geothermal field, Baja California, Mexico: Berkeley, Calif., Lawrence Berkeley Laboratory (for U.S. Department of Energy), Report LBL-10540 (CP11), 95 p.
- Macdonald, G.A., and Katsura, T., 1964, Chemical composition of Hawaiian lavas: *Journal of Petrology*, v. 5, pt. 1, p. 82-133.
- MacLeod, N.S., 1978a, Newberry volcano in Oregon [work in progress], in *Geological Survey Research 1978: U.S. Geological Survey Professional Paper 1100*, p. 194.
- 1978b, Newberry volcano, Oregon: Preliminary results of new field investigations [abs.]: *Geological Society of America Abstracts with Programs*, v. 10, no. 3, p. 115.
- MacLeod, N.S., and Sammel, E.A., 1982, Newberry volcano, Oregon: A Cascade Range geothermal prospect: Oregon Department of Geology and Mineral Industries, Oregon Geology, v. 44, no. 11, p. 123-131.
- MacLeod, N.S., and Sherrod, D.R., 1979, Latest eruptions at Newberry volcano in Oregon [work in progress], in *Geological Survey Research 1979: U.S. Geological Survey Professional Paper 1150*, p. 182-183.
- MacLeod, N.S., Sherrod, D.R., and Chitwood, L.A., 1982, Geologic map of Newberry volcano, Deschutes, Klamath, and Lake Counties, Oregon: U.S. Geological Survey Open-File Report 82-847, 27 p., scale 1:62,500.
- MacLeod, N.S., Sherrod, D.R., Chitwood, L.A., and McKee, E.H., 1981, Newberry volcano, Oregon, in Johnston, D.A., and Donnelly-Nolan, J., eds., *Guides to some volcanic terranes in Washington, Idaho, Oregon, and northern California*: U.S. Geological Survey Circular 838, p. 85-103.
- MacLeod, N.S., Walker, G.W., and McKee, E.H., 1975, Geothermal significance of eastward increase in age of upper Cenozoic rhyolitic domes in southeastern Oregon, in *Second United Nations Symposium on the Development and Use of Geothermal Resources*, San Francisco, California, 1975, Proceedings: Washington, D.C., U.S. Government Printing Office, v. 1, p. 465-474.
- Magill, J., and Cox, A., 1980, Tectonic rotation of the Oregon Western Cascades: Oregon Department of Geology and Mineral Industries Special Paper 10, 67 p.
- Mariner, R.H., Swanson, J.R., Orris, G.J., Presser, J.S., and Evans, W.C., 1980, Chemical and isotopic data for water from thermal springs and wells of Oregon: U.S. Geological Survey Open-File Report 80-737, 50 p.
- Mase, C.W., Sass, J.H., Lachenbruch, A.H., and Munroe, R.J., 1982, Preliminary heat flow investigations of the California Cascades: U.S. Geological Survey Open-File Report 82-150, 240 p.

- Matlick, J.S., III, and Buseck, P.R., 1976, Exploration for geothermal areas using mercury—a new geochemical technique, in *Second United Nations Symposium on the Development and Use of Geothermal Resources*, San Francisco, California, 1975, Proceedings: Washington, D.C., U.S. Government Printing Office, v. 1, p. 785-792.
- Maynard, L.C., 1974, *Geology of Mount McLoughlin: Eugene, Oreg.*, University of Oregon master's thesis, 139 p.
- McBirney, A.R., Sutter, J.F., Naslund, H.R., Sutton, K.G., and White, C.M., 1974, Episodic volcanism in the central Oregon Cascade Range: *Geology*, v. 2, no. 12, p. 585-589.
- McKee, E.H., Duffield, W.A., and Stern, R.J., 1983, Late Miocene and early Pliocene basaltic rocks and their implications for crustal structure, northeastern California and south-central Oregon: *Geological Society of America Bulletin*, v. 94, no. 2, p. 292-304.
- McKenzie, W.F., and Truesdell, A.H., 1977, Geothermal reservoir temperatures estimated from the oxygen isotope compositions of dissolved sulfate and water from hot springs and shallow drill holes: *Geothermics*, v. 5, p. 51-61.
- McLain, W.H., 1981, Geothermal and structural implications of magnetic anomalies observed over the southern Oregon Cascade Mountains and adjoining Basin and Range province: *Corvallis, Oreg.*, Oregon State University master's thesis, 151 p.
- McNitt, J.R., Sanyal, S.K., Klein, C.W., Che, M., Tolentino, B.S., Alcaraz, A., and Datuin, R., 1982, Temperature and pressure distribution in the Palimpinon geothermal field, southern Negros, Philippines: *Geothermal Resources Council Transactions*, v. 6, p. 293-296.
- Miyashiro, A., 1974, Volcanic rock series in island arcs and active continental margins: *American Journal of Science*, v. 274, no. 4, p. 321-355.
- Molloy, M.W., 1982, Baca geothermal demonstration project—reservoir definition review: *Geothermal Resources Council Transactions*, v. 6, p. 301-303.
- Munts, S.R., 1978, *Geology and mineral deposits of the Quartzville mining district, Linn County, Oregon: Eugene, Oreg.*, University of Oregon master's thesis, 213 p.
- Nakamura, K., 1977, Volcanoes as possible indicators of tectonic stress orientation—principle and proposal: *Journal of Volcanology and Geothermal Research*, v. 2, no. 1, p. 1-16.
- Naslund, H.R., 1977, *The geology of the Hyatt Reservoir and Surveyor Mountain quadrangles, Oregon: Eugene, Oreg.*, University of Oregon master's thesis, 127 p.
- Newcomb, R.C., 1969, Effect of tectonic structure on the occurrence of ground water in the basalt of the Columbia River Group of The Dalles area, Oregon and Washington: *U.S. Geological Survey Professional Paper 383-C*, 33 p.
- Newcomb, R.C., and Hart, D.H., 1958, Preliminary report on the ground-water resources of the Klamath River basin, Oregon: *U.S. Geological Survey Open-File Report 58-73*, 248 p.
- O'Hara, M.J., 1965, Primary magmas and the origin of basalts: *Scottish Journal of Geology*, v. 1, pt. 1, p. 19-40.
- Oki, Y., and Hirano, T., 1970, The geothermal system of Hakone volcano: *Geothermics*, Special Issue 2, v. 2, pt. 2, p. 1157-1166.
- 1974, Hydrothermal system and seismic activity of Hakone volcano, in Colp, J.L., and Furumoto, A.S., eds., *The utilization of volcano energy: Albuquerque, N. Mex.*, Sandia Laboratories, p. 13-40.
- Olson, J.P., 1978, *Geology and mineralization of the North Santiam mining district, Marion County, Oregon: Corvallis, Oreg.*, Oregon State University master's thesis, 135 p.
- Oregon Department of Geology and Mineral Industries (DOGAMI), 1982, *Geothermal resources of Oregon, 1982: DOGAMI/National Oceanic and Atmospheric Administration (for U.S. Department of Energy)*, 1 sheet, map scale 1:500,000.
- Parchman, W.L., and Knox, J.W., 1981, Exploration for geothermal resources in Dixie Valley, Nevada: *Geothermal Resources Council Bulletin*, v. 10, no. 5, p. 3-6.
- Parmentier, P.P., and Hayashi, M., 1981, Geologic model of the "vapor-dominated" reservoir in Yunotani geothermal field, Kyushu, Japan: *Geothermal Resources Council Transactions*, v. 5, p. 201-204.
- Peacock, M.A., 1931, Classification of igneous rock series: *Journal of Geology*, v. 39, no. 1, p. 54-67.
- Peck, D.L., Griggs, A.B., Schlicker, H.G., Wells, F.G., and Dole, H.M., 1964, *Geology of the central and northern parts of the Western Cascade Range in Oregon: U.S. Geological Survey Professional Paper 449*, 56 p.
- Peterson, N.V., 1962, *Geology of Collier State Park area, Klamath County, Oregon: Oregon Department of Geology and Mineral Industries, Ore Bin*, v. 24, no. 6, p. 88-97.
- Peterson, N.V., and Groh, E.A., eds., 1965, *Lunar Geological Field Conference guidebook: Oregon Department of Geology and Mineral Industries Bulletin 57*, 51 p.
- 1967, *Geothermal potential of the Klamath Falls area, Oregon—a preliminary study: Oregon Department of Geology and Mineral Industries, Ore Bin*, v. 29, no. 11, p. 209-231.
- Peterson, N.V., Groh, E.A., Taylor, E.M., and Stensland, D.E., 1976, *Geology and mineral resources of Deschutes County, Oregon: Oregon Department of Geology and Mineral Industries Bulletin 89*, 66 p.
- Peterson, N.V., and McIntyre, J.R., 1970, *The reconnaissance geology and mineral resources of eastern Klamath County and western Lake County, Oregon: Oregon Department of Geology and Mineral Industries Bulletin 66*, 70 p.
- Pitts, G.S., 1979, *Interpretation of gravity measurements made in the Cascade Mountains and adjoining Basin and Range province in central Oregon: Corvallis, Oreg.*, Oregon State University master's thesis, 186 p.
- Pitts, G.S., and Couch, R.W., 1978, *Complete Bouguer gravity anomaly map, Cascade Mountain Range, central Oregon: Oregon Department of Geology and Mineral Industries Geological Map Series GMS-8*, scale 1:125,000.
- Power, S.G., and Field, C.W., 1982, *Mining districts of the Western Cascades: Oregon Department of Geology and Mineral Industries unpublished report*, 73 p.
- Power, S.G., Field, C.W., Armstrong, R.L., and Harakal, J.E., 1981, *K-Ar ages of plutonism and mineralization, Western Cascades, Oregon and southern Washington: Isochron/West*, no. 31, p. 27-29.
- Priest, G.R., 1982, Overview of the geology and geothermal resources of the Mount Hood area, in Priest, G.R., and Vogt, B.F., eds., *Geology and geothermal resources of the Mount Hood area, Oregon: Oregon Department of Geology and Mineral Industries Special Paper 14*, p. 6-15.
- Priest, G.R., Beeson, M.H., Gannett, M.W., and Berri, D., 1982a,



- Geology, geochemistry and geothermal resources of the Old Maid Flat area, Oregon, in Priest, G.R., and Vogt, B.F., eds., *Geology and geothermal resources of the Mount Hood area, Oregon*: Oregon Department of Geology and Mineral Industries Special Paper 14, p. 16-30.
- Priest, G.R., Black, G.L., Woller, N.M., and King, W.L., 1982b, *Geothermal exploration in Oregon, 1981*: Oregon Department of Geology and Mineral Industries, Oregon Geology, v. 44, no. 6, p. 63-68.
- Priest, G.R., Hadden, M.M., Woller, N.M., and Brand, C.B., [in press], Preliminary soil-mercury survey of Newberry volcano, in Oregon Department of Geology and Mineral Industries, Survey of potential geothermal exploration sites at Newberry volcano, Deschutes County, Oregon: Oregon Department of Geology and Mineral Industries Open-File Report O-83-3.
- Priest, G.R., Riccio, J.F., Woller, N.M., Gest, D., and Pitts, G.S., 1980, Heat flow along the High Cascade-Western Cascade transition zone, Oregon [abs.]: Oregon Academy of Science Proceedings, v. 16, p. 15.
- Priest, G.R., and Vogt, B.F., eds., 1982a, *Geology and geothermal resources of the Cascades, Oregon*: Oregon Department of Geology and Mineral Industries Open-File Report O-82-7, 206 p.
- 1982b, *Geology and geothermal resources of the Mount Hood area, Oregon*: Oregon Department of Geology and Mineral Industries Special Paper 14, 100 p.
- Priest, G.R., and Woller, N.M., 1982, Preliminary geology of the Outerson Mountain-Devils Creek area, Marion County, Oregon, in Priest, G.R., and Vogt, B.F., eds., *Geology and geothermal resources of the Cascades, Oregon*: Oregon Department of Geology and Mineral Industries Open-File Report O-82-7, p. 71-91.
- Priest, G.R., Woller, N.M., and Evans, S.H., Jr., 1981, Late Cenozoic modification of calc-alkalic volcanism, central Oregon Cascades [abs.]: American Association for the Advancement of Science, Pacific Division, 62nd Annual Meeting, Eugene, Oreg., 1981, Abstracts, p. 32.
- Pungrasami, T., 1970, *Geology of the western Detroit Reservoir area, Quartzville and Detroit quadrangles, Linn and Marion Counties, Oregon*: Corvallis, Oreg., Oregon State University master's thesis, 76 p.
- Ringwood, A.E., 1975, *Composition and petrology of the earth's mantle*: New York, N.Y., McGraw-Hill, 618 p.
- Ritchey, J.L., 1979, *Origin of divergent magmas at Crater Lake, Oregon*: Eugene, Oreg., University of Oregon doctoral dissertation, 209 p.
- Robinson, P.T., and Brem, G.F., 1981, Guide to geologic field trip between Kimberly and Bend, Oregon, with emphasis on the John Day Formation, in Johnston, D.A., and Donnelly-Nolan, J., eds., *Guides to some volcanic terranes in Washington, Idaho, Oregon, and northern California*: U.S. Geological Survey Circular 838, p. 29-40.
- Robinson, J.H., Forcella, L.S., and Gannett, M.W., 1981, Data from geothermal test wells near Mount Hood, Oregon: U.S. Geological Survey Open-File Report 81-1002, 24 p.
- Robison, J.H., Keith, T.E.C., Beeson, M.H., and Bargar, K.E., 1982, Map showing geothermal investigations in the vicinity of the Mount Hood Wilderness, Clackamas and Hood River Counties, Oregon: U.S. Geological Survey Miscellaneous Field Studies Map MF-1379-B, scale 1:62,500.
- Robison, J.H., and Laenen, A., 1976, *Water resources of the Warm Springs Indian Reservation, Oregon*: U.S. Geological Survey Water Resources Investigations 76-26, 85 p.
- Rollins, A., 1976, *Geology of the Bachelor Mountain area, Linn and Marion Counties, Oregon*: Corvallis, Oreg., Oregon State University master's thesis, 83 p.
- Roy, R.F., Decker, E.R., Blackwell, D.D., and Birch, F., 1968, Heat flow in the United States: *Journal of Geophysical Research*, v. 73, no. 16, p. 5207-5221.
- Sammel, E.A., 1976, *Hydrologic reconnaissance of the geothermal area near Klamath Falls, Oregon*: U.S. Geological Survey Water Resources Investigation WRI 76-127, 129 p.
- 1980, *Hydrogeologic appraisal of the Klamath Falls geothermal area, Oregon*: U.S. Geological Survey Professional Paper 1044-G, 45 p.
- 1981, *Results of test drilling at Newberry volcano, Oregon*: Geothermal Resources Council Bulletin, v. 10, no. 11, p. 3-8.
- Sass, J.H., Lachenbruch, A.H., and Munroe, R.J., 1971, Thermal conductivity of rocks from measurements on fragments and its application to heat flow determinations: *Journal of Geophysical Research*, v. 76, no. 14, p. 3391-3401.
- Sass, J.H., and Sammel, E.A., 1976, Heat flow data and their relation to observed geothermal phenomena near Klamath Falls, Oregon: *Journal of Geophysical Research*, v. 81, no. 26, p. 4863-4868.
- Schaubs, M.P., 1978, *Geology and mineral deposits of the Bohemia mining district, Lane County, Oregon*: Corvallis, Oreg., Oregon State University master's thesis, 135 p.
- Schlicker, H.G., and Finlayson, C.T., 1979, *Geology and geologic hazards of northwestern Clackamas County, Oregon*: Oregon Department of Geology and Mineral Industries Bulletin 99, 79 p.
- Scholz, C.H., Barazangi, M., and Sbar, M.L., 1971, Late Cenozoic evolution of the Great Basin, western United States, as an ensialic interarc basin: *Geological Society of America Bulletin*, v. 82, no. 11, p. 2979-2990.
- Schumacher, C.A., 1981, Index to published geologic mapping in Oregon, 1898-1979: Oregon Department of Geology and Mineral Industries Geological Map Series GMS-14.
- Scott, W.E., 1977, Quaternary glaciation and volcanism, Metolius River area, Oregon: *Geological Society of America Bulletin*, v. 88, no. 1, p. 113-124.
- Sherrod, D.R., Moyle, P.R., Rumse, C.M., and MacLeod, N.S., [in press], *Geology and mineral resource potential of the Diamond Peak Wilderness, Lane and Klamath Counties, Oregon*: U.S. Geological Survey open-file report.
- Smith, J.G., 1979, Cenozoic volcanism in the Cascade Range, Medford 2° sheet, southern Oregon [abs.]: *Geological Society of America Abstracts with Programs*, v. 11, no. 3, p. 128.
- Smith, J.G., and Page, N.J., 1977, Preliminary reconnaissance geologic map of part of Jackson County, Oregon: U.S. Geological Survey Open-File Report 77-318, scale 1:250,000.
- Smith, J.G., Page, N.J., Johnson, M.G., Moring, B.C., and Gray, F., 1982, Preliminary geologic map of the Medford 1°×2° quadrangle, Oregon and California: U.S. Geological Survey Open-File Report 82-955, scale 1:250,000.
- Smith, J.G., Sawlan, M.S., and Katcher, A.C., 1980, An important lower Oligocene welded-tuff marker bed in the Western Cascade Range of southern Oregon [abs.]: *Geological Society of America Abstracts with Programs*, v. 12, no. 3, p. 153.
- Smith, R.L., and Bailey, R.A., 1968, Resurgent cauldrons, in Coats, R.R., Hay, R.L., and Anderson, C.A., eds., *Studies in volcanology*: Boulder, Colo., Geological Society of America Memoir 116, p. 613-662.

- Smith, R.L., and Shaw, H.R., 1973, Volcanic rocks as geologic guides to geothermal exploration and evaluation [abs.]: EOS (American Geophysical Union Transactions), v. 54, no. 11, p. 1213.
- 1979, Igneous-related geothermal systems, in Muffler, L.J.P., ed., Assessment of geothermal resources of the United States—1978: U.S. Geological Survey Circular 790, p. 12-17.
- Sorey, M.L., Lewis, R.E., and Olmsted, F.H., 1978, The hydrothermal system of Long Valley caldera, California: U.S. Geological Survey Professional Paper 1044-A, 60 p.
- Steele, J.L., Blackwell, D.D., and Robison, J.H., 1982, Heat flow in the vicinity of the Mount Hood volcano, Oregon, in Priest, G.R., and Vogt, B.F., eds., Geology and geothermal resources of the Mount Hood area, Oregon: Oregon Department of Geology and Mineral Industries Special Paper 14, p. 31-42.
- Steiner, A., 1977, The Wairakei geothermal area, North Island, New Zealand: Its subsurface geology and hydrothermal rock alteration: New Zealand Geological Survey Bulletin 90, 136 p.
- Stewart, J.H., 1978, Basin-Range structure in western North America: A review, in Smith, R.B., and Eaton, G.P., eds., Cenozoic tectonics and regional geophysics of the Western Cordillera: Boulder, Colo., Geological Society of America Memoir 152, p. 1-31.
- Storch, S.G.P., 1978, Geology of the Blue River mining district, Linn and Lane Counties, Oregon: Corvallis, Ore., Oregon State University master's thesis, 70 p.
- Sutter, J.F., 1978, K-Ar ages of Cenozoic volcanic rocks from the Oregon Cascades west of 121°30': Isochron/West, no. 21, p. 15-21.
- Sutton, K.G., 1974, The geology of Mount Jefferson: Eugene, Ore., University of Oregon master's thesis, 120 p.
- Swanson, F.J., and James, M.E., 1975, Geology and geomorphology of the H.J. Andrews Experimental Forest, Western Cascades, Oregon: Portland, Ore., U.S. Forest Service, Pacific Northwest Forest and Range Experiment Station, 14 p.
- Swanson, D.A., Wright, T.L., Hooper, P.R., and Bentley, R.D., 1979, Revisions in stratigraphic nomenclature of the Columbia River Basalt Group: U.S. Geological Survey Bulletin 1457-G, 59 p.
- Taylor, E.M., 1967, Recent volcanism between Three Fingered Jack and North Sister, Oregon Cascade Range: Pullman, Wash., Washington State University doctoral dissertation, 84 p.
- 1968, Roadside geology, Santiam and McKenzie Pass Highways, Oregon, in Dole, H.M., ed., Andesite Conference guidebook: Oregon Department of Geology and Mineral Industries Bulletin 62, p. 3-33.
- 1973a, Geochronology and structure of the central part of the Cascade Range, Oregon: Unpublished report to Oregon Academy of Science, 31st Annual Meeting, Corvallis, Ore., 1973.
- 1973b, Geology of the Deschutes Basin, in Beaulieu, J.D., field trip committee chairman, Geologic field trips in northern Oregon and southern Washington: Oregon Department of Geology and Mineral Industries Bulletin 77, p. 29-32.
- 1978, Field geology of S.W. Broken Top quadrangle, Oregon: Oregon Department of Geology and Mineral Industries Special Paper 2, 50 p.
- 1980, Volcanic and volcanoclastic rocks on the east flank of the central Cascade Range to the Deschutes River, Oregon, in Oles, K.F., Johnson, J.G., Niem, A.R., and Niem, W.A., eds., Geologic field trips in western Oregon and southwestern Washington: Oregon Department of Geology and Mineral Industries Bulletin 101, p. 1-7.
- 1981, Central High Cascade roadside geology—Bend, Sisters, McKenzie Pass, and Santiam Pass, Oregon, in Johnston, D.A., and Donnelly-Nolan, J., eds., Guides to some volcanic terranes in Washington, Idaho, Oregon, and northern California: U.S. Geological Survey Circular 838, p. 55-58.
- Taylor, H.P., Jr., 1971, Oxygen isotope evidence for large-scale interaction between meteoric ground waters and Tertiary granodiorite intrusions, Western Cascade Range, Oregon: Journal of Geophysical Research, v. 76, no. 32, p. 7855-7874.
- Thayer, T.P., 1936, Structure of the North Santiam River section of the Cascade Mountains in Oregon: Journal of Geology, v. 44, no. 6, p. 701-716.
- 1937, Petrology of later Tertiary and Quaternary rocks of the north-central Cascade Mountains in Oregon, with notes on similar rocks in western Nevada: Geological Society of America Bulletin, v. 48, no. 11, p. 1611-1651.
- 1939, Geology of the Salem Hills and the North Santiam River basin, Oregon: Oregon Department of Geology and Mineral Industries Bulletin 15, 40 p.
- Timm, S., 1979, The structure and stratigraphy of the Columbia River basalt in the Hood River Valley, Oregon: Portland, Ore., Portland State University master's thesis, 60 p.
- U.S. Army Corps of Engineers, 1964, Cougar Reservoir, South Fork McKenzie River, Oregon, foundation report: Portland, Ore., U.S. Army Corps of Engineers, Portland District, var. pag.
- Veen, C.A., 1981, Gravity anomalies and their structural implications for the southern Oregon Cascade Mountains and adjoining Basin and Range province: Corvallis, Ore., Oregon State University master's thesis, 86 p.
- Venkatakrishnan, R., Bond, J.G., and Kauffman, J.D., 1980, Geological linears of the northern part of the Cascade Range, Oregon: Oregon Department of Geology and Mineral Industries Special Paper 12, 25 p.
- Vogt, B.F., 1979, Columbia River Basalt Group stratigraphy and structure in the Bull Run Watershed, Western Cascades, northern Oregon [abs.]: Oregon Academy of Science Proceedings, v. 15, p. 51-52.
- 1981, The stratigraphy and structure of the Columbia River Basalt Group in the Bull Run Watershed, Multnomah and Clackamas Counties, Oregon: Portland, Ore., Portland State University master's thesis, 151 p.
- Walker, G.W., 1977, Geologic map of Oregon east of the 121st meridian: U.S. Geological Survey Miscellaneous Investigations Series Map I-902, scale 1:500,000.
- Walker, G.W., Greene, R.C., and Pattee, E.C., 1966, Mineral resources of the Mount Jefferson Primitive Area, Oregon: U.S. Geological Survey Bulletin 1230-D, 32 p., map scale 1:62,500.
- Waring, G.A. [revised by Blankenship, R.R., and Bantall, R.], 1965, Thermal springs of the United States and other countries of the world—a summary: U.S. Geological Survey Professional Paper 492, p. 38-41.
- Waters, A.C., 1955, Geomorphology of south-central Washington, illustrated by the Yakima East quadrangle: Geological Society of America Bulletin, v. 66, no. 6, p. 663-684.
- 1968a, Reconnaissance geologic map of the Dufur quadrangle, Hood River, Sherman, and Wasco Counties, Oregon: U.S. Geological Survey Miscellaneous Geologic Investigations Map I-556, scale 1:125,000.
- 1968b, Reconnaissance geologic map of the Madras quadrangle, Jefferson and Wasco Counties, Oregon: U.S. Geological

- Survey Miscellaneous Geologic Investigations Map I-555, scale 1:125,000.
- Wells, F.G., 1956, Geology of the Medford quadrangle, Oregon-California: U.S. Geological Survey Geologic Quadrangle Map GQ-89, scale 1:96,000.
- Wells, F.G., and Peck, D.L., 1961, Geologic map of Oregon west of the 121st meridian: U.S. Geological Survey Miscellaneous Investigations Series Map I-325, scale 1:500,000.
- White, C.M., 1980a, Geology of the Breitenbush Hot Springs quadrangle, Oregon: Oregon Department of Geology and Mineral Industries Special Paper 9, 26 p.
- 1980b, Geology and geochemistry of Mt. Hood volcano: Oregon Department of Geology and Mineral Industries Special Paper 8, 26 p.
- 1980c, Geology and geochemistry of volcanic rocks in the Detroit area, Western Cascade Range, Oregon: Eugene, Oreg., University of Oregon doctoral dissertation, 178 p.
- White, C.M., and McBirney, A.R., 1978, Some quantitative aspects of orogenic volcanism in the Oregon Cascades, in Smith, R.B., and Eaton, G.P., eds., *Cenozoic tectonics and regional geophysics of the western Cordillera*: Boulder, Colo., Geological Society of America Memoir 152, p. 369-388.
- Williams, D.L., and Finn, C., 1981a, Evidence from gravity data on the location and size of subvolcanic intrusions: Preliminary results [abs.]: Society of Exploration Geophysicists, 51st Annual International Meeting, Los Angeles, Calif., 1981, Technical Program Abstracts, p. 15.
- 1981b, Gravity anomalies and subvolcanic intrusions in the Cascade Range and at other selected volcanoes: Preliminary results: Unpublished manuscript.
- Williams, D.L., Hull, D.A., Ackermann, H.D., and Beeson, M.H., 1982, The Mount Hood region: Volcanic history, structure, and geothermal energy potential: *Journal of Geophysical Research*, v. 87, no. B4, p. 2767-2781.
- Williams, D.L., and von Herzen, R.P., 1982, On the terrestrial heat flow and physical limnology of Crater Lake, Oregon: *Journal of Geophysical Research*, v. 88, no. B2, p. 1094-1104.
- Williams, H., 1933, Mount Thielsen, a dissected Cascade volcano: Berkeley, Calif., University of California Publications in Geological Sciences, v. 23, no. 6, p. 195-214.
- 1935, Newberry volcano of central Oregon: *Geological Society of America Bulletin*, v. 46, no. 2, p. 253-304.
- 1942, The geology of Crater Lake National Park, Oregon, with a reconnaissance of the Cascade Range southward to Mount Shasta: Carnegie Institution of Washington Publication 540, 162 p.
- 1944, Volcanoes of the Three Sisters region, Oregon Cascades: Berkeley, Calif., University of California Publications in Geological Sciences, v. 27, no. 3, p. 37-83.
- 1949, Geology of the Macdoel quadrangle [California]: California Division of Mines and Geology Bulletin 151, p. 7-60.
- 1953, The ancient volcanoes of Oregon (2nd ed.): Eugene, Oreg., Oregon State System of Higher Education, Condon Lectures, 68 p.
- 1957, A geologic map of the Bend quadrangle, Oregon, and a reconnaissance geologic map of the central portion of the High Cascade Mountains: Oregon Department of Geology and Mineral Industries, 1 sheet, scales 1:125,000 and 1:250,000.
- Wise, W.S., 1969, Geology and petrology of the Mount Hood area: A study of High Cascade volcanism: *Geological Society of America Bulletin*, v. 80, no. 6, p. 969-1006.
- Woller, N.M., 1982, Geology of the Swift Creek area, Lane County, Oregon, in Priest, G.R., and Vogt, B.F., eds., *Geology and geothermal resources of the Cascades, Oregon*: Oregon Department of Geology and Mineral Industries Open-File Report O-82-7, p. 135-151.
- Wozniak, K.C., 1982, Geology of the northern part of the Southeast Three Sisters quadrangle, Oregon: Corvallis, Oreg., Oregon State University master's thesis, 98 p.
- Yamasaki, T., and Hayashi, M., 1976, Geologic background of Otake and other geothermal areas in north-central Kyushu, southwestern Japan, in *Second United Nations Symposium on the Development and Use of Geothermal Resources*, San Francisco, California, 1975, Proceedings: Washington, D.C., U.S. Government Printing Office, v. 1, p. 673-684.
- Yoder, H.S., Jr., 1976, Generation of basaltic magma: Washington, D.C., National Academy of Science, 265 p.
- Yoder, H.S., Jr., and Tilley, C.E., 1962, Origin of basalt magmas: An experimental study of natural and synthetic rock systems: *Journal of Petrology*, v. 3, pt. 3, p. 342-532.
- Youngquist, W.L., 1980, Geothermal gradient drilling, north-central Cascades of Oregon, 1979: Oregon Department of Geology and Mineral Industries Open-File Report O-80-12, 47 p.
- Zoback, M.L., and Thompson, G.A., 1978, Basin and Range rifting in northern Nevada: Clues from a mid-Miocene rift and its subsequent offsets: *Geology*, v. 6, no. 2, p. 111-116.



## APPENDIX A.

NEW K-Ar DATA<sup>1</sup>

Table A.1. New K-Ar data, Oregon

Plate no. <sup>2</sup>	Figure no. <sup>2</sup>	Sample no. on plate/figure <sup>2</sup>	Sample no.	Geologic unit	Material dated	% K	<sup>40</sup> Ar/ <sup>atm</sup>	Moles/g Ar <sup>40</sup> (x10 <sup>11</sup> ) <sup>3</sup>	Age <sup>3</sup> (m.y. ± 1σ)	Township (S.)/Range (E.)/Section <sup>4</sup>	Latitude (N.)	Longitude (W.)
-	3.2	6	Devil 440	Tmo	Whole rock	0.53	87	0.492	5.34±0.58 <sup>5</sup>	10/ 7/11Aa	44°43'24"	121°54'24"
-	3.2	6E	DC-4	Tmp	Whole rock	0.66	90	1.089	9.5 ±1.3	10/ 7/ 2Add	44°44' 9"	121°54'25"
-	3.2	16	DC-114	Tmp	Whole rock	1.61	37	1.762	6.30±0.22	10/ 7/ 4Ddd	44°43'47"	121°56'54"
-	3.2	18	DC-14	Tmp	Whole rock	0.49	91	0.514	6.0 ±0.9	10/ 7/10Dac	44°43' 7"	121°55'46"
2	-	23	Ri-85	Tmrt	Plagioclase	0.349	74	0.838	13.8 ±0.8	16/ 4/36Ddb	44° 7'41"	122°16'18"
2	-	25	Tmwl	Tmw	Whole rock	0.440	93	0.950	12.4 ±2.5 <sup>5</sup>	17/ 5/ 8Bbd	44° 6'12"	122°14'10"
2	-	28	Ri-22	Tmw	Whole rock	1.32	72	3.029	13.2 ±0.7	17/ 5/16Abc	44° 5'49"	122°12'27"
2	-	34	Cougar	Tmvic	Whole rock	0.237	87	0.669	16.2 ±1.8	16/ 5/32Cca	44° 7'43"	122°14'11"
2	-	35	Ri-136	Tmcr	Whole rock	0.755	66	1.2232	9.31±0.44	16/ 5/28Add	44° 8'45"	122°12'30"
2	-	37	Ri-62	Tml	Whole rock	0.48	86	0.651	7.80±0.77	17/ 5/21Abd	44° 4'54"	122°12'19"
2	-	39	Ri-64	Tml	Whole rock	1.39	64	2.274	9.41±0.42	17/ 5/22Cbb	44° 4'38"	122°11'46"
2	-	-	Ri-112 <sup>2</sup>	Tmw	Plagioclase	0.208	65	0.414	11.4 ±0.5	17/ 4/12Bcb	44° 7' 0"	122°17' 7"
-	-	-	Tmw-top	-	Whole rock	1.12	39	1.726	8.80±0.34	16/ 5/ 3Cbd	42°12'11"	122°11'46"
-	-	-	Tpb-L0	-	Whole rock	0.365	61	0.529	8.34±0.36	16/ 5/ 3Bdc	44°12'28"	122°11'31"
-	-	-	Foley Ridge	-	Whole rock	0.548	95	0.193	2.03±0.52	16/ 5/14Bcb	44°10'49"	122°10'35"
-	-	-	MO-159	-	Whole rock	0.332	92	0.392	6.80±1.18	17/6½/21Daa	44° 4'39"	122° 0'20"
-	-	-	MO-160	-	Whole rock	0.357	89	0.476	7.67±0.96	17/6½/21Bcb	44° 4'42"	122° 0'50"
-	-	-	MO-ENG B	-	Whole rock	0.191	86	0.340	10.2 ±1.0	17/ 6/22Ddc	44° 4'12"	122° 3'49"
-	-	-	MO-ENG B	-	Whole rock	0.191	81	0.319	9.6 ±1.5	17/ 6/22Ddc	44° 4'12"	122° 3'49"
-	-	-	MB-133	-	Whole rock	0.432	91	0.167	2.23±0.37	16/ 6/17D	44°10'28"	122° 6'12"
-	5.2	41	BB-16	Totl	Whole rock	0.810	83	3.489	24.7 ±2.0 <sup>5</sup>	20/ 2/26Dda	43°48'02"	122°36'42"
-	5.2	45	BB-30	Tml	Whole rock	0.515	89	1.970	21.9 ±2.9 <sup>5</sup>	20/ 2/22Cda	43°48'40"	122°33'35"
-	5.2	48	BB-35	Tml	Whole rock	0.540	65	2.074	22.0 ±1.0	20/ 2/22Daa	43°48'57"	122°32'58"
-	5.2	52	BB-PAT	Tma	Whole rock	0.100	98	0.145	8.3 ±5.5 <sup>5</sup>	21/ 2/ 7Cbd	43°45'34"	122°37'25"
-	5.2	53	BB-NSH	Tma	Whole rock	0.241	97	0.668	15.9 ±7.6 <sup>5</sup>	20/ 2/14Dda	43°48'56"	122°31'42"
-	5.2	55	BB-PPAT	Tmu	Whole rock	0.91	70	0.918	5.81±0.30	21/ 1/12Aba	43°45'59"	122°37'54"
-	5.2	56	BB-Tpba	QTb	Whole rock	1.18	95	0.114	0.56±0.16	20/ 2/18Abc	43°50' 6"	122°36'56"
-	-	-	OM-5	-	Plagioclase	0.340	65.6	1.2644	21.3 ±1.0 <sup>5</sup>	22/ 4/31Bcc	43°34'15"	122°20' 9"
-	-	-	OM-49	-	Whole rock	0.755	53.1	2.2824	17.3 ±0.7 <sup>5</sup>	20/ 4/19Dac	43°36'41"	122°23'24"
-	-	-	OM-520	-	Plagioclase	0.511	66.7	1.6673	18.7 ±0.9 <sup>5</sup>	23/ 4/ 4Abb	43°48'45"	122°22'15"
3	-	63	T-10	Tmb	Whole rock	1.10	53	2.984	15.6 ±0.6	24/ 4/24Dcb	43°28'29"	122°16'58"
3	-	65	T-14	Tmb	Whole rock	0.66	72	1.957	17.0 ±0.9	24/ 4/ 1Dcd	43°30'53"	122°16'33"
3	-	70	P-624	Tmb	Whole rock	0.89	82	2.095	13.5 ±1.1	23/ 5/30Cda	43°17'40"	122°15'27"
3	-	71	P-626	Tmb	Whole rock	0.87	68	1.985	13.1 ±0.6	23/ 4/25Ddd	43°17'38"	122°16'13"
3	-	72	T-F1ZZ	Tmb	Whole rock	0.80	74	1.964	14.1 ±0.8 <sup>5</sup>	24/ 4/18Cbb	43°29'23"	122°16' 8"
3	-	81	P-509	Tma	Whole rock	0.67	62	2.022	17.3 ±0.8	23/ 5/19Bac	43°34' 6"	122°14'20"
3	-	82	P-616	Tpb	Whole rock	1.25	85	0.937	4.32±0.40	23/ 5/33Ddd	43°31'44"	122°10'30"
3	-	37E	P-PHL	Tpb	Whole rock	0.90	76	0.869	5.56±0.34	23/ 5/16Dcc	43°34'15"	122°13'12"
3	-	36E	P-324	Tpb	Whole rock	0.94	81	0.903	5.53±0.41	23/ 5/14Aab	43°35' 7"	122°10'30"
3	-	83	P-22	QTb	Whole rock	0.71	89	0.244	1.98±0.25	23/ 5/ 9Bbb	43°35'47"	122°13'47"
3	-	84	P-NOTCH	QTb	Whole rock	0.863	96	0.147	0.98±0.34	23/ 5/14Bdd	43°34'41"	122°10'52"
3	-	85	T-208	QTb	Whole rock	0.62	95	0.083	0.77±0.21	24/ 5/16Cda	43°29'11"	122°13'24"
3	-	86	T-210	QTb	Whole rock	0.81	99	0.024	0.17±0.48	24/ 5/18Adc	43°29'36"	122°15' 9"
3	-	87	T-211	QTb	Whole rock	0.68	97	0.115	0.97±0.46	24/ 5/18Ddb	43°29'17"	122°15' 9"
2	-	31	Ri-28	Tmw	Whole rock	0.52	95	0.734	8.1 ±2.3 <sup>5</sup>	17/ 5/ 4Cba	44° 7' 5"	122°12'54"

<sup>1</sup> Stanley H. Evans, Jr., and Francis H. Brown, University of Utah Research Institute, analysts.<sup>2</sup> The map numbers are the sequential sample numbers listed in Appendix B and are plotted on the geologic maps of this report. Unnumbered samples either are from areas outside of the map areas or lack chemical data (i.e., Ri-112).<sup>3</sup> Constants used:  $\lambda_{\beta} = 4.962 \times 10^{-10}/\text{yr}$ ;  $\lambda_{\epsilon} = 0.581 \times 10^{-10}/\text{yr}$ ;  $^{40}\text{K}/\text{K}_{\text{Tot}} = 1.167 \times 10^{-4} \text{ atom/atom}$ .<sup>4</sup> For explanation of township-range location system, see Appendix C.<sup>5</sup> Date may be affected by low-grade rock alteration.

## APPENDIX B.

## CHEMICAL ANALYSES OF ROCK SAMPLES

Table B.1. Rock chemistry, Outerson Mountain-Devils Creek area, Marion County, Oregon. Sample localities are shown on Figure 3.2.

Sample no. on Figure 3.2	1	2	3	4	5	6	7	8 ***	9	10 ***
Geol. unit	Lavas of Outerson Mountain									
Map symbol	Tmo	Tmo	Tmo	Tmo	Tmo	Tmo	Tmo		Tmo	
Field no.	Devil-60'	Devil-120'	Devil-210'	Devil-260'	Devil-340'	Devil-440'	Devil-480'	DC-4	DC-5	DC-1
Location	T10S/R7E/11Aad	T10S/R7E/11Aad	T10S/R7E/11Aad	T10S/R7E/11Aad	T10S/R7E/11Aad	T10S/R7E/11Aad	T10S/R7E/11Aad		T10S/R7E/2A <sub>da</sub>	
SiO <sub>2</sub>	49.60	52.20	51.50	53.00	52.20	53.70	52.80		54.00	
TiO <sub>2</sub>	1.21	1.20	1.17	1.11	1.23	1.14	1.15		1.36	
Al <sub>2</sub> O <sub>3</sub>	19.10	18.54	18.73	17.60	17.70	18.15	18.03		18.72	
Fe <sub>2</sub> O <sub>3</sub>	[ 9.48	[ 9.26	[ 8.74	[ 8.41	[ 9.18	[ 8.66	[ 8.55		[ 8.83	
FeO										
MnO	0.13	0.14	0.14	0.15	0.13	0.13	0.15		0.13	
MgO	5.41	5.23	4.82	4.89	5.32	5.12	4.90		4.63	
CaO	8.11	7.54	8.33	7.99	7.96	8.08	7.83		8.27	
Na <sub>2</sub> O	3.34	3.30	3.40	3.30	3.51	3.57	3.59		3.42	
K <sub>2</sub> O	0.41	0.65	0.48	0.58	0.78	0.61	0.73		0.53	
H <sub>2</sub> O <sup>+</sup>	[ 1.57	[ 1.92	[ 1.36	[ 0.82	[ 0.55	[ 0.64	[ 0.74		[ 1.38	
H <sub>2</sub> O <sup>-</sup>										
P <sub>2</sub> O <sub>5</sub>	0.37	0.36	0.35	0.35	0.34	0.35	0.37		0.34	
Total	98.73	100.34	99.02	98.20	98.90	100.15	98.84		101.61	
Total FeO*	9.76	9.41	8.95	8.64	9.33	8.70	8.72		8.81	
CIPW norms										
Q	0.55	6.28	3.10	5.83	1.40	4.25	3.59		5.85	
Or	2.42	3.84	2.84	3.43	4.61	3.60	4.31		3.13	
Ab	28.30	27.90	28.80	27.90	29.70	30.20	30.40		28.90	
an	35.90	29.00	34.40	31.40	30.40	31.70	30.90		34.20	
Di(C)	1.79	( 1.78)	4.00	5.15	5.85	5.20	4.79		3.86	
Hy	21.40	21.60	18.10	17.50	18.80	18.20	17.80		17.40	
Ol	0.00	0.00	0.00	0.00	0.00	0.00	0.00		0.00	
Mt	3.00	2.93	2.77	2.67	2.90	2.75	2.71		2.80	
Il	2.30	2.28	2.22	2.11	2.34	2.17	2.18		2.58	
Trace elements										
(ppm)										
Rb	-----	-----	-----	-----	-----	-----	-----		-----	
Ba	340	394	331	385	358	394	412		331	
Sr	652	628	659	637	629	665	657		599	
Co	27	27	30	26	32	72	35		35	
Ni	73	69	67	62	77	63	54		43	
Cr	99	84	92	98	107	79	72		66	
Zn	82	85	76	86	79	77	77		74	
Cu	64	58	59	66	70	58	53		44	
Li	15	12	16	11	8	11	11		13	

\*Total iron recalculated to Fe<sup>+2</sup>, volatile-free.

\*\*Outside map area.

\*\*\* Reassigned to unit Tmpu; see Table B.5.

## APPENDIX B.

## CHEMICAL ANALYSES OF ROCK SAMPLES

Table B.1. Rock chemistry, Outerson Mountain-Devils Creek area, Marion County, Oregon. Sample localities are shown on Figure 3.2.--Continued

Sample no. on Figure 3.2	11	12	13	14	15	16	17	18	(Not on map) Pigeon Prairie
Geol. unit	Tuffs of Outerson Mountain					Upper Miocene-Pliocene lavas			
Map symbol	Tmt	Tmt	Tmt	Tmt	Tmt	Tmp	Tmp	Tmp	----
Field no.	DC-103	DC-104	DC-105	DC-107	DC-109B	DC-114	DC-111	DC-14	P.P.
Location	T10S/R7E/9Caa	T10S/R7E/9Dbb	T10S/R7E/9Dbb	T10S/R7E/9Dbb	T10S/R7E/9Dbb	T10S/R7E/4Ddd	T10S/R7E/9Ac	T10S/R7E/10Dac	---
SiO <sub>2</sub>	64.18	60.70	61.49	55.29	68.60	56.10	52.80	53.40	48.60
TiO <sub>2</sub>	0.50	1.17	0.73	1.54	0.38	1.14	1.40	1.45	1.23
Al <sub>2</sub> O <sub>3</sub>	18.12	16.40	15.78	16.35	14.99	17.76	17.38	17.09	17.06
Fe <sub>2</sub> O <sub>3</sub>	[ 3.59	[ 6.47	[ 4.98	[ 7.79	[ 3.17	[ 8.44	[ 9.90	[ 9.47	3.87
FeO									6.21
MnO	0.09	0.11	0.15	0.12	0.06	0.16	0.14	0.14	0.19
MgO	4.84	2.63	1.86	2.91	1.32	3.86	5.31	4.61	7.58
CaO	2.89	4.69	2.98	7.07	2.24	7.52	9.11	8.85	9.55
Na <sub>2</sub> O	1.07	3.82	3.61	2.12	2.74	3.83	3.36	3.49	3.36
K <sub>2</sub> O	0.42	1.79	2.67	1.58	4.70	2.57	0.66	0.70	0.43
H <sub>2</sub> O <sup>+</sup>	[ 7.06	[ 3.50	[ 4.76	[ 6.17	[ 3.96	[ 0.22	[ 0.00	[ 0.55	[ ----
H <sub>2</sub> O <sup>-</sup>									
P <sub>2</sub> O <sub>5</sub>	0.05	0.25	0.12	0.34	0.06	0.57	0.31	0.26	0.39
Total	102.81	101.53	99.13	101.28	102.22	102.17	100.37	100.01	98.47
Total FeO*	3.75	6.60	5.28	8.19	3.23	8.28	9.86	9.52	9.88
CIPW norms									
Q	41.50	15.80	19.30	15.90	26.60	2.22	2.80	4.33	0.00
Or	2.48	10.60	15.80	9.34	27.80	15.20	3.90	4.14	2.58
Ab	9.05	32.30	30.60	17.90	23.20	32.40	28.40	29.15	28.92
An	14.20	21.90	14.20	30.40	11.00	23.70	30.40	28.90	30.71
Di(C)	(10.3 )	( 0.15)	( 1.75)	2.27	( 1.36)	8.64	10.60	11.10	12.08
Hy	15.40	12.00	9.23	12.50	6.30	13.10	17.00	14.40	6.08
Ol	0.00	0.00	0.00	0.00	0.00	0.00	0.00	0.00	12.86
Mt	1.13	2.04	1.58	2.46	1.00	2.67	3.15	3.00	3.48
Il	0.95	2.22	1.39	2.92	0.72	2.17	2.66	2.75	2.38
Trace elements									
(ppm)									
Rb	----	----	----	----	----	----	----	----	5
Ba	242	403	465	287	752	1110	269	242	279
Sr	297	447	322	674	269	1312	578	548	581
Co	38	27	70	126	25	34	48	78	59
Ni	6	11	9	13	11	39	45	22	158
Cr	< 2	10	8	6	10	46	83	63	283
Zn	66	83	84	87	54	81	67	65	88
Cu	13	21	15	31	17	91	53	60	59
Li	29	14	16	7	20	12	7	6	10

\*Total iron recalculated to Fe<sup>+2</sup>, volatile-free.

\*\*Outside map area.



## APPENDIX B.

## CHEMICAL ANALYSES OF ROCK SAMPLES

Table B.2. Rock chemistry, Cougar Reservoir area, Lane County, Oregon. Sample localities are shown on Plate 2.

Sample no. on Plate 2.	19	20	21	22	23	24	25	26	27
Geol. unit	Tuffs of Cougar Reservoir				Tuffs of Rush Creek		Andesites of Walker Creek		
Map symbol	Totc Ri-LB	Totc Ri-87	Totc Ri-149	Totc Ri-150	Tmrt Ri-85	Tmrt Ri-99a	Tmw Tmw1	Tmw Ri-40	Tmw Ri-43
Field no.	T16S/R4E/36Ddd	T17S/R4E/1Aad	T16S/R5E/29Bca	T16S/R5E/30Add	T16S/R4E/36Ddb	T17S/R4E/14Dda	T17S/R5E/8Bbd	T17S/R5E/15Cab	T17S/R5E/15AcB
Location									
SiO <sub>2</sub>	55.60	58.70	71.46	64.03	61.42	60.66	54.86	57.22	61.08
TiO <sub>2</sub>	0.82	1.47	0.36	0.48	0.44	0.60	0.88	0.89	0.86
Al <sub>2</sub> O <sub>3</sub>	15.71	15.47	15.15	12.10	12.83	15.01	17.03	17.12	17.04
Fe <sub>2</sub> O <sub>3</sub>	-----	2.55	2.36	2.71	1.88	2.00	2.12	3.21	2.45
FeO	5.35	4.68	0.40	0.71	0.92	1.56	4.70	3.62	2.80
MnO	0.10	0.13	0.09	0.03	0.04	0.08	0.13	0.12	0.10
MgO	2.52	2.39	0.38	1.30	1.69	1.85	5.29	4.02	2.47
CaO	5.08	6.30	1.66	4.65	3.59	4.38	8.41	7.22	5.59
Na <sub>2</sub> O	4.42	3.64	4.85	0.43	1.25	2.72	3.00	3.89	3.56
K <sub>2</sub> O	1.81	1.33	2.31	2.06	1.88	1.91	0.49	1.20	2.06
H <sub>2</sub> O <sup>+</sup>	[ 6.06	1.30	0.95	5.31	5.61	3.43	0.88	0.40	1.18
H <sub>2</sub> O <sup>-</sup>		2.12	0.87	5.87	8.70	6.13	1.13	1.05	0.37
P <sub>2</sub> O <sub>5</sub>	0.19	0.49	0.11	0.06	0.07	0.10	0.16	0.17	0.19
Total	97.66	100.57	100.95	99.74	100.32	100.43	99.08	100.13	99.75
Total FeO*	5.84	7.20	2.55	3.55	3.05	3.71	6.82	6.62	5.10
CIPW norms									
Q		15.60	30.37	45.81	41.66	26.64	9.16	7.99	15.84
Or		8.10	13.85	13.78	12.96	12.43	2.99	7.22	12.43
Ab		31.77	41.63	4.12	12.29	25.33	26.17	33.39	30.76
An		22.59	7.63	25.66	20.20	23.22	32.52	26.10	24.88
Di(C)		5.25	( 1.94)	( 0.96)	( 2.77)	( 0.83)	7.62	7.49	1.76
Hy		10.14	2.73	7.23	7.90	8.73	17.04	13.38	10.44
Ol		0.00	0.00	0.00	0.00	0.00	0.00	0.00	0.00
Mt		2.53	0.90	1.26	1.07	1.31	2.40	2.33	1.80
Il		2.87	0.69	1.03	0.97	1.26	1.72	1.71	1.67
Trace elements									
(ppm)									
Rb	----	24	47	35	47	41	9	22	27
Ba	269	387	497	467	611	530	180	337	578
Sr	343	476	189	913	453	333	628	642	503
Co	17	18	20	3.0	22	33	47	39	31
Ni	13	11	10	7.8	7	12	6	52	21
Cr	16	11	10	12	12	14	132	27	17
Zn	46	85	51	46	49	51	63	78	74
Cu	32	33	18	20	16	17	53	66	26
Li	22	7.5	26	24	13	135	9	13	10

\*Total iron recalculated to Fe<sup>+2</sup>, volatile-free.

## APPENDIX B.

## CHEMICAL ANALYSES OF ROCK SAMPLES

Table B.2. Rock chemistry, Cougar Reservoir area, Lane County, Oregon. Sample localities are shown on Plate 2.--Continued

Sample no. on Plate 2	28	29	30	31	32	33	34	35	36
Geol. unit	Andesites of Walker Creek			Basaltic lavas of the East Fork			Dacite intrusive of Cougar Dam	Andesites of Castle Rock	Lavas of Tipsoo Butte
Map symbol	Tmw	Tmw	Tmw	Tme	Tme	Tme	Tmvic	Tmcr	Tml
Field no.	Ri-22	Ri-60	Ri-146	Ri-28	Ri-34a	EFKA	Cougar Dam	Ri-136	Ri-45
Location	T17S/R5E/16Abb	T17S/R5E/16Ca	T18S/R4E/1Dd	T17S/R5E/4Cba	T17S/R5E/9Daa	T17S/R5E/4Cab	T16S/R5E/32Cca	T16S/R5E/28Acd	T17S/R5E/15Ad
SiO <sub>2</sub>	59.10	59.60	58.77	51.66	51.47	53.41	61.95	58.66	51.32
TiO <sub>2</sub>	0.85	0.84	0.95	1.01	1.06	0.90	1.10	1.06	1.47
Al <sub>2</sub> O <sub>3</sub>	18.20	18.53	19.97	16.70	16.83	16.83	15.32	16.95	16.26
Fe <sub>2</sub> O <sub>3</sub>	-----	-----	2.53	3.83	2.61	3.19	1.81	3.06	4.42
FeO	6.69	6.56	3.50	5.03	5.93	4.45	3.94	3.26	6.80
MnO	0.09	0.15	0.12	0.14	0.14	0.13	0.12	0.10	0.18
MgO	3.23	3.14	2.17	7.65	7.37	6.54	2.36	3.14	5.30
CaO	6.49	5.72	6.28	8.92	8.61	8.85	5.10	6.56	7.90
Na <sub>2</sub> O	3.94	3.80	4.21	3.26	3.34	3.24	4.65	3.85	3.45
K <sub>2</sub> O	1.77	1.78	1.12	0.61	0.77	0.79	1.08	0.94	1.09
H <sub>2</sub> O <sup>+</sup>	[ 0.40	[ 0.99	0.69	0.64	1.00	0.74	2.23	0.65	0.57
H <sub>2</sub> O <sup>-</sup>			0.85	0.76	0.94	1.33	0.57	0.97	0.47
P <sub>2</sub> O <sub>5</sub>	0.16	0.16	0.27	0.14	0.18	0.11	0.21	0.19	0.64
Total	100.92	101.27	100.43	100.35	100.25	100.51	100.44	99.39	99.87
Total FeO*	6.66	6.54	5.84	8.59	8.44	7.46	5.72	6.15	10.95
CIPW norms									
Q	9.20	11.20	11.47	0.00	0.00	2.70	16.24	13.21	1.02
Or	10.50	10.50	6.64	3.67	4.61	4.74	6.54	5.68	6.51
Ab	33.30	32.2	35.67	27.97	28.79	27.89	40.32	33.40	29.59
An	26.80	27.7	29.47	29.46	29.16	29.58	18.18	26.84	26.02
Di(C)	3.85	0.21	0.00	11.68	10.63	11.63	5.23	4.31	7.77
Hy	12.3	14.00	11.21	19.70	18.63	18.87	8.85	11.89	20.90
Ol	0.00	0.00	0.00	2.23	2.74	0.00	0.00	0.00	0.00
Mt	2.12	2.07	2.04	3.02	2.97	2.63	2.01	2.17	3.85
Il	1.61	1.60	1.81	1.94	2.05	1.73	2.14	2.06	2.84
Trace elements									
(ppm)									
Rb	-----	-----	-----	8.8	8.5	14	31	16	12
Ba	358	546	505	196	171	380	355	365	696
Sr	643	512	524	418	407	491	313	458	594
Co	35	63	33	42	44	47	24	42	50
Ni	29	13	24	147	140	46	21	33	96
Cr	30	24	14	378	304	331	16	59	125
Zn	52	65	70	77	84	74	74	87	103
Cu	45	46	50	41	172	38	30	80	94
Li	9	15	17	12	9.8	9.9	6.2	13	12

\*Total iron recalculated to Fe<sup>+2</sup>, volatile-free.

## APPENDIX B.

## CHEMICAL ANALYSES OF ROCK SAMPLES

Table B.2. Rock chemistry, Cougar Reservoir area, Lane County, Oregon. Sample localities are shown on Plate 2.--Continued

Sample no. on Plate 2	37	38	39	40
Geol. unit	Lavas of Tipsoo Butte			
Map symbol	Tm1	Tm1	Tm1	Tm1
Field no.	Ri-62	Ri-64	Ri-63	Ri-46
Location	T17S/R5E/21Aca	T17S/R5E/22Bcc	T17S/R5E/21Abd	T17S/R5E/15Ada
SiO <sub>2</sub>	47.35	53.42	47.64	48.20
TiO <sub>2</sub>	2.37	1.26	1.46	1.36
Al <sub>2</sub> O <sub>3</sub>	16.69	16.93	16.90	17.81
Fe <sub>2</sub> O <sub>3</sub>	2.98	2.38	1.99	-----
FeO	8.84	6.86	9.21	11.86
MnO	0.20	0.17	0.20	0.18
MgO	6.29	4.29	7.87	7.97
CaO	8.50	7.52	9.72	9.34
Na <sub>2</sub> O	3.21	3.83	2.42	2.31
K <sub>2</sub> O	0.61	1.64	0.38	0.38
H <sub>2</sub> O <sup>+</sup>	1.00	0.46	0.79	[ 1.53
H <sub>2</sub> O <sup>-</sup>	0.75	0.07	0.53	
P <sub>2</sub> O <sub>5</sub>	0.68	0.87	0.47	0.32
Total	99.47	99.70	99.58	101.26
Total FeO*	11.84	9.03	11.22	11.89
CIPW norms				
Q	0.00	2.19	0.00	0.00
Or	3.66	9.76	2.30	2.25
Ab	27.76	32.71	20.80	19.26
An	30.06	24.36	34.72	37.10
Di(C)	6.98	6.24	9.10	5.91
Hy	14.69	17.12	19.81	23.5
Ol	6.46	0.00	5.41	3.48
Mt	4.16	3.20	3.94	3.76
Il	4.62	2.41	2.81	2.58
Trace elements				
(ppm)				
Rb	1.5	15	5.9	-----
Ba	733	878	317	233
Sr	571	636	398	295
Co	51	38	49	44
Ni	105	46	129	127
Cr	124	63	350	211
Zn	116	101	83	66
Cu	98	81	72	73
Li	12	13	8.3	8

\*Total iron recalculated to Fe<sup>+2</sup>, volatile-free.

## APPENDIX B.

## CHEMICAL ANALYSES OF ROCK SAMPLES

Table B.3. Rock chemistry, Lookout Point area, Lane County, Oregon. Sample localities are shown on Figure 5.2.

Sample no. on Figure 5.2	41	42	43	44	45	46	47	48	49
	Oligocene-lower Miocene		Lavas of	Lavas of			Lavas of Black Canyon		
Geol. unit	tuffs and lavas		Lookout Point	Hardesty Mtn.					
Map symbol	Totl	Totl	Tolp	Toh	Tml	Tml	Tml	Tml	Tml
Field no.	BB-16	BB-21	Tolpa	BB-203	BB-30	BB-32	BB-33	Stack (BB-35)	BB-36
Location	T20S/R2E/26Dad	T20S/R2E/35Add	T20S/R2E/35Cbd	T20S/R1E/23Bdb	T20S/R2E/22Cda	T20S/R2E/22Cad	T20S/R2E/22Cad	T20S/R2E/22Daa	T20S/R2E/23Cca
SiO <sub>2</sub>	55.00	70.00	67.86	57.83	50.11	52.22	55.23	56.62	58.42
TiO <sub>2</sub>	0.64	0.97	0.81	1.08	1.53	1.27	1.22	1.95	1.44
Al <sub>2</sub> O <sub>3</sub>	16.57	14.48	14.05	15.39	16.74	17.72	16.01	14.32	15.52
Fe <sub>2</sub> O <sub>3</sub>	3.55	3.40	0.31	7.23	7.68	4.43	4.07	4.32	0.16
FeO	3.91	0.85	0.88	1.74	3.35	5.97	6.25	5.79	7.84
MnO	0.16	0.07	0.10	0.12	0.27	0.18	0.18	0.19	0.15
MgO	5.72	0.27	1.23	1.93	3.82	3.56	3.93	3.25	2.89
CaO	9.24	2.61	3.42	5.94	7.30	8.53	7.85	6.77	6.28
Na <sub>2</sub> O	2.52	4.29	3.98	3.38	4.65	3.30	3.59	4.02	4.07
K <sub>2</sub> O	0.90	1.49	1.55	1.01	0.58	0.51	0.66	0.62	0.84
H <sub>2</sub> O <sup>+</sup>	-----	-----	1.89	1.26	2.02	0.88	0.30	0.76	0.47
H <sub>2</sub> O <sup>-</sup>	-----	-----	0.53	2.08	2.51	1.32	0.70	1.34	1.19
P <sub>2</sub> O <sub>5</sub>	0.20	0.20	0.19	0.32	0.40	0.29	0.27	0.35	0.46
Total	98.41	98.63	96.80	99.31	100.96	100.18	100.26	100.30	99.72
Total Fe*	7.26	3.98	1.23	8.60	10.72	10.21	10.03	9.82	8.14
CIPW norms									
Q	8.51	32.92	31.82	17.23	0.00	5.45	7.67	11.21	13.18
Or	5.41	8.95	9.71	6.25	3.57	3.08	3.94	3.74	5.05
Ab	21.71	36.90	36.68	29.97	41.03	28.56	30.66	34.71	35.05
An	31.81	11.83	16.66	24.98	24.08	32.76	25.86	19.59	21.98
Di(C)	10.99	( 1.57)	( 0.07)	3.13	9.10	7.14	9.68	10.26	5.53
Hy	17.31	4.09	3.54	12.48	8.75	16.27	15.72	12.42	12.47
Ol	0.00	0.00	0.00	0.00	5.71	0.00	0.00	0.00	0.00
Mt	2.55	1.40	0.43	3.05	3.77	3.59	3.53	3.48	2.86
Il	1.24	1.87	1.63	2.15	3.03	2.47	2.34	3.78	2.78
Trace elements									
(ppm)									
Rb	21	36	59	19	9.1	8.5	11	1.0	13
Ba	250	469	411	243	160	183	213	250	305
Sr	470	226	221	357	360	416	421	407	417
Co	43	23	13.3	24	34	41	40	33	28
Ni	35	3	12	13	19	38	17	15	8.5
Cr	160	11	11	13	26	12	13	11	11
Zn	74	90	90	88	108	97	97	119	102
Cu	40	29	29	30	9.7	133	25	41	9.0
Li	15	24	15	12	39	5.9	13	8.6	24

\*Total iron recalculated to Fe<sup>+2</sup>, volatile-free.



## APPENDIX B.

## CHEMICAL ANALYSES OF ROCK SAMPLES

Table B.3. Rock chemistry, Lookout Point area, Lane County, Oregon. Sample localities are shown on Figure 5.2.--Continued

Sample no. on Figure 5.2	50	51	52	53	54	55	56
Geol. unit	Lavas of Black Canyon	←←←←←Miocene	andesitic	lavas→→→→→	Miocene-andesitic intrusives	Upper Miocene lavas	Pliocene- Pleistocene(?) basaltic lavas
Map symbol	Tm1	Tma	Tma	Tma	Tmi	Tmu	QTb
Field no.	BB-227	BB-37	BB-PAT	BB-NSH	BB-SSL	BB-PPAT	BB-Tpba
Location	T20S/R2E/33Bda	T20S/R2E/23Bdc	T21S/R2E/7Cbd	T20S/R2E/14Dda	T20S/R2E/20	T21S/R1E/12Aba	T20S/R2E/18Acba
SiO <sub>2</sub>	57.00	55.99	58.97	67.28	60.64	51.30	54.42
TiO <sub>2</sub>	1.17	1.29	1.07	0.85	1.41	1.34	1.23
Al <sub>2</sub> O <sub>3</sub>	15.88	16.15	16.85	15.63	15.23	16.23	17.11
Fe <sub>2</sub> O <sub>3</sub>	5.69	2.72	3.84	3.49	2.78	-----	4.03
FeO	4.06	4.52	3.00	0.75	4.08	10.07	2.83
MnO	0.17	0.14	0.14	0.09	0.15	0.15	0.10
MgO	2.82	3.16	2.61	0.79	2.12	8.32	6.00
CaO	7.12	8.01	6.51	3.36	5.72	8.28	8.60
Na <sub>2</sub> O	3.84	3.47	3.99	4.68	4.03	3.38	4.18
K <sub>2</sub> O	0.65	0.63	1.00	1.98	1.12	1.25	1.37
H <sub>2</sub> O <sup>+</sup>	-----	1.50	-----	0.80	0.93	[ 0.00	0.15
H <sub>2</sub> O <sup>-</sup>	-----	2.05	-----	0.83	1.45		0.15
P <sub>2</sub> O <sub>5</sub>	0.32	0.29	0.29	0.21	0.34	0.38	0.45
Total	98.72	99.92	98.27	100.74	100.00	100.70	100.62
Total Fe*	9.35	7.25	6.60	3.94	6.77	10.00	6.46
CIPW norms							
Q	11.34	12.15	13.38	23.34	17.42	0.00	0.00
Or	3.91	3.87	6.03	11.84	6.79	7.39	8.09
Ab	53.03	30.50	34.44	40.06	34.97	28.60	35.34
An	24.57	27.66	25.62	15.47	20.68	25.40	23.86
Di(C)	7.70	9.59	4.46	( 0.18)	5.11	11.00	12.75
Hy	13.15	10.44	11.01	5.60	9.10	11.40	12.73
Ol	0.00	0.00	0.00	0.00	0.00	9.63	1.56
Mt	3.29	2.55	2.32	1.39	2.38	3.19	2.27
Il	2.26	2.55	2.07	1.63	2.75	2.54	2.33
Trace elements							
(ppm)							
Rb	14	10	20	47	23	-----	8.4
Ba	213	418	312	266	379	502	650
Sr	476	588	509	280	304	987	451
Co	33	31	25	15	23	50	30
Ni	3	11	11	10	16	161	139
Cr	6.5	15	22	11	14	236	255
Zn	116	97	95	80	97	90	86
Cu	12.8	47	32	7.4	55	67	75
Li	9.4	8.3	12	24	20	9	12

\*Total iron recalculated to Fe<sup>+2</sup>, volatile-free.

## APPENDIX B.

## CHEMICAL ANALYSES OF ROCK SAMPLES

Table B.4. Rock chemistry, Waldo Lake-Swift Creek area, Lane County, Oregon. Sample localities are shown on Plate 3.

Sample no. on Plate 3	(Not on map)								
	57	58	59	60	61	62	63	64**	65
Geol. unit	Basaltic lavas of Tumblebug Creek								
Map symbol	Tmb	Tmb	Tmb	Tmb	Tmb	Tmb	Tmb	Tmb	Tmb
Field no.	T-1	T-2	T-3	T-4	T-7	T-9	T-10	T-13	T-14
Location	T24S/R4E/13Ada	T24S/R5E/19Baa	T24S/R5E/19Dbc	T24S/R4E/24Ddb	T24S/R5E/19Cba	T24S/R4E/24Dbc	T24S/R4E/24Caa	T24S/R4E/25Abd	T24S/R4E/1Dcc
SiO <sub>2</sub>	49.40	54.40	53.20	53.40	52.80	51.60	54.85	53.20	53.60
TiO <sub>2</sub>	1.25	1.36	1.08	1.03	1.03	1.42	1.13	1.01	0.91
Al <sub>2</sub> O <sub>3</sub>	16.12	16.57	17.40	16.43	17.75	17.14	17.06	17.58	17.54
Fe <sub>2</sub> O <sub>3</sub>	6.02	6.38	3.70	3.18	3.17	4.02	4.31	4.31	4.49
FeO	3.08	2.65	5.09	5.56	5.58	5.19	3.36	3.85	3.77
MnO	0.17	0.16	0.18	0.16	0.16	0.17	0.15	0.16	0.16
MgO	6.40	5.37	5.21	6.56	5.32	6.13	4.47	5.32	5.22
CaO	7.99	8.62	8.32	8.63	9.00	8.50	8.60	8.50	8.53
Na <sub>2</sub> O	3.18	3.48	3.53	3.26	3.67	3.50	3.43	3.24	3.55
K <sub>2</sub> O	1.59	1.05	1.00	0.67	0.73	0.66	1.24	0.83	0.83
H <sub>2</sub> O <sup>+</sup>	-----	-----	-----	-----	-----	-----	-----	-----	-----
H <sub>2</sub> O <sup>-</sup>	-----	-----	-----	-----	-----	-----	-----	-----	-----
P <sub>2</sub> O <sub>5</sub>	0.64	0.55	0.63	0.33	0.39	0.33	0.32	0.37	0.38
Total	95.84	100.59	99.34	99.21	99.60	98.66	98.92	98.37	98.98
Total FeO*	8.92	8.39	8.51	8.51	8.49	8.97	7.35	7.89	7.93
CIPW norms									
Q	0.00	4.12	2.81	3.16	1.11	0.64	5.52	4.34	3.23
Or	9.84	6.20	5.96	4.00	4.34	3.96	7.43	5.00	4.97
Ab	28.19	29.40	30.12	27.84	31.21	30.08	29.42	27.94	30.43
An	26.21	26.45	28.92	28.48	29.96	29.56	27.86	31.57	29.86
Di(C)	8.88	10.32	6.99	10.19	10.10	9.00	10.82	7.29	8.56
Hy	14.81	16.41	18.68	20.61	17.43	20.10	13.44	18.27	17.53
Ol	4.89	0.00	0.00	0.00	0.00	0.00	0.00	0.00	0.00
Mt	3.14	2.95	2.99	3.00	2.99	3.15	2.59	2.78	2.79
Il	2.49	2.58	2.07	1.97	1.97	2.74	2.18	1.96	1.75
Trace elements									
(ppm)									
Rb	25	14	11	6.5	5.0	6.2	21	10	10
Ba	708	438	456	267	409	311	483	598	400
Sr	745	819	854	759	815	569	508	538	560
Co	42	48	65	55	66	53	46	58	42
Ni	97	81	72	150	67	129	68	89	75
Cr	156	154	106	224	106	133	96	118	101
Zn	93	90	98	86	90	84	78	86	87
Cu	66	71	68	72	54	62	77	73	75
Li	13	11	11	8.3	9.5	8.8	9.1	9.1	9.9

\*Total iron recalculated to Fe<sup>+2</sup>, volatile-free.

\*\* Outside map area.

## APPENDIX B.

## CHEMICAL ANALYSES OF ROCK SAMPLES

Table B.4. Rock chemistry, Waldo Lake-Swift Creek area, Lane County, Oregon. Sample localities are shown on Plate 3.--Continued

Sample no. on Plate 3	66	67	69**	70	71	72	73	74
Geol. unit	Basaltic lavas of Tumblebug Creek						Andesitic lavas of Moss Mountain	
Map symbol	Tmb	Tmb	Tmb	Tmb	Tmb	Tmb	Tma	Tma
Field no.	T-19	T-25	P-50	P-624	P-626	T-FIZZ	P-Tmo	P-604
Location	T24S/R5E/6Bac	T24S/R4E/2Ccntr.	T24S/R5E/28Cdd	T23S/R5E/30Cad	T23S/R5E/30Ccc	T24S/R5E/18Cbb	T23S/R5E/8Baa	T23S/R5E/9Acc
SiO <sub>2</sub>	53.20	51.00	53.93	53.40	56.00	53.93	55.70	56.50
TiO <sub>2</sub>	0.76	1.31	1.12	1.11	1.07	1.04	0.95	0.94
Al <sub>2</sub> O <sub>3</sub>	17.27	18.10	17.01	17.36	17.61	16.65	18.54	18.61
Fe <sub>2</sub> O <sub>3</sub>	5.21	4.91	3.03	3.07	-----	5.74	[ 7.83	[ 7.69
FeO	4.01	4.38	4.70	4.67	8.24	2.22		
MnO	0.17	0.18	0.15	0.15	0.13	0.15	0.13	0.06
MgO	6.04	6.23	4.79	4.76	4.97	4.36	4.48	3.74
CaO	8.46	8.46	8.25	8.67	7.91	7.96	7.63	6.60
Na <sub>2</sub> O	3.65	3.23	3.27	3.39	3.34	3.46	3.28	2.76
K <sub>2</sub> O <sup>+</sup>	0.61	0.56	1.02	1.06	1.12	1.25	0.89	0.79
H <sub>2</sub> O <sup>+</sup>	-----	-----	-----	-----	[ ( 0.21)	-----	[ 0.89	[ 2.48
H <sub>2</sub> O <sup>-</sup>	-----	-----	-----	-----				
P <sub>2</sub> O <sub>5</sub>	0.36	0.40	0.26	0.30	0.30	0.54	0.30	0.15
Total	99.74	98.76	97.53	97.94	100.90	97.30	100.62	100.32
Total FeO*	8.77	8.95	7.64	7.61	8.18	7.64	7.85	7.86
CIPW norms								
Q	1.37	1.01	5.89	4.02	6.82	5.78	8.21	14.80
Or	3.63	3.36	6.19	6.40	6.68	7.62	5.20	4.67
Ab	31.06	27.75	28.41	29.33	28.30	30.21	27.80	23.4
An	29.10	33.75	29.49	29.67	29.70	27.05	33.30	32.0
Di(C)	8.77	5.06	8.80	10.03	6.38	8.23	2.38	( 1.49)
Hy	20.70	22.46	15.75	15.01	16.90	15.09	17.40	16.42
Ol	0.00	0.00	0.00	0.00	0.00	0.00	0.00	0.00
Mt	3.08	3.15	2.69	2.68	2.61	2.69	2.48	2.44
Il	1.45	2.53	2.18	2.16	2.03	2.04	1.80	1.82
Trace elements								
(ppm)								
Rb	6.2	2.0	16	15		21	---	---
Ba	339	477	399	417	375	559	293	179
Sr	598	538	514	561	563	556	694	602
Co	52	62	42	45	32	33	34	17
Ni	134	142	54	66	49	60	43	22
Cr	190	270	45	80	81	86	44	34
Zn	89	92	88	84	74	95	73	61
Cu	58	53	61	63	63	59	66	34
Li	9.8	9.2	6.5	7.8	9	7.8	6	13

\*Total iron recalculated to Fe<sup>+2</sup>, volatile-free.

\*\*In this report, there is no sample 68 on Plate 3.

## APPENDIX B.

## CHEMICAL ANALYSES OF ROCK SAMPLES

Table B.4. Rock chemistry, Waldo Lake-Swift Creek area, Lane County, Oregon. Sample localities are shown on Plate 3.--Continued

Sample no. on Plate 3	75	76	77	78	79	80	81	82
Geol. unit	Andesitic lavas of Moss Mountain							Miocene-Pliocene basaltic lavas
Map symbol	Tma	Tma	Tma	Tma	Tma	Tma	Tma	Tpb
Sample no.	P-21	P-28	P-32	P-33	P-39	P-40	P-509	P-616
Location	T23S/R5E/9Bbd	T23S/R5E/20Bdc	T23S/R5E/19AcB	T23S/R5E/19Aca	T23S/R5E/19Bda	T23S/R5E/20Bdd	T23S/R5E/19Bac	T23S/R5E/33Ddd
SiO <sub>2</sub>	53.50	55.70	55.78	55.60	52.60	56.15	56.29	51.20
TiO <sub>2</sub>	0.73	0.92	0.95	0.90	0.92	0.62	0.84	0.76
Al <sub>2</sub> O <sub>3</sub>	19.29	18.58	18.31	18.01	19.96	18.37	18.27	17.53
Fe <sub>2</sub> O <sub>3</sub>	3.93	4.04	2.13	3.62	3.57	4.04	3.36	5.12
FeO	3.26	2.85	4.98	3.53	3.66	3.05	3.62	4.32
MnO	0.17	0.12	0.12	0.13	0.13	0.12	0.10	0.17
MgO	3.80	4.17	4.60	4.36	3.77	4.20	4.32	7.30
CaO	8.78	7.55	8.28	7.91	9.08	7.62	7.91	8.78
Na <sub>2</sub> O	3.67	3.42	3.55	3.54	3.77	3.58	3.53	3.43
K <sub>2</sub> O	0.60	0.71	0.70	0.74	0.45	0.72	0.73	0.70
H <sub>2</sub> O <sup>+</sup>	-----	-----	-----	-----	-----	-----	0.84	-----
H <sub>2</sub> O <sup>-</sup>	-----	-----	-----	-----	-----	-----	0.50	-----
P <sub>2</sub> O <sub>5</sub>	0.17	0.15	0.14	0.15	0.14	0.15	0.14	0.27
Total	97.90	98.21	99.54	98.49	98.05	98.62	100.45	99.58
Total FeO*	6.97	6.64	6.95	6.92	7.03	6.81	6.72	9.01
CIPW norms								
Q	4.29	8.95	6.79	7.59	2.76	8.20	8.27	0.00
Or	3.63	4.28	4.16	4.45	2.72	4.33	4.36	4.17
Ab	31.80	29.54	30.19	30.48	32.60	30.79	30.19	29.23
An	35.21	33.94	32.12	31.61	37.00	32.45	32.19	30.59
Di(C)	6.77	2.69	6.72	5.98	6.64	4.07	5.34	9.35
Hy	14.04	16.13	15.44	15.38	13.70	16.21	15.34	14.78
Ol	0.00	0.00	0.00	0.00	0.00	0.00	0.00	6.64
Mt	2.45	2.33	2.44	2.43	2.48	2.40	2.37	3.17
Il	1.42	1.78	1.81	1.74	1.79	1.20	1.61	1.45
Trace elements								
(ppm)								
Rb	6.5	6.5	6.5	8.0	3.0	8.0	7.9	5.0
Ba	179	180	203	181	217	180	150	429
Sr	744	744	784	763	885	767	822	659
Co	43	44	48	51	144	50	34	48
Ni	46	46	59	52	52	48	40	182
Cr	197	44	54	57	58	42	42	292
Zn	71	71	84	81	74	72	71	86
Cu	98	32	53	62	98	61	23	65
Li	7.1	7.1	6.3	7.1	8.4	5.8	7.4	10

\*Total iron recalculated to Fe<sup>+2</sup>, volatile-free.



## APPENDIX B.

## CHEMICAL ANALYSES OF ROCK SAMPLES

Table B.4. Rock chemistry, Waldo Lake-Swift Creek area, Lane County, Oregon. Sample localities are shown on Plate 3.--Continued

Sample no. on Plate 3	83	84	85	86	87	88
Geol. unit	Pleistocene basaltic rocks					Holocene(?)
Map symbol						air-fall pumice
Field no.	P-22	Qb P-Notch	Qb T-208	Qb T-210	Qb T-211	(Not shown) P-302
Location	T23S/R5E/9Bbb	T23S/R5E/14Bdd	T24S/R5E/16Cdb	T24S/R5E/18Add	T24S/R5E/18Dac	T23S/R5E/15Cntr.
SiO <sub>2</sub>	53.30	57.04	52.20	52.80	50.32	33.74
TiO <sub>2</sub>	0.81	0.83	1.29	1.03	1.27	0.92
Al <sub>2</sub> O <sub>3</sub>	17.62	18.39	16.82	17.50	17.01	8.25
Fe <sub>2</sub> O <sub>3</sub>	4.13	2.90	5.33	4.74	6.81	0.92
FeO	3.74	4.00	4.07	3.69	2.19	0.90
MnO	0.14	0.14	0.18	0.17	0.14	0.03
MgO	6.41	2.99	6.89	6.56	5.57	0.52
CaO	8.53	7.35	8.90	8.10	9.02	1.66
Na <sub>2</sub> O	3.74	4.02	3.57	3.82	2.85	2.30
K <sub>2</sub> O	0.82	1.07	0.70	0.71	0.39	1.05
H <sub>2</sub> O <sup>+</sup>	-----	-----	-----	-----	1.44	6.51
H <sub>2</sub> O <sup>-</sup>	-----	-----	-----	-----	3.36	42.96
P <sub>2</sub> O <sub>5</sub>	0.32	0.37	0.33	0.39	0.33	0.06
Total	99.56	99.10	100.28	99.51	100.70	99.82
Total FeO*	7.53	6.69	8.89	8.04	8.74	3.45
CIPW norms						
Q	0.21	8.37	0.00	0.00	4.08	23.61
Or	4.88	6.39	4.14	4.23	2.41	12.34
Ab	31.87	34.37	30.22	32.58	25.27	38.67
An	29.07	29.28	27.81	28.73	34.03	15.59
Di (C)	9.37	4.23	11.52	7.46	8.64	( 0.91)
Hy	19.71	12.55	17.98	21.21	19.16	3.90
Ol	0.00	0.00	1.99	0.10	0.00	0.00
Mt	2.65	2.35	3.13	2.83	3.07	1.21
Il	1.55	1.59	2.45	1.97	2.53	3.47
Trace elements						
(ppm)						
Rb	10	15	6.9	11	9.7	22
Ba	412	444	302	382	230	380
Sr	898	683	738	673	696	166
Co	59	30	51	44	36	0
Ni	158	68	134	156	76	7.8
Cr	197	51	219	253	145	11
Zn	79	80	92	92	114	22
Cu	98	66	57	52	56	10
Li	10	11	10	12	13	15

\*Total iron recalculated to Fe<sup>+2</sup>, volatile-free.

## APPENDIX B.

## CHEMICAL ANALYSES OF ROCK SAMPLES

Table B.5. New chemical data for the Outerson Mountain-Devils Creek and Waldo Lake-Swift Creek areas, Oregon (sample numbers with "E" suffix).

Sample no. on plate or figure	/-----Outerson Mountain-Devils Creek (Figure 3.2)-----							
	1E	2E	3E	4E	5E	6E	7E	8E
Geol. unit	Lavas of Outerson Mountain				/-----Lower Miocene-Pliocene lavas-----/-----Upper Miocene-Pliocene lavas-----			
Map symbol	Tmo	Tmpl	Tmpl	Tmpl	Tmpu	Tmpu	Tmpu	Tmpu
Field no.	DC-418	DC-412	DC-471A	DC-480	DC-1	DC-4	DC-420	DC-422
Location	T10S/R7E/3Ccc	T10S/R7E/3Cca	T10S/R7E/11Dad	T10S/R7E/11Dda	T9S/R7E/35Cab	T10S/R7E/2Aac	T10S/R7E/11Cbba	T10S/R7E/11Cbdd
SiO <sub>2</sub>	53.02	53.02	50.52	51.71	54.40	54.89	52.98	50.58
TiO <sub>2</sub>	1.16	1.35	1.24	1.15	1.08	1.14	1.36	1.35
Al <sub>2</sub> O <sub>3</sub>	16.99	16.98	17.25	17.21	18.40	17.92	16.94	17.50
Fe <sub>2</sub> O <sub>3</sub>	2.85	2.51	4.44	6.04			3.56	1.97
FeO	5.82	6.63	4.51	2.77	8.80	7.82	5.43	7.04
MnO	0.15	0.16	0.16	0.15	0.105	0.111	0.17	0.15
MgO	5.41	5.95	6.83	6.16	4.99	5.01	4.90	6.99
CaO	8.48	8.66	9.38	9.00	8.82	9.08	9.38	9.31
Na <sub>2</sub> O	3.50	3.59	3.18	3.33	3.65	3.28	3.52	3.18
K <sub>2</sub> O	0.90	0.51	0.59	0.68	1.09	0.915	0.80	0.38
H <sub>2</sub> O <sup>+</sup>	0.38	0.32	0.40	0.54			0.41	0.41
H <sub>2</sub> O <sup>-</sup>	0.50	0.25	0.28	0.48	0.99	0.39	0.35	0.31
P <sub>2</sub> O <sub>5</sub>	0.37	0.32	0.27	0.28	0.283	0.207	0.31	0.26
Total	99.53	100.25	99.05	99.50	102.61	100.76	100.11	99.42
Total FeO*	8.53	8.94	8.69	8.47	8.66	7.79	8.72	8.95
CIPW norms								
Q	2.62	2.18	0.00	0.98	2.17	5.38	2.52	0.00
Or	5.40	3.02	3.55	4.10	6.44	5.38	4.77	2.27
Ab	30.05	30.49	27.42	28.73	30.90	27.80	30.00	27.30
An	28.40	28.80	31.64	30.59	30.60	31.50	28.28	32.80
Di(C)	9.65	9.94	11.33	10.61	9.55	10.10	13.57	9.96
Hy	17.80	19.10	17.89	19.16	15.70	14.60	14.45	20.20
Ol	0.00	0.00	2.075	0.00	0.00	0.00	0.00	1.20
Mt	3.00	3.14	3.055	2.95	2.73	2.48	3.07	3.15
Il	2.34	2.57	2.40	2.23	2.05	2.17	2.60	2.60
Trace elements								
(ppm)								
Rb	----	----	6.9	9.7	----	----	11	3.3
Ba	400	327	260	291	429	251	290	273
Sr	674	398	505	558	908	550	603	583
Co	38	41	46	42	33	49	33	45
Ni	81	96	138	120	47	34	31	132
Cr	94	159	253	214	54	97	96	213
Zn	92	101	84	89	61	57	83	115
Cu	86	69	64	69	83	44	64	65
Li	10	12	11	9.1	9	9	8.4	9.7

\*Total iron recalculated to Fe<sup>+2</sup>, volatile-free.

## APPENDIX B.

## CHEMICAL ANALYSES OF ROCK SAMPLES

Table B.5. New chemical data for the Outerson Mountain-Devils Creek and Waldo Lake-Swift Creek areas, Oregon (sample numbers with "E" suffix)--Continued.

Sample no. on plate or figure	9E	10E	11E	12E	13E	14E	15E	16E***
Geol. unit	Upper Miocene-Pliocene lavas		Andesitic intru- sive rocks	Oligocene-Miocene rhyodacites-----/-----Oligocene-Miocene lavas-----				
Map symbol	Tmpu	Tmpu	Tmia	Tomr	Tomr	Tomr	Toml	
Field no.	DC-459	DC-462	DC-421	P-777	P-825	P-821	P-738	
Location	T10S/R7E/2Adb	T9S/R7E/35Cddd	T10S/R7E/11Cbca	T22S/R5½E/29Ca	T22S/R5½E/29Cb	T22S/R5½E/29Dd	T22S/R5E/8Dbc	T22S/R5E/26Ab
SiO <sub>2</sub>	54.83	51.39	57.95	72.37	72.56	73.06	54.08	
TiO <sub>2</sub>	1.62	1.18	1.11	0.14	0.13	0.14	0.88	
Al <sub>2</sub> O <sub>3</sub>	16.74	17.83	16.81	15.30	14.81	14.71	18.34	
Fe <sub>2</sub> O <sub>3</sub>	2.86	4.27	3.12	1.01	0.72	0.68	3.79	
FeO	5.78	4.62	4.31	0.56	0.87	0.83	3.79	
MnO	0.17	0.16	0.14	0.03	0.06	0.05	0.14	
MgO	3.26	5.44	2.80	0.18	0.13	0.20	4.51	
CaO	7.10	9.33	5.95	1.35	1.19	1.18	8.97	
Na <sub>2</sub> O	4.07	3.00	4.58	4.67	4.36	4.63	3.37	
K <sub>2</sub> O	1.68	0.56	1.60	3.16	3.14	3.01	0.72	
H <sub>2</sub> O <sup>+</sup>	0.71	0.85	0.26	0.24	1.28	1.29	0.66	
H <sub>2</sub> O <sup>-</sup>	0.48	0.65	0.43	0.32	0.36	0.17	0.50	
P <sub>2</sub> O <sub>5</sub>	0.63	0.21	0.53	0.05	0.35	0.05	0.17	
Total	99.93	99.49	99.59	99.38	99.96	100.00	99.92	
Total FeO*	8.49	8.67	7.23	1.49	1.54	1.46	7.29	
CIPW norms								
Q	4.75	2.81	7.75	29.72	32.40	31.65	5.12	
Or	10.06	3.39	9.57	18.91	18.94	18.06	4.32	
Ab	34.91	25.97	39.24	40.02	37.66	39.77	28.93	
An	22.75	34.30	20.84	6.45	5.76	5.61	33.27	
Di(C)	7.26	9.50	4.49	0.00	0.00	0.00	8.79	
Hy	12.69	18.21	12.08	2.11	2.14	2.17	14.90	
Ol	0.00	0.00	0.00	0.00	0.00	0.00	0.00	
Mt	2.985	3.05	2.54	0.52	0.55	0.52	2.58	
Il	3.12	2.29	2.135	0.27	0.25	0.27	1.70	
Trace elements								
(ppm)								
Rb	20	5.5	25	72	81	75	9.7	
Ba	555	238	368	758	720	768	200	
Sr	590	424	582	122	107	120	614	
Co	26	38	17	0	0	0	34	
Ni	7.3	31	6.5	2.8	2.8	3.7	28	
Cr	4.8	115	4.7	0	0	2.3	56	
Zn	101	89	100	44	58	42	86	
Cu	49	44	35	8.8	5.7	5.2	57	
Li	9.7	11	11	20	45	26	10	

\*Total iron recalculated to Fe<sup>+2</sup>, volatile-free.

\*\* Outside map area

\*\*\* Chemical analysis of this sample has been eliminated from this table.

## APPENDIX B.

## CHEMICAL ANALYSES OF ROCK SAMPLES

Table B.5. New chemical data for the Outerson Mountain-Devils Creek and Waldo Lake-Swift Creek areas, Oregon (sample numbers with "E" suffix)--Continued.

-----Waldo Lake-Swift Creek (Plate 3)-----							
Sample no. on plate or figure	17E	18E	19E	20E	21E	22E	23E
Geol. unit	Oligocene-Miocene lavas		/-----Basaltic lavas of Koch Mountain-----				
Map symbol	Toml	Toml	Tmk	Tmk	Tmk	Tmk	Tmk
Field no.	P-744	P-743	WL18	WL27	WL31	WL41	WL46-8
Location	T22S/R5E/27Aac	T22S/R5E/27Abd	T21S/R5E/25Ada	T21S/R5E/25Add	T21S/R5E/25Add	T21S/R5E/25Dab	T21S/R5E/25Dac
SiO <sub>2</sub>	54.83	56.89	52.64	52.45	52.20	53.77	52.33
TiO <sub>2</sub>	1.35	0.88	1.13	1.22	1.30	1.06	1.29
Al <sub>2</sub> O <sub>3</sub>	17.14	18.54	18.00	16.86	17.50	18.03	17.39
Fe <sub>2</sub> O <sub>3</sub>	2.99	3.97	2.93	2.66	4.42	2.82	3.79
FeO	4.89	3.05	5.49	6.24	4.81	5.08	4.82
MnO	0.20	0.11	0.14	0.16	0.15	0.15	0.14
MgO	4.33	2.32	5.86	6.93	4.73	4.36	4.50
CaO	8.10	7.08	8.32	8.28	7.70	7.61	7.11
Na <sub>2</sub> O	3.54	4.29	3.71	3.33	3.98	3.66	3.92
K <sub>2</sub> O	0.53	1.24	0.80	1.20	1.28	0.80	1.46
H <sub>2</sub> O <sup>+</sup>	0.76	0.34	0.35	0.20	0.67	0.88	0.80
H <sub>2</sub> O <sup>-</sup>	0.85	0.44	0.45	0.14	0.62	0.61	0.72
P <sub>2</sub> O <sub>5</sub>	0.43	0.20	0.24	0.34	0.84	0.46	0.84
Total	99.94	99.35	100.06	100.01	100.20	99.29	99.11
Total FeO*	7.71	6.72	8.19	8.66	8.88	7.79	8.43
CIPW norms							
Q	8.09	7.43	0.36	0.00	0.32	5.36	1.55
Or	3.19	7.45	4.77	7.12	7.67	4.84	8.86
Ab	30.50	36.92	31.66	28.29	34.13	31.70	34.05
An	29.85	28.14	30.35	27.62	26.45	31.12	26.22
Di(C)	6.71	5.21	7.88	9.23	5.49	3.64	3.57
Hy	15.33	10.32	19.38	20.93	18.34	17.44	18.26
Ol	0.00	0.00	0.00	0.65	0.00	0.00	0.00
Mt	2.72	2.37	2.89	3.06	3.14	2.75	2.98
Il	2.61	1.70	2.16	2.33	2.50	2.06	2.52
Trace elements							
(ppm)							
Rb	6.9	24	13	14	10	11	12
Ba	480	336	383	747	594	710	716
Sr	636	628	790	1006	769	728	701
Co	30	20	40	43	35	33	32
Ni	36	15	81	147	61	60	54
Cr	54	7.2	195	192	110	100	104
Zn	93	82	85	109	122	116	106
Cu	74	45	79	95	42	79	86
Li	12	5.2	11	9.1	9	11	9.9

\*Total iron recalculated to Fe<sup>+2</sup>, volatile-free.

\*\* Sample location not shown on map.



## APPENDIX B.

## CHEMICAL ANALYSES OF ROCK SAMPLES

Table B.5. New chemical data for the Outerson Mountain-Devils Creek and Waldo Lake-Swift Creek areas, Oregon (sample numbers with "E" suffix)--Continued.

Sample no. on plate or figure	24E	25E	26E	27E	28E	29E	30E	31E	32E
Geol. unit	Andesitic lavas of Moss Mountain-----/-----				Miocene-Pliocene basaltic lavas-----				
Map symbol	Tma	Tma	Tma	Tma	Tpb	Tpb	Tpb	Tpb	Tpb
Field no.	WL191	WL303	WL86	WL247	WL7	WL12	WL16	WL17	WL248
Location	T22S/R5½E/2Caa	T21S/R5E/17Cdd	T21S/R5½E/21Ccd	T21S/R5E/29Cdc	T21S/R5E/25Aad	T21S/R5E/25Ada	T21S/R5E/25Ada	T21S/R5E/25Ada	T21S/R5E/33Dbb
SiO <sub>2</sub>	62.69	57.06	60.07	60.24	50.95	50.77	50.77	51.20	51.44
TiO <sub>2</sub>	0.71	1.20	0.80	1.00	1.65	1.27	1.21	1.22	1.37
Al <sub>2</sub> O <sub>3</sub>	17.12	18.27	17.40	17.41	17.94	17.32	17.05	16.64	17.29
Fe <sub>2</sub> O <sub>3</sub>	2.65	3.90	2.65	2.74	3.05	2.92	2.58	2.11	3.63
FeO	2.72	3.49	3.21	3.63	6.61	6.62	6.92	6.79	5.89
MnO	0.10	0.11	0.11	0.14	0.17	0.17	0.17	0.16	0.18
MgO	2.09	3.38	2.97	2.61	5.44	6.96	6.59	7.41	7.00
CaO	4.69	6.81	5.52	5.34	9.49	8.79	9.01	8.65	8.38
Na <sub>2</sub> O	4.58	3.72	4.39	3.96	3.60	3.49	3.40	3.40	3.37
K <sub>2</sub> O	2.06	1.23	1.75	0.56	0.46	0.66	0.76	0.81	0.65
H <sub>2</sub> O <sup>+</sup>	0.19	0.38	0.24	0.58	0.42	0.06	0.06	0.13	0.17
H <sub>2</sub> O <sup>-</sup>	0.23	0.49	0.30	0.61	0.36	0.09	0.13	0.21	0.24
P <sub>2</sub> O <sub>5</sub>	0.21	0.31	0.23	0.21	0.35	0.36	0.29	0.35	0.30
Total	100.04	100.35	99.64	99.03	100.49	99.48	98.94	99.08	99.91
Total FeO*	5.12	7.04	5.70	6.23	9.38	9.31	9.36	8.80	9.20
CIPW norms									
Q	13.64	9.39	10.41	17.94	0.00	0.00	0.00	0.00	0.00
Or	12.24	7.32	10.45	3.39	2.73	3.93	4.55	4.85	3.87
Ab	38.96	31.71	37.53	34.29	30.58	29.75	29.14	29.14	28.70
An	20.18	29.74	22.84	25.71	31.55	29.86	29.39	28.10	30.33
Di(C)	1.52	1.85	2.72	0.00	10.95	9.50	11.36	10.55	7.74
Hy	9.82	14.48	11.98	12.93	15.63	14.72	14.72	16.87	21.70
Ol	0.00	0.00	0.00	0.00	1.30	5.69	4.53	4.22	1.10
Mt	1.81	2.49	1.99	2.20	3.31	3.28	3.30	3.10	3.25
Il	1.36	2.30	1.54	1.99	3.15	2.43	2.33	2.35	2.62
Trace elements									
(ppm)									
Rb	43	21	36	31	2.8	10	13	13	12
Ba	640	396	532	488	390	314	340	376	263
Sr	487	518	539	417	835	606	672	672	562
Co	14	26	20	21	41	35	47	47	44
Ni	17	40	33	21	54	128	93	160	135
Cr	16	54	46	33	83	179	187	245	234
Zn	68	94	69	76	93	91	91	86	92
Cu	36	70	52	50	82	45	54	48	62
Li	19	9.1	18	16	10	9.8	12	9.9	10

\*Total iron recalculated to Fe<sup>+2</sup>, volatile-free.

## APPENDIX B.

## CHEMICAL ANALYSES OF ROCK SAMPLES

Table B.5. New chemical data for the Outerson Mountain-Devils Creek and Waldo Lake-Swift Creek areas, Oregon (sample numbers with "E" suffix)--Continued.

-----Waldo Lake-Swift Creek (Plate 3)-----								
Sample no. on plate or figure	33E	34E	35E	36E	37E	38E	39E	40E
Geol. unit	-----Miocene-Pliocene basaltic lavas-----					Upper Tertiary- Quaternary lavas (undifferentiated)	Pleistocene basaltic lavas	
Map symbol	Tpb	Tpb	Tpb	Tpb	Tpb	Qtu	Qtb	Qtb
Field no.	WL251	WL149	P716	P324	P-PHL	T-205a	WL227	WL239
Location	T21S/R5E/35Cbd	T22S/R5E/1Caa	T23S/R5E/6Aad	T23S/R5E/12Ccc	T23S/R5E/16Dcc	T24S/R5E/23Ddd	T22S/R5E/10Aca	T22S/R5E/22Acd
SiO <sub>2</sub>	50.60	51.27	51.95	52.08	48.70	51.20	52.57	52.94
TiO <sub>2</sub>	1.31	1.28	1.11	1.24	1.88	1.10	1.18	1.27
Al <sub>2</sub> O <sub>3</sub>	17.21	17.85	17.10	17.58	15.78	17.26	18.58	18.44
Fe <sub>2</sub> O <sub>3</sub>	3.06	2.57	2.58	2.03	11.79	5.69	2.28	2.43
FeO	5.78	6.28	6.00	6.95		4.06	5.61	5.51
MnO	0.17	0.16	0.16	0.18	0.17	0.18	0.15	0.15
MgO	7.02	5.44	5.78	5.17	7.50	5.76	5.52	5.30
CaO	9.56	8.93	8.26	8.55	9.41	8.50	8.68	9.03
Na <sub>2</sub> O	3.14	3.74	3.66	3.75	3.14	3.53	3.65	3.78
K <sub>2</sub> O	0.63	0.64	1.03	0.93	1.26	0.87	0.95	1.06
H <sub>2</sub> O <sup>+</sup>	0.24	0.32	0.30	0.41	----		0.31	0.17
H <sub>2</sub> O <sup>-</sup>	0.15	0.36	0.34	0.30	----	----	0.18	0.16
P <sub>2</sub> O <sub>5</sub>	0.37	0.31	0.47	0.56	0.55	0.44	0.39	0.47
Total	99.24	99.15	98.74	99.73	100.18	98.59	100.05	100.71
Total FeO*	8.63	8.73	8.48	8.86	11.77	9.37	7.70	7.67
CIPW norm								
Q	0.00	0.00	0.07	0.35	0.00	0.00	0.38	0.00
Or	3.77	3.84	6.21	5.55	7.45	5.23	5.64	6.24
Ab	26.91	32.15	31.59	32.04	26.60	30.40	31.04	31.88
An	31.40	30.51	27.73	28.67	25.20	29.19	31.66	30.12
Di(C)	11.48	10.15	8.90	8.57	14.90	8.83	7.35	9.33
Hy	17.60	15.27	19.25	18.01	3.04	18.75	18.06	16.13
Ol	2.42	1.80	0.00	0.00	13.06	1.13	0.00	0.10
Mt	3.05	3.08	2.99	3.12	3.74	3.29	2.71	2.70
Il	2.52	2.47	2.15	2.38	3.57	2.13	2.25	2.40
Trace elements								
(ppm)								
Rb	5.9	10	12	6.9	-----	10	11	11
Ba	281	295	492	489	570	546	479	559
Sr	673	564	801	765	852	626	933	1023
Co	27	36	39	38	42	55	35	33
Ni	88	63	80	56	96	119	56	44
Cr	248	117	140	105	194	93	111	99
Zn	84	84	87	94	96	92	82	99
Cu	56	58	64	36	64	120	94	60
Li	8.6	11	10	9.2	9	10	11	11

\*Total iron recalculated to Fe<sup>+2</sup>, volatile-free.

## APPENDIX B.

## CHEMICAL ANALYSES OF ROCK SAMPLES

Table B.5. New chemical data for the Outerson Mountain-Devils Creek and Waldo Lake-Swift Creek areas, Oregon (sample numbers with "E" suffix)--Continued.

Sample no. on Waldo Lake-Swift Creek (Plate 3)--/  
plate or figure 41E 42E

Geol. unit Pleistocene basaltic lavas

Map symbol	Qtb	Qtb
Field no.	WL109	WL278
Location	T21S/R5½E/28Cdb	T21S/R5½E/34Baa
SiO <sub>2</sub>	53.83	49.48
TiO <sub>2</sub>	1.13	1.65
Al <sub>2</sub> O <sub>3</sub>	17.29	17.28
Fe <sub>2</sub> O <sub>3</sub>	3.78	4.58
FeO	4.06	5.78
MnO	0.15	0.18
MgO	6.22	7.49
CaO	7.84	8.62
Na <sub>2</sub> O	3.72	3.24
K <sub>2</sub> O	0.96	0.96
H <sub>2</sub> O <sup>+</sup>	0.20	0.33
H <sub>2</sub> O <sup>-</sup>	0.25	0.31
P <sub>2</sub> O <sub>5</sub>	0.33	0.49
Total	99.76	100.39
Total FeO*	7.51	9.93

CIPW norm

Q	1.89	0.00
Or	5.72	5.70
Ab	31.76	27.55
An	27.89	29.91
Di(C)	7.42	7.98
Hy	19.72	11.38
Ol	0.00	9.70
Mt	2.65	3.51
Il	2.17	3.15

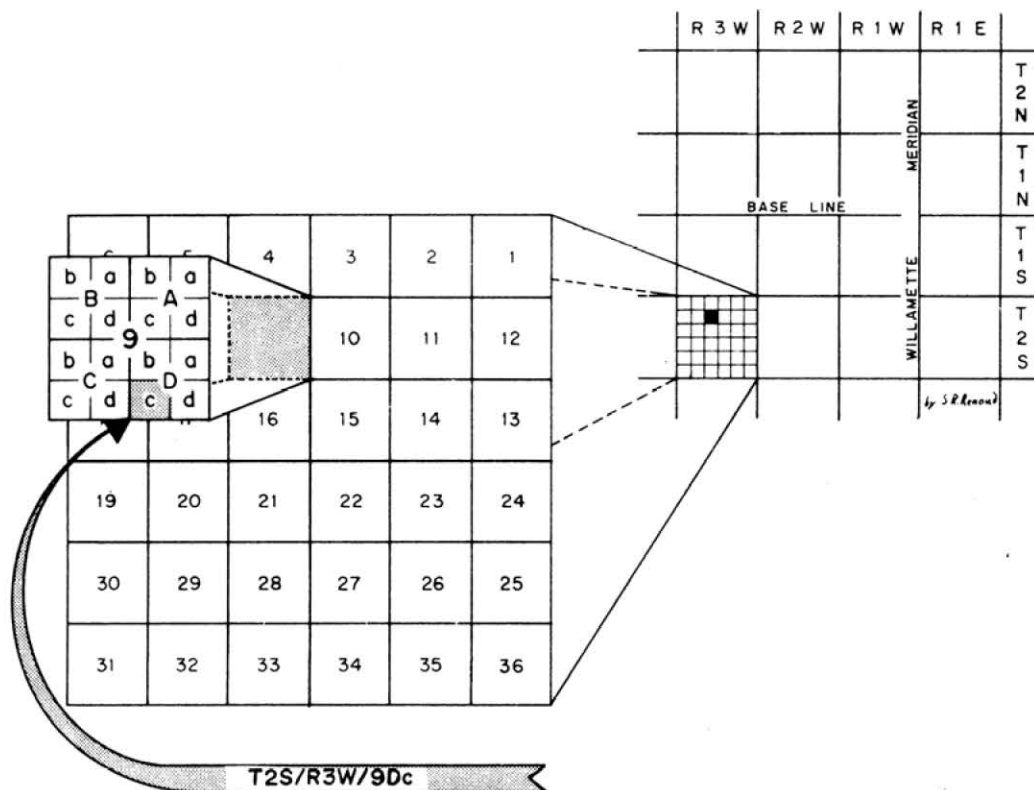
Trace elements

(ppm)		
Rb	11	8.8
Ba	409	534
Sr	691	776
Co	35	38
Ni	182	146
Cr	228	235
Zn	82	110
Cu	75	74
Li	9.8	8.3

\*Total iron recalculated to Fe<sup>+2</sup>, volatile-free.

# APPENDIX C.

## EXPLANATION OF THE TOWNSHIP-RANGE LOCATION SYSTEM



Locations listed in this report are designated according to official systems for the rectangular subdivision of public lands. The numbers indicate the location by township, range, section, and position within the section. In the symbol T2S/R3W/9Dc, the "T2S" indicates the township south of the base line and "R3W" the range west of the Willamette Meridian. The "9" indicates the section, "D" the quarter section, and "c" the 40-acre plot within that quarter.



## APPENDIX D.

## TEMPERATURE AND HEAT-FLOW DATA

Table D.1. Temperature and heat-flow data for the Oregon Cascades

Location	Prov. <sup>a</sup>	N. lat. deg.-min.	W. long. deg.-min.	Hole name (date)	Hole type <sup>b</sup>	Collar elev. (m)	Total depth (m)	Depth interval (m)	Average thermal conductivity	Uncorr. grad. <sup>c</sup> °C/km (1σ)	Corr. grad. <sup>c</sup> (°C/km)	Corr. heat flow <sup>c</sup> mW/m <sup>2</sup>	Quality <sup>d</sup>	Lithologic summary
T6S/R1E/13Da	WC	45-2.8	122-37.2	TWW (10/6/76)	WW	326	140	35-95 95-140	1.59 (1.17)	26.2 (0.1) 34.7 (0.7)	28.6 37.7	45 44	A A	Basalt and siltstone
T6S/R1E/35Cb	WC	45-0.3	122-39.4	MC-WW (10/6/76)	WW	285	195	95-195	(1.17)	30.9 (0.2)	34.3	40	C	Siltstone
T6S/R2E/18Ba	WC	45-3.3	122-36.7	QWW (10/6/76)	WW	259	90	55-90	----	29.1 (0.5)	29.0	--	B	Oligocene marine sediments
T6S/R6E/23Ca1	WC	45-1.8	122-2.7	DH-5000 (11/4/75)	FS	487	22.5	15-22.5	----	70 (4.3)	----	--	D	Oligocene and Miocene volcanics
T6S/R6E/34Cd	WH	44-60.0	122-3.8	RDHCRCR (9/30/76)	TG	487	150	10-150	1.64 (0.04)	81.8 (0.5)	65.0	106	A	Diorite sill, basalt
T6S/R7E/4Dc	HC	45-4.3	121-57.6	RDHCRLKH (7/25/77)	TG	686	40	0-38	----	----	----	--	X	Porphyritic andesite
T6S/R7E/21Cd	WH	45-1.8	121-57.7	AUST HSE (6/29/77)	TG	603	40	10-40	1.47 (0.07)	231.6 ( 8.7)	162.8	239	B	Basalt, tuff and andesite
T6S/R7E/30Bb	WH	45-1.3	122-0.5	RDHCRAHS (9/30/76)	TG	512	132.5	95-130	1.65 (0.08)	240.7 ( 2.0)	169.5	279	B	Basalt, tuff and rhyolite
T7S/R1E/11Aca	WC	44-58.8	122-38.8	OW-W1 (7/ /62)	OW	214	2379	0-2379	(1.59)	26.0	26.0	41	C	Eugene and Spencer Fms.
T7S/R7E/4Dd	HC	44-59.0	121-57.0	EWEB-TS (5/28/80)	TG	1273	193.5	165-190	1.62 (0.04)	----	----	--	X	Basalt (Q)
T7S/R8E/5Dd	HC	44-59.0	121-50.8	EWEB-PC (5/28/80)	TG	975	187	70-185	1.58 (0.04)	----	----	--	X	Basalt (Q)
T7S/R8E/10Ad	HC	44-58.5	121-48.4	EWEB-CC (5/30/80)	TG	1140	137	110-137	1.45 (0.10)	----	----	--	X	Basalt (Q)
T7S/R5E/22Aa	WC	44-57.1	122-10.4	CR-BHS (9/30/76)	TG	655	152	20-90	1.46 (0.05)	84.3	66.8	97	B	Basalt, 10-85 m
T8S/R1W/32Bb	WC	44-50.3	122-50.4	SWW (9/27/76)	WW	115	80	30-80	(1.59)	34.4 (0.4)	34.4	54	C	Basalt
T8S/R2W/24Bc	WC	44-51.7	122-53.0	CWW (8/10/76)	WW	127	61	22.5-60	(1.59)	24.7 (0.2)	24.7	39	C	Col. Riv. Basalt
T8S/R1E/8Db	WC	44-53.3	122-42.5	H-1-WW (10/8/76)	WW	303	218	95-215	1.72	27.6 ( 0.1)	27.6	47	B	Basalt
T8S/R1E/9Bd	WC	44-53.47	122-41.63	WOLFF (4/30/80)	WW	338	100	30-100	----	34.9 ( 4.7)	----	--	C	Basalt
T8S/R1E/17Da	WC	44-52.3	122-42.3	SM-WW (10/6/76)	WW	315	112	10-110	(1.59)	28.5	27.0	43	C	Basalt
T8S/R5E/31Cc	WC	44-49.9	122-14.8	CDR CRK (10/26/77)	ME	705	345	35-345	1.80 (0.33)	32.3 ( 0.5)	28.6	51	A	Volcanics
T8S/R8E/6Dd	HC	44-54.3	121-52.9	EWEB-SB (4/29/80)	TG	860	460	150-460	1.49 (0.13)	71.5 ( 1.1)	63.3	94	B	Basalt and andesite
T8S/R8E/31C	HC	44-50.0	121-52.9	CUB-CRK (9/28/79)	TG	1072	98	70-98	1.47 (0.08)	37.8 ( 1.4)	34.0	50	C	Basalt and andesite
T9S/R2E/21Da	WC	44-46.2	122-33.6	GI-WW (10/7/76)	WW	213	49	22.5-47.5	1.26	53.2 ( 2.4)	47.5	59	B	Tuffs and clays
T9S/R3E/11Ba	WC	44-48.5	122-24.5	EV2-WW (10/14/76)	WW	317	85	47.5-85	1.34	27.3 ( 0.8)	24.0	32	B	Clay

## APPENDIX D.

## TEMPERATURE AND HEAT-FLOW DATA

Table D.1. Temperature and heat-flow data for the Oregon Cascades --Continued

Location	Prov. <sup>a</sup>	N. lat. deg.-min.	W. long. deg.-min.	Hole name (date)	Hole type	Collar elev. (m)	Total depth (m)	Depth interval (m)	Average thermal conductivity	Uncorr. grad.C °C/km (1σ)	Corr. grad.C (°C/km)	Corr. heat flowC mW/m <sup>2</sup>	Quality <sup>d</sup>	Lithologic summary
T9S/R3E/11Cb	WC	44-48.1	122-24.8	EV1-WW (10/7/76)	WW	333	67	25-60	1.34	26.5 (0.1)	23.6	31	B	Clay and sandstone
T9S/R3E/28Cb	WC	44-45.4	122-27.1	GR-WW (10/14/76)	WW	268	55	25-52.5	----	30.0	28.0	--	C	----
T9S/R6E/23Bb	WH	44-47.0	122-2.4	RDH-BHSW (9/30/76)	TG	550	150	30-105	1.61 (0.11)	67.6 (0.4)	55.7	89	B	Crystal lithic tuff
T9S/R7E/20Aa	WH	44-46.9	121-58.3	BEAMER 3 (4/29/80)	WW	677	309.5	5-35	1.27 (0.13)	1300	1100	1393	B	Tuff, clay, and basalt
								0-309.5	1.55 (0.13)	277.2	261.0	404	B	
T9S/R7E/20Ac	WH	44-46.9	121-58.6	BEAMER 1 (2/6/78)	WW	682	150	0-150	(1.46)	600.0	521.7	763	D	Tuff, clay, and basalt
T9S/R7E/20Ad	WH	44-46.8	121-58.3	BEAMER 2 (4/29/80)	WW	680	74	6-74	1.27 (0.13)	407.3 (40.3)	339.4	430	B	Tuff, clay, and basalt
T9S/R7E/21Ad	WH	44-46.7	121-57.1	RDH-BHSE (9/30/76)	TG	725	152	90-150	1.65	92.9 (1.4)	82.6	135	B	Tuff, clays and basalt
T10S/R5E/3Dcc	WH	44-43.7	122-10.8	FS-DRSWW (6/26/78)	WW	518	180.5	10-170	(1.17)	52.0	43.2	50	C	Volcanics
T10S/R7E/11Aa	HC	44-43.4	121-54.4	RDH-DVCK (11/5/79)	TG	1194	155	70-150	1.40 (0.04)	83.5 (1.6)	72.6	101	B	Basalt
T11S/R1W/14Dd	WC	44-36.5	122-45.9	BL-WW (10/4/76)	WW	182	160	30-125	1.17	41.3 (0.3)	42.3	49	B	Claystone
T11S/R1W/32Bbb	WV	44-36.6	122-50.6	OW-LCD (12/11/58)	OW	108	1350	0-1345	(1.59)	18.9	18.9	30	C	Tuff, basalt, silt- stone
T11S/R1E/7Da	WC	44-37.5	122-43.3	RL-WW (10/13/76)	WW	158	58	40-57.5	1.34	28.1 (1.4)	26.7	35	C	Claystone
T11S/R6E/22Db	WH	44-36.01	122-3.39	BUCK MTN (7/31/80)	TG	1333	152	30-50	----	90.8 (4.1)	----	--	X	0-110 m andesite
T11S/R7E/10Dc	HC	44-37.6	121-56.1	RDH-MTCK (7/31/80)	TG	762	109	30-109	1.64 (0.13)	68.4 (3.7)	64.0	105	D	Basalt, andesite, and mudflows
T11S/R10E/5AcB	DU	44-38.78	121-33.47	CASTLERX (7/23/80)	TG	1194	153	25-153	----	18.2 (1.1)	----	--	X	Lavas with auto- breccia
T12S/R1W/4Dc	WC	44-33.1	122-48.6	B-9 (10/29/74)	WW	135	65	30-65	1.34 (0.13)	37.1 (1.0)	36.4	50	A	Volcanic conglomerate
T12S/R1W/30Ca	WC	44-29.7	122-51.3	MC PHRSON (4/10/79)	WW	219	125	180-125	(1.59)	34.2 (0.4)	34.2	54	B	Basalt
T12S/R1W/30Db	WC	44-29.7	122-51.1	LEBN GLF (4/10/79)	WW	170	70	40-70	(1.59)	28.3 (1.0)	28.3	45	C	Basalt
T12S/R7E/9Da	HC	44-32.7	121-57.8	EWEB-TM (5/29/80)	TG	1195	600	300-600	1.36 (0.08)	71.4 (1.3)	69.4	94	B	Volcanics
T12S/R9E/1Bcd	DU	44-33.70	121-36.42	GREENRDG (7/23/80)	TG	999	152	70-105	(1.60)	79.2 (1.5)	(63.4)(101)		B	Tuff, conglomerate, basalt
T13S/R2W/3Aa	WV	44-28.3	122-54.4	TVR-WW (8/25/76)	WW	317	95	40-95	1.34	29.0 (0.5)	29.4	39	B	Sandstone and basalt

## APPENDIX D.

## TEMPERATURE AND HEAT-FLOW DATA

Table D.1. Temperature and heat-flow data for the Oregon Cascades --Continued

Location	Prov. <sup>a</sup>	N. lat. deg.-min.	W. long. deg.-min.	Hole name (date)	Hole type <sup>b</sup>	Collar elev. (m)	Total depth (m)	Depth interval (m)	Average thermal conductivity	Uncorr. grad. <sup>c</sup> °C/km (1σ)	Corr. grad. <sup>c</sup> (°C/km)	Corr. heat flow <sup>c</sup> mW/m <sup>2</sup>	Quality <sup>d</sup>	Lithologic summary
T13S/R2W/18Cb	WV	44-26.2	122-59.1	WB-WW (8/25/76)	WW	378	198	95-190	(1.59)	15.5 (0.1)	25.8	37	C	Basalt
T13S/R1W/8Db	WC	44-27.1	122-49.9	RJ-WW (10/12/76)	WW	329	95	15-95	(1.59)	19.0 (0.3)	20.0	31	B	Basalt
T13S/R1W/10Ca	WC	44-27.1	122-47.7	BJ-WW (8/11/76)	WW	149	62.5	27.5-62.5	1.34	23.3 (0.6)	22.7	30	C	Claystone and sediments
T13S/R1E/20Ba	WC	44-25.9	122-43.0	MR-WW (8/11/76)	WW	402	130	90-130	(1.34)	33.6 (1.8)	39.9	53	C	Basalt and sandstone
T13S/R1E/35Ab	WC	44-24.1	122-38.9	MMW (8/11/76)	WW	310	152	90-150	(1.34)	31.5 (0.3)	37.4	50	C	Consolidated sedi- ments, basalt, sand- stone
T13S/R7E/9Abb	WC	44-27.7	121-58.97	DETRO-FM (7/23/80)	WW	1128	79	----	----	----	----	--	X	Olivine basalt
T13S/R7E/32Dc	HC	44-23.3	121-59.7	EWEB-CL (10/30/79)	TG	955	557	50-205	1.44	112.0 (2.2)	102.8	148	B	Andesite and volcanics
								0-555	1.40	25.6 (11.4)	23.9	33	C	
T13S/R10E/5Ab	DU	44-28.75	121-33.41	FLY CRK (7/24/80)	TG	1194	120	----	----	----	----	--	X	Basaltic andesite
T14S/R6E/32Dc	WH	44-18.2	122-7.3	WOLF MDW (8/1/80)	TG	999	155	42.5-155	1.46 (0.13)	87.2 1.6	72.7	110	B	Altered basalt and breccia
T14S/R3W/24Dc	WV	44-20.0	122-59.6	NWW (10/1/76)	WW	207	47.5	10-47.5	(1.59)	24.7 (0.4)	25.0	39	D	Claystone
T15S/R6E/11Dc	WH	44-16.1	122-3.3	RDHCRBTR (7/26/77)	TG	716	64	0-52	----	----	----	--	X	Basalt and cinders
T15S/R7E/28Aa	WH	44-14.8	121-58.4	RDH-CRSM (7/26/77)	TG	1143	55	----	----	----	----	--	X	Basalt and cinders
T15S/R10E/5Bb	HC	44-18.3	121-34.4	CENTWEST (4/5/80)	WW	978	106	10-30	----	104.8 (14.5)	----	--	C	----
T16S/R2E/26Bc1	WC	44-9.0	122-32.5	OH-22 (11/26/75)	FS	310	30	20-30	----	25.0 (0.6)	----	--	X	----
T16S/R4E/14Db	WC	44-10.1	122-17.5	BH-32 (11/26/75)	FS	457	45	12.5-45	1.80 (0.33)	37.8 (0.4)	35.0	63	D	Volcanics
T16S/R5E/30Ab	WH	44-9.2	122-14.9	DDH-15 (6/26/78)	FS	367	85	15-85	1.33	54.0	51.0	68	D	Tuff and basalt
T16S/R5E/30Ab	WH	44-9.1	122-15.0	ST DAM 1 (8/8/79)	FS	368	80	45-70	----	55.9 (2.8)	53.0	--	C	Alluvium
T16S/R5E/30Aa	WH	44-9.3	122-14.6	ST DAM 2 (8/8/79)	FS	389	87	25-61	1.32	56.3 (1.2)	53.0	70	C	Tuff
T16S/R6E/2Ca	WH	44-12.1	122-3.0	RDH-CRFP (8/5/76)	TG	701	150	100-150	1.74 (0.03)	84.1 (1.4)	88.3	153	C	Andesite
T16S/R6E/27Bb	WH	44-9.1	122-4.7	RDH-CRHC (9/29/76)	TG	573	152	30-150	1.57 (0.05)	96.2 (0.9)	70.9	111	B	Basalts and tuffs
T17S/R1W/26Da	WC	44-3.7	122-47.1	CWW (9/29/76)	WW	327	145	20-145	(1.59)	26.2 (0.2)	25.6	40	B	Basalt and cinders

## APPENDIX D.

## TEMPERATURE AND HEAT-FLOW DATA

Table D.1. Temperature and heat-flow data for the Oregon Cascades --Continued

Location	Prov. <sup>a</sup>	N. lat. deg.-min.	W. long. deg.-min.	Hole name (date)	Hole type <sup>b</sup>	Collar elev. (m)	Total depth (m)	Depth interval (m)	Average thermal conductivity	Uncorr. grad. <sup>c</sup> °C/km ( $\sigma$ )	Corr. grad. <sup>c</sup> (°C/km)	Corr. heat flow <sup>c</sup> mW/m <sup>2</sup>	Quality <sup>d</sup>	Lithologic summary
T17S/R1W/32Cc	WC	44-2.5	122-50.5	DWW (10/1/76)	WW	292	133	50-130	(1.17)	35.4 (0.9)	37.7	44	B	Pyroclastics or sediments
T17S/R2W/36Ca	WC	44-2.8	122-52.7	79S-WW (9/29/76)	WW	213	106	40-105	(1.17)	29.5 (0.3)	26.7	31	C	Claystone
T17S/R5E/8Ac	WH	44-6.4	122-14.0	WLKR-CR (7/24/80)	TG	585	155	105-155	(1.59)	54.1 (0.7)	52.0	83	B	Pyroxene andesite
T17S/R5E/20Ba	WH	44-4.9	122-13.8	RIDR-CRK (7/31/80)	TG	536	154	60-154	2.64 (0.04)	128.5 (3.6)	97.5	159	B	Andesite
T17S/R6E/25Ad	HC	44-3.9	122-1.4	RDH-MQCK (8/1/80)	TG	1005	152	115-152	1.55	62.8 (1.4)	73.8	114	C	Basaltic andesite
T18S/R2W/4Ad	WC	44-2.2	122-55.8	HB-WW (9/2/76)	WW	175	125	45-125	(1.17)	38.0 (0.5)	36.1	42	B	Claystone, sandstone
T18S/R1W/32Cc	WC	43-57.3	122-50.4	PR-WW (8/26/76)	WW	192	215	70-215	(1.17)	39.4 (0.3)	38.4	45	B	Claystone
T18S/R5E/11Bd	WH	44-1.1	122-9.8	RDH-RBCK (7/31/80)	TG	780	152	55-78	1.55	34.4 (1.0)	36.6	56	C	Basaltic andesite
T19S/R2W/2Ac	WV	43-56.9	122-53.8	JA-WW (8/19/76)	WW	231	120	25-120	(1.26)	35.5 (0.3)	34.6	43	C	Sandstone, shale
T19S/R2W/10Ad	WV	43-55.9	122-54.6	ER-WW (9/30/76)	WW	218	108	42.5-105	(1.17)	34.6 (0.5)	31.5	36	B	----
T19S/R4E/29Cc	WC	43-53.0	122-22.15	CHRS-CRK (7/31/80)	TG	579	154	70-154	1.75 (0.09)	64.0 (1.1)	52.3	92	B	Silicified dacite plug
T19S/R5E/27B	WH	43-53.1	122-12.61	BRCK-CRK (7/31/80)	TG	987	154	135-154	1.75 (0.09)	65.8 (0.4)	65.6	115	B	Olivine basalt flow
T19S/R6E/8Ba	HC	43-57.0	122-1.8	RDHELKCK (7/9/80)	TG	877	135	40-135	1.22 (0.04)	43.2 (1.0)	33.3	41	B	Sand and gravel
T19S/R6E/25Dc	HC	43-53.0	122-4.11	N. FORK (7/31/80)	TG	951	154	30-154	1.35 (0.05)	78.4 (5.1)	67.5	91	B	Olivine basalt
T20S/R2E/35Ac	WC	43-47.5	122-32.0	BTBR-CRK (7/2/80)	TG	160	155	20-155	(1.41)	42.6 (2.3)	34.1	48	B	Lithic-rich laharic tuff
T20S/R3E/26Cd	WC	43-47.9	122-25.2	AE-WW (8/19/76)	WW	707	124	10-80	(1.59)	25.8 (0.5)	25.6	40	B	Basalt and cinders
T20S/R3E/26Da	WC	43-48.0	122-25.0	CS-WW (9/28/76)	WW	719	142	45-70	(1.59)	25.3 (1.8)	25.1	39	B	Basalt and cinders
								70-140	(1.17)	39.0 (0.5)	38.8	45	B	
T20S/R4E/27Dd	WC	43-47.9	122-18.8	WALL-CRK (7/11/80)	TG	582	137	30-135	1.13 (0.13)	72.6 (0.9)	60.5	69	B	Tuff
T21S/R3E/10Ad	WC	43-45.6	122-25.9	FC-WW (9/28/76)	WW	548	100	25-100	(1.17)	36.5 (0.5)	35.6	41	B	Quaternary basalt
T21S/R3E/17Da	WC	43-44.8	122-28.3	OAKR-CW6 (11/8/80)	TG	345	345	70-240	(1.82)	47.7 (2.9)	40.5	74	B	Sandstone
								240-340	(1.84)	42.3	36.0	66	B	
T21S/R3E/26Caa	WC	43-43.05	122-25.17	HILLSCDRM (11/8/80)	TG	427	160	30-160	(3.71)	36.9	31.3	116	B	Silicified volcanics



## APPENDIX D.

## TEMPERATURE AND HEAT-FLOW DATA

Table D.1. Temperature and heat-flow data for the Oregon Cascades --Continued

Location	Prov. <sup>a</sup>	N. lat. deg.-min.	W. long. deg.-min.	Hole name (date)	Hole type <sup>b</sup>	Collar elev. (m)	Total depth (m)	Depth interval (m)	Average thermal conductivity	Uncorr. grad. <sup>c</sup> °C/km (1σ)	Corr. grad. <sup>c</sup> (°C/km)	Corr. heat flow <sup>c</sup> mW/m <sup>2</sup>	Quality <sup>d</sup>	Lithologic summary
T21S/R4E/28Ad	WH	43-43.1	122-20.0	CR-MCHSE (9/29/76)	TG	533	154	10-150	1.67	82.3 (0.4)	60.0	99	B	Intrusives, lithic tuff
T21S/R5E/16Ac	WH	43-44.9	122-13.0	BLCK-CRK (8/1/80)	TG	829	104	45-104	----	6.2 (0.6)	----	--	X	Basalt
T21S/R11E/25Bb	HL	43-43.9	121-21.7	BFZ-MB (8/4/76)	TG	1515	35	27.5-35	1.51	65.3 (4.3)	65.3	100	C	Obsidian and cinders, rhyolite
T22S/R3E/10Dd	WC	43-40.3	122-27.0	PCCPG-WW (6/28/78)	WW	490	106	20-90	1.33	39.0 (0.6)	40.0	53	B	Claystone, sandstone
T22S/R5E/26Bc	WH	43-38.2	122-11.3	RDH-MHSW (9/29/76)	TG	975	155	30-150	1.97 (0.06)	54.0 (0.4)	51.8	102	B	Amgydaloidal basalt, andesite
T23S/R5E/8Da	WH	43-35.5	122-14.0	PNT0-CRK (8/1/80)	TG	1219	154	40-154	1.52 (0.04)	83.3 (3.3)	66.1	101	B	Andesite and tuff
T23S/R9E/36Bb	HC	43-32.6	121-36.1	SH-WW (10/1/75)	WW	1320	130	----	----	----	----	--	X	Basalt (QTb)
T24S/R5E/18Ca	WH	43-29.4	122-15.9	TBUG-CRK (8/1/80)	TG	951	155	35-154	----	54.2 (8.6)	----	--	C	Basalt and altered basalt
T24S/R7E/7Db	HC	43-30.3	121-55.8	WP-WW (10/5/76)	WW	1463	45	----	----	----	----	--	X	Quaternary basalt
T26S/R2W/23Aa	WC	43-17.8	122-53.5	SUSCRCPG (7/24/81)	WW	289	52	----	----	----	----	--	-	Alluvium and basalt(?)
T26S/R3E/25Aa	WH	43-17.0	122-24.0	PPL-TCS (7/23/81)	WW	780	25	7.5-25	----	41.7	----	--	C	----
T28S/R8E/5Aa	BR	43-10.8	121-47.0	SHD-1 (8/25/73)	WW	1430	75	----	----	----	----	--	X	----
T29S/R6E/9Bc	HC	43-5.6	122-5.4	CLKPRK (8/2/81)	WW	1844	305	----	----	----	----	--	X	Pyroclastics
T31S/R2W/11Bc	WC	42-54.2	122-56.0	JWILSON (7/21/81)	WW	466	67.5	----	----	----	----	--	-	Silicic lithic tuffs
T31S/R3E/3Da	WH	42-54.2	122-26.5	USFS-NUC (7/23/81)	WW	1024	52.5	----	----	----	----	--	X	Silicic pyroclastics, basalt
T32S/R2W/4Ca	WC	42-49.0	122-56.4	CLR-7 (12/29/72)	WW	937	215	105-215	2.93 (0.17)	20.5 (0.4)	20.9	61	A	Chlorite schist
T32S/R3E/29Ba	HC	42-45.8	122-29.3	USFSRPS (7/23/81)	WW	805	46	----	----	----	----	--	X	High Cascade clas- tics
T33S/R2E/11Ac	WC	42-43.0	122-32.7	WILDWOOD (8/7/77)	WW	705	60	----	----	----	----	--	X	----
T33S/R2E/17Add	WC	42-42.1	122-35.9	LCRKDAM2 (7/22/81)	FS	597	92.5	----	----	----	----	--	-	Basalt
T33S/R2E/17Adc	WC	42-42.2	122-36.0	LCRKDAM1 (7/22/81)	FS	683	131	----	----	----	----	--	-	Basalt
T33S/R2E/19Dd	WC	42-40.9	122-37.3	DMND-CRK (8/18/77)	WW	592	45	----	----	----	----	--	X	----
T34S/R1W/4Dd	WC	42-38.3	122-49.2	MARTINSN (7/31/81)	WW	491	212	----	----	----	----	--	-	Basalt and andesite

## APPENDIX D.

## TEMPERATURE AND HEAT-FLOW DATA

Table D.1. Temperature and heat-flow data for the Oregon Cascades --Continued

Location	Prov. <sup>a</sup>	N. lat. deg.-min.	W. long. deg.-min.	Hole name (date)	Hole type <sup>b</sup>	Collar elev. (m)	Total depth (m)	Depth interval (m)	Average thermal conductivity	Uncorr. grad. <sup>c</sup> °C/km (1σ)	Corr. grad. <sup>c</sup> (°C/km)	Corr. heat flow <sup>c</sup> mW/m <sup>2</sup>	Quality <sup>d</sup>	Lithologic summary
T34S/R1E/34Aa	WC	42-34.5	122-40.7	JVARGO (7/30/81)	WW	548	40	7.5-35	----	49.7	----	--	C	Volcanics
T34S/R1E/34Bb	WC	42-34.7	122-41.6	MATHER (7/31/81)	WW	555	52.5	10-52.5	----	33.2	----	--	C	Basalt flows(?)
T35S/R2W/28Cc	WC	42-29.5	122-57.1	SAMS VAL (8/9/77)	WW	389	165	30-165	(1.88)	16.7 (0.5)	17.0	33	B	Claystone
T35S/R2W/30Da	WC	42-29.8	122-58.5	SAMS VLF (8/9/77)	WW	395	85	10-85	(1.88)	19.2 (1.7)	19.0	33	B	Claystone
T35S/R1E/13Ad	WC	42-31.8	122-38.3	RAMBO (8/15/77)	WW	853	40	25-40	(1.59)	29.6 (1.4)	31.0	49	C	Basalt (Miocene)
T36S/R2W/31Dc	WC	42-23.4	122-58.7	WLWCK-2 (8/10/77)	WW	443	150	95-150	(1.88)	12.9 (0.1)	12.0	40	B	Mudstone
T36S/R2W/31Dd	WC	42-23.3	122-58.8	WLWCK-1 (8/10/77)	WW	437	40	----	----	----	----	--	X	----
T36S/R1E/18Cc	WC	42-26.1	122-45.3	OWENS (8/10/77)	WW	437	45	10-45	----	35.3 (1.3)	35.3	--	B	Volcanic flows
T37S/R2W/34Dc	WC	42-18.2	122-55.3	JCKSNVIL (8/10/77)	WW	449	40	20-40	----	19.6 (1.4)	18.0	--	C	Mudstone
T37S/R1W/27Cb	WC	42-19.4	122-48.7	PHOEN-BL (8/9/77)	WW	529	220	75-220	(1.88)	25.0	24.0	46	B	Mudstone
T37S/R2E/4Ad	WC	42-23.0	122-34.8	MORTEN (8/27/81)	WW	561	96.5	30-96.5	----	34.6	----	--	-	Basalt
T37S/R7E/15Ba	BR	42-21.4	121-59.0	WEYEH (75)	--	---	---	-----	----	----	----	42	D	----
T38S/R2E/25Bb	WC	42-14.6	122-32.4	MILLER (8/26/81)	WW	1164	29	10-29	----	50.0	----	--	C	Volcanic sediments and basalts
T38S/R2E/27Ca	WC	42-14.2	122-34.2	HARRGTON (8/81)	WW	963	46	20-46	----	68.8	----	--	C	Andesite(?)
T38S/R2E/35Ac	WC	42-13.4	122-32.4	JM MILLR (8/4/81)	WW	1231	45	15-45	----	14.3	----	--	C	Basalt
T38S/R3E/12Ad	WH	42-17.0	122-24.5	LILYGLEN (8/4/81)	WW	1400	38.5	-----	----	----	----	--	-	Sediments and basalt
T38S/R9E/20Ac	BR	42-15.1	121-46.9	PH-WW (8/21/74)	WW	1329	465	0-465	> 0.75	160.0	160.0	121	C	----
T38S/R9E/28Ac	BR	42-14.3	121-46.0	MOLATORE (6/16/79)	WW	1359	170	105-170	----	71.9	----	--	C	----
T38S/R9E/28Dc	BR	42-14.0	121-46.8	BH-WW (7/17/74)	WW	1292	78	0-78	> 0.75	950.0	950.0	715	C	----
T38S/R9E/29Aa	BR	42-14.4	121-46.6	PF-WW (7/18/74)	WW	1277	60	0-59	> 0.75	130.0	130.0	98	C	----
T38S/R9E/32Da	BR	42-13.2	121-46.6	MODCLMR (9/22/81)	WW	1247	631	380-625	----	186	----	--	B	----
T38S/R9E/33Ab	BR	42-13.6	121-45.7	AG-WW (7/17/74)	WW	1262	109	0-109	> 0.75	716.0	716.0	537	C	----
T39S/R1E/2Bc	WC	42-12.7	122-40.6	COOK (8/4/81)	WW	622	180	20-177	----	27.5	----	--	A	Siltstone and sand- stone

## APPENDIX D.

## TEMPERATURE AND HEAT-FLOW DATA

Table D.1. Temperature and heat-flow data for the Oregon Cascades --Continued

Location	Prov. <sup>a</sup>	N. lat. deg.-min.	W. long. deg.-min.	Hole name (date)	Hole type <sup>b</sup>	Collar elev. (m)	Total depth (m)	Depth interval (m)	Average thermal conductivity	Uncorr. grad. <sup>c</sup> °C/km (1σ)	Corr. grad. <sup>c</sup> (°C/km)	Corr. heat flow <sup>c</sup> mW/m <sup>2</sup>	Quality <sup>d</sup>	Lithologic summary
T39S/R1E/4Bb	WC	42-12.7	122-42.8	ASLDGRHSE (10/14/81)	WW	536	136	18-136	----	76.5	----	--	C	-----
T39S/R1E/13Da	WC	42-31.6	122-38.5	RAMBO (8/1/81)	WW	884	69	40-68	----	21.1	----	--	C	-----
T39S/R1E/15Cdb	WC	42-10.4	122-41.3	STURDEVNT (8/3/81)	WW	731	257	----	----	18.0	----	--	-	-----
T39S/R1E/32Acd	WC	42-08.1	122-43.5	WC 1	TG	1025	310	283-310	3.05 (0.06)	16.27 ( 0.08)	----	42	A	Granodiorite
T39S/R2E/7Cc	WC	42-11.3	122-38.2	LITHIASP (8/8/77)	WW	583	130	95-130	(2.09)	16.6 ( 0.3)	15.0	31	B	Claystone
T39S/R8E/31Ac	BR	42-8.0	122-55.2	RP-WW (3/8/74)	WW	1262	52	15-52	> 0.75	55.0	55.0	> 42	C	-----
T39S/R9E/3Dd	BR	42-12.0	121-44.3	CW-WW (1/25/74)	WW	1251	150	25-150	> 0.75	170.0	170.0	>130	C	-----
T39S/R9E/8Ad	BR	42-11.7	121-46.5	KLADZ-WW (8/26/74)	WW	1247	85	4-84	> 0.75	160.5	160.5	>121	C	-----
T39S/R9E/12Bc	BR	42-11.5	121-42.8	GH-WW (8/22/79)	WW	1259	150	80-150	> 0.75	138.0	138.0	>105	C	-----
T39S/R9E/7Da	BR	42-11.5	121-48.0	FRHVNSCH (8/18/77)	WW	1282	50	15-50	> 0.75	245.7 ( 34.6)	223.0	>167	C	Pliocene-Pleistocene volcanics
T39S/R9E/2Cd	BR	42-12.1	121-43.6	WP-WW (8/22/74)	WW	1262	290	30-290	> 0.75	165.0	165.0	>125	C	-----
T39S/R9E/9Cb	BR	42-11.4	121-46.3	KLAOI-WW (8/26/74)	WW	1257	69	15-69	> 0.75	110.0	110.0	> 84	C	-----
T39S/R9E/30Ad	BR	42-9.3	121-41.9	ED-WW (1/25/74)	WW	1251	70	40-70	> 0.75	90.0	90.0	> 67	C	-----
T39S/R9E/35Cb	BR	42-8.0	121-44.1	JB-WW (6/12/74)	WW	1247	50	10-50	> 0.75	86.0	86.0	> 63	C	-----
T39S/R10E/6Cd	BR	42-12.1	121-41.5	OWC-WW (8/18/74)	WW	1304	223	0-223	1.05	104.0	104.0	105	C	-----
T39S/R10E/14Cc	BR	42-10.4	121-37.1	MB-WW (6/18/74)	WW	1268	115	0-115	> 0.75	400.0	400.0	>301	C	-----
T39S/R10E/18Bc	BR	42-10.7	121-41.7	HW-1-WW (6/18/74)	WW	1268	80	30-80	> 0.75	48.0	48.0	> 33	C	-----
T39S/R10E/19Ac	BR	42-9.9	121-40.9	KT-1-WW (5/29/74)	WW	1256	120	100-120	> 0.75	28.5	28.5	> 21	C	-----
T39S/R10E/21Bb	BR	42-10.2	121-39.2	CT-WW (6/5/74)	WW	1253	48	10-48	> 0.75	47.0	47.0	> 33	C	-----
T39S/R10E/30Ad	BR	42-9.0	121-40.7	BA-WW (5/20/74)	WW	1248	73	20-73	> 0.75	80.0	80.0	> 59	C	-----
T39S/R10E/30Ad	BR	42-8.9	121-40.7	EJ-WW (5/20/74)	WW	1248	54	20-54	> 0.75	82.0	82.0	> 63	C	-----
T40S/R2W/21Bb	KM	42-5.0	122-57.0	USGS	TG(?)	1245	---	----	2.72	----	12.3	63	A	-----
T40S/R1E/36Ab	WC	42-3.3	122-38.7	COLESTIN (8/11/77)	WW	1094	140	10-140	(1.88)	31.2 ( 0.7)	28.0	52	B	Colestin Fm., volcanic conglomer- ates

## APPENDIX D.

## TEMPERATURE AND HEAT-FLOW DATA

Table D.1. Temperature and heat-flow data for the Oregon Cascades --Continued

Location	Prov. <sup>a</sup>	N. lat. deg.-min.	W. long. deg.-min.	Hole name (date)	Hole type <sup>b</sup>	Collar elev. (m)	Total depth (m)	Depth interval (m)	Average thermal conductivity	Uncorr. grad. <sup>c</sup> °C/km (1σ)	Corr. grad. <sup>c</sup> (°C/km)	Corr. heat flow <sup>c</sup> mW/m <sup>2</sup>	Quality <sup>d</sup>	Lithologic summary
T40S/R2E/6Bb	WC	42-5.6	122-32.3	FORD (8/25/81)	WW	963	137	20-137	----	24.6	----	--	C	Fine sediments
T40S/R2E/12Acc	WC	42-6.3	122-31.8	HARRELL (8/26/81)	WW	817	47	10-47	----	47.0	----	--	C	Basalts
T40S/R3E/5Ddd	WC	42-6.8	122-29.0	MURRAY (8/27/81)	WW	1359	73	45-73	----	26.4	----	--	C	Basalt
T40S/R8E/3Cd2	BR	42-6.8	121-51.9	VW-WW (5/21/74)	WW	1245	72	20-72	> 0.75	146.0	146.0	>109	C	-----
T40S/R8E/17Ba	BR	42-5.7	121-54.2	EG-17-WW (3/18/74)	WW	1254	55	15-55	> 0.75	17.0	17.0	> 13	D	-----
T40S/R9E/6Ab	BR	42-7.5	121-48.1	RD-WW (6/20/74)	WW	1248	150	0-150	> 0.75	----	50.0	> 4	D	-----
T40S/R9E/19Dc	BR	42-4.2	121-48.3	TF-1-WW (6/4/74)	WW	1243	50	28-50	> 0.75	45.0	45.0	> 33	C	-----
T40S/R9E/28Ad	BR	42-3.8	121-45.5	LA-WW (6/14/74)	WW	1256	30	20-30	> 0.75	74.0	74.0	> 54	C	-----
T40S/R10E/17Cc	BR	42-5.1	121-40.5	JG-WW (2/8/74)	WW	1245	58	18-49	----	----	82.0	--	D	-----
T40S/R10E/18Cb	BR	42-5.3	121-41.8	CM-WW (6/13/74)	WW	1245	140	12-140	> 0.75	77.0	77.0	> 59	C	-----
T40S/R10E/26Bc2	BR	42-3.8	121-36.9	BHL-WW (6/26/74)	WW	1262	89	60-89	> 0.75	58.0	58.0	> 42	C	-----
T40S/R10E/25Cc	BR	42-3.3	121-35.8	LC-WW (6/27/74)	WW	1280	38	20-38	> 0.75	120.0	120.0	92	C	-----
T41S/R8E/13Ac	BR	42-0.3	121-49.3	LISKEY-WW	WW	1244	179	51-179	0.75 (0.01)	16.8 ( 0.9)	16.8 ( 0.9)	13	A	-----
T41S/R9E/3Db	BR	42-1.8	121-44.8	OC-1-WW (8/21/74)	WW	1244	176	53-176	0.75 (0.01)	78.6 ( 0.3)	78.6 ( 0.3)	60	A	-----
T41S/R10E/1Cd2	BR	42-1.5	121-35.5	BC-WW (5/11/74)	WW	1240	87	25-87	> 0.75	74.0	74.0	> 54	C	-----
T41S/R10E/7Db	BR	42-1.0	121-41.1	OC-3-WW (1/24/74)	WW	1253	150	0-150	> 0.75	130.0	130.0	> 96	C	-----
T41S/R10E/15Ab	BR	42-0.4	121-37.7	RK-WW (6/13/74)	WW	1248	73	45-73	> 0.75	110.0	110.0	> 84	C	-----

## FOOTNOTES FOR TABLE D.1.

<sup>a</sup> Physiographic province: BR = Basin and Range; HL = High Lava Plains; DU = Deschutes-Umatilla Plateau; HC = High Cascades; WC = Western Cascades; WV = Willamette Valley; KM = Klamath Mountains; WH = Western-High Cascade boundary.

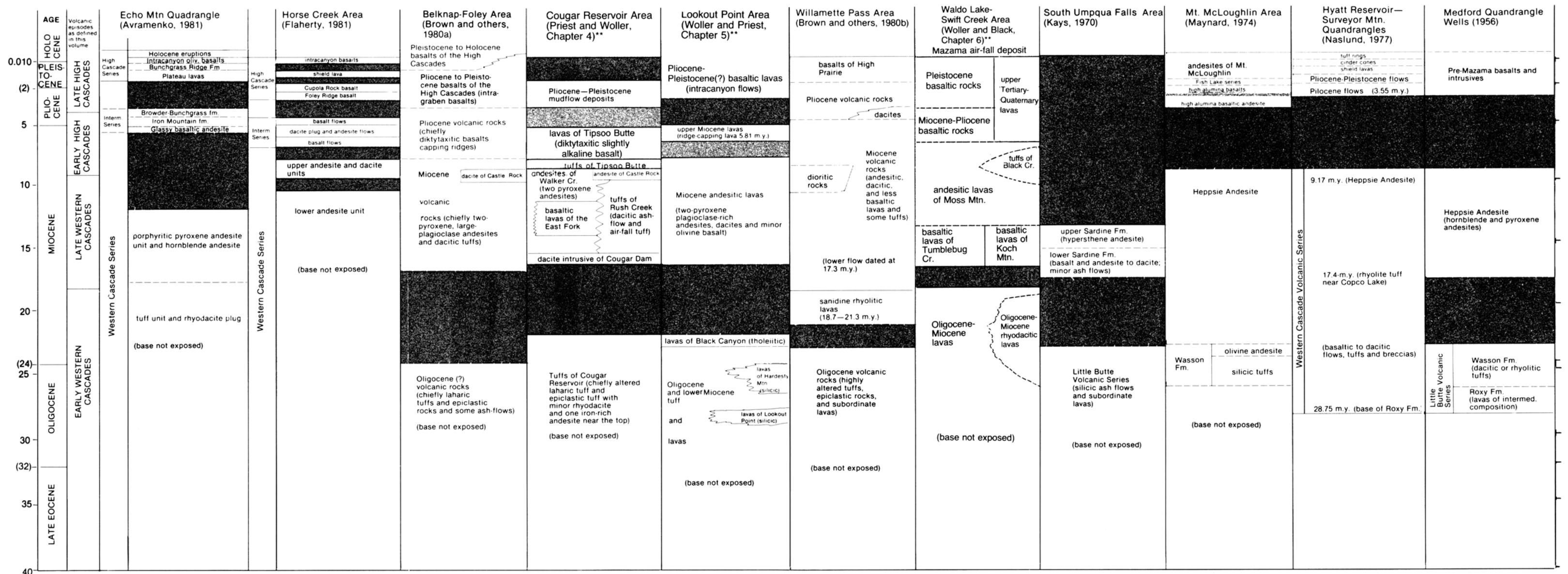
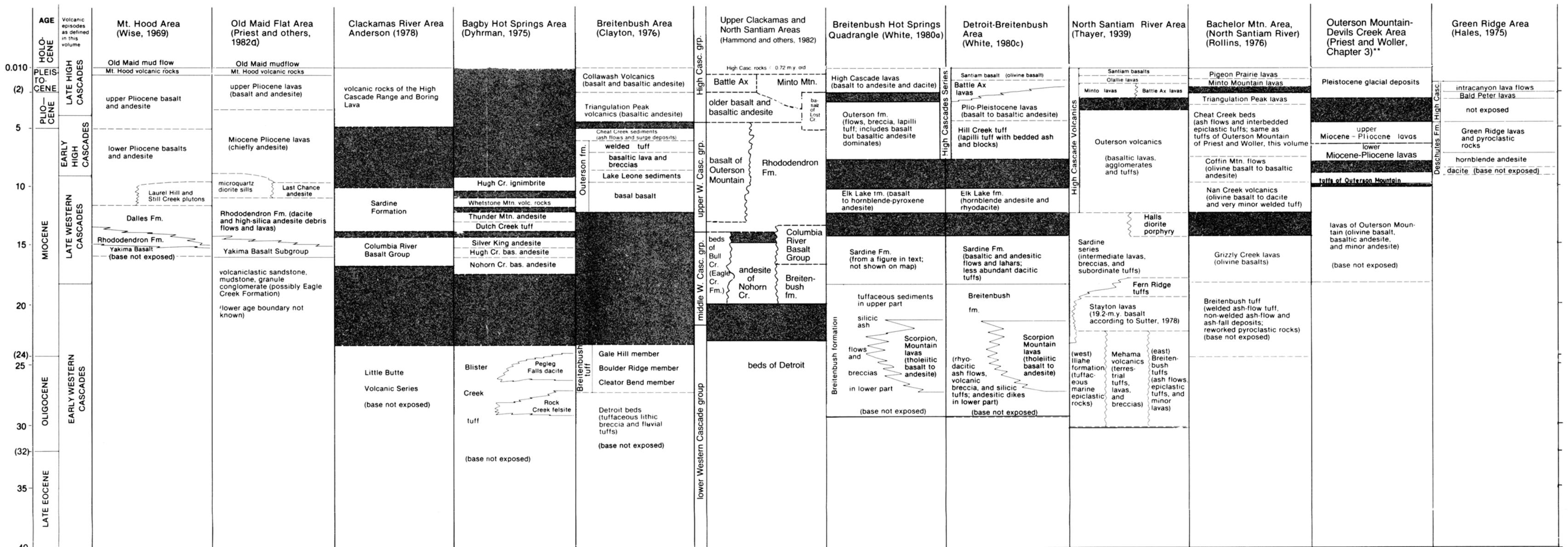
<sup>b</sup> Hole type: WW = water wells; OW = oil and gas prospects; TG = temperature-gradient holes; FS = damsite foundation studies; ME = mineral exploration holes.

<sup>c</sup> Calculations performed under direction of David D. Blackwell, Southern Methodist University, Dallas, Texas.

<sup>d</sup> Heat-flow quality: Assessment of reliability of heat-flow determination. A±=5 percent; B±=10 percent; C±=25 percent; D = uncertain reliability; X = temperature-depth data not suitable for heat-flow determinations.



# LOCAL STRATIGRAPHIC COLUMNS OF REGIONAL INTEREST IN THE OREGON CASCADES\*

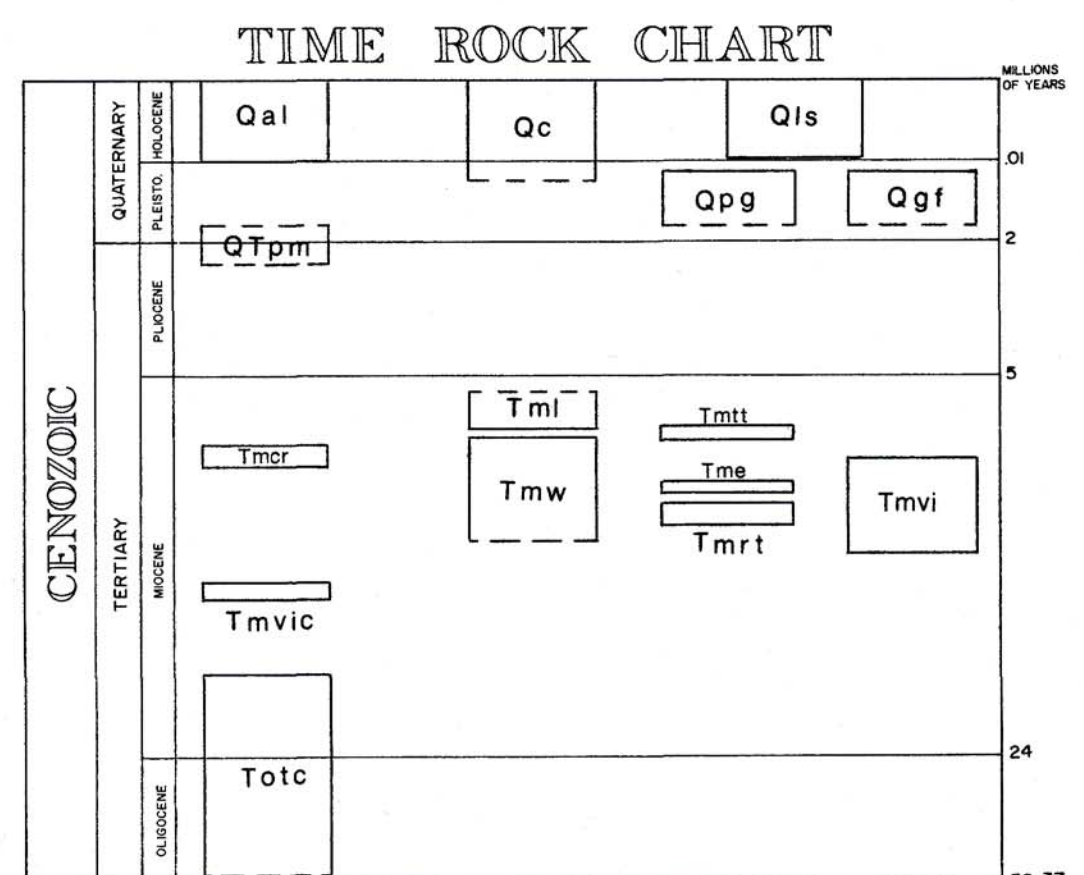


\* Time boundaries are assigned to match, as closely as possible, the intent of the original reference; poorly consolidated Pleistocene and younger sedimentary deposits not included. Initial capital letters are used to indicate names of units that are recognized by the U.S. Geological Survey or the Oregon Department of Geology and Mineral Industries. References cited in Plate 1 appear in list of references cited at the end of Special Paper 15.  
\*\* This paper.



Contains  
Recycled  
Materials





**EXPLANATION**

### SUBFICIAL DEPOSITS

- |     |                                                                                                                                                                                                                                                                                   |
|-----|-----------------------------------------------------------------------------------------------------------------------------------------------------------------------------------------------------------------------------------------------------------------------------------|
| Qal | <b>Alluvium (Quaternary):</b> <i>Recent unconsolidated sediments located in present river and creek channels</i>                                                                                                                                                                  |
| Qc  | <b>Recent colluvium (Quaternary):</b> <i>Includes talus debris slopes as well as thin soil cover. Where bedrock lithology can be inferred below thin soil cover, bedrock unit is shown</i>                                                                                        |
| Qls | <b>Landslide deposits (Quaternary):</b> <i>Unconsolidated landslide debris; includes slumps and slide blocks</i>                                                                                                                                                                  |
| Qpg | <b>Glacial outwash deposits (Quaternary):</b> <i>Unconsolidated sands and sandy gravels with moderately good sorting and stratification; found at lower elevations; Pleistocene in age</i>                                                                                        |
| Qgl | <b>Glacial and fluvial deposits (Quaternary):</b> <i>Unconsolidated sedimentary deposits of glacial and fluvial origin; includes tills and unconsolidated outwash deposits of Pleistocene age; found at higher elevations; may be partly a result of local igneous alteration</i> |

### BEDROCK GEOLOGIC UNITS

- Piobocene-Pleistocene mudflow deposits (Piobocene-Pleistocene):** Semiconsolidated clastic units bearing andesitic, lithic fragments and cobbles in indurated, silty and matrix, brown-gray. Mapped as unit Tm by Wells and Peck (1981) and as Oligocene and Pleistocene by Wells and others (1988). Occurs as outcrops along the river margins; clearly controlled by present topography which developed after about 5.0 m. B.P.
- Volcanic rocks of the early High Cascade period**
- Lavas of Tipsoo Butte (upper Piobocene):** Unit caps ridges on east side of Cougar Reservoir; appears conformable on unit Tm at Tipsoo Butte. Dikeless, ophiolite basaltic and basaltic andesite, light to medium gray. Olivines inclined to indiginate. Clinopyroxene in groundmass is ophitic to intergranular and may be titanium-rich. Three flows recognized on Tipsoo Butte. Flows originate from east of map area and are undifferentiated. Equivalent to uppermost part of the Outcrop below. (See also the map of the area.)
- Intermediate series of Flaherty (1981):** Basal flow of Tipsoo Butte K-Ar dated at  $7.80 \pm 0.77$  m. B.P.; basal flow at Lookout Ridge K-Ar dated at  $8.34 \pm 0.34$  m. B.P.; flow near top of section of Tipsoo Butte K-Ar dated at  $9.41 \pm 0.42$  m. B.P.

### Volcanic rocks of the late Western Cascade episode

- |        |                                                                                                                                                                                                                                                                                                                                                                                                                                                                                                                                                                                                                                                                                                                                                                                                                                                                                                                                                                      |
|--------|----------------------------------------------------------------------------------------------------------------------------------------------------------------------------------------------------------------------------------------------------------------------------------------------------------------------------------------------------------------------------------------------------------------------------------------------------------------------------------------------------------------------------------------------------------------------------------------------------------------------------------------------------------------------------------------------------------------------------------------------------------------------------------------------------------------------------------------------------------------------------------------------------------------------------------------------------------------------|
| Tmtrt  | <b>Tuffs of Tipsoo Butte (Miocene):</b> Unit flowed into canyons cut into <b>Tuw</b> at <b>Tipsoo Butte</b> and is overlain (conformably) by unit <b>Tml</b> . Hornblende-bearing two-pyroxene dacite nonwelded ash-flow tuff and probable sparse deposit. White granitic and fine-grained, cream-colored matrix; thick bedded at almost flat basal angle attitude. Lies on top of <b>Tml</b> dated at 9.4 to 7.8 m.y. B.P. but above parts of unit <b>Tuw</b> dated at 13.2 to 8.83 m.y. B.P.                                                                                                                                                                                                                                                                                                                                                                                                                                                                       |
| Tmcr   | <b>Andesites of Castle Rock (Miocene):</b> Intrusive plug dome and possible flows at <b>Castle Rock</b> . Pilolitic hypersthene and quartz, fine-grained, light gray, olivine-gray. K-Ar dated at 9.31 to 4.0 m.y. B.P.                                                                                                                                                                                                                                                                                                                                                                                                                                                                                                                                                                                                                                                                                                                                              |
| Tmvi   | <b>Andesitic intrusives (Miocene):</b> Generally two-pyroxene plagioclase-arsenite. Composition and textures similar to unit <b>Tuw</b>                                                                                                                                                                                                                                                                                                                                                                                                                                                                                                                                                                                                                                                                                                                                                                                                                              |
| Tmw    | <b>Andesites of Walker Creek (Miocene):</b> Plagioclase-rich two-pyroxene andesites, usually reddish gray. Unit flowed into canyons cut into unit <b>Tote</b> and is interbedded with unit <b>Turt</b> on the west side of the reservoir. Equivalent to <b>Sardine Formation</b> of Peck and others (1964), <b>Rhododendron Formation</b> of Hedge (1933), and <b>Miocene volcanics</b> of Brown and others (1980). Includes intrusions of labradorite and augite and some compositionally similar dacite as an interbedded sequence. The upper part is a fine-grained, cream-colored, nonwelded ash-flow tuff. The sequence exceeds 752 m (2,467 ft), 610 m (2,000 ft) exposed at <b>Walker Creek</b> . Slightly altered flow at base of section on east side of reservoir. K-Ar dated at 13.2 to 8.83 m.y. B.P. <b>Tipsoo Butte</b> is a small, isolated, conical hill. Unit <b>Tmw</b> interbedded tuffs at <b>Rush Creek</b> K-Ar dated at 13.2 to 0.7 m.y. B.P. |
| Tme    | <b>Basaltic lavas of the East Fork (Miocene):</b> Gray-black, almost aphyric olivine-bearing basalts and basaltic andesites. At least 120 m (396 ft) thick. Mapped as <b>Sardine Formation</b> by Peck and others (1964) and as <b>Miocene volcanic rocks</b> by Brown and others (1980). Olivine is altered to iddingsite. Interbedded within unit <b>Tmw</b> . Folded and faulted; probably older than unit <b>Tuw</b> flow and dated at 13.2 to 0.7 m.y. B.P.                                                                                                                                                                                                                                                                                                                                                                                                                                                                                                     |
| Tmrt   | <b>Tuffs of Rush Creek (Miocene):</b> Dacite welded and nonwelded ash flows; generally cream-colored or gray. Dacite bearing hypersthene and plagioclase phenocrysts with or without minor hornblende. Contains interbeds of siltstone. Unconformably on unit <b>Tote</b> . Flowed into canyons cut into unit <b>Tuw</b> and is also interbedded within unit <b>Tuw</b> . Mapped as <b>Sardine Formation</b> by Peck and others (1964) and <b>Miocene volcanics</b> by Brown and others (1980). Folded and faulted. One of the highest flows in the sequence K-Ar dated at 13.2 to 0.8 m.y. B.P.                                                                                                                                                                                                                                                                                                                                                                     |
| Tmrvic | <b>Dacite intrusive of Cougar Dam (Miocene):</b> Two-pyroxene-bearing dacite; black; glassy with irregular jointing. Dike-like intrusion on east side of reservoir; becomes both dike- and sill-like in west-side dam exposure. Equivalent to unit <b>Tote</b> . K-Ar dated at 13.2 to 0.7 m.y. B.P. Mapped as <b>Sardine Formation</b> by Peck and others (1964); equivalent to <b>Miocene intrusive rocks</b> of Brown and others (1980).                                                                                                                                                                                                                                                                                                                                                                                                                                                                                                                          |










### Volcanic rocks of the early Western Cascade episode

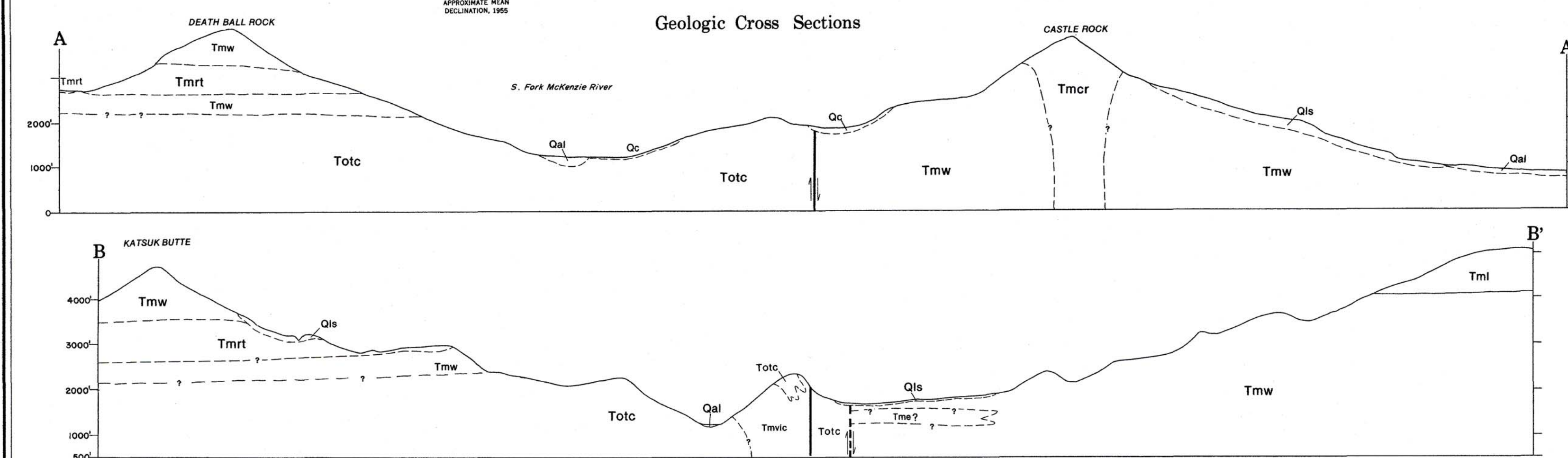
- [illegible]

## REFERENCES

- Brown, D.E., Melson, D.G., Pyle, G.R., Woller, N.M., and Black, G.L., 1980. Preliminary geology and geothermal resource potential of the Belding-People Geopark. Oregon: Oregon Department of Geology and Mineral Industries Open-File Report 0-80, 58 pp.
- Flaherty, J.R., 1981. The Western Cascade-High Cascade transition in the McElaine Basin area, central Oregon Cascade Range, Eugene, Oregon. University of Oregon master's thesis, 178 p.
- Hammond, P.E., Anderson, J.L., and Manning, K.J., 1980. Guide to the geology of the upper Clackamas and North Santiam rivers in the Cascade Range, in Oles, K.P., Johnson, J.G., Niemi, A.R., and Niemi, W.A., eds. *Geological field trips in western Oregon and southwestern Washington*. Oregon Department of Geology and Mineral Industries Bulletin 110, 1-130.
- Hock, D.L., 1983. Age of Schickler Highway and lower canyon lake. *Geological Society of America Bulletin*, v. 44, pt. 1: 156-157.
- Peck, D.L., Griggs, A.B., Schickler, H.G., Wells, F.G., and Dale, H.M., 1964. Geology of the central and northern parts of the Cascade Range in Oregon. U.S. Geological Survey Professional Paper 449, 56 p.
- Sutton, J.P., 1978. K-Ar ages of the Cascade Range, in Oles, K.P., Johnson, J.G., Niemi, A.R., and Niemi, W.A., eds. *Geological field trips in western Oregon and southwestern Washington*. Oregon Department of Geology and Mineral Industries Bulletin 110, 21, p. 15-21.
- Thompson, J.R., 1980. Structure of the North Santiam River section of the Cascade Mountains in Oregon. *Journal of Geology*, v. 88, no. 6: 701-716.
- 1989. Geology of the Salween Hills, in Oles, K.P., Johnson, J.G., Niemi, A.R., and Niemi, W.A., eds. Oregon Department of Geology and Mineral Industries Special Paper 5, 26 p.
- Wells, F.G., and Peck, D.L., 1961. Geologic map of Oregon west of the 121st meridian. U.S. Geological Survey Miscellaneous Investigations Series Map 1-326, scale 1:500,000.
- White, J.D., 1980a. Geology of the Interlachen Hot Springs quadrangle, Oregon. Oregon Department of Geology and Mineral Industries Special Paper 5, 26 p.
- 1980b. Geology and geochemistry of volcanic rocks in the Detroit area, Western Cascade Range, Eugene, Oregon. Oregon Department of Geology and Mineral Industries Special Paper 5, 26 p.

### GEOLOGIC SYMBOLS

-  **Fault:** Solid where visible, dashed where approximately located, dotted where concealed by alluvium, landslide, or reservoir. Dip on fault plane indicated; bar and ball on downthrown side
-  **Strike and dip**
-  **Contact:** Solid where visible, dashed where inferred below cover or from photo interpretation
-  **Strike and dip of fault zone:** Orientation of plane and slickensides shown
-  **Geothermal test hole:** With terrain-corrected gradient ( $^{\circ}\text{C/km}$ ) and heat flow ( $\text{mW/m}^2$ ) shown
-  **Geochemical sample**
-  **K-Ar date:** With age in millions of years
-  **Dike:** Dip shown
-  **Shear zone with brecciation**





GEOLOGIC MAP OF THE WALDO LAKE - SWIFT CREEK AREA,  
LANE AND KLAMATH COUNTIES, OREGON

1983

STATE OF OREGON  
DEPARTMENT OF GEOLOGY AND MINERAL INDUSTRIES  
DONALD A. HULL, STATE GEOLOGIST

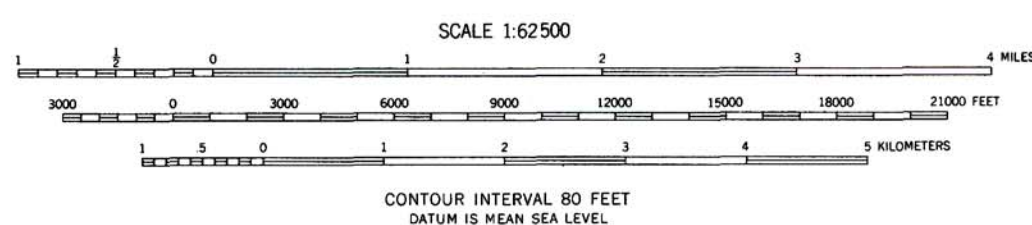
Sp. P. 15

Geology and Geothermal Resources  
of the Central Oregon Cascade Range  
Edited by George R. Priest and Beverly F. Vogt  
This work was supported by the United States Department of Energy  
(Cooperative agreement No. DE-FC-07-79ID12044).

PLATE 3



Base map by U.S. Geological Survey-Waldo Lake, Oakridge, Toketa Falls, and Summit Lake quadrangles.  
Control by USGS and USCGS  
Topography from aerial photographs by multiple methods  
Aerial photographs taken 1954. Field check 1955-56  
Polyconic projection. 1927 North American datum  
10,000-foot grid based on Oregon coordinate system,  
north zone.  
1000-meter Universal Transverse Mercator grid ticks,  
zone 10  
Dashed lines indicate approximate locations

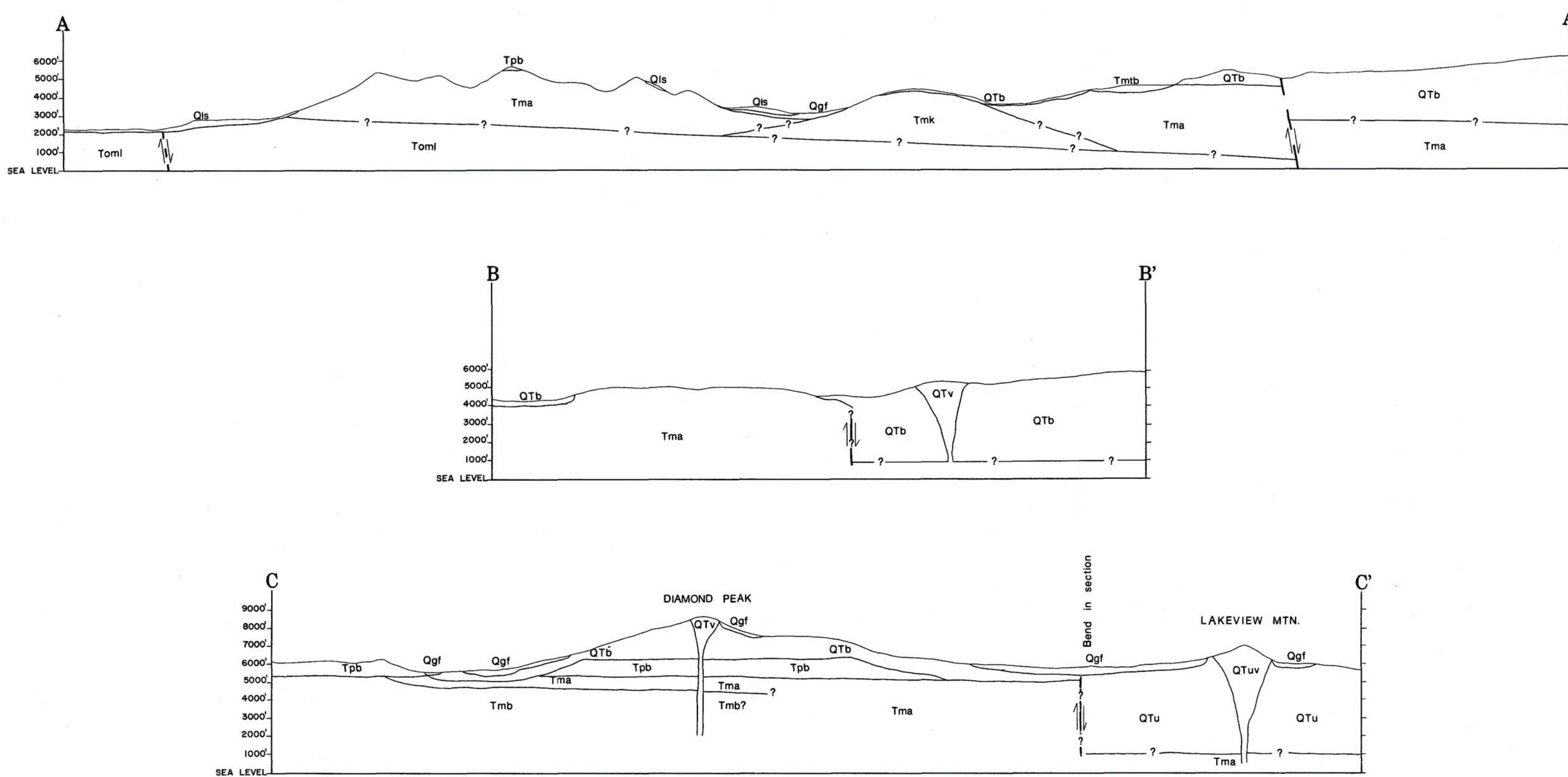


Geology by Neil M. Woller and Gerald L. Black

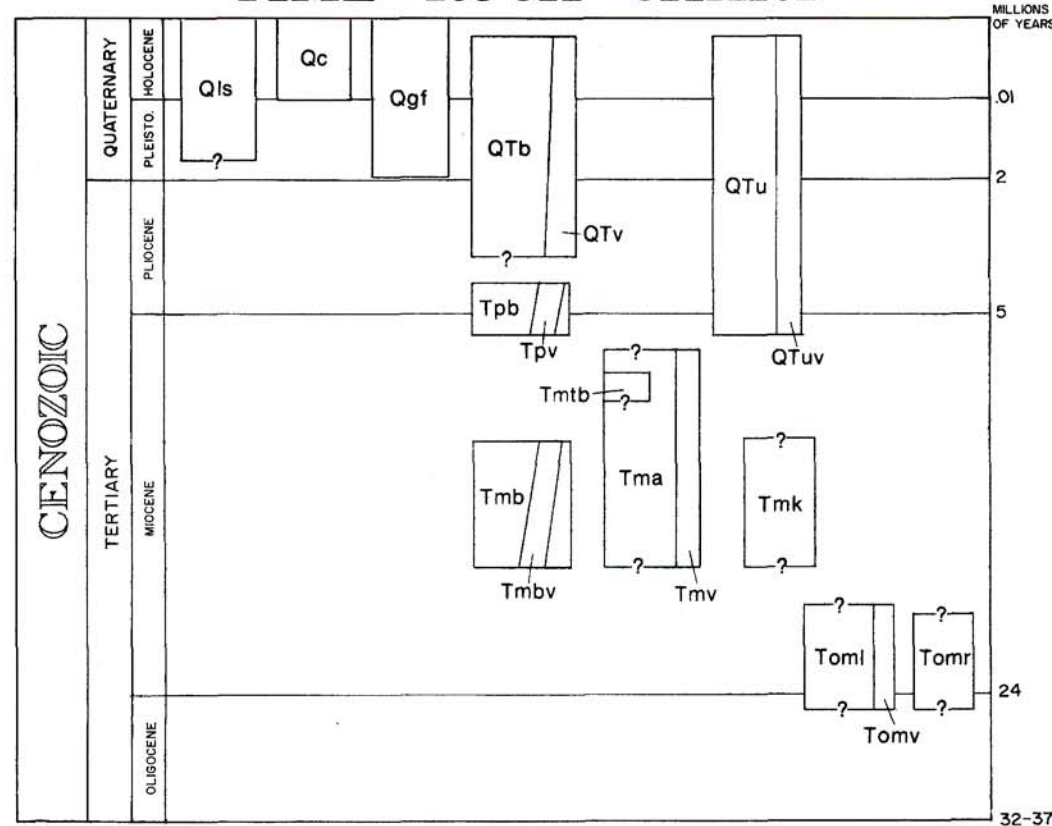
Field work, 1980-1982

Geologic mapping of the Diamond Peak Wilderness area  
from Sherrod and others (in press)

Geologic Cross Sections



TIME ROCK CHART



EXPLANATION

SURFICIAL DEPOSITS

- Qc Colluvium (Quaternary): Recent unconsolidated deposits including debris slopes and local  
Massena ash and pumice lapilli aerial deposits. Mapped separately only where colluvial  
deposits are thick and the nature of underlying bed rock is uncertain
- Qls Landslide deposits (Quaternary): Unconsolidated landslide debris; includes slumps and  
slide blocks
- Qgl Glacial and fluvial deposits (Quaternary): Unconsolidated and semiconsolidated  
sedimentary deposits of glacial and fluvial origin; includes terrace deposits, tills, and  
moraines. Bed rock shown where till is thin

BEDROCK GEOLOGIC UNITS

- Volcanic rock of the early and late High Cascade episodes
- Qtb, Qtu, Qtv Upper Tertiary-Quaternary lavas, undifferentiated (Pliocene-Pleistocene): Olivine  
basalts and basaltic andesites, light to dark gray, compact to dikeitic, fresh. Flows are  
mapped as unit Qtb, vents and plugs as unit Qtv. Includes all lavas and vents that cannot  
be assigned with confidence to either unit Qtb or unit Qtv. Also includes  
epistatic volcanic rocks and sediments. Equivalent to volcanic rocks of the High Cascades  
and Boring Lavas (Peck and others, 1964) and Outers formation and High Cascade lavas of  
White (1980a)
- Volcanic rocks of the late High Cascade episode
- Qtb, Qtv Pleistocene basaltic lavas (upper Pliocene?-Holocene?): Olivine basalt and basaltic  
andesites, yellow-brown when weathered, light to dark gray when fresh, compact to  
dikeitic, undifferentiated, very fresh. Flows are mapped as unit Qtb, vents and plugs as unit  
Qtv. Includes interbedded epistatic volcanic rocks and sediments. Units mapped as lavas  
conform to any or all of the following criteria: (1) they either flowed into canyons cut into the  
existing topography of the Western Cascades or are associated with other flows that did; (2)  
they possess surficial flow morphologies and/or relationships to glacial features which  
indicate a Pleistocene or younger age; or (3) they are associated with K-Ar-dated lavas which  
are younger than 2 m.y. Equivalent to High Cascade lavas of White (1980a) and basaltic  
of High Prairie of Brown and others (1980b); partially equivalent to volcanic rocks of the  
High Cascades (undivided) of Peck and others (1964). Oldest dated flow 1.98 ± 0.25 m.y. B.P.;  
youngest dated flow 0.17 ± 0.45 m.y. B.P.
- Volcanic rocks of the early High Cascade episode
- Tpb, Tpv Miocene-Pliocene basaltic lavas (middle Miocene-middle Pliocene): Olivine basalt  
and basaltic andesites, gray, compact to dikeitic, fresh to slightly altered, faulted. Caps  
highest ridges of Western Cascades. Flows mapped as unit Tpb, vents and plugs as unit Tpv.  
In eastern half of map area, conformably underlies unit Qtb, from which it is  
indistinguishable unless it is sheeted or altered. Includes sedimentary interbeds. Equivalent  
to Outers volcanics of Thayer (1939). Pliocene volcanic rocks of Brown and others (1980b),  
and Outers formation of White (1980a). Oldest dated flow 5.56 ± 0.35 m.y. B.P.; youngest  
dated flow 4.32 ± 0.4 m.y. B.P.
- Volcanic rocks of the late Western Cascade episode
- Tma, Tmv Andesitic lavas of Moss Mountain (middle Miocene-upper Miocene?): Plagioclase-  
phyric two-pyroxene andesites, olive-clinopyroxene basaltic andesites, and hornblende  
and/or orthopyroxene dacites. Gray to dark-gray, compact, fresh to altered. Flows are  
mapped as unit Tma, vents and plugs as unit Tmv. Includes interbedded epistatic volcanic  
rocks and sediments and minor thin ash flows. Equivalent to Sardine Formation of Peck  
and others (1964). Miocene volcanic rocks of Brown and others (1980b), andesites of Walker  
Creek of Priest and Woller (this volume), Sardine series of Thayer (1939), Elk Lake  
Formation and Sardine Formation of White (1980a), and other volcanoclastic sediments and  
lavas of Walker (1939). One unit within this unit has been mapped separately as unit  
Tmb (below)
- Tmb Tufts of Black Creek (upper Miocene): Equivalent to Sardine Formation of Peck  
and others (1964). Miocene volcanic rocks of Brown and others (1980b), andesites of Walker  
Creek of Priest and Woller (this volume), Sardine series of Thayer (1939), Elk Lake  
Formation and Sardine Formation of White (1980a), and other volcanoclastic sediments and  
lavas of Woller (1982). Ductile(?) pumiceous ash-flow tufts, gray when weathered,  
buff to pink when fresh, well-indurated but unwelded, contain almost equal amounts of  
pumice and dark-gray dacitic(?) lithic fragments with subordinate plagioclase crystals.  
Also includes poorly indurated fine-grained tufts, unthrifted pumice falls and flows, and  
rare thin two-pyroxene andesite flows. Total thickness may be as much as 111 m (365 ft).  
Very poorly exposed on benches along Black Creek which lie at elevations of 1,340-  
1,460 m (4,400-4,800 ft)
- Tmk Basaltic lavas of Koch Mountain (middle Miocene): Olivine basalt and basaltic  
andesites, red-brown weathering, dark-gray to black when fresh, compact, occasionally  
dikeitic. Indurated olivine is typically phenocryst mineral. Extensively altered to  
smectites. Equivalent to Sardine Formation of Peck and others (1964). Miocene volcanic  
rocks of Brown and others (1980b), Sardine series of Thayer (1939), Sardine Formation of  
White (1980a), and basaltic lavas of Tumblebug Creek (this map)
- Tmbv, Tmv Basaltic lavas of Tumblebug Creek (middle Miocene): Olivine basalt and basaltic  
andesites, black to gray, compact to dikeitic, generally fresh. Flows are mapped as unit  
Tmbv, vents and plugs as unit Tmv. Includes interbedded epistatic volcanic rocks and  
sediments and minor thin ash flows. Equivalent to Sardine Formation of Peck and others  
(1964). Miocene volcanic rocks of Brown and others (1980b), Sardine series of Thayer (1939),  
Sardine Formation of White (1980a), and basaltic lavas of Koch Mountain (this map). K-Ar  
dates between 17.0 and 13.1 m.y. B.P. were obtained on various parts of the sequence
- Volcanic rocks of the early Western Cascade episode
- Toml, Tmtr Olivocene-Miocene lavas, undifferentiated (Oligocene-Miocene): Rhyolite to basaltic  
andesites, red-brown weathering, dark-gray to black when fresh, compact, occasionally  
dikeitic. Includes fragment-rich tuff and interbedded sediments. Includes green-yellow  
lithic-fragment-rich tuff and interbedded sediments. Includes altered to amictic, apatitic,  
zeolitic, and chlorophanitic. Equivalent to Little Butte Volcanic Series of Peck and others  
(1964) and Kays (1970). Oligocene volcanic rocks of Brown and others (1980a,b), and  
Breitenbush formation of White (1980a) and Hammond and others (1980)
- Tmtrv Olivocene-Miocene rhyolite-dacite lavas (Oligocene-Miocene): Predominantly aphyric  
rhyolite, although some rhyolite may be present. A moderately thick sequence is exposed  
on lower southeast flank of Mount David Douglas. Typical colors are pink, gray, white, and  
buff. Unit is commonly flow banded. Unit contains interbedded dacitic and andesitic flows  
similar to those mapped elsewhere as unit Toml but included in unit Tmtrv at this locality.  
Equivalent to Miocene silicic rocks of Brown and others (1980b), Little Butte Volcanic Series  
of Peck and others (1964) and Kays (1970), and Breitenbush formation of White (1980a)  
and Hammond and others (1980)

REFERENCES

- Brown, D.E., McLean, G.D., Priest, G.R., Woller, N.M., and Black, G.L., 1980a, Preliminary geology and  
geothermal resource potential of the Belknap-Poly area, Oregon: Oregon Department of Geology  
and Mineral Industries Open-File Report 0-80-2, 58 p.
- Brown, D.E., McLean, G.D., Woller, N.M., and Black, G.L., 1980b, Preliminary geology and geothermal  
resource potential of the Willamette Falls area, Oregon: Oregon Department of Geology and Mineral  
Industries Open-File Report 0-80-3, 65 p.
- Hammond, P.E., Anderson, J.L., and Manning, K.J., 1980, Guide to the geology of the upper Clackamas  
and North Santiam River areas, northern Oregon Cascade Range, in Oles, R.F., Johnson, J.G.,  
Niem, A.B., and Niem, W.A., eds., Geologic field trips in western Oregon and southwestern  
Washington: Oregon Department of Geology and Mineral Industries Bulletin 101, p. 153-167.
- Kays, M.A., 1970, Western Cascade volcanic series, South Umpqua Falls region, Oregon: Oregon  
Department of Geology and Mineral Industries, Ore. Div., v. 32, no. 5, p. 81-94.
- Peck, D.L., Griggs, A.B., Schlicker, H.G., Wells, F.G., and Dohy, H.M., 1964, Geology of the central and  
northern parts of the Western Cascade Range in Oregon: U.S. Geological Survey Professional Paper  
449, 56 p.
- Sherrod, D.R., Moyle, P.R., Ramsey, C.M., and MacLeod, N.S., in press, Geology and mineral resource  
potential of the Diamond Peak Wilderness, Lane and Klamath Counties, Oregon: U.S. Geological  
Survey open-file report.
- Thayer, T.P., 1939, Geology of the Salem Hills and the North Santiam basin, Oregon: Oregon Department  
of Geology and Mineral Industries Bulletin 15, 40 p.
- White, C.M., 1980a, Geology of the Breitenbush Hot Springs quadrangle, Oregon: Oregon Department  
of Geology and Mineral Industries Special Paper 9, 26 p.
- , 1980b, Geology and geochemistry of Mt. Hood volcano: Oregon Department of Geology and  
Mineral Industries Special Paper 8, 39 p.
- Woller, N.M., 1982, Geology of the Swift Creek area, Lane County, Oregon, in Priest, G.R., and Vogt,  
B.F., eds., Geology and geothermal resources of the Cascades, Oregon: Oregon Department of  
Geology and Mineral Industries Open-File Report 0-82-7, p. 155-151.

GEOLOGIC SYMBOLS

- Contact: Solid where visible, dashed where approximately located
- Strike and dip
- Shear: With dip of plane
- Shear: With dip of plane and rake of slickensides
- Mafic to intermediate dike: Dip shown
- Chemical sample number
- K-Ar date: With age in millions of years. "a" indicates K-Ar date may be affected by rock  
alteration. Parentheses around K-Ar date indicate that sample had less than 10% radiogenic  
argon
- Fault: Solid where visible, dashed where inferred, dotted where concealed by younger units,  
questioned where questionable. Ball and bar on downthrown side. Dip of plane shown if known
- Fault: With brecciation
- Geothermal test hole: With terrain-corrected temperature gradient (upper number) and  
heat flow (lower number). "Iso" denotes isothermal gradient